

Non-perturbative renormalization group analysis of nonlinear spiking networks

Braden A. W. Brinkman¹

¹Department of Neurobiology and Behavior, Stony Brook University, Stony Brook, NY, 11794, USA

(Dated: January 24, 2023)

The critical brain hypothesis posits that neural circuits may operate close to critical points of a phase transition, which has been argued to have functional benefits for neural computation. Theoretical and computational studies arguing for or against criticality in neural dynamics largely rely on establishing power laws or scaling functions of statistical quantities, while a proper understanding of critical phenomena requires a renormalization group (RG) analysis. However, neural activity is typically non-Gaussian, nonlinear, and non-local, rendering models that capture all of these features difficult to study using standard statistical physics techniques. Here, we overcome these issues by adapting the non-perturbative renormalization group (NPRG) to work on (symmetric) network models of stochastic spiking neurons. By deriving a pair of Ward-Takahashi identities and making a “local potential approximation,” we are able to calculate non-universal quantities such as the effective firing rate nonlinearity of the network, allowing improved quantitative estimates of network statistics. We also derive the dimensionless flow equation that admits universal critical points in the renormalization group flow of the model, and identify two important types of critical points: in networks with an absorbing state there is Directed Percolation (DP) fixed point corresponding to a non-equilibrium phase transition between sustained activity and extinction of activity, and in spontaneously active networks there is a *complex valued* critical point, corresponding to a spinodal transition observed, e.g., in the Lee-Yang ϕ^3 model of Ising magnets with explicitly broken symmetry. Our Ward-Takahashi identities imply trivial dynamical exponents $z_* = 2$ in both cases, rendering it unclear whether these critical points fall into the known DP or Ising universality classes.

There is little hope of understanding how each of the $\mathcal{O}(10^{11})$ neurons contributes to the functions of the brain [1]. These neurons must operate amid constantly changing and noisy environmental conditions and internal conditions of an organism [2], rendering neural circuitry stochastic and often far from equilibrium. Experimental work has demonstrated that neural circuitry can operate in many different regimes of activity [3–15], and theoretical and computational work suggests that transitions between these different operating regimes of collective activity may be sharp, akin to phase transitions observed in statistical physics. Some neuroscientists argue that circuitry in the brain is actively maintained close to critical points—the dividing lines between phases—as a means of minimizing reaction time to perturbations and switching between computations, or for maximizing information transmitted. This has become known as the “critical brain hypothesis” [15–18]. While the hypothesis has garnered experimental and theoretical support in its favor, it has also become controversial, with many scientists arguing that key signatures of criticality, such as power law scaling, may be produced by non-critical systems [19, 20], or are potentially artifacts of statistical inference in sub-sampled recordings [21, 22].

The tools of non-equilibrium statistical physics have been built to investigate such dynamic collective activity. However, there are several obstacles to the application of these tools to neural dynamics: neurons are not arranged in translation-invariant lattices with simple nearest-neighbor connections, and neurons communicate with all-or-nothing signals called “spikes,” the statistics of which are very non-Gaussian. These are all features very unlike the typical systems studied in soft condensed

matter physics, and hence methods developed to treat such systems often cannot be applied to models of neural activity without drastically simplifying neural models to fit these unrealistic assumptions.

Tools that have been somewhat successful at treating neural spiking activity on networks include mean-field theory, linear response theory, and diagrammatic perturbative calculations to correct these approximations [23–26]. However, these tools break down when the synaptic connections between neurons are strong, particularly when the system is close to a bifurcation. A powerful approach for studying the statistical behavior of strongly coupled systems is the non-perturbative renormalization group (NPRG), which has been successfully used to study many problems in condensed matter physics [27–38]. However, because these methods have been developed for lattices or continuous media in which the fluctuations are driven by Gaussian noise, they cannot be straightforwardly applied to spiking network models. Previous work has studied phase transitions in neuron models primarily either through simulations, data analysis [13, 15, 39], or by applying renormalization group methods to models from statistical mechanics that have been reinterpreted in a neuroscience context as firing rate models or coarse-grained activity states (e.g., “active” or “quiescent”) [14, 40, 41], but not spikes.

In this work we adapt the non-perturbative renormalization group method to apply to a stochastic spiking network model commonly used in neuroscience. We show that we are able to investigate both universal and non-universal properties of the spiking network statistics, even away from phase transitions, on both lattices and random networks, as depicted in Fig. 1. We begin by

briefly reviewing the spiking network model and the types of phase transitions predicted by a mean-field analysis (Sec. I). We then introduce the core idea of the NRG method and derive the flow equations for the spiking network model (Sec. II), which we use to calculate non-universal quantities like the effective nonlinearity that predicts how a neuron's mean firing rate is related to its mean membrane potential. To investigate universal properties, we then present the rescaled RG flow equations and conditions under which non-trivial critical points exist (Sec. III). The properties of these critical points depend on an effective dimension d , which coincides with spatial dimension in nearest-neighbor networks. We end this report by discussing the implications of this work for current theoretical and experimental investigations of collective activity in spiking networks, both near and away from phase transitions (Sec. IV).

I. SPIKING NETWORK MODEL

A. Model definition

We consider a network of N neurons that stochastically fire action potentials, which we refer to as “spikes.” The probability that neuron i fires $\dot{n}_i(t)dt$ spikes within a small window $[t, t+dt]$ is given by a counting process with expected rate $\phi(V_i(t))dt$, where $\phi(V)$ is a non-negative firing rate nonlinearity, conditioned on the current value of the membrane potential $V_i(t)$. We assume $\phi(V)$ is the same for all neurons, and for definiteness we will take the counting process to be Poisson or Bernoulli, though the properties of the critical points are not expected to depend on this specific choice.

The membrane potential of each neuron obeys leaky dynamics,

$$\tau \frac{dV_i}{dt} = -(V_i - \mathcal{E}_i) + \sum_{j=1}^N J_{ij} \dot{n}_j(t), \quad (1)$$

$$\dot{n}_i(t)dt \sim \text{Poiss}[\phi(V_i(t))dt] \quad (2)$$

where τ is the membrane time constant, \mathcal{E}_i is the rest potential, and J_{ij} is the weight of the synaptic connection from pre-synaptic neuron j to post-synaptic neuron i . We allow J_{ii} to be non-zero in general to allow for, e.g., refractory effects that would otherwise be absent in this model (i.e., there is no hard reset of the membrane potential after a neuron fires a spike). For simplicity, we model the synaptic input as an instantaneous impulse, referred to as a “pulse coupled” network. It is straightforward to generalize J_{ij} to a general time-dependent linear filter of the incoming spikes, but this would complicate the upcoming calculations. Similarly, for technical reasons explained later, we restrict our analysis to symmetric networks, $J_{ij} = J_{ji}$.

B. Mean-field analysis and phase transitions

The stochastic system defined by Eqs. (1)-(2) cannot be solved in closed form, and understanding the statistical dynamics of these networks has historically been accomplished through simulations and approximate analytic or numerical calculations.

A qualitative picture of the dynamics of the model can be obtained by a mean-field approximation in which fluctuations are neglected, such that $\langle \dot{n}_i(t) \rangle = \langle \phi(V_i(t)) \rangle \approx \phi(\langle V_i(t) \rangle)$, and solving the dynamics

$$\tau \frac{d\langle V_i(t) \rangle}{dt} = -(\langle V_i(t) \rangle - \mathcal{E}_i) + \sum_{j=1}^N J_{ij} \phi(\langle V_i(t) \rangle).$$

Many different types of dynamical behaviors and transitions among behaviors are possible depending on the properties of the connections J_{ij} and nonlinearity $\phi(V)$ [3], including bump attractors [4–7], pattern formation in networks of excitatory and inhibitory neurons [8–10], transitions to chaos [11, 12], and avalanche dynamics [13–15]. Many networks admit a steady-state for which $d\langle V_i \rangle / dt = 0$ for all i as $t \rightarrow \infty$, which gives the self-consistent mean-field equations

$$\langle V_i \rangle = \mathcal{E}_i + \sum_{j=1}^N J_{ij} \phi(\langle V_j \rangle). \quad (3)$$

This equation of state does reasonably well at predicting the steady state statistics of the network when synaptic coupling and nonlinearity are weak. As synaptic coupling grows stronger the fluctuations become important and the mean-field predictions no longer agree well with simulation data; see Fig. 3. A typical situation in which fluctuations grow strong enough to invalidate the mean-field predictions is when the system approaches a phase transition. In this work we will focus on transitions from quiescent or low activity steady states characterized by $\langle V_i(t) \rangle = 0$ to active states characterized by $\langle V_i(t) \rangle \neq 0$. In order for $\langle V_i \rangle = 0$ to be a steady state, Eq. (3) imposes

$$\mathcal{E}_i + \sum_j J_{ij} \phi(0) = 0.$$

Deviations of this quantity from zero act like an external field in magnetic systems, with positive (negative) deviations biasing $\langle V \rangle$ to values above (below) zero. At exactly zero the mean-field approximation predicts a continuous phase transition to an active state.

For analytic $\phi(V) = \phi(0) + \phi'(0)V + AV^{1+\beta^{-1}} + \dots$, where $V^{1+\beta^{-1}}$ is the lowest order nonlinear dependence (i.e., $\beta^{-1} > 0$), we can estimate the dynamics of the mean

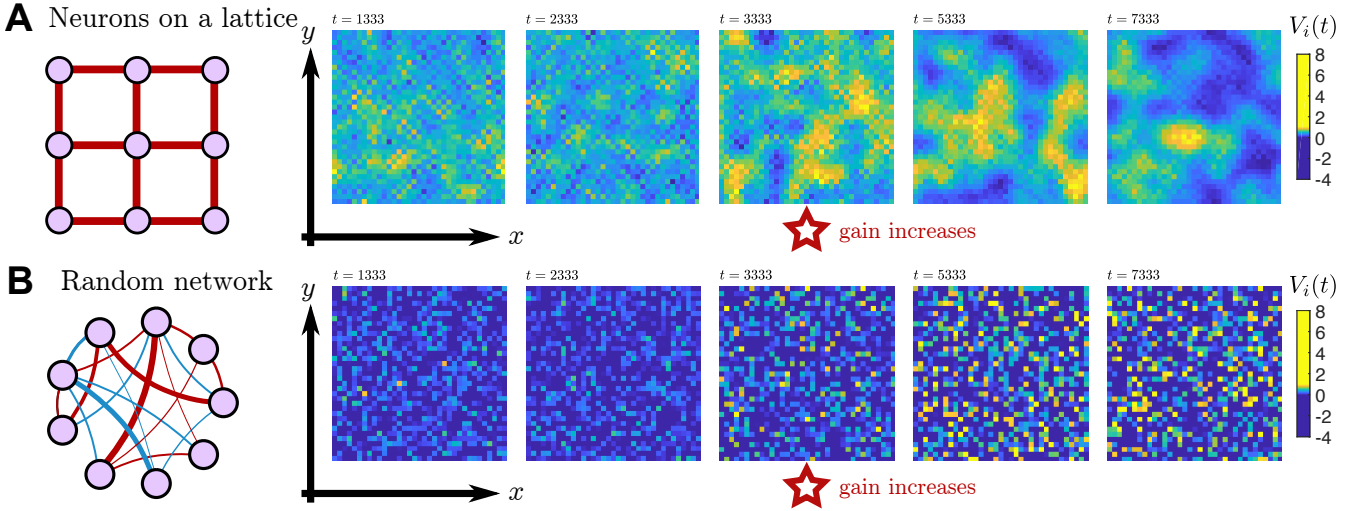


FIG. 1. **Dynamics of neurons on lattices versus networks** can appear to differ substantially, depending on features like the statistics of synaptic connections between neurons and the signs of those synaptic connections. For example, **A**) shows the dynamics of a simulated network of excitatory neurons connected to their neighbors on a 2-dimensional lattice. Initially, the neurons fire asynchronously at intermediate rates. At $t = 3333$ timesteps into the simulation, the gain of the neurons is increased (reflecting, for example, changes in attention of the organism), which creates two metastable states of high or low firing rate that drift through the network. In comparison, for the network of **B**) neurons are connected randomly with synaptic strengths of either sign. Because there is not spatial organization, it is not clear if the increase in gain creates metastable states of activity in the network, or if it merely increases the variance of the network. Network models like this have been studied extensively using approximate techniques like mean-field theory, but understanding the roles that stochastic fluctuations play in these systems demands the use of tools from the renormalization group (RG).

membrane potentials when $\langle V \rangle$ is close to 0 from above:

$$\begin{aligned} \tau \frac{d\langle V_i(t) \rangle}{dt} &\approx - \sum_{j=1}^N (\delta_{ij} - J_{ij}\phi'(0))\langle V_j(t) \rangle \\ &\quad + \sum_{j=1}^N AJ_{ij}\langle V_j(t) \rangle^{1+\beta^{-1}} + \dots \end{aligned}$$

In the subcritical or critical regimes in which $\langle V_i(t) \rangle$ decays to 0, the projection of $\langle V_i(t) \rangle$ onto the eigenmode of J_{ij} with the largest eigenvalue, Λ_{\max} , will have the slowest rate of decay, so we may approximate $\langle V_i(t) \rangle$ by the dynamics of this leading order mode:

$$\tau \frac{d\langle V \rangle}{dt} \approx -(1 - \Lambda_{\max}\phi'(0))\langle V \rangle + Ac\langle V \rangle^{1+\beta^{-1}} + \dots,$$

where $c = \Lambda_{\max} \sum_j P_{\Lambda_{\max},j} P_{j,\Lambda_{\max}}^{1+\beta^{-1}}$, with $P_{i\lambda} = (P^T)_{\lambda i}$ the eigenmode of J_{ij} with eigenvalue λ . When $r \equiv 1 - \Lambda_{\max}\phi'(0) > 0$ the solution decays to zero exponentially, whereas $\langle V(t) \rangle$ decays algebraically when $r = 0$:

$$\langle V(t) \rangle \sim \begin{cases} \exp(-rt/\tau), & r > 0 \\ t^{-\beta}, & r = 0 \end{cases}. \quad (4)$$

For $r < 0$ the zero solution of the mean-field equation becomes unstable. In networks with homogeneous excitatory couplings $J_{ij} = 0$ or $J > 0$, two non-zero steady-

state solutions emerge (assuming $Ac < 0$),

$$\langle V(\infty) \rangle \sim (r/(Ac))^\beta,$$

with an exponential decay $\exp(-\beta^{-1}|r|t/\tau)$ toward these values. Note that for even $\beta^{-1} \geq 2$ there are two solutions of opposite sign, whereas for odd β^{-1} there is one real positive solution. Typically, $\beta^{-1} = 1$ or 2 for nonlinearities $\phi(y)$ commonly used in spiking network models.

The argument above is expected to work well for networks with excitatory homogeneous synaptic strength $J_{ij} = J > 0$ if neurons i and j are connected and 0 otherwise, as the leading order mode will be homogeneous. For random networks with synapses of either sign the behavior in the supercritical regime is more complicated, and we defer discussion of this case until we have accounted for fluctuations.

We focus on two important universality classes of phase transitions that may occur with this mean-field analysis: i) “absorbing state networks”, for which $\phi(V)$ is 0 when $V \leq 0$, and there are no fluctuations in activity once the network has reached this state; and ii) spontaneous networks, for which $\phi(0) \neq 0$ and neurons can stochastically fire even if the network has become quiescent for some period of time. In the case of absorbing state networks, we consider $\beta = 1$, and the transition from $\langle V \rangle = 0$ to $\langle V \rangle \sim r$ is a bifurcation similar to the directed percolation phase transition, a genuinely non-equilibrium phase transition between a quiescent absorbing state and an active state. In spontaneous networks we will typically

consider sigmoidal nonlinearities that have $\beta = 1/2$, and the transition from $\langle V \rangle = 0$ to one of the metastable states $\langle V \rangle \sim \pm \sqrt{r}$ is reminiscent of the Ising universality class phase transition. In our discussion of non-universal quantities, we will focus on spontaneous networks, but we will cover both types of classes in our investigation of critical points in the renormalization group flow.

Typically, mean-field theory gives a good qualitative picture of the collective dynamics of a system. However, it is well known that fluctuations can alter the predictions of critical exponents, like the algebraic decay of $\langle V(t) \rangle$ or how the active state scales with r , meaning these quan-

ties may not be equal to the exponent β . Fluctuations can also qualitatively change the mean-field predictions, for example by changing second order transitions into first order transitions or vice versa. Indeed, we will see that fluctuations of the spontaneous spiking network result in a first order transition, not a second order transition, as predicted by the mean-field analysis.

A tractable way to go beyond mean-field theory and account for fluctuations is to formulate the model as a non-equilibrium statistical field theory. The stochastic network dynamics (1) and (2) can be formulated as a path integral with an action [26, 42]

$$S[\tilde{V}, V, \tilde{n}, \dot{n}] = \sum_{i=1}^N \int_{-\infty}^{\infty} dt \left\{ \tilde{V}_i(t) \left(V_i(t) - \mathcal{E}_i - \sum_{j=1}^N \int_{-\infty}^{\infty} dt' J_{ij}(t-t') \dot{n}_j(t') \right) + \tilde{n}_i(t) \dot{n}_i(t) - (e^{\tilde{n}_i(t)} - 1) \phi(V_i(t)) \right\}, \quad (5)$$

where we have formally solved Eq. (1) to write $V_i(t) = \mathcal{E}_i + \sum_j J_{ij}(t-t') \dot{n}_j(t')$, with $J_{ij}(t) \equiv J_{ij} \tau^{-1} e^{-t/\tau} \Theta(t)$, with $\Theta(t)$ the Heaviside step-function. In fact, Eq. (5) holds for any model in which the membrane potential linear filters spike trains through $J_{ij}(t-t')$, and our NPRG formalism will apply for any such choice, though we focus on the case in which the dynamics correspond to Eq. (1). In addition to the membrane fields V and spike fields \dot{n} , the action is a functional of auxiliary “response fields” \tilde{V} and \tilde{n} that arise in the Martin-Siggia-Rose-Janssen-De Dominicis (MSRJD) construction of the path integral [23, 25, 26, 42]. The term $(e^{\tilde{n}_i(t)} - 1) \phi(V_i(t))$ arises from choosing the conditional spike probabilities to be Poisson or Bernoulli. We have neglected terms corresponding to initial conditions, as we will primarily be interested in steady state statistics, or in the non-equilibrium responses of a network perturbed out of a quiescent steady state. To lighten notation going forward, we will use the shorthands $a \cdot b = \sum_{i,\alpha} \int dt a_i^\alpha(t) b_i^\beta(t)$ and $a \cdot M \cdot b = \sum_{ij,\alpha\beta} \int dt dt' a_i^\alpha(t) M_{ij}^{\alpha\beta}(t-t') b_j^\beta(t')$, where i, j run over neuron indices, α, β index the different fields $\{V, \tilde{V}, \tilde{n}, \dot{n}\}$ (or their corresponding sources, to be introduced), and $t, t' \in \mathbb{R}$ are times.

This field theory was first developed for the spiking dynamics (marginalized over V, \tilde{V}) by [23], who also developed the perturbative diagrammatic rules for calculating the so-called loop corrections to the mean-field approximation with “tree level” corrections (corresponding to approximating the spiking process as Gaussian fluctuations around the mean-field prediction), and [26] extends the diagrammatic approach to actions of the form (5) (with an additional nonlinearity to implement hard resets of the membrane potential, which we do not consider here). This formalism is useful in the subcritical regime where mean-field theory paints a qualitatively accurate

picture of the dynamics, but ultimately breaks down as a phase transition is approached (see Fig. 3).

The standard approach for extending the applicability of the path integral formalism into parameter regimes where phase transitions occur is to develop a perturbative renormalization group (RG) approach. In lattice systems this is normally accomplished by taking a continuum limit of the model, in which the lattice becomes a continuous medium. However, it is not clear what the appropriate continuum limit of an arbitrary network is, rendering it unclear how to perform a perturbation renormalization group scheme of this model on networks instead of translation-invariant lattices.

An alternative to the perturbative renormalization group method that has been successful in analyzing challenging models in statistical physics is the “non-perturbative renormalization group” (NPRG). In this work we adapt the NPRG method to apply to this spiking network model, and show that we can quantitatively estimate both non-universal and universal statistics of the network’s behavior, even in regimes where even the loop corrections break down. Importantly, we show that our approach works for neurons arranged in lattices or random networks, currently restricted to networks with symmetric connections $J_{ij} = J_{ji}$.

To this end, in the next section we will introduce the NPRG method through our derivation of its extension to the spiking network model, and the approximations we implement to solve the resulting equations in practice. We will show that incorporating the effects of fluctuations replaces the bare nonlinearity $\phi(\langle V \rangle)$ in the mean-field equations with an effective nonlinearity $\Phi_1(\langle V \rangle)$, a non-universal quantity which we will calculate numerically. We will show that our method predicts this nonlinearity well for a variety of network structures, in sub- and supercritical cases.

After our investigation of the non-universal firing rate nonlinearity in Sec. II, we will show how to rescale the RG equations to obtain fixed points of the renormalization group procedure, and thereby investigate critical points and universality in this spiking network model in Sec. III.

II. THE NON-PERTURBATIVE RENORMALIZATION GROUP EXTENDED TO THE SPIKING NETWORK MODEL

In any statistical model, one would in principle like to compute the moment generating functional (MGF) $\mathcal{Z}[\mathcal{A}]$ or the related cumulant generating functional (CGF) $\mathcal{W}[\mathcal{A}]$,

$$\begin{aligned} \mathcal{Z}[\mathcal{A}] &\equiv \exp(\mathcal{W}[\mathcal{A}]) \\ &= \int \mathcal{D}[\tilde{V}, V, \tilde{n}, \dot{n}] e^{-S[\tilde{V}, V, \tilde{n}, \dot{n}] + \tilde{V} \cdot h + V \cdot \tilde{h} + \tilde{n} \cdot j + \dot{n} \cdot \tilde{j}}, \end{aligned} \quad (6)$$

a functional of “source fields” $\mathcal{A} = \{h, \tilde{h}, j, \tilde{j}\}$. (Note that we use the convention of pairing source fields with tildes to their partners without tildes, and vice versa, as all fields with tildes may be taken to be purely imaginary). Derivatives of the MGF evaluated at zero sources yield statistical moments and response functions. In practice, computing $\mathcal{Z}[\mathcal{A}]$ or $\mathcal{W}[\mathcal{A}]$ exactly is intractable except in special cases.

The key idea behind the non-perturbative renormalization group (NPRG) method is to define a one-parameter family of models that interpolate from a solvable limit of

the theory to the full theory by means of a differential equation that allows for tractable and non-trivial approximations that do not rely on series expansions. In Eq. (5) the interactions between neurons arise only through the bilinear term $\tilde{V} \cdot J \cdot \dot{n}$, and the MGF is solvable in the absence of coupling, $J = 0$, as then it just consists of a collection of independent Poisson neurons with rates $\phi(\mathcal{E}_i)$. This motivates us to define our family of models by regulating the synaptic interactions between neurons, replacing the interaction term, $\tilde{V} \cdot J \cdot \dot{n}$ with $\tilde{V} \cdot J_\Lambda \cdot \dot{n}$, depending on a parameter $\Lambda \in [\Lambda_{\min}, \Lambda_{\max}]$, such that $J_{ij; \Lambda=\Lambda_{\min}}(t-t') = 0$ and $J_{ij; \Lambda=\Lambda_{\max}}(t-t') = J_{ij}(t-t')$. We will choose the parameter Λ to be a threshold on the eigenvalues of J_{ij} , for reasons that will become evident shortly.

Following the standard NPRG approach (see [43] for pedagogical introductions in equilibrium and [27, 30, 44, 45] for non-equilibrium systems, and [46] for a broad overview), we derive the flow equation for the regulated average effective action (AEA) $\Gamma_\Lambda[\chi] = -\mathcal{W}_\Lambda[\mathcal{A}] + \chi \cdot \mathcal{A} - \frac{1}{2}\chi \cdot R_\Lambda \cdot \chi$, where $\chi = \{\tilde{\psi}, \psi, \tilde{\nu}, \nu\}$ are “fluctuation-corrected” versions of the fields $\{\tilde{V}, V, \tilde{n}, \dot{n}\}$, respectively. The regulator R_Λ is chosen so that $\Gamma_{\Lambda=\Lambda_{\min}} = S[\chi]$ is the mean-field theory of the spiking network model and $\Gamma_{\Lambda=\Lambda_{\max}}[\chi] = \Gamma[\chi]$, the true AEA of the model. We will define R_Λ explicitly momentarily. The AEA is a modified Legendre transform of the CGF of the model and hence contains all statistical and response information about the network [45, 46]. The fields χ are defined by derivatives of the CGF $\mathcal{W}_\Lambda[\mathcal{A}]$,

$$\tilde{\psi}_i(t) = \frac{\delta \mathcal{W}_\Lambda[\mathcal{A}]}{\delta h_i(t)}, \quad \psi_i(t) = \frac{\delta \mathcal{W}_\Lambda[\mathcal{A}]}{\delta \tilde{h}_i(t)}, \quad \tilde{\nu}_i(t) = \frac{\delta \mathcal{W}_\Lambda[\mathcal{A}]}{\delta j_i(t)}, \quad \nu_i(t) = \frac{\delta \mathcal{W}_\Lambda[\mathcal{A}]}{\delta \tilde{j}_i(t)}; \quad (7)$$

for $\Lambda = \Lambda_{\max}$ the definition of $\Gamma_\Lambda[\chi]$ reduces to the standard Legendre transform, and the fields \mathcal{A} can be recovered from derivatives of $\Gamma_{\Lambda=\Lambda_{\max}}[\chi] = \Gamma[\chi]$:

$$h_i(t) = \frac{\delta \Gamma[\chi]}{\delta \tilde{\psi}_i(t)}, \quad \tilde{h}_i(t) = \frac{\delta \Gamma[\chi]}{\delta \psi_i(t)}, \quad j_i(t) = \frac{\delta \Gamma[\chi]}{\delta \tilde{\nu}_i(t)}, \quad \tilde{j}_i(t) = \frac{\delta \Gamma[\chi]}{\delta \nu_i(t)}, \quad (8)$$

For $\Lambda \neq \Lambda_{\max}$, the fields \mathcal{A} can be defined in terms of $\Gamma_\Lambda[\chi]$, with R_Λ -dependent corrections in Eqs. (8); see Appendix B.

Owing to the bilinearity of the interaction $J_{ij}(t)$, the AEA obeys the celebrated Wetterich flow equation [47],

$$\partial_\Lambda \Gamma_\Lambda = \frac{1}{2} \text{Tr} \left[\partial_\Lambda \mathbf{R}_\Lambda \cdot \left[\Gamma_\Lambda^{(2)} + \mathbf{R}_\Lambda \right]^{-1} \right], \quad (9)$$

where Tr denotes a super-trace over field indices χ , neuron indices, and times. The regulator $\mathbf{R}_\Lambda(t-t')$ is a $4N \times 4N$ matrix that couples only the $\tilde{\psi}$ and ν fields. In particular, $R_{ij; \Lambda}^{\tilde{\psi}, \nu}(t-t') = J_{ij}(t-t') - J_{ij; \Lambda}(t-t')$ and

$R_{ij; \Lambda}^{\chi, \chi'}(t-t') = 0$ for any other pair of fields $(\chi, \chi') \neq (\tilde{\psi}, \nu)$ or $(\nu, \tilde{\psi})$. $\Gamma_\Lambda^{(2)}$ is a $4N \times 4N$ matrix of second derivatives of Γ_Λ with respect to pairs of the fields χ , and the factor $\left[\Gamma_\Lambda^{(2)} + \mathbf{R}_\Lambda \right]^{-1}$ is an inverse taken over matrix indices, field indices, and time.

The Wetterich equation is exact, but being a functional integro-partial differential equation it cannot be solved in practice, and approximations are still necessary. The advantage of using $\Gamma_\Lambda[\chi]$ over $\mathcal{Z}_\Lambda[\mathcal{A}]$ is that the AEA shares much of its structure with the original action S , allowing us to better constrain our non-perturbative approximation. The standard approach is to make an *ansatz* for

the form of the solution, constrained by symmetries or Ward-Takahashi identities and employing physical intuition. The action of the spiking network model does not readily admit any obvious symmetries; however, we can derive a pair of Ward-Takahashi identities that allows us to restrict the form of the AEA.

A. Ward-Takahashi identities

The derivation of the Ward-Takahashi identities for this model makes use of the fact that we can marginalize over either the spiking fields or the membrane potential fields when computing the moment generating functional $\mathcal{Z}[\mathcal{A}]$ (Eq. (6)):

$$\mathcal{Z}[\mathcal{A}] = e^{j \cdot \tilde{j}} \int \mathcal{D}[\tilde{V}, V] e^{-S_{\text{volt}}[\tilde{V}, V | \tilde{j}] + \tilde{V} \cdot h + V \cdot \tilde{h}} \quad (10)$$

$$= e^{\tilde{h} \cdot (h + \mathcal{E})} \int \mathcal{D}[\tilde{n}, \dot{n}] e^{-S_{\text{spike}}[\tilde{n}, \dot{n} | h] + \tilde{n} \cdot j + \dot{n} \cdot \tilde{j}}, \quad (11)$$

where the marginalized actions are

$$S_{\text{volt}}[\tilde{V}, V | \tilde{j}] \equiv \sum_i \int dt \left\{ \tilde{V}_i(t)(V_i(t) - \mathcal{E}_i) - \phi(V_i(t)) \left(e^{\tilde{j}_i(t) + \sum_j \int dt' \tilde{V}_j(t') J_{ji}(t' - t)} - 1 \right) \right\},$$

$$S_{\text{spike}}[\tilde{n}, \dot{n} | h] \equiv \sum_i \int dt \left[\tilde{n}_i(t) \dot{n}_i(t) - \left(e^{\tilde{n}_i(t)} - 1 \right) \phi \left(\sum_j \int dt' J_{ij}(t - t') \dot{n}_j(t') + \mathcal{E}_i(t) + h_i(t) \right) \right].$$

Taking a derivative of Eq. (10) with respect to $j_i(t)$ and writing it in terms of $\mathcal{W}[\mathcal{A}]$ gives

$$\frac{\delta \mathcal{W}[\mathcal{A}]}{\delta j_i(t)} = \tilde{j}_i(t) + \sum_j \int dt' \frac{\delta \mathcal{W}[\mathcal{A}]}{\delta h_j(t')} J_{ji}(t' - t).$$

Identifying $\tilde{\nu}_i(t) = \frac{\delta \mathcal{W}[\mathcal{A}]}{\delta j_i(t)}$, $\tilde{\psi}_i(t) = \frac{\delta \mathcal{W}[\mathcal{A}]}{\delta h_i(t)}$, and $\tilde{j}_i(t) = \frac{\delta \Gamma[\chi]}{\delta \nu_i(t)}$ yields the identity

$$\tilde{\nu}_i(t) = \frac{\delta \Gamma[\chi]}{\delta \nu_i(t)} + \sum_j \int dt' \tilde{\psi}_j(t') J_{ji}(t' - t). \quad (12)$$

Next, we take a derivative of Eq. (11) with respect to $\tilde{h}_i(t)$, giving

$$\frac{\delta \mathcal{W}[\mathcal{A}]}{\delta \tilde{h}_i(t)} = h_i(t) + \mathcal{E}_i(t) + \sum_j \int dt' J_{ij}(t - t') \frac{\delta \mathcal{W}[\mathcal{A}]}{\delta \tilde{j}_j(t')}.$$

Identifying $\tilde{\psi}_i(t) = \frac{\delta \mathcal{W}[\mathcal{A}]}{\delta h_i(t)}$, $\nu_i(t) = \frac{\delta \mathcal{W}[\mathcal{A}]}{\delta j_i(t)}$, and $h_i(t) = \frac{\delta \Gamma[\chi]}{\delta \tilde{\psi}_i(t)}$ yields the identity

$$\psi_i(t) = \frac{\delta \Gamma[\chi]}{\delta \tilde{\psi}_i(t)} + \mathcal{E}_i(t) + \sum_j \int dt' J_{ji}(t' - t) \nu_j(t'). \quad (13)$$

Combining the anti-derivatives of Eqs. (12) and (13) shows that the AEA *must* have the form

$$\Gamma_\Lambda[\tilde{\psi}, \psi, \tilde{\nu}, \nu] = \tilde{\psi} \cdot (\psi - \mathcal{E} - J \cdot \nu) + \tilde{\nu} \cdot \nu + \Upsilon_\Lambda[\tilde{\nu}, \psi], \quad (14)$$

where J is the true synaptic coupling, not the regulated coupling J_Λ , and the unknown renormalized functional $\Upsilon_\Lambda[\tilde{\nu}, \psi]$ couples only the spike-response fields $\tilde{\nu}$ and the membrane-potential fields ψ . Before we move on to use this result to form our ansatz, we note that these Ward-Takahashi identities can be derived in the traditional manner, perturbing the fields $\tilde{V}_i(t)$ or $\dot{n}_i(t)$ by infinitesimal amounts and demanding that the variation of the action vanish. However, the advantage of the derivation given here is that it also works with the discrete time formulation of the model, in which it is questionable whether the discrete time form of $\dot{n}_i(t)$ can be infinitesimally perturbed. We also note that there is a symmetry of the model that arises from the fact that only potential differences are meaningful. If we add an explicit offset to $\phi(V) \rightarrow \phi(V - V_0)$, then we may shift $V_i(t) \rightarrow V_i(t) + \theta$, $\mathcal{E}_i \rightarrow \mathcal{E}_i + \theta$ and $V_0 \rightarrow V_0 + \theta$ for any constant θ and the action remains unchanged. However, this symmetry does not provide any additional constraints on the form of the action (see Appendix C), and we set $V_0 = 0$ in this work.

B. Local potential approximation

Now that we have restricted the form of Γ_Λ we may make an ansatz for the renormalized piece $\Upsilon_\Lambda[\tilde{\nu}, \psi]$. The initial condition for this piece is $\Upsilon_{\Lambda=\Lambda_{\min}}[\tilde{\nu}, \psi] = - \sum_i \int dt (e^{\tilde{\nu}_i(t)} - 1) \phi(\psi_i(t))$, which is a local functional of the fields $\tilde{\nu}_i(t)$ and $\psi_i(t)$, depending only on a single time t and neuron index i , integrated over all time and summed over all neuron indices. This motivates us to follow the example of previous NRG work and assume that

Υ_Λ remains a local functional of the fields all throughout the flow, called the “local potential approximation” (LPA):

$$\Upsilon_\Lambda[\tilde{\nu}, \psi] = - \sum_i \int dt U_\Lambda(\tilde{\nu}_i(t), \psi_i(t)). \quad (15)$$

We will not assume that the “local potential” function $U_\Lambda(\tilde{\nu}_i(t), \psi_i(t))$ is a separable function of $\tilde{\nu}_i(t)$ and $\psi_i(t)$, as this property is not preserved by the RG flow. The effective firing rate nonlinearity $\Phi_1(y)$, the key quantity

we focus on predicting in this work, is defined by

$$\nu_i(t) = U_{\Lambda_{\max}}^{(1,0)}(0, \psi_i(t)) \equiv \Phi_1(\psi_i(t)). \quad (16)$$

This relationship reveals that, just as at the mean-field level, a scatter plot of the mean firing rates against the mean membrane potentials should yield a functional relationship.

Using the ansatz (15), we compute the functional derivatives of Γ_Λ , evaluate them at constant values $\tilde{\nu}_i(t) \rightarrow \tilde{x}$ and $\psi_i(t) \rightarrow y$, and insert them into the Wetterich flow equation (9) to obtain a flow equation for the function $U_\Lambda(\tilde{x}, y)$. The result for finite N and arbitrary regulated coupling $\mathbf{J}(\omega)$ —represented in the Fourier domain—is

$$\begin{aligned} \partial_\Lambda U_\Lambda(\tilde{x}, y) = & \frac{1}{2} \int_{-\infty}^{\infty} \frac{d\omega}{2\pi} \text{tr} \left[\partial_\Lambda \mathbf{J}_\Lambda(\omega) \left[U_\Lambda^{(1,1)}(\tilde{x}, y) \mathbb{I}_{N \times N} - \left(U_\Lambda^{(1,1)}(\tilde{x}, y)^2 - U_\Lambda^{(2,0)}(\tilde{x}, y) U_\Lambda^{(0,2)}(\tilde{x}, y) \right) \mathbf{J}_\Lambda^T(-\omega) \right] \mathbf{\Xi}_\Lambda(\omega) \right. \\ & \left. + \partial_\Lambda \mathbf{J}_\Lambda^T(-\omega) \mathbf{\Xi}_\Lambda(\omega) \left[U_\Lambda^{(1,1)}(\tilde{x}, y) \mathbb{I}_{N \times N} - \left(U_\Lambda^{(1,1)}(\tilde{x}, y)^2 - U_\Lambda^{(2,0)}(\tilde{x}, y) U_\Lambda^{(0,2)}(\tilde{x}, y) \right) \mathbf{J}_\Lambda(\omega) \right] \right], \end{aligned} \quad (17)$$

where the trace tr is over neural indices and

$$\mathbf{\Xi}_\Lambda(\omega) = \left[\mathbb{I}_{N \times N} - U_\Lambda^{(1,1)}(\tilde{x}, y) (\mathbf{J}_\Lambda(\omega) + \mathbf{J}_\Lambda^T(-\omega)) + \left(U_\Lambda^{(1,1)}(\tilde{x}, y)^2 - U_\Lambda^{(2,0)}(\tilde{x}, y) U_\Lambda^{(0,2)}(\tilde{x}, y) \right) \mathbf{J}_\Lambda(\omega) \mathbf{J}_\Lambda^T(-\omega) \right]^{-1}. \quad (18)$$

This form of the flow equation holds for any synaptic coupling filter $\mathbf{J}(\omega)$. For the remainder of this work we will focus on the specific case of pulse-coupled networks described by Eq. (1), for which $\mathbf{J}_\Lambda(t) = \mathbf{J}_\Lambda \tau^{-1} \exp(-t/\tau) \Theta(t)$ (where τ is the membrane time-constant and $\Theta(t)$ is the Heaviside step function), or $\mathbf{J}_\Lambda(\omega) = \mathbf{J}_\Lambda / (-i\omega\tau + 1)$. We also consider only symmetric connections $\mathbf{J}_\Lambda = \mathbf{J}_\Lambda^T$ that can be diagonalized. For the pulse-coupled network the frequency integrals can be completed exactly using the residue theorem, and symmetric couplings allow us to diagonalize the matrices and reduce the trace to a sum over eigenvalues of \mathbf{J}_Λ . We choose to regulate the synaptic couplings by replacing

the eigenvalues λ of the true \mathbf{J} with regulated values

$$\lambda_\Lambda(\lambda) = \lambda \Theta(\Lambda - \lambda). \quad (19)$$

The regulated eigenvalues are interpreted as the limit of a smooth function that tends to the step function Θ . That is, eigenvalues greater than the threshold Λ are set to 0 while smaller eigenvalues retain their values (Recall that eigenvalues are purely real for symmetric matrices). In lattice systems the eigenvalues λ are related to momentum, and this procedure is similar to momentum shell integration, but done directly in energy space. We illustrate the effect this coarse-graining has on the synaptic connections $J_{ij;\Lambda}$ in lattices and random networks in Fig. 2.

Evaluating the frequency integrals and taking the infinite network limit $N \rightarrow \infty$, the flow equation for $U_\Lambda(\tilde{x}, y)$ reduces to

$$\partial_\Lambda U_\Lambda(\tilde{x}, y) = \frac{1}{2\tau} \rho_\lambda(\Lambda) \left\{ 1 - \Lambda U_\Lambda^{(1,1)}(\tilde{x}, y) - \sqrt{\left(1 - \Lambda U_\Lambda^{(1,1)}(\tilde{x}, y) \right)^2 - \Lambda^2 U_\Lambda^{(0,2)}(\tilde{x}, y) U_\Lambda^{(2,0)}(\tilde{x}, y)} \right\}, \quad (20)$$

where $\rho_\lambda(\lambda)$ is the eigenvalue density, also known as the

density of states when the synaptic connections form a

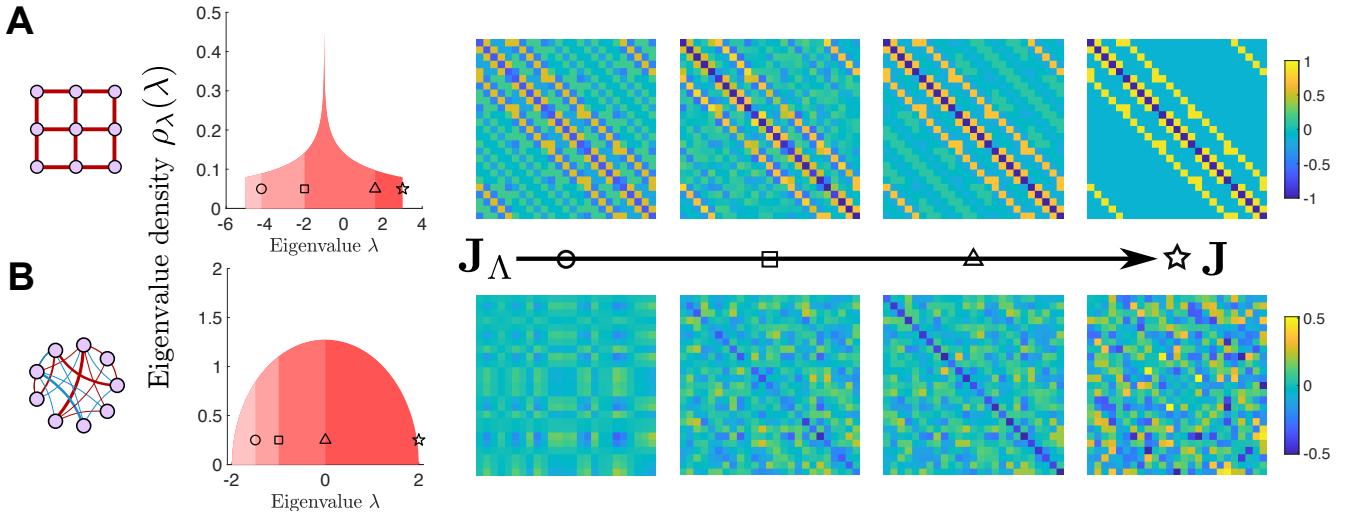


FIG. 2. **Dynamics of neurons on lattices versus networks** can appear to differ substantially, depending on features like the statistics of synaptic connections between neurons and the signs of those synaptic connections. For example, **A**) shows the dynamics of a simulated network of excitatory neurons connected to their neighbors on a 2-dimensional lattice. Initially, the neurons fire asynchronously at intermediate rates. At $t = 3333$ timesteps into the simulation, the gain of the neurons is increased (reflecting, for example, changes in attention of the organism), which creates two metastable states of high or low firing rate that drift through the network. In comparison, for the network of **B**) neurons are connected randomly with synaptic strengths of either sign; we set $J_{ii} = 0$ for this example. Because there is not spatial organization, it is not clear if the increase in gain creates metastable states of activity in the network, or if it merely increases the variance of the network. Network models like this have been studied extensively using approximate techniques like mean-field theory, but understanding the roles that stochastic fluctuations play in these systems demands the use of tools from the renormalization group (RG).

nearest-neighbor lattice. An important result is that the flow equation is independent of the eigenvectors of J_{ij} . Thus, any networks with the same eigenvalue density and bare nonlinearity $\phi(y)$ will have the same effective firing rate nonlinearity within the local potential approximation. However, the statistics of the network activity will depend on the eigenvectors through the solution of the self-consistent equations $\nu_i = \Phi_1(\psi_i)$, $\psi_i = \mathcal{E}_i + \sum_j J_{ij} \nu_j$.

By construction, the initial condition of Eq. (20) is $U_{\Lambda=\Lambda_{\min}}(\tilde{x}, y) = (e^{\tilde{x}} - 1)\phi(y)$. The boundary conditions are a more subtle issue, and most papers on the NPRG method do not discuss them in depth. The most common means of dealing with the boundary conditions are to i) compute derivatives at the boundaries of the numerical grid using a stencil method that only uses points internal to the grid [38], ii) impose that the solution matches the mean-field or 1-loop approximations at the numerical boundaries [48], or iii) expand the function in a power series around some point and truncating the series at some order, resulting in a system of ordinary differential equations that need only an initial condition (however, the truncation is equivalent to implicitly imposing the missing boundary conditions [49]). In this work we focus on a combination of method iii with ii, using a series expansion to eliminate \tilde{x} and solving a resulting system of partial differential equations, as it is numerically the most tractable. We have obtained similar results solving the full two-dimensional partial differential equation (20) using methods i and ii for subcritical networks.

Expanding $U_\Lambda(\tilde{x}, y)$ in a series around $\tilde{x} = 0$ and truncating at a finite power \tilde{x}^m yields a hierarchy of flow equations for the effective nonlinearities

$$\Phi_{m,\Lambda}(y) \equiv U_\Lambda^{(m,0)}(0, y)$$

for $m > 0$. The rationale for expanding around $\tilde{x} = 0$ is that this is the expected value of the membrane response field $\tilde{\psi}_i(t) = \langle \tilde{V}_i(t) \rangle$ when the network reaches a steady state. All of these nonlinearities share the initial condition $\Phi_{m,\Lambda_{\min}}(y) = \phi(y)$, for all m . Flow equations for these nonlinearities may be derived by differentiating the flow equation for $U_\Lambda(\tilde{x}, y)$ with respect to \tilde{x} m times and then setting $\tilde{x} = 0$. This procedure yields an infinite hierarchy of equations in which the m^{th} nonlinearity is coupled to the previous $m - 1$ nonlinearities as well as the $(m + 1)^{\text{th}}$ nonlinearity. That is, the hierarchy has the structure

$$\partial_\Lambda \Phi_{1,\Lambda}(y) = \mathcal{F}_1(\Phi_{1,\Lambda}, \Phi_{2,\Lambda}) \quad (21)$$

$$\partial_\Lambda \Phi_{2,\Lambda}(y) = \mathcal{F}_2(\Phi_{1,\Lambda}, \Phi_{2,\Lambda}, \Phi_{3,\Lambda}) \quad (22)$$

$$\partial_\Lambda \Phi_{3,\Lambda}(y) = \mathcal{F}_3(\Phi_{1,\Lambda}, \Phi_{2,\Lambda}, \Phi_{3,\Lambda}, \Phi_{4,\Lambda}) \quad (23)$$

⋮

$$\partial_\Lambda \Phi_{m,\Lambda}(y) = \mathcal{F}_m(\Phi_{1,\Lambda}, \Phi_{2,\Lambda}, \dots, \Phi_{m,\Lambda}, \Phi_{m+1,\Lambda}) \quad (24)$$

⋮

where the functions \mathcal{F}_m depend on the nonlinearities as

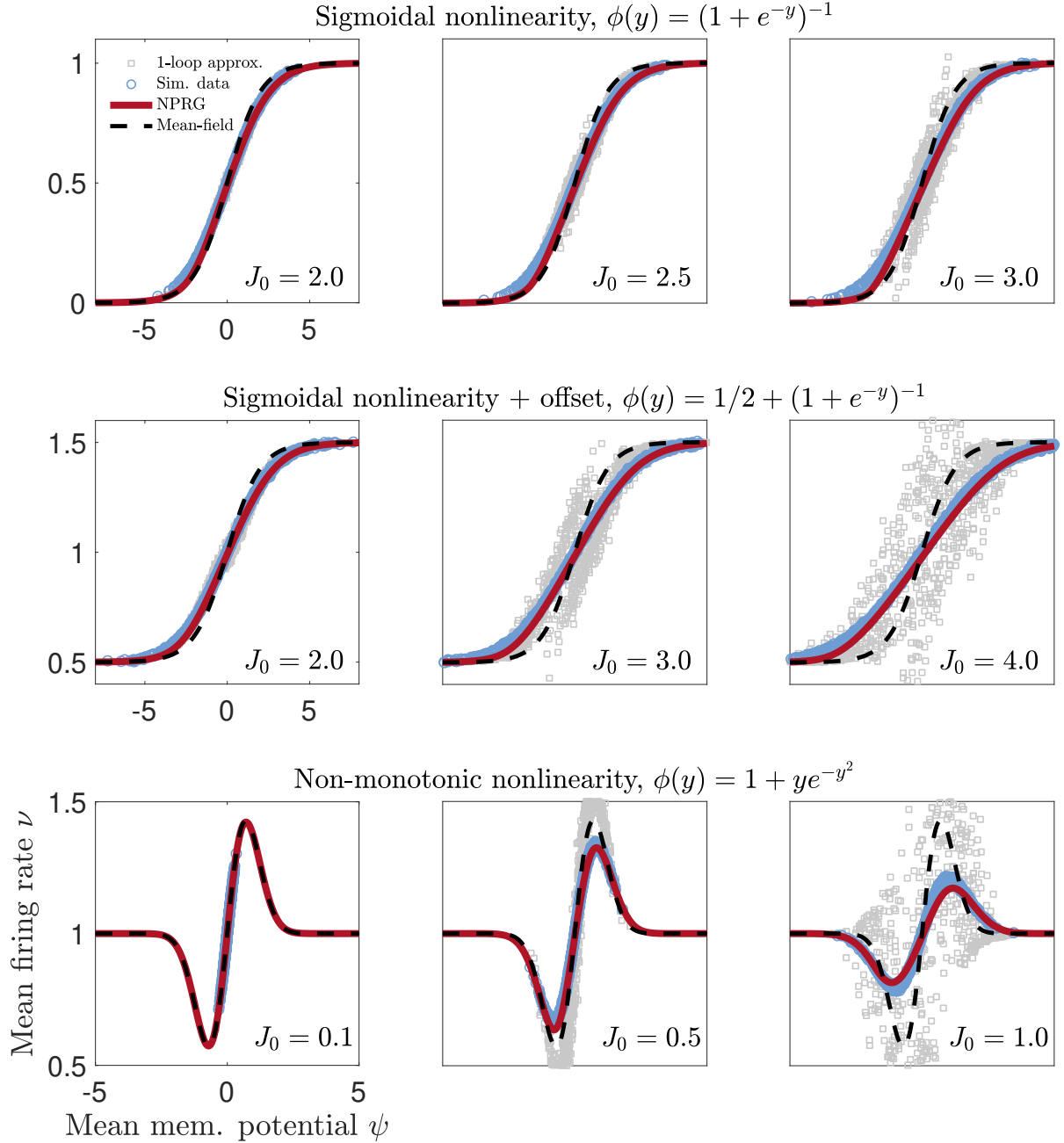


FIG. 3. **Effective nonlinearities as functions of synaptic strength** in networks of $N = 10^3$ neurons and for three different choices of the bare nonlinearity $\phi(V)$ (in dimensionless units). Top row: Sigmoidal nonlinearity $\phi(y) = (1 + \exp(-y))^{-1}$ and synaptic weight variance $J_0 = 2.0$ (left) 2.5 (middle), and 3.0 (right). Middle row: Sigmoidal nonlinearity with a non-zero minimum baseline firing rate, $\phi(y) = 1/2 + 1/(1 + \exp(-y))$ and synaptic weight variance $J_0 = 2.0$ (left) 3.0 (middle), and 4.0 (right). Bottom: Results for a non-monotonic nonlinearity with $\phi(y) = 1 + y \exp(-y^2)$ and synaptic weight variance $J_0 = 0.1$ (left) 0.5 (middle), and 1.0 (right). Our non-perturbative renormalization group analysis predicts that scatter-plots of the mean firing rates ν_i versus mean membrane potentials $\psi_i = \mathcal{E}_i + \sum_j J_{ij} \nu_j$ should lie along a nonlinear curve, confirmed by the simulation data (blue data points). Our prediction of the effective nonlinearity is given by the solid red curve, obtained by solving Eq. (20) numerically. For comparison, we show the mean field prediction (black dashed lines) and the 1-loop predictions obtained using Ref. [23]'s diagrammatic methods (grey data points). We see that for strong coupling strengths our non-perturbative predictions continue to predict the firing rates well when other methods break down.

well as derivatives of those nonlinearities, which are not denoted explicitly as arguments in Eqs (21)-(24).

Because each nonlinearity is coupled to the subsequent nonlinearity in the hierarchy, we need to make some approximation to close the hierarchy at a finite order of m in order to solve it. The simplest such approximation consists of setting the nonlinearities on the right hand side of Eqs (21)-(24) to their initial values $\phi(y)$. However, this is approximation amounts to the one-loop approximation [50], and we do not expect it to perform better than the perturbative diagrammatic methods of [23, 25]. In particular, we expect it to break down at the mean-field phase transition, when $\Lambda\phi'(0)$ approaches 1, at which point a singularity develops in the flow equation.

We can instead improve on this approximation by truncating at order m and approximating only $\Phi_{m+1,\Lambda}(y) \approx \phi(y)$. For example, if we close the hierarchy at order 3 by approximating $\Phi_{4,\Lambda} = \phi(y)$, we would solve the following

system of equations for $\Phi_{1,\Lambda}(y)$, $\Phi_{2,\Lambda}(y)$, and $\Phi_{3,\Lambda}(y)$:

$$\partial_\Lambda \Phi_{1,\Lambda}(y) = \mathcal{F}_1(\Phi_{1,\Lambda}, \Phi_{2,\Lambda}) \quad (25)$$

$$\partial_\Lambda \Phi_{2,\Lambda}(y) = \mathcal{F}_2(\Phi_{1,\Lambda}, \Phi_{2,\Lambda}, \Phi_{3,\Lambda}) \quad (26)$$

$$\partial_\Lambda \Phi_{3,\Lambda}(y) \approx \mathcal{F}_3(\Phi_{1,\Lambda}, \Phi_{2,\Lambda}, \Phi_{3,\Lambda}, \phi). \quad (27)$$

This approximation does not suffer the same issues as the 1-loop approximation, which breaks down when $1 - \Lambda\phi'(0)$ vanishes. In the hierarchy (25)-(27) (and higher-order truncations), the factor of $\phi(y)$ only appears in numerators. The singular factor is instead $1 - \Lambda\Phi'_{1,\Lambda}(y)$, but renormalization of $\Phi'_{1,\Lambda}(0)$ results in the solution persisting until we chose a Λ_{\max} such that $1 - \Lambda_{\max}\Phi'_{1,\Lambda_{\max}}(0) = 0$, corresponding to the phase transition. Beyond this value of Λ_{\max} the solution becomes non-analytic, out of the range of perturbative calculations. This singularity does cause problems for our numerical solution of the hierarchy, but we will show that we can still obtain a semi-quantitative solution and understand the supercritical behavior of the network qualitatively.

To show an explicit example of a hierarchy, Eqs. (28)-(29) give the equations for the hierarchy truncated at second order ($\Phi_{3,\Lambda}(y) \approx \phi(y)$); for the subcritical results shown in this paper we truncate at order 4, and for the supercritical results we truncate at order 1.

$$\partial_\Lambda \Phi_{1,\Lambda}(y) = \frac{\rho_\lambda(\Lambda)\Lambda^2}{4\tau} \frac{\Phi_{2,\Lambda}(y)\Phi''_{1,\Lambda}(y)}{|1 - \Lambda\Phi'_{1,\Lambda}(y)|}, \quad (28)$$

$$\partial_\Lambda \Phi_{2,\Lambda}(y) = \frac{\rho_\lambda(\Lambda)\Lambda^2}{8\tau} \left[\frac{\Lambda^2\Phi_{2,\Lambda}(y)^2\Phi''_{1,\Lambda}(y)^2}{|1 - \Lambda\Phi'_{1,\Lambda}(y)|^3} + \frac{4\Lambda\Phi_{2,\Lambda}(y)\Phi'_{2,\Lambda}(y)\Phi''_{1,\Lambda}(y)}{|1 - \Lambda\Phi'_{1,\Lambda}(y)|^2} + \frac{4\phi(y)\Phi''_{1,\Lambda}(y) + 2\Phi_{2,\Lambda}(y)\Phi''_{2,\Lambda}(y)}{|1 - \Lambda\Phi'_{1,\Lambda}(y)|} \right], \quad (29)$$

with initial conditions $\Phi_{m,\Lambda_{\min}}(y) = \phi(y)$ and boundary conditions $\lim_{|y| \rightarrow \infty} \Phi_{m,\Lambda_{\min}}(y) \sim \phi(y)$ for $m = 1, 2$.

For sufficiently small $\Lambda_{\max}\phi'(0)$ the denominator $1 - \Lambda\Phi'_{1,\Lambda}(y)$ remains positive for the duration of the flow, and the solution is analytic. However, at a critical value of $\Lambda_{\max}\phi'(0)$ the denominator vanishes at the end of the flow, $1 - \Lambda_{\max}\Phi'_{1,\Lambda_{\max}}(0) = 0$, corresponding to a critical point. Above this critical value of $\Lambda_{\max}\phi'(0)$ the solution develops a range of y for which $1 - \Lambda\Phi'_{1,\Lambda}(y) = 0$, compensated by the second derivatives of the $\Phi''_{m,\Lambda}(y)$ vanishing on this range. This corresponds a supercritical regime in which the solution is non-analytic, analogous to the development of the non-analyticity in the free-energy of the Ising model in the ordered phase [51].

We present results for a few choices of $\phi(y)$ in Fig. 3, showing how well the numerical solution predicts the effective nonlinearity $\Phi_1(\psi)$, even when the synaptic strength exceeds the value of mean-field prediction for the phase transition ($1 = \Lambda_{\max}\phi'(0)$), for which perturbative approximations like the loop expansion [23, 25]

break down. Although we focus on sigmoidal nonlinearities in this work, we show an example of a non-monotonic nonlinearity to show that the method does not just coincidentally do well on sigmoidal nonlinearities. In these examples we used fully connected networks with Gaussian distributed weights to demonstrate the success of the method on random networks. For this first demonstration we do not tune these networks to criticality, instead fixing $\mathcal{E}_i = 0$ for all neurons. As a result of the heterogeneity of the neurons, there is a distribution of firing rates across the population, which allows us to resolve the effective nonlinearity $\Phi_1(\psi)$ by making a scatter plot of ν_i versus ψ_i .

Numerical solutions for the effective nonlinearities agree well with simulated data, especially compared to perturbative calculations. However, our approximation does systematically undershoot the data near the negative tail of the distribution. It is unclear if this is an artifact of the local potential approximation itself, the hierarchy closure approximation, or finite-size effects in

the simulations.

In the subcritical regime the flow equations can be numerically integrated to predict the effective nonlinearity, and we have implemented this solution up to order 4 ($\Phi_{5,\Lambda}(y) \approx \phi(y)$). The solutions are reasonably good for $\Phi_{1,\Lambda}(y)$ and $\Phi_{2,\Lambda}(y)$ when truncated at this order, with $\Phi_{3,\Lambda}(y)$ showing some influence of the truncation and $\Phi_{4,\Lambda}(y)$ showing the most influence. In principle, going to even higher orders should improve the numerical solutions further, though the flow equations become increasingly complicated.

In the supercritical regime the numerical solution becomes increasingly challenging. The development of the non-analytic behavior is straightforwardly observed at the order 1 approximation ($\Phi_{2,\Lambda}(y) \approx \phi(y)$). At higher orders it is difficult to coax Mathematica to integrate through the development of the non-analyticity, reminiscent of barriers integrating through the development of non-analytic shocks in nonlinear wave equations [52]. Nevertheless, we obtain a qualitative picture of what happens in the supercritical regime: in order for the flow to be finite, the nonlinearity develops a piecewise linear region for $y \in [\psi_-, \psi_+]$ —where the endpoints of this region, ψ_{\pm} , depend on the initial value of $\phi'(0)\Lambda_{\max}$ —such that second order derivatives in the numerator vanish and cancel out the singularity caused by $1 - \Lambda\Phi'_1(y) = 0$ in the denominator. Outside of this region $1 - \Lambda\Phi'_1(y) < 0$ and the nonlinearity is smooth and continuous. We will use this semi-quantitative picture later when investigating the dynamics of the mean membrane potentials in the supercritical regime (Sec. II D).

C. Examples of effective nonlinearities for different networks

To further evaluate our NPRG method on different types of networks, we calculate the effective nonlinearities for i) hypercubic lattices in dimensions $d = 2$ and 3 with excitatory connections (Fig. 4), ii) random regular graphs of degrees 3, 4, and 5 (but all effective dimension $d = 3$) with excitatory connections (Fig. 5), and iii) fully connected networks with Gaussian-distributed synaptic weights (Fig. 6, also shown in Fig. 3 for different nonlinearities). As observed, the predictions of the NPRG nonlinearities agree well with simulation data, particularly for the sub- and near-critical cases, which are calculated by closing Eqs. (24) at order $m = 4$. The biggest discrepancy between the numerical solutions and the simulated data occurs near the negative tail of the nonlinearity.

The super-critical nonlinearities do not agree as well quantitatively, as the flow equation must be integrated through the development of a singularity in the flow equation, which leads to a non-analytic solution. For these cases we solve for $\Phi_1(\psi)$ by closing Eqs. (24) at order $m = 1$, setting $\Phi_2(y) = \phi(y)$.

We remind the reader that the effective nonlinearity is a non-universal quantity, depending on the choice of the

bare nonlinearity $\phi(V)$ and the network architecture. It is worth noting that the non-perturbative renormalization group method is most commonly used to estimate universal properties, which are less sensitive to features of approximations like the local potential approximation. The reasonably good quantitative agreement between our NPRG predictions of this non-universal quantity is therefore a pleasant surprise.

D. Phase transition analysis with effective nonlinearities

Now that we understand the qualitative behavior of the effective nonlinearities, we can revisit the phase transition analysis discussed in the context of mean-field theory in Sec. I B. The conditions for a phase transition become

$$\mathcal{E}_i + \sum_j J_{ij}\Phi(0) = 0, \quad (30)$$

$$\tau/\tau_{\text{relax}} = 1 - \Lambda_{\max}\Phi'(0) = 0 \quad (31)$$

as $N \rightarrow \infty$, where $\Phi(\psi) \equiv U_{\Lambda=\Lambda_{\max}}^{(1,0)}(0, \psi)$ is the effective nonlinearity, which we remind the reader determines the expected firing rates via the relation $\langle \dot{n}_i(t) \rangle = \Phi(\langle V_i(t) \rangle)$. The first condition just means that the mean input into a neuron is 0, and hence $\langle V_i(t) \rangle = 0$ self-consistently (as we inserted $\langle V_i(t) \rangle = 0$ into $\Phi(\langle V_j(t) \rangle)$). The second condition says that the largest relaxation time τ_{relax} of the network diverges, equivalent to the divergence of the temporal correlation length.

In the subcritical regime $1 - \Lambda_{\max}\Phi'_1(0) > 0$, the mean-field analysis does not change, as $\Phi_1(\psi)$ is analytic, and so we expect an exponential decay to $\psi_i(t) = \langle V_i(t) \rangle = 0$. Qualitatively, the critical case is not expected to change either, giving rise to an algebraic decay of $\psi_i(t)$. However, one generally expects the power of this decay to be modified at the critical point, as the leading order super-linear behavior of $\Phi_1(\psi)$ is expected to be non-analytic at the critical point. We cannot solve the flow equations with enough precision to try and predict this exponent quantitatively, but we revisit this exponent in the next section on universality.

Finally, the dynamics in the supercritical regime are much different than the mean-field analysis suggests, due to the development of the piecewise-linear region of $\Phi_1(\psi)$. The “extremal” values of the membrane potential, corresponding to the values of ψ at which $\Phi_1(\psi)$ switches from the linear behavior to the nonlinear behavior, are fixed points of the membrane dynamics, at least in a homogeneous excitatory network. These two values therefore represent two extremal metastable states of the network, analogous to the positive and negative magnetization phases of the Ising model. Homogeneous excitatory networks can be prepared such that they remain in either state for extended periods of time, or even exhibit phase separation (Fig. 1A). The two metastable states can be observed by driving the networks with a global

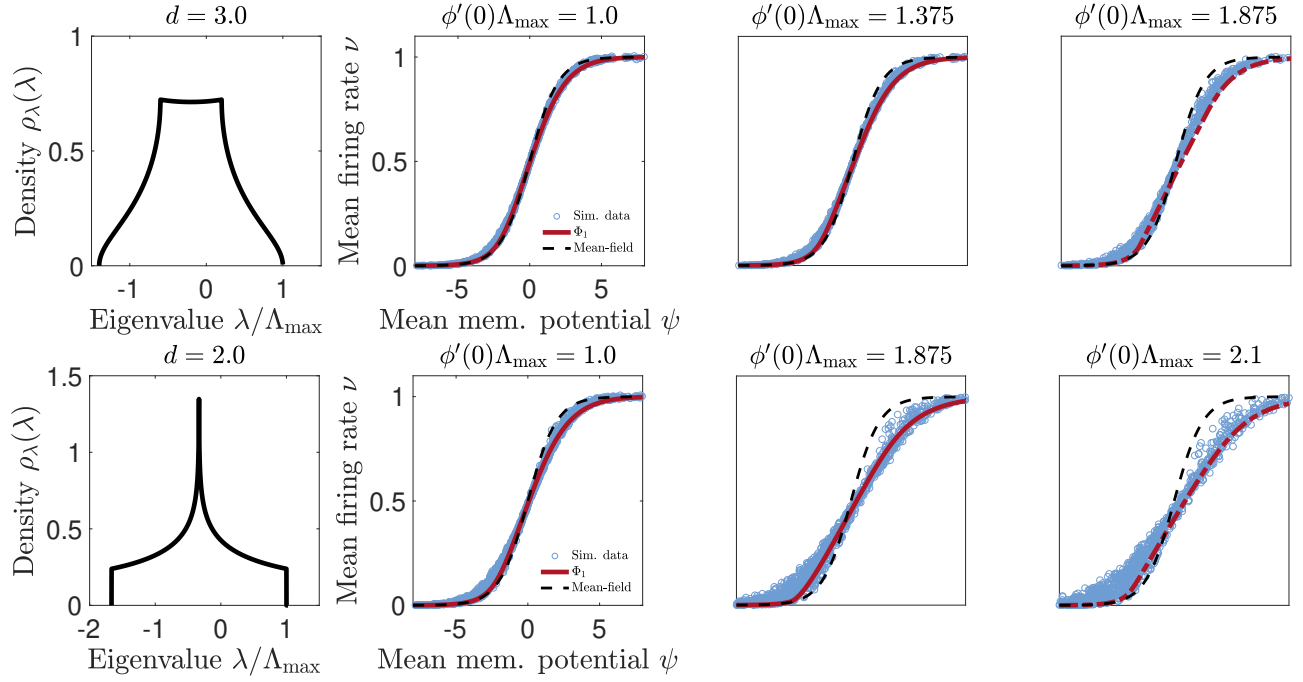


FIG. 4. **Effective nonlinearities on hypercubic lattices** of dimensions $d = 3$ (top row) and $d = 2$ (bottom row), along with their corresponding eigenvalue distributions $\rho_\lambda(\lambda)$ (far left). For each dimension we show a subcritical nonlinearity (left), a near-critical nonlinearity (middle), and a supercritical nonlinearity (right), although the networks themselves are not critical due to the heterogeneity of the neurons. The red curves are the predictions of the hierarchy of nonlinearities (Eq. (24), truncated at fourth order for subcritical and critical cases and first order for the supercritical case, using the results of [53] to compute the eigenvalue distributions. Blue data points are simulated data, using networks of $N = 10^3$ in $d = 3$ and $N = 35^2$ in $d = 2$.

current input I , starting from a very negative value of I , such that network firing is suppressed, and increasing it toward large positive current values. If we then decrease the current back toward negative values the population-averaged firing rates $\nu = \frac{1}{NT} \sum_{i=1}^N \int_{t_0}^{t_0+T} dt \dot{n}_i(t)$ trace out different trajectories in the ν - I plane when the networks are tuned to the supercritical regime, as shown in Fig. 7. The population averages are estimated by holding the current I fixed for a duration T , which we take to be 500 time steps in the simulations shown in Fig. 7.

For random networks J_{ij} with both excitatory and inhibitory connections, we cannot tune the entire network to occupy just one of the extremal states. In fact, because the synaptic connections J_{ij} are symmetric, we expect the network to be in a spin glass regime. The population-distribution of the membrane potentials can be understood using the dynamical mean-field theory method for spin glasses [54] applied to the dynamical equations for $\psi_i(t)$:

$$\tau \frac{d\psi_i(t)}{dt} = -\psi_i(t) + \sum_{j=1}^N J_{ij} (\Phi_1(\psi_j(t)) - \Phi_1(0)),$$

where we have assumed $\mathcal{E}_i = -\sum_j J_{ij} \Phi_1(0)$. The key difference between the standard dynamic mean-field calculations and our case is that the nonlinearity $\Phi_1(\psi)$ changes with the tuning parameter Λ_{\max} , whereas in pre-

vious treatments the nonlinearity is a fixed quantity. The dynamic mean-field calculation is not as tractable as it is in the case of asymmetric random networks with independent J_{ij} and J_{ji} [24, 55] or the original spin-glass treatment of the Ising model [54], owing in part to the non-analyticity of the nonlinearity in the supercritical regime. However, we can exploit the fact that the effective nonlinearity is predicted to be piecewise linear in the super-critical regime to obtain rough estimates of the population statistics. Our analysis does well at predicting the trend of standard deviation of the membrane potentials of the population varies with $\Phi_1'(0) = \Lambda_{\max}^{-1}$, the gain of the nonlinearity in the supercritical regime, though our calculation over-estimates the standard deviation compared to simulations of the network model, as shown in Fig. 8, likely due to neglecting the saturating behavior of the effective nonlinearity.

III. UNIVERSALITY IN THE RENORMALIZATION GROUP FLOW

So far, our renormalization group (RG) treatment of the spiking network model has implemented the first step of an RG procedure, coarse-graining. This has allowed us to calculate non-universal features of the network statistics that hold regardless of whether the network is close to a phase transition. In this section we turn our atten-

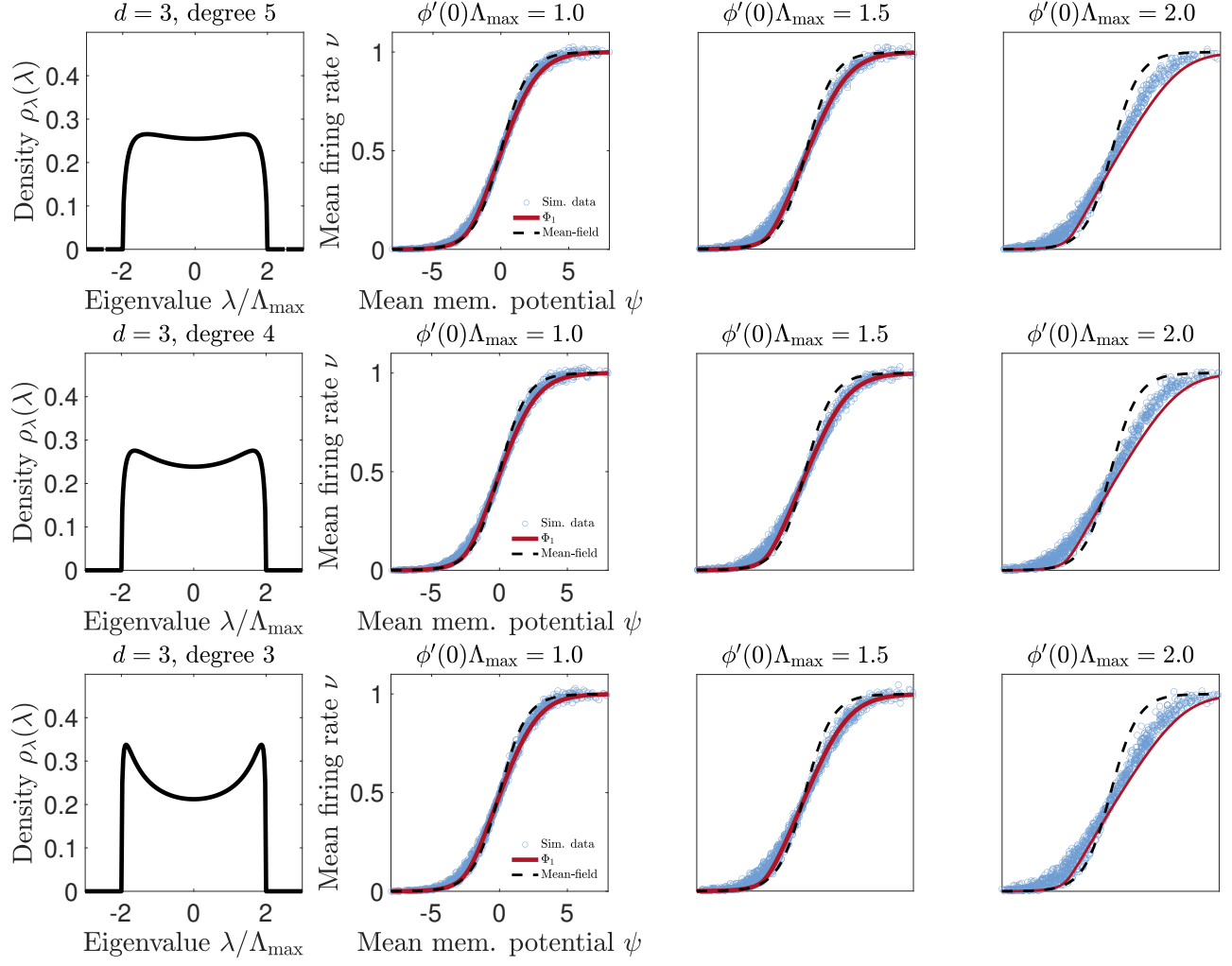


FIG. 5. **Effective nonlinearities on excitatory random regular graphs** of effective dimension $d = 3$ (all cases) and degrees 5 (top row), 4 (middle row), and 3 (bottom row), along with their corresponding eigenvalue distributions $\rho_\lambda(\lambda)$ (far left). For each degree we show a subcritical nonlinearity (left), a near-critical nonlinearity (middle), and a supercritical nonlinearity (right), tuned by varying the global excitatory coupling $J_0 = \Lambda_{\max}/2$. We map out the nonlinearity synthetically by assigning a distribution of rest potentials \mathcal{E}_i . The red curves are the predictions of the hierarchy of nonlinearities (Eq. (24), truncated at fourth order for subcritical and near-critical cases and first order for the supercritical case. Blue data points are simulated data, using networks of $N = 10^3$ neurons.

tion to networks tuned to a phase transition, at which the statistics are expected to exhibit universal scale-invariant properties that can in principle be measured in experiments. To investigate these universal features, we must implement the second step of the RG procedure, rescaling. In the non-perturbative renormalization group (NPRG) context, the rescaling procedure will amount to identifying an appropriate non-dimensionalization of the flow equation Eq. (20) and searching for fixed points.

This section proceeds as follows: we will first identify the rescaling of the NPRG flow equations that renders them dimensionless, and will admit fixed points. We will search for these fixed points using a combination of a perturbation expansion and non-perturbative truncations. This will show that the mean-field prediction of

a second-order transition are qualitatively invalidated in spontaneous networks, even at the level of the local potential approximation employed in this work.

A. Non-dimensionalization of the flow equation

In translation-invariant lattices and continuous media, rescaling a theory is typically done by scaling variables and fields with powers of momentum; it is not *a priori* obvious how to perform this step for general networks. The resolution in this more general setting is that near a critical point quantities will scale as powers of $\delta\Lambda \equiv \Lambda_{\max} - \Lambda$.

To isolate the singular behavior of the RG flow as

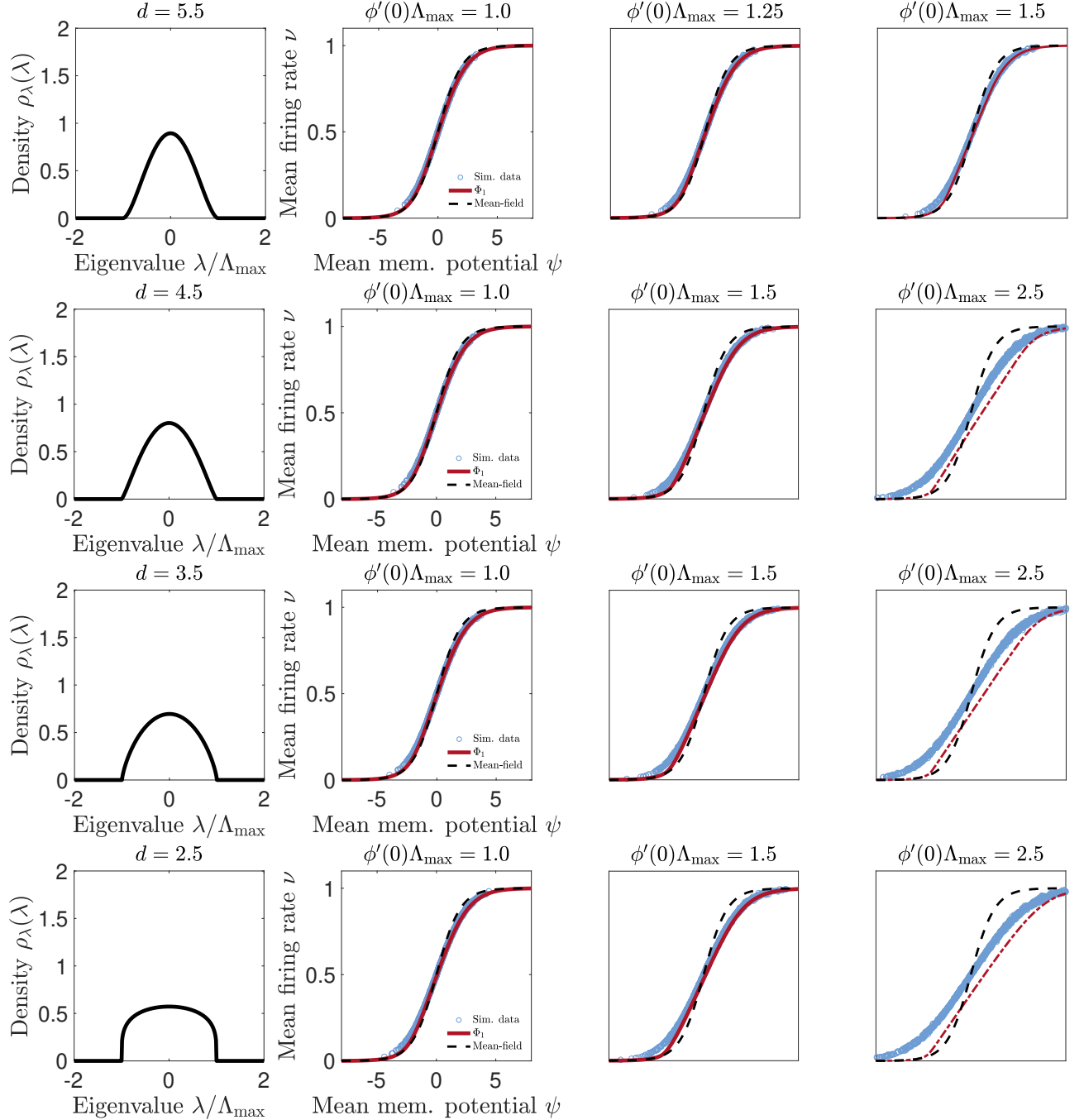


FIG. 6. **Effective nonlinearities on random networks** of effective dimensions $d = 5.5$ (top row) to $d = 2.5$ (bottom row), along with their corresponding eigenvalue distributions $\rho_\lambda(\lambda)$ (far left). For each dimension we show a subcritical nonlinearity (left), a near-critical nonlinearity (middle), and a supercritical nonlinearity (right), although the networks themselves are not critical due to the heterogeneity of the neurons. The red curves are the predictions of the hierarchy of nonlinearities (Eq. (24), truncated at fourth order for subcritical and critical cases and first order for the supercritical case, using the results of [53] to compute the eigenvalue distributions. Blue data points are simulated data, using networks of $N = 10^3$ neurons.

it approaches a critical point, it is convenient to define $U_\Lambda(\tilde{x}, y) = \Lambda_{\max}^{-1} \tilde{x}y + W_\Lambda(\tilde{x}, y)$, where Λ_{\max}^{-1} is the critical value of $G_{11, \Lambda=\Lambda_{\max}} \equiv U_{\Lambda=\Lambda_{\max}}^{(1,1)}(0, 0)$, such that $W_{\Lambda=\Lambda_{\max}}^{(1,1)}(0, 0) = 0$ at the critical point. We look for a scale invariant solution by making the change of variables

$W_\Lambda(\tilde{x}, y) = \Omega_\Lambda w_s(\tilde{z}, z)$ with $\tilde{z} = \tilde{x}/\tilde{X}_\Lambda$ and $z = y/Y_\Lambda$, where Ω_Λ , \tilde{X}_Λ , and Y_Λ are running scales to be determined and $s = -\ln\left(\frac{\Lambda_{\max}-\Lambda}{\Lambda_{\max}-\Lambda_{\min}}\right) \in [0, \infty)$ is the ‘‘RG time’’ (which we define to be positive, in contrast to the convention in some NRG works).

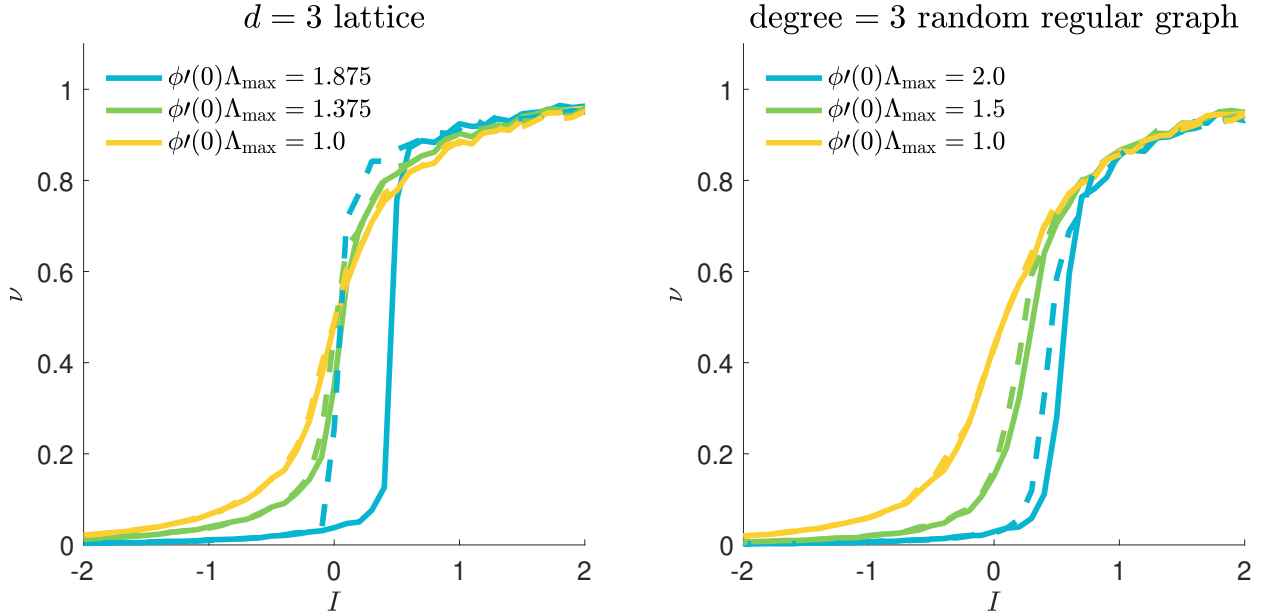


FIG. 7. **Hysteresis in homogeneous excitatory networks** on a $d = 3$ hypercubic lattice (left) and a random regular graph of degree 3 (right). The neurons in the network are tuned to have $\mathcal{E}_i = -\sum_j J_{ij}\phi(0) + I$, where I is a global external current, initially set to be very negative. As I increases the firing rates of the network will increase until they saturate at large I (solid lines). We then decrease I back toward large negative values (dashed lines). When the networks are in the supercritical regime we observe hysteresis: the upward and downward sweeps trace out different trajectories in the current I versus population-averaged firing rate $\nu = \sum_i \int dt \dot{n}_i(t)/(NT)$ plane, where the number of spike is averaged over a duration of $T = 500\Delta t$, with $\Delta t = 0.1$.

A straightforward way to determine the running scales Ω_Λ , \tilde{X}_Λ , and Y_Λ is to require the flow equation (20) to become asymptotically autonomous as $s \rightarrow \infty$. One can also find these scalings by rescaling the full average effective action (AEA), but it is more involved, and requires a careful consideration of the $N \rightarrow \infty$ limit in the eigenbasis of J_{ij} ; we give this derivation in Appendix H. In the scalings that follow below, we define the effective dimension d by the scaling of the eigenvalue distribution near Λ_{\max} , $\rho_\lambda(\Lambda) \sim \delta\Lambda^{d/2-1}$. This definition is chosen so that the effective dimension is equal to the spatial dimension when J_{ij} is a nearest-neighbor lattice with homogeneous coupling. With this definition,

we find $\Omega_\Lambda \sim \delta\Lambda^{d/2+1} \sim e^{-s(d/2+1)}$ and the combination $\tilde{X}_\Lambda Y_\Lambda \sim \Omega_\Lambda/\delta\Lambda \sim \delta\Lambda^{d/2}$. Importantly, we can only constrain the combination $\tilde{X}_\Lambda Y_\Lambda$, which means that there is a “redundant parameter”, similar to the case in models with absorbing state transitions [56]. This allows us to introduce a running exponent η_s^X by defining $\tilde{X}_\Lambda \sim \delta\Lambda^{\eta_s^X} = e^{-s\eta_s^X}$ and $Y_\Lambda \sim \delta\Lambda^{d/2-\eta_s^X} = e^{-s(d/2-\eta_s^X)}$. Note that this exponent does not arise from any field renormalizations, as our Ward-Takahashi identity guarantees no such field renormalizations exist. We will discuss the determination of \tilde{X}_Λ shortly. First, we present the dimensionless flow equation, whose asymptotically autonomous form as $\delta\Lambda \rightarrow 0$ is

$$\partial_s w_s - \left(\frac{d}{2} + 1\right) w_s + \eta_s^X \tilde{z} w_s^{(1,0)} + \left(\frac{d}{2} - \eta_s^X\right) z w_s^{(0,1)} = 1 - w_s^{(1,1)} - \sqrt{\left(1 - w_s^{(1,1)}\right)^2 - w_s^{(0,2)} w_s^{(2,0)}}, \quad (32)$$

Although Eq. (32) is only valid for RG-times $s \rightarrow \infty$, we retain some autonomous time-dependence for the purposes of performing linear stability analyses around fixed points of the flow. For the fully non-autonomous flow, see Appendix G.

We will not solve Eq. (32) directly, as its numerical solution is rendered delicate by the divergence of w_s when

it is not near a critical manifold. This is in contrast to its dimensionful counterpart Eq. (20), which remains finite over the course of integration and can be solved numerically when sufficient precision is specified. To assess the critical properties of the model, we will focus on searching for fixed point solutions, using a combination of traditional perturbative techniques and additional functional

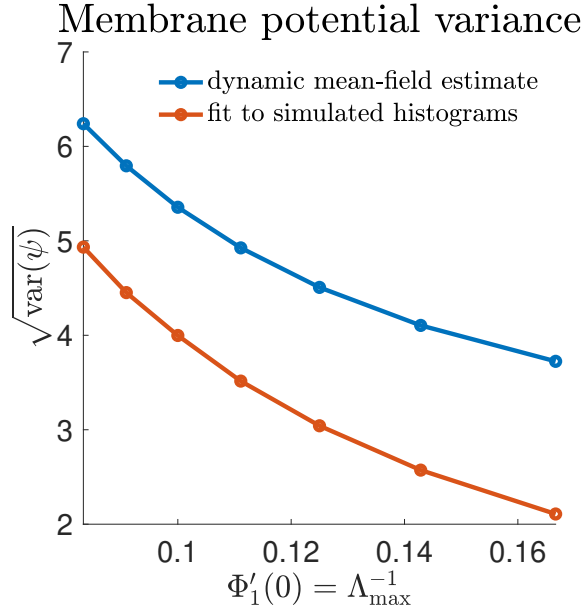


FIG. 8. **Population variance of the membrane potentials in random Gaussian networks** with effective dimension $d = 3$, as a function of $\Phi'_1(0) = \Lambda_{\max}^{-1}$, the gain of the effective nonlinearity $\Phi_1(\psi)$ in the supercritical regime.

truncations of $w_*(\tilde{z}, z)$ to a finite number of couplings that can be treated non-perturbatively.

To find fixed point solutions, we need to make a choice of the running scale \tilde{X}_Λ . We will briefly discuss the most natural choice $\tilde{X}_\Lambda = 1$, and then focus on two choices corresponding to networks with absorbing states and spontaneously active networks.

B. Pure annihilation fixed point

The variable \tilde{x} , corresponding to the spike response fields $\tilde{\nu}_i(t)$, is dimensionless, appearing in the bare potential through $e^{\tilde{x}} - 1$. Its “dimensionless” counterpart $\tilde{z} = \tilde{x}/\tilde{X}_\Lambda$ could therefore be chosen to be equal to \tilde{x} itself by setting $\tilde{X}_\Lambda = 1$. However, as we will see momentarily, the resulting fixed points $w_*(\tilde{z}, z)$ are unstable to couplings in the model that cannot all be simultaneously tuned to put the RG flow on the stable manifold of these fixed points.

One fixed point is the trivial solution $w_*(\tilde{z}, z) = 0$. This is analogous to the Gaussian fixed point in most field theoretic RG studies. A linear stability analysis around the trivial fixed point reveals that perturbations to all couplings of order z^0 and z^1 are unstable (“relevant”) in any dimension d , independent of \tilde{z} . This means that in order to tune the network to this trivial critical point, one has to adjust entire functions of \tilde{z} to some “critical functions.” For our initial condition $w_0(\tilde{z}, z)$ these functions start at $(e^{\tilde{z}} - 1)\phi(0)$ and $(e^{\tilde{z}} - 1)\phi'(0)z$, and it is not clear that the two parameters $\phi(0)$ and $\phi'(0)$ are suf-

cient to tune the entire model to this critical point. We therefore expect that for effective dimensions $d > 2$ any phase transitions are more likely to be controlled by some other fixed points, which we will find by using non-trivial choices of the running scale \tilde{X}_Λ .

Before we turn to these other cases, we briefly note that the trivial critical point develops an additional unstable direction as d crosses below 2, when the z^2 terms become unstable. For these dimensions we can find a pure annihilation fixed point following the prescription of [32], characterized by couplings $g_{mn}^* \equiv w_*^{(m,n)}(0, 0)$ that are zero for $m > n$. Moreover, other work has suggested that the pure annihilation fixed point becomes unstable to a fixed point with non-zero branching rate below $d \simeq 4/3$ [28, 57–60]. Because the initial condition for the spiking network model contains infinitely many couplings $g_{mn,0}$ with $m > n$, it may not be possible to tune the network close to the annihilation fixed point in $d < 2$, and it may be more likely that the model is controlled by other fixed points. The other non-trivial fixed point in $d \lesssim 4/3$ could potentially become important in networks with low enough effective dimension. In typical network models the effective dimension may not be so low, however, so we leave such a possibility for future investigations, and turn our focus now to fixed points in dimensions $d \geq 2$.

C. Absorbing state networks

A commonly used class of nonlinearities in network models are “rectified units,” which vanish when the membrane potential is less than a particular value (here, 0): $\phi(V) = 0$ for $V \leq 0$. Neurons with rectified nonlinearities are guaranteed not to fire when their membrane potentials are negative, and as a result the network boasts an “absorbing state:” once the membrane potentials of *all* neurons drop below this threshold the network will remain silent. It is possible, in the $N \rightarrow \infty$ limit, that mutually excitatory neurons can maintain network activity at a high enough level that the network never falls into the absorbing state and remains active. Non-equilibrium models with absorbing states often fall into the directed percolation universality class [61], with exceptions when there are additional symmetries satisfied by the microscopic action [62].

The primary symmetry of the directed percolation (DP) universality class is the “rapidity symmetry,” a name inherited from high-energy physics. Translated into the spiking network model, rapidity symmetry would correspond to an invariance of the average effective action under the transformation $\tilde{\nu}_i(t) \leftrightarrow -c\psi_i(t)$, where c is a specific constant, chosen so that the terms $\tilde{\nu}_i(t)\psi_i(t)^2$ and $\tilde{\nu}_i(t)^2\psi_i(t)$ transform into each other (including their coefficients). It is straightforward to check that the action of the spiking network does not obey this symmetry; however, most models in the DP universality class do not exhibit rapidity symmetry exactly, and it is instead an

emergent symmetry that satisfied after discarding irrelevant terms in an action tuned to the critical point [63]. We will show that this is true of the RG flow of the absorbing state spiking network.

The spiking network action does not appear to admit any obvious symmetries beyond the the Ward-Takahashi identities. One of the consequences of these identities is the prediction that the dynamic exponent is $z_* = 2$, unmodified from its “mean-field” value. A trivial dynamic exponent is also a feature of the “directed percolation with coupling to a conserved quantity” (DP-C) universality class [61], which is another possible candidate for the universality class of the spiking network. The DP-C class has a symmetry that also predicts a correlation length exponent of $\nu_* = 2/d$, which is not guaranteed by our Ward-Takahashi identities but could be an emergent property if the model is in the DP-C class. (Note that we will give critical exponent symbols $*$ subscripts to distinguish them from the variables z and field ν). To demonstrate that the spiking network model supports a DP-like critical point, we will choose the running scale \tilde{X}_Λ to impose the rapidity symmetry relationship on the lowest order couplings. We assume that $\phi'(0^+) > 0$ and $\phi''(0^+) < 0$, and choose $\tilde{X}_\Lambda = Y_\Lambda |W_\Lambda^{(1,2)}(0,0)|/W_\Lambda^{(2,1)}(0,0)$. This renders $g_{21,s} = -g_{12,s}$ for all s , a hallmark of the Reggeon field theory action that describes the directed percolation universality class [44, 61]. We can then show that $w_*(\tilde{z}, z) = 0$, $\eta_*^X = d/4$ is a trivial fixed point for which the combination of terms $\tilde{z}z^2 - \tilde{z}^2z$ loses stability below the upper critical dimension $d_c = 4$.

Then, the exponent η_s^X can be defined by differentiating Eq. (32) to derive equations for $g_{12,s}$ and $-g_{21,s}$ and equating them. This reveals that

$$\eta_s^X = \frac{d}{4} + \frac{1}{2} \frac{g_{13,s} - g_{31,s}}{1 - g_{11,s}}. \quad (33)$$

In general, rapidity symmetry requires $g_{mn}^* = (-1)^{m+n} g_{nm}^*$ [44]. Under this assumption, $\eta_*^X = d/4$.

To capture the key features of the RG flow, we expand the running potential $w_s(\tilde{z}, z)$ and truncate,

$$\begin{aligned} w_s(\tilde{z}, z) &= g_{11,s} \tilde{z}z + \frac{g_{12,s}}{2!} (\tilde{z}z^2 - \tilde{z}^2z) + \frac{g_{22,s}}{2!2!} \tilde{z}^2z^2 \\ &+ \frac{g_{13,s}}{3!} \tilde{z}z^3 + \frac{g_{31,s}}{3!} \tilde{z}^3z + \frac{g_{23,s}}{2!3!} \tilde{z}^2z^3 + \frac{g_{32,s}}{2!3!} \tilde{z}^3z^2 \\ &+ \frac{g_{33,s}}{3!3!} \tilde{z}^3z^3 + \dots \end{aligned}$$

setting higher order terms to zero. A system of differential equations is obtained by differentiating Eq. (32) with respect to the appropriate powers of \tilde{z} and z and evaluating at $(\tilde{z}, z) = (0, 0)$. In this expansion we have $g_{12,s} = -g_{21,s}$ by construction, but we need not impose the rapidity symmetry on the higher order terms, so that we may check how the lack of this symmetry at the dimensionful level affects the RG flow. Note that because rapidity symmetry imposes a relationship between g_{mn}^* and g_{nm}^* , any truncation we make must include both such

terms. We will denote the “order” of our truncations by $[m, m]$ if the truncation includes all couplings up to an including g_{mm}^* , and (m, m) if the truncation does not include g_{mm}^* .

If we truncate w_s at the first two couplings, g_{11} and $g_{21,s}$ (order $(2, 2)$), the resulting system of equations is simple enough that we obtain analytic expressions for the fixed points and critical exponent ν_* . In principle, truncating at higher orders should improve the results, as well as allow us to check that rapidity symmetry emerges even if the initial condition does not satisfy rapidity symmetry. However, the fixed point equations at higher order truncations also introduce many spurious roots. In order to identify the correct roots, we will perform a perturbative expansion around the upper critical dimension $d = 4$, using the results of the minimal truncation at $g_{21,s}$ to guide the form of this expansion. The perturbative results are in principle exact close to the upper critical dimension, and can be used to seed the first iteration of a numerical root finder for $d \approx 4$, which uses the previously discovered root as d is decreased.

1. Minimal truncation

The fixed point solution for the minimal truncation is

$$\begin{aligned} \eta_*^X &= \frac{d}{4} \\ g_{11}^* &= \frac{4-d}{12-d} \\ g_{21}^* &= \frac{4\sqrt{4-d}}{\sqrt{d^2 - 24d + 144}}, \end{aligned}$$

with $g_{12}^* = -g_{21}^*$. From this solution we see that the fixed point values of the couplings scale as powers of $\sqrt{4-d}$. This suggests this is the appropriate small quantity for a perturbative expansion. i.e., if we set $\epsilon = 4-d$, then our series expansion should be in powers of $\sqrt{\epsilon}$.

By performing a linear stability analysis around the trivial and non-trivial fixed points we can estimate the correlation length exponent ν_* from the largest eigenvalue of the stability matrix, μ : $\nu_* = (2\mu)^{-1}$. (The factor of 1/2 is included so that the value of ν_* matches the numerical values obtained in prior work in translation invariant systems). For the trivial fixed point the eigenvalues are $\mu = (1, (4-d)/4)$, while the non-trivial fixed point has eigenvalues

$$\mu = \left(\frac{1}{16} \left(5d - 12 - \sqrt{41d^2 - 376d + 912} \right), \frac{1}{16} \left(5d - 12 + \sqrt{41d^2 - 376d + 912} \right) \right). \quad (34)$$

When $d > 4$ both eigenvalues of the non-trivial fixed point are positive, while the second eigenvalue of the trivial fixed point is negative, signaling the fact we must

tune one parameter to arrive at this fixed point. Thus, the eigenvalue $\mu = 1$ controls the correlation length exponent in $d > 4$, giving $\nu_* = 1/2$, as expected. In $d < 4$ the trivial fixed point becomes unstable, and the first eigenvalue of Eq. (34) becomes negative, and thus the second eigenvalue determines the critical point. As $d \rightarrow 4^-$ the critical exponent is

$$\nu_* \approx \frac{1}{2} + \frac{4-d}{16} - \frac{7}{128}(4-d)^2 + \dots$$

Although g_{21}^* scales as $\sqrt{4-d}$, the lowest order dependence of ν_* is linear. The expansion of ν_* near $d = 4^-$ matches the one-loop approximation of ν_* for Reggeon field theory, the first suggestion that the spiking network is more like the standard DP class, not the DP-C class, for which $\nu_* = 2/d \approx 1/2 + (4-d)/8 + \dots$ [61].

Although the result for ν_* is reasonable close to $d = 4^-$, a plot of the exact expression on the range $d \in [1, 4]$ reveals a non-monotonic behavior, with ν_* decreasing as d is lowered below ~ 3.2 . This non-monotonic behavior is an artifact of the truncation, as we will show by increasing the truncation order. To facilitate our higher order truncations we first turn to a perturbative expansion.

2. Perturbative fixed point solution in powers of $\sqrt{4-d}$

One can implement the so-called “ ϵ -expansion” in the NRG framework by assuming the fixed point solution $w_*(\tilde{z}, z)$ can be expanded in a series of powers of the distance from the upper critical dimension, $\epsilon \equiv d_c - d$. As our minimal truncation showed, however, we expect some of the couplings to depend on $\sqrt{\epsilon}$, which we will use as our expansion parameter:

$$w_*(\tilde{z}, z) = \epsilon^{1/2} w_1(\tilde{z}, z) + \epsilon w_2(\tilde{z}, z) + \epsilon^{3/2} w_3(\tilde{z}, z) + \epsilon^2 w_4(\tilde{z}, z) + \dots \quad (35)$$

$$\eta_*^X = 1 + \epsilon^{1/2} \delta\eta_1 + \epsilon \delta\eta_2 + \epsilon^{3/2} \delta\eta_3 + \epsilon^2 \delta\eta_4 + \dots \quad (36)$$

Because the trivial fixed point is $w_*(\tilde{z}, z) = 0$, there are no ϵ^0 terms. For this calculation we will not assume $\eta_*^X = d/4 = 1 - \epsilon/4$ at the outset, to allow for the possibility of discovering a solution that does not obey rapidity symmetry, though it turns out there is no such solution perturbatively.

We insert the expansions (35)-(36) into Eq. (32) and expand in powers of $\epsilon^{1/2}$, resulting in a hierarchy of linear equations whose solutions depend on the previous solutions in the hierarchy. A valid critical point solution must exist for all \tilde{z} and z , so we fix constants of integration and the coefficients of η_*^X order by order to eliminate terms that are not polynomially bounded in z . The result to $\mathcal{O}(\epsilon^2)$ is

$$w_*(\tilde{z}, z) = 2a \frac{\tilde{z}^2 z - \tilde{z} z^2}{2!} \epsilon^{1/2} + 2a^2 \tilde{z} z \epsilon - \frac{544a^5}{48a^2 - 1} \frac{\tilde{z}^2 z - \tilde{z} z^2}{2!} \epsilon^{3/2} + \left(\left(\frac{1088a^6}{48a^2 - 1} + 4a^4 \right) \tilde{z} z + 72a^4 \frac{\tilde{z}^2 z^2}{2!2!} - 48a^4 \frac{\tilde{z}^3 z + \tilde{z} z^3}{3!} \right) \epsilon^2 + \mathcal{O}(\epsilon^{5/2}), \quad (37)$$

where $a = 0, \pm 1/4$. The first choice of a corresponds to the trivial solution, while the second corresponds to two equivalent non-trivial solutions; we take the positive value $a = 1/4$ to match the sign of our initial condition. We see that at order ϵ^2 the combination $\tilde{z}^3 z + \tilde{z} z^3$ appears, which obeys the expected rapidity symmetry. Accordingly, the exponent is

$$\eta_*^X = 1 - \frac{\epsilon}{4} + \mathcal{O}(\epsilon^{5/2}),$$

which is just the exact result $\eta_*^X = d/4$.

The dimensionless effective nonlinearity $\varphi_{1*}(z) \equiv w_*^{(1,0)}(0, z)$ is

$$\varphi_{1*}(z) = \left(\frac{\epsilon}{8} + \frac{19}{128} \epsilon^2 \right) z - \left(\frac{\sqrt{\epsilon}}{4} + \frac{17}{128} \epsilon^{3/2} \right) z^2 - \frac{\epsilon^2}{32} z^3.$$

We can estimate the linear stability of the solution by the standard method of perturbing $w_s(\tilde{z}, z) = w_*(\tilde{z}, z) + e^{\mu s} \delta w(\tilde{z}, z)$, and expanding $\mu = \mu_0 + \epsilon^{1/2} \mu_1 + \epsilon \mu_2 + \dots$, choosing μ_0 to correspond to the eigenvalue of the largest allowed eigenvalue to zeroth order, and the remaining terms to non-polynomial divergent terms at large z . In this analysis we will assume rapidity symmetry to hold, such that we may fix $\eta_*^X = d/4$. In our higher-order non-perturbative analysis we will relax this assumption. We find that the largest eigenvalue of this fixed point is

$$\mu(\epsilon) = 1 - \frac{\epsilon}{8} - \frac{10}{256} \epsilon^2 + \mathcal{O}(\epsilon^3),$$

which yields a correlation exponent of

$$\nu_*(\epsilon) = \frac{1}{2} + \frac{\epsilon}{16} + \frac{7}{256} \epsilon^2 + \mathcal{O}(\epsilon^3). \quad (38)$$

To first order this agrees with both our minimal truncation and the epsilon expansion for the Reggeon field theory. The second order correction is numerically close to the 2-loop expansion for the Reggeon field theory, but is not the same. The discrepancy could be an artifact of our sharp regulator or our local potential approximation. Our result suggests that the universality class of this fixed point is more consistent with the regular DP class, rather than the DP-C class. However, it remains that Ward-Takahashi identities predict a dynamic exponent of $z_* = 2$ for all effective dimensions d , in contrast with the perturbative results for the Reggeon field theory. It is not clear whether this indicates that the spiking network is truly in a separate universality class from the DP class, or if there is an assumption in the analysis that erroneously restricts $z_* = 2$. We return to this issue in the Discussion.

3. Non-perturbative truncation up to order $\tilde{z}^5 z^5$

Because the ϵ -expansion is expected to be exact close to $d = 4^-$, we can use the results of our perturbative calculation as initial guesses in a numerical root-finding scheme in a higher order non-perturbative truncation. Once the roots are found numerically, we can decrease the value of d and use the previously obtained numerical root as the initial guess for the root finder. We proceed iteratively in this way, allowing us to continuously track the non-trivial fixed point as we decrease d from 4, avoiding the erroneous roots introduced by our truncation.

We have performed our truncation at orders $\tilde{z}^3 z^3$, $\tilde{z}^4 z^4$, and $\tilde{z}^5 z^5$, beyond which the calculations become computationally expensive. We indeed still find a non-trivial fixed point with rapidity symmetry, for which we estimate the critical exponent ν_* by analyzing the eigenvalues of the flow. We insert the expression Eq. (33) for η_s^X into the flow equations before linearizing, such that we can verify that the fixed point with rapidity symmetry is not unstable to some other fixed point lacking that symmetry, at least for some finite range of $d < 4$. We indeed find that the DP fixed point has a single relevant direction for $2.78 \lesssim d < 4$. As $d \rightarrow 2.78^+$ the estimates for ν_* diverge for our $\tilde{z}^3 z^3$ and $\tilde{z}^4 z^4$ truncations, and cannot be continued for lower d for our $\tilde{z}^5 z^5$ truncation, as shown in Fig. 9. Interestingly, the estimate of ν_* in the $(5, 5)$ truncation appears to be quite close to the ϵ -expansion up to the dimension where the solution ends. The restriction of this range indeed appears to be due to the development of an additional positive eigenvalue for $d \lesssim 2.78$, indicating the DP-like fixed point becomes unstable to some other fixed point in this regime. We leave investigation of what this other fixed point might be for future studies.

The non-perturbative truncation allows another check that the rapidity symmetric fixed point is approached even when the initial conditions do not obey the rapidity symmetry. To demonstrate this, we use the $\tilde{z}^3 z^3$ truncation. As shown in Fig. 10, even though $g_{13,0} \neq g_{31,0}$ and

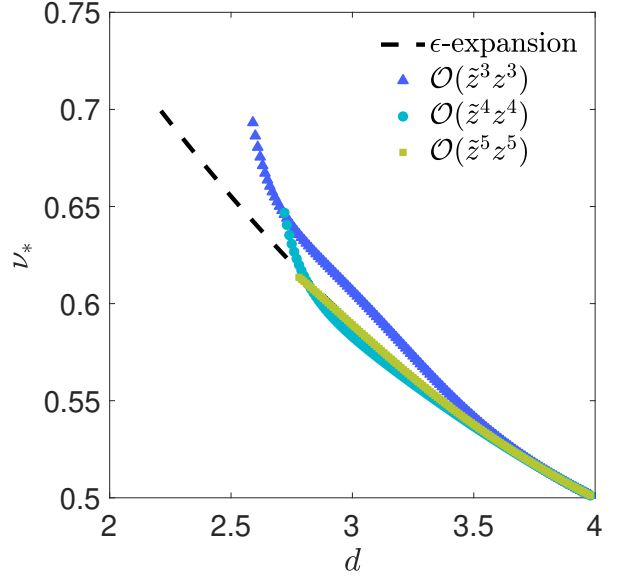


FIG. 9. **Correlation length exponent for the absorbing state network** as a function of the effective dimension d . Obtained using the third (dark blue triangles), fourth (light blue circles), and fifth order (green squares) truncations. The estimates are compared to Eq. (38), the perturbative ϵ -expansion estimate (black dashed line). The non-perturbative analysis suggests the fixed point becomes unstable toward another fixed point in $d \lesssim 2.78$.

$g_{23,0} \neq g_{32,0}$, the curves rapidly merge, and the rapidity symmetry is satisfied as the models flows toward the fixed point. We also see that $g_{22,s}$ flows to a positive value, despite starting at a negative value. The initial signs of the couplings are chosen in accordance with the signs of the coefficients in the initial condition of the full $w_0(\tilde{z}, z)$. This suggests it is possible that the spiking network, despite not possessing rapidity symmetry at the level of the microscopic action, can indeed flow to a fixed point with emergent rapidity symmetry.

D. Spontaneous networks

We now consider the case of spontaneously active networks, for which $\phi(0) \neq 0$. The probability of firing a spike is never 0 at any finite V , so there is no absorbing state in this network. Instead, we anticipate that the network may be able to achieve a steady-state, though potentially one far from equilibrium.

The fact that there is a membrane potential-independent component of the fluctuations in the spontaneous networks suggests we should choose the running scale $\tilde{X}_\Lambda = \sqrt{\Omega_\Lambda/W_\Lambda^{(2,0)}(0,0)}$. This choice renders $g_{20,s} = w_s^{(2,0)}(0,0) = 1$ for all s , which is in essence like choosing the Gaussian part of the action to be invariant under the RG procedure. This restriction puts a constraint on the exponent η_s^X in terms of the couplings

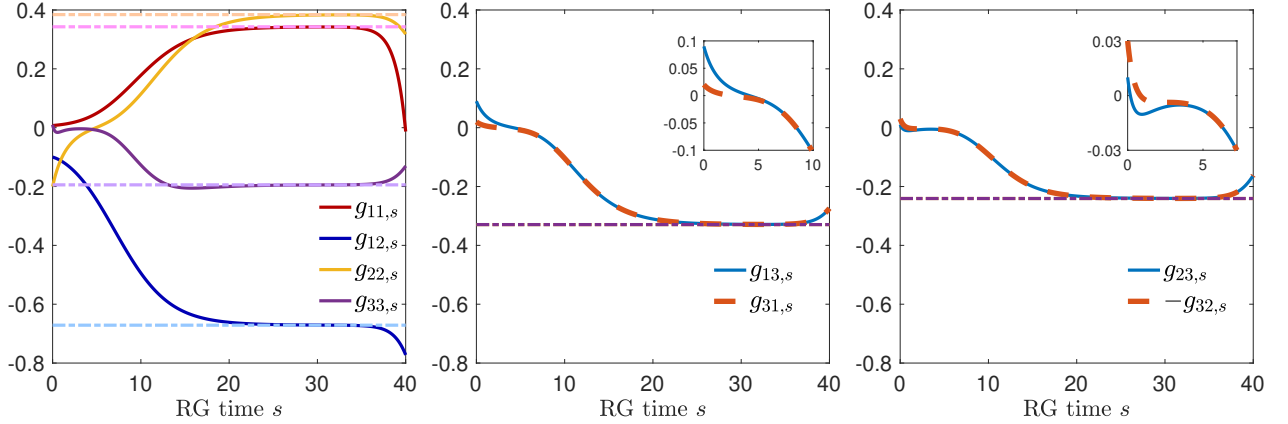


FIG. 10. **Flow of the couplings** $g_{mn,s}$ for the absorbing state network in $d = 3$, truncated at order $\tilde{z}^3 z^3$. **A)** Flow of $g_{11,s}$, with initial condition tuned such that the system is transiently close to the fixed point between $20 \lesssim s \lesssim 35$, shown with the flows of $g_{12,s} = -g_{21,s}$ (relationship fixed by construction), $g_{22,s}$ and $g_{33,s}$. **B)** Flow of $g_{13,s}$ and $g_{31,s}$, and **C)** $g_{23,s}$ and $-g_{32,s}$ with insets zoomed in on the initial transient regime for which the couplings do not respect rapidity symmetry, which emerges near the fixed point as the curves merge together. Dot-dashed lines indicate fixed point values predicted by solving the steady-state equations.

$g_{mn,s}$:

$$\begin{aligned} \eta_s^X &= \frac{d+2}{4} + \frac{1}{4} \frac{g_{22,s} + 2g_{12,s}g_{30,s}}{1 - g_{11,s}} \\ &+ \frac{1}{2} \frac{g_{12,s}g_{21,s}}{(1 - g_{11,s})^2} + \frac{1}{8} \frac{g_{12,s}^2}{(1 - g_{11,s})^3} \end{aligned} \quad (39)$$

The reader can check that $w_*(\tilde{z}, z) = \tilde{z}^2/2$, $\eta_*^X = \frac{d+2}{4}$ is a trivial fixed point solution. A linear stability analysis of this fixed point shows that the couplings $g_{10,s}$ and $g_{11,s}$ are unstable (Appendix I). The divergent flow of $g_{10,s}$ does not contribute to any other coupling, only to the renormalized value of $\Phi_1(0)$, which is compensated by tuning the rest potentials \mathcal{E}_i . The flow of $g_{11,s}$ is the key relevant term; its initial value $g_{11,0}$ must be tuned so that the RG flow takes the model to the critical point.

A linear stability analysis of the trivial fixed point predicts that as the effective dimension d is lowered the couplings $g_{1n,s}$ become relevant sequentially, with g_{12} becoming relevant at $d = 6$, then g_{13} at $d = 4$, and so on until all couplings are relevant in $d = 2$. This is the standard sequence predicted for scalar field theories, like ϕ^4 theory with symmetry breaking terms. The coefficients $g_{mn,s}$ ($n \geq 1$) are all irrelevant above $d = 2$ for any $m \geq 2$ (Appendix I).

In our exemplar case in the mean-field analysis explored in Sec. I B, we chose a bare nonlinearity $\phi(V) = (1 + \exp(-V))^{-1}$, which has $\phi''(0) = 0$. Naively, then, it appears that $g_{12,0} = 0$, and we might expect to find a Wilson-Fisher fixed point in $d < 4$ related to the Ising universality class. While we will show our dimensionless flow equations do admit such a fixed point solution, the \mathbb{Z}_2 symmetry of this fixed point is *not* a symmetry of the initial action for this model. Such a symmetry would manifest as an invariance to the transformation

$w_s(\tilde{z}, z) = w_s(-\tilde{z}, -z)$, which the initial condition—a scaled version of $(e^{\tilde{x}} - 1)\phi(V) - \phi(0)\tilde{x}$ —does not satisfy. Thus, even though $g_{12,s} = 0$ initially, we expect this term to be generated by the RG flow, and the mean-field prediction for this case will be *qualitatively* invalidated.

1. Minimal truncation

We validate our above claims by making a minimal truncation of $w_s(\tilde{z}, z) = \tilde{z}^2/2 + \tilde{z}(g_{11,s}z + g_{12,s}z^2/2 + g_{13,s}z^3/3!)$. As expected, we find three valid fixed points: a trivial fixed point, a fixed point with a \mathbb{Z}_2 symmetry, and a third fixed point for which $g_{12}^* \neq 0$. The \mathbb{Z}_2 -symmetric fixed point has values

$$g_{11}^* = \frac{4-d}{10-d} \quad (40)$$

$$g_{13}^* = -12 \frac{4-d}{(10-d)^2} \quad (41)$$

$$\eta_*^X = \frac{d+2}{4}, \quad (42)$$

with $g_{12}^* = 0$. Because of the trivial \tilde{z} dependence and the \mathbb{Z}_2 symmetry, the exponent η_*^X takes on its trivial value, indicating that the anomalous exponent is zero within this truncation.

The third fixed point is rather unwieldy in its exact form, so we instead give its behavior near the dimension

$d = 6$, where it coincides with the trivial solution:

$$g_{11}^* = \frac{6-d}{9} + \frac{(6-d)^2}{81} + \dots \quad (43)$$

$$g_{12}^* = \pm i \frac{\sqrt{2}}{3} \sqrt{6-d} \mp i \frac{5}{27\sqrt{2}} (6-d)^{3/2} + \dots \quad (44)$$

$$g_{13}^* = \frac{4}{27} (6-d)^2 + \dots \quad (45)$$

$$\eta_*^X = 2 - \frac{5}{18} (6-d) - \frac{2}{81} (6-d)^2 + \dots \quad (46)$$

The most striking feature of this fixed point solution is that the coupling g_{12}^* is *imaginary*. This is not an artifact of the truncation, but a signature of a spinodal point in the model, as observed in the critical ϕ^3 theory. Indeed, [64, 65] argue that imaginary fixed points correspond to spinodal points associated with *first order* transitions, yet still possess several features of continuous transitions, such as universal critical exponents. i.e., the imaginary couplings have real physical consequences. Importantly, the anomalous exponents and correlation length exponent ν_* are purely real.

We estimate the exponents for all fixed points via a linear stability analysis. The trivial critical point has eigenvalues $\mu = (1, (6-d)/4, (4-d)/2)$ with corresponding eigenvectors $(\delta g_{11}, \delta g_{12}, \delta g_{13}) = (1, 0, 0), (0, 1, 0)$, and $((2-d)^{-1}, 0, 1)$. The first eigenvectors shows that g_{11} is relevant in all dimensions, while the second and third confirm that g_{12} and g_{13} become relevant in $d = 6$ and $d = 4$, respectively.

The \mathbb{Z}_2 -symmetric Wilson-Fisher-like fixed point has eigenvalues

$$\mu = \left(\frac{1}{6} \left(\sqrt{7d^2 - 62d + 145} + 2d - 5 \right), \frac{d-2}{4}, \right. \\ \left. \frac{1}{6} \left(-\sqrt{7d^2 - 62d + 145} + 2d - 5 \right) \right),$$

ordered in terms of size. For $d > 4$ all three eigenvalues are positive, while the third eigenvalue is negative in $d < 4$. The first and third eigenvalues have associated eigenvectors with components only in the g_{11} and g_{13} directions, indicating the relevance of g_{11} in all d . The second eigenvalue's eigenvector is $(0, 1, 0)$, indicating that g_{12} is a relevant perturbation at this WF-like fixed point.

The spinodal fixed point's eigenvalues cannot be solved in closed form, but numerical evaluation confirms it has two unstable directions in $d > 6$ and one unstable direction for $d < 6$, indicating that it is the controlling critical point for the spiking network model, even for small dimensions $d < 4$.

We will verify that higher order truncations give a consistent qualitative picture that agrees with the above analysis. To assist in this endeavor, we first derive the fixed point solution using an ϵ -expansion. Following our minimal truncation, we will expand in powers of $\sqrt{\epsilon}$, with $\epsilon = 6 - d$.

2. Perturbative fixed point solution in powers of $\sqrt{6-d}$

The ϵ -expansion proceeds similarly to the absorbing state network, though it ends up being slightly more complicated. We expand

$$w_*(\tilde{z}, z) = \frac{\tilde{z}^2}{2} + \epsilon^{1/2} w_1(\tilde{z}, z) + \epsilon w_2(\tilde{z}, z) \\ + \epsilon^{3/2} w_3(\tilde{z}, z) + \epsilon^2 w_4(\tilde{z}, z) + \dots \\ \eta_*^X = 2 + \epsilon^{1/2} \delta\eta_1 + \epsilon \delta\eta_2 + \epsilon^{3/2} \delta\eta_3 + \epsilon^2 \delta\eta_4 + \dots$$

and insert this expansion into Eq. (32), deriving a hierarchy of linear equations. Demanding that the solutions are polynomially bounded as z grows large yields the trivial solution as well as two equivalent non-trivial *complex* fixed points:

$$w_*(\tilde{z}, z) = \frac{\tilde{z}^2}{2} + \frac{i}{12\sqrt{2}} \tilde{z} (4z^2 - 2) \epsilon^{1/2} + \frac{\tilde{z}z}{9} \epsilon \\ - \frac{i}{216\sqrt{2}} \tilde{z} \left(\tilde{z}^2 + 12\tilde{z}z + 16z^2 + 4(2z^2 - 1) \left(-2 + \psi^{(0)}\left(-\frac{1}{2}\right) - \psi^{(0)}\left(\frac{1}{2}\right) \right) \right) \epsilon^{3/2} \\ + \left[\frac{1}{162} \tilde{z} \left(z^2 - \frac{1}{2} \right) (z(4z^2 + 19) - (8z^4 + 26z^2 + 19) F(z)) \right. \\ \left. + \frac{1}{324} \tilde{z} ((2z^2 - 1) F(z) - z) \left(8z^4 + 2z^2 \left(5 + 4\psi^{(0)}\left(-\frac{1}{2}\right) - 4\psi^{(0)}\left(\frac{1}{2}\right) \right) + 11 - 4\psi^{(0)}\left(\frac{1}{2}\right) + 4\psi^{(0)}\left(-\frac{1}{2}\right) \right) \right. \\ \left. + \frac{\tilde{z}^2 z^2}{54} + \frac{5\tilde{z}^3 z}{972} + \frac{5\tilde{z}^4}{10368} \right] \epsilon^2, \quad (47)$$

with effective nonlinearity $\varphi_{1*}(z) \equiv w_*^{(1,0)}(0, z)$

$$\begin{aligned} \text{Re}[\varphi_{1*}(z)] &= \frac{z}{9}\epsilon + \left[\frac{1}{324} (2z^2 - 1) (z(4z^2 + 19) - (8z^4 + 26z^2 + 19) F(z)) \right. \\ &\quad \left. + \frac{1}{324} ((2z^2 - 1) F(z) - z) \left(8z^4 + 2z^2 \left(5 + 4\psi^{(0)}\left(-\frac{1}{2}\right) - 4\psi^{(0)}\left(\frac{1}{2}\right) \right) \right. \right. \\ &\quad \left. \left. + 11 - 4\psi^{(0)}\left(\frac{1}{2}\right) + 4\psi^{(0)}\left(-\frac{1}{2}\right) \right) \right] \epsilon^2 \end{aligned} \quad (48)$$

$$+ 11 - 4\psi^{(0)}\left(\frac{1}{2}\right) + 4\psi^{(0)}\left(-\frac{1}{2}\right) \Bigg] \epsilon^2 \quad (49)$$

$$\text{Im}[\varphi_{1*}(z)] = \frac{2z^2 - 1}{6\sqrt{2}}\epsilon^{1/2} + \frac{(16z^2 + 4(2z^2 - 1)(-2 + \psi^{(0)}(-\frac{1}{2}) - \psi^{(0)}(\frac{1}{2})))}{216\sqrt{2}}\epsilon^{3/2} \quad (50)$$

where $\psi^{(0)}(\cdot)$ is the Poly-Gamma function ($\psi^{(0)}(-1/2) \approx 0.03649$, $\psi^{(0)}(1/2) \approx -1.96351$) and $F(z) = \frac{\sqrt{\pi}}{2}e^{-z^2/2}\text{erfi}(z)$ is the Dawson F function with $\text{erfi}(z) = \frac{2}{\sqrt{\pi}} \int_0^z dt e^{+t^2}$ the “imaginary error function.” The second non-trivial solution is the complex conjugate. As in the minimal truncation, the exponents turn out to be purely real:

$$\eta_*^X = 2 - \frac{5}{18}\epsilon + \frac{29}{648}\epsilon^2 + \mathcal{O}(\epsilon^{5/2}),$$

with anomalous exponent

$$\delta\eta_*^X \equiv \eta_*^X - \frac{d+2}{4} = -\frac{1}{36}\epsilon + \frac{29}{648}\epsilon^2 + \mathcal{O}(\epsilon^{5/2}).$$

We may attempt a linear stability analysis to estimate the critical exponent ν_* , but the standard approach of perturbing $w_s(\tilde{z}, z) = w_*(\tilde{z}, z) + e^{\mu s}\delta w(\tilde{z}, z)$ is complicated by the fact that η_s^X flows near this fixed point and should be perturbed as well. Nonetheless, we calculate a rough estimate by fixing η_s^X to its fixed point value, which we will find agrees with our other estimates to at least $\mathcal{O}(\epsilon^{3/2})$. We find that the largest positive eigenvalue is

$$\mu(\epsilon) = 1 - \frac{2}{9}\epsilon + \mathcal{O}(\epsilon^2);$$

to obtain the ϵ^2 term we would need to go to order $\epsilon^{5/2}$ in our expansion of w_* and η_*^X . The correlation exponent ν_* is therefore:

$$\nu_* = \frac{1}{2} + \frac{\epsilon}{9} + \mathcal{O}(\epsilon^2). \quad (51)$$

Interestingly, only the non-analytic powers of ϵ give rise to imaginary terms, suggesting that the fixed point is purely real in $d > 6$. It also turns out the real component of $\varphi_{1*}(z)$ is odd in z , while the imaginary components are even in z .

The fact that the critical point is complex implies the following behavior as one translates from the dimensionless flow to the dimensioned flow: when starting

from real-valued initial conditions, the dimensionless flow equation will eventually blow up at a finite scale of the RG flow, but this divergence can be analytically continued into the complex plane, such that the flow is able to arrive at the critical point (for a fine-tuned initial condition). If the initial condition is complex to begin with, we expect this divergence does not occur, as was shown for a toy example of a complex fixed point in [64].

3. Higher order truncations

With the ϵ -expansion we can now return to the non-perturbative truncations of the flow equations, using the perturbative results as seeds for the initial guess of a root finding algorithm near $d = 6^-$. Unlike the absorbing state network, we do not have to truncate symmetrically in \tilde{z} and z . The simplest truncation consists of setting $\varphi_{2*}(z) = 1$ and $\varphi_{m*}(z) = 0$ for $m \geq 3$, and truncating $\varphi_{1*}(z)$ at a finite power z^n . We have performed this truncation up to $n = 10$, though the numerical solution becomes increasingly difficult at this order.

The estimates of ν_* shown in Fig. 11A change quantitatively as we increase n , but qualitatively still display the non-monotonic behavior observed in the minimal truncation. We have attempted higher order truncations of the general form (m, n) for $m = 2$ and $n \leq 6$ the estimates, in Fig. 11B. These estimates appear to show some convergence for $5 \lesssim d < 6$, but for $d < 5$ the estimates do not agree and numerical solution of the roots becomes increasingly difficult and unreliable. In particular, the eigenvalues of the linear stability analysis abruptly develop non-negligible imaginary components, jumping from $\mathcal{O}(10^{-17} \sim 10^{-15})$ to $\mathcal{O}(10^{-4} \sim 1)$, which is most likely an artifact of the truncation or numerical evaluation, and not a real emergence of complex eigenvalues in the RG flow.

The inconsistent and non-monotonic estimates of ν_* below $d \approx 5$ could be a consequence of the local potential approximation. [66] used NPRG methods to study the spinodal point in the Yang-Lee model (ϕ^3 theory with imaginary coupling), using the derivative expansion to go

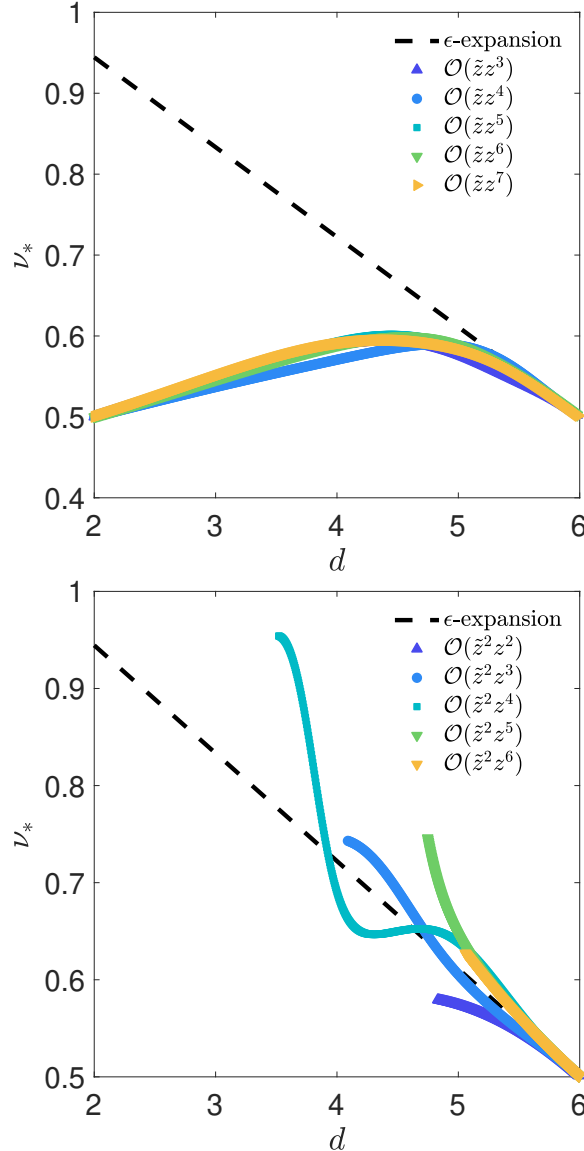


FIG. 11. Correlation length estimates for the spinodal fixed point as a function of the effective dimension d . Top panel: Estimates obtained using truncations at linear order in \tilde{z} and up to order z^7 . Bottom panel: Estimates obtained using a truncation up to \tilde{z}^2 and z^6 . The estimates are compared to Eq. (51), the perturbative ϵ -expansion estimate (black dashed line). The non-perturbative analysis suggests the results may be reliable for $d \gtrsim 5$, but may require a more refined approximation than the local potential approximation in lower dimensions.

beyond the local potential approximation. They found that truncations at the local potential level failed to yield fixed points below $d \approx 5.6$. While the structure of the spiking network model differs in several important ways (notably, the lack of field renormalizations), it could be that to fully capture the behavior of the critical exponents as a function of dimension we need to generalize the derivative expansion to the present case. There are technical obstacles to doing so [67], so we leave this as a direction for future work.

4. Wilson-Fisher-like fixed point

Although we expect the spinodal fixed point to control critical phenomena in the spontaneous network, it is useful to investigate the \mathbb{Z}_2 -invariant Wilson-Fisher-like (WF-like) fixed point and compare the results to previous NRG investigations of the Ising model.

Performing a perturbative expansion in $\epsilon = 4 - d$ yields an approximate solution for $w_*(\tilde{z}, z)$ to $\mathcal{O}(\epsilon^2)$:

$$w_*(\tilde{z}, z) = \frac{\tilde{z}^2}{2} + \frac{1}{36}\tilde{z}(6z - 2z^3)\epsilon + \left(\frac{\tilde{z}z^3}{108} + \frac{\tilde{z}^2z^2}{72}\right)\epsilon^2 + \mathcal{O}(\epsilon^3) \quad (52)$$

with $\eta_*^X = 3/2 - \epsilon/4 + \epsilon^2/72$. The anomalous exponent is $\epsilon^2/72$, second order as expected for the Wilson-Fisher critical point in the Ising model.

We use the perturbative results to seed the root finder for the truncations used for the spinodal fixed point. We find similar results: the estimates of ν_* appear to converge near the upper critical dimension, but become non-monotonic and truncations at higher orders in \tilde{z} develop erroneous imaginary components as the dimension is lowered. The truncations at higher powers of z appear to indicate that ν_* exceeds the predictions of the first order ϵ -expansion. Unlike the DP fixed point, there is no indication of the emergence of another fixed point near the values where the estimates become unreliable, possibly indicating limitations of the local potential approximation rather than a transition to a new critical point.

For the WF-like fixed point we have also succeeded in performing a $(2, \infty)$ truncation, setting $w_*(\tilde{z}, z) = \tilde{z}\varphi_{1s}(z) + \tilde{z}^2\varphi_{2s}(z)/2$ and numerically solving the flow equations. By fine-tuning $g_{11,0}$ the solution can transiently flow to the fixed point solution, before being repelled away. The flow equations for this restricted truncation reduce to

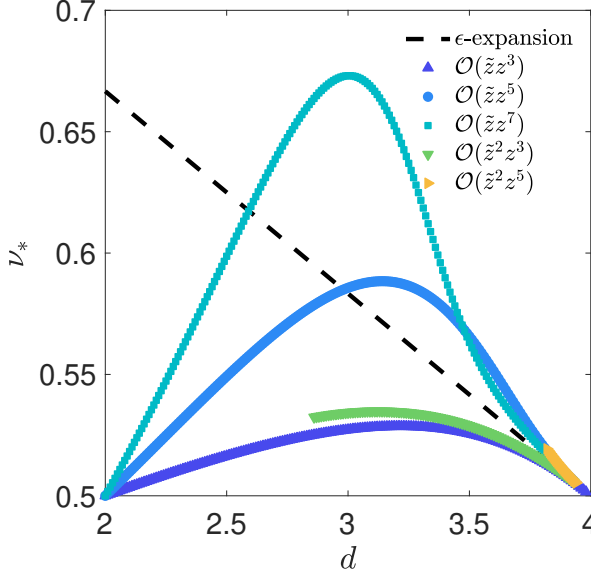


FIG. 12. **Correlation length exponent (ν^*) estimates for the Wilson-Fisher-like fixed point** as a function of the effective dimension d , obtained using several truncations up to quadratic order in \tilde{z} and seventh order in z .

$$\partial_s \varphi_{1s}(z) - \left(\frac{d}{2} + 1 - \eta_s^X \right) \varphi_{1s}(z) + \left(\frac{d}{2} - \eta_s^X \right) z \varphi'_{1s}(z) = \frac{1}{2} \frac{\varphi''_{1s}(z) \varphi_{2s}(z)}{1 - \varphi'_{1s}(z)} \quad (53)$$

$$\begin{aligned} \partial_s \varphi_{2s}(z) - \left(\frac{d}{2} + 1 - 2\eta_s^X \right) \varphi_{2s}(z) + \left(\frac{d}{2} - \eta_s^X \right) z \varphi'_{2s}(z) \\ = \frac{1}{2} \frac{\varphi_{2s}(z) \varphi''_{2s}(z) + 2\varphi''_{1s}(z) \varphi_{3s}(z)}{1 - \varphi'_{1s}(z)} + \frac{\varphi_{2s}(z) \varphi'_{2s}(z) \varphi''_{1s}(z)}{(1 - \varphi'_{1s}(z))^2} + \frac{1}{4} \frac{\varphi_{2s}(z)^2 \varphi''_{1s}(z)^2}{(1 - \varphi'_{1s}(z))^3} \end{aligned} \quad (54)$$

(c.f. Eqs. (28)-(29)), with η_s^X given by Eq. (39). For completeness, we have included the next order term in the expansion, $\varphi_{3s}(z)$, but will impose it to be zero in the numerical solution. If we were to instead assume a truncation at an earlier order, imposing which $\varphi_{2s}(z) = 1$ for all s , then the flow equation for $-\varphi_{1*}(z)$ turns out map exactly onto the flow equation for the derivative of the effective potential of the ϕ^4 theory using an ultra-sharp regulator in the LPA approximation [48, 68]. This flow equation has been extensively studied, and we have used these results to help find the numerical solutions when keeping the next order nonlinearity $\varphi_{2*}(z)$. This allows us to estimate contributions to the anomalous exponent $\delta\eta_*^X = \eta_*^X - (d+2)/4$, but unfortunately estimating the correlation exponent ν_* and crossover exponent from this method are more numerically sensitive, and we do not pursue those estimates here. We plot the numerical solution of the fixed point function in $d = 3, 3.2, 3.5$ and 4 in Fig. 13). Below this dimension the numerical solution becomes increasingly unstable, and we were unable to find an initial value of $g_{11,0}$ that drove the flow close

to a fixed point. This numerical instability is potentially related to the emergence of additional fixed points that split off from the trivial fixed point as d moves below 3. We give the technical details of the solution in Appendix K.

E. Singular contributions to the firing rate nonlinearity at criticality

We end our current investigation of universality in the spiking network model by discussing the non-analytic contributions to the effective firing rate nonlinearity $\Phi_1(\psi)$. The critical effective firing rate nonlinearity is related to its dimensionless counterpart via

$$\begin{aligned} \Phi_1(\psi) = \Lambda_{\max}^{-1} \psi + \lim_{s \rightarrow \infty} e^{-s(d/2+1-\eta_s^X)} \varphi_{1*} \left(\psi e^{s(d/2-\eta_s^X)} \right) \\ + \text{analytic terms.} \end{aligned} \quad (55)$$

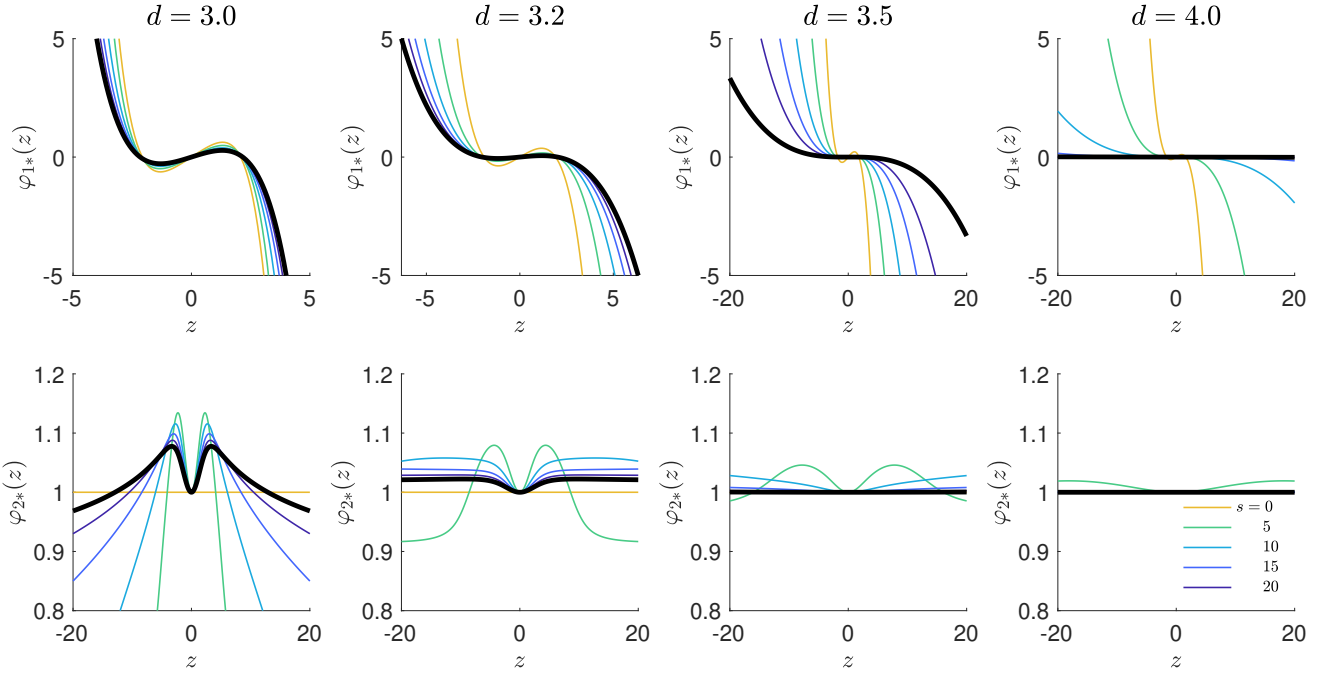


FIG. 13. **Fixed point functions of the spontaneous network Wisher-Fisher point in effective dimensions $3 \leq d \leq 4$.** We solve Eqs. (53) and (54) by fine-tuning the initial value of $g_{11,0}$ by dichotomy, until the solution displays a transient behavior close to the Wilson-Fisher fixed point. Thin curves show the progression of the solution as a function of RG-time s , converging approximately to the fixed point solution (thick black curve). Note the difference in the horizontal axis scale for $\varphi_{1*}(z)$ in dimensions $d = 3.0, 3.2$ compared to the other plots. Note this fixed point is unstable toward the spinodal fixed point.

The analytic terms arise from deviations of $\varphi_{1s}(z)$ away from the critical point, such as irrelevant couplings that are non-zero in the bare nonlinearity $\phi(V)$. The critical point $\varphi_*(z)$ gives rise to the singular non-analytic behavior that emerges at the critical point, which is in principle observable when the network is tuned to the critical point, though the analytic terms can make it difficult to measure the singular behavior, even if the system is close to a critical point. Because the effective firing rate nonlinearity $\Phi_1(\psi)$ must be real and finite, $\varphi_*(z)$ must behave as a power-law for large z , such that the dependence on s in Eq. (55) cancels out [32]. This yields

$$\begin{aligned} \text{Re}[\Phi_1(\psi)] &= \lim_{s \rightarrow \infty} e^{-s(d/2+1-\eta_*^X)} \text{Re}[\varphi_{1*}(\psi e^{s(d/2-\eta_*^X)})] \\ &\sim \mathcal{A}_d \psi^{\frac{d/2+1-\eta_*^X}{d/2-\eta_*^X}}, \\ \text{Im}[\Phi_1(y)] &= \lim_{s \rightarrow \infty} e^{-s(d/2+1-\eta_*^X)} \text{Im}[\varphi_{1*}(\psi e^{s(d/2-\eta_*^X)})] \\ &\rightarrow 0, \end{aligned}$$

where \mathcal{A}_d is a d -dependent constant and $\text{Im}[\varphi_{1*}(z)]$ must grow more slowly than $z^{\frac{d/2+1-\eta_*^X}{d/2-\eta_*^X}}$ as $z \rightarrow \infty$.

Because our analyses of the flow equations are based on truncating the dimensionless function $w_*(\tilde{z}, z)$ in small powers of \tilde{z} or ϵ , we cannot predict the coefficient \mathcal{A}_d . However, because we have estimates of η_*^X for our various

cases, we can estimate the exponent

$$\beta^{-1} = \frac{1}{d/2 - \eta_*^X},$$

where we previously defined β^{-1} by the leading order nonlinear scaling of $\Phi_1(\psi) \sim \psi^{1+\beta^{-1}}$. In the absorbing state universality class we found $\eta_*^X = d/4$ for $d < 4$, which yields an exponent of

$$\beta_{\text{AS}} = \frac{d}{4}.$$

Because of the emergent rapidity symmetry, this is exact within our local potential approximation, at least for $2.78 \lesssim d \leq 4$ where our analysis predicts this critical point exists.

We have checked that simulations of the absorbing state network on excitatory lattices agree with the prediction $\eta_*^X = d/4$ for dimensions $d = 2$ and 3 , shown in Fig. 14. The agreement in $d = 2$ suggests that the relevant fixed point in this dimension may still exhibit an emergent rapidity symmetry, or the loss of stability of the DP-like fixed point below $d \lesssim 2.78$ is an artifact of the truncation or local potential approximation. In $d = 4$ we do not find power-law scaling consistent with $d/4$, but this is likely due to logarithmic corrections known to occur at the upper critical dimension [51], which we do not attempt to estimate.

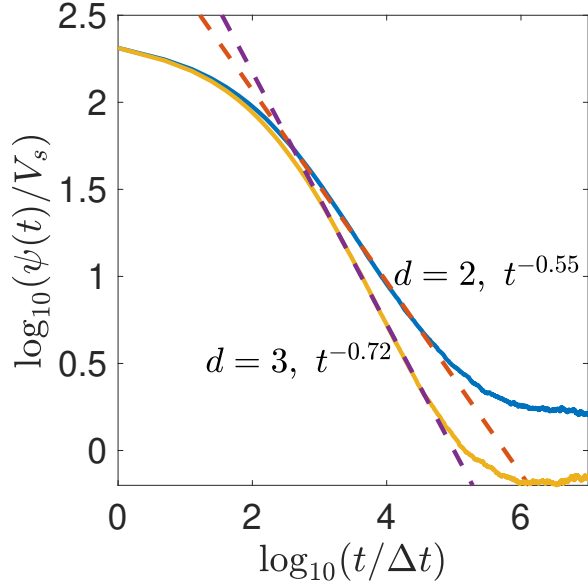


FIG. 14. **Decay of mean membrane-potential near criticality in $d = 2$ and 3-dimensional lattices** for excitatory absorbing state networks with $N = 1000$. All neuron membrane potentials start at $V_i(0)/V_s = 0.2$, where V_s is a scale factor with units of the membrane potential. Network dynamics are simulated for 1500 time-steps of size $\Delta t = 0.1$ and averaged over 100 trials. Plots show the population average of these trial averages to eliminate stochastic variability. There is a region of the decay of both curves that is consistent with a power-law $t^{-\beta}$ with exponents that agree with the predicted value $\beta = d/4$.

On networks with random synaptic connections this behavior may be modified or obscured by the randomness of the connections [69], so although we expect this critical point to shape the effective nonlinearity of the network, it is more difficult to predict the dynamics of the random networks compared to lattices, and we do not pursue these estimates in this work.

With this exponent we may use our estimates of ν_* and z_* to calculate the exponents measured in neural avalanches in slice tissue. In slices neurons are not very spontaneously active, and the absorbing state network may be an appropriate model for this situation. A neural avalanche is triggered when a single neuron fires due to external stimulation (either injected by the experimenter or due to environmental noise), and triggers a cascade of subsequent firing events. Key statistical measurements are the distribution of avalanche sizes, S , which is predicted to scale as $S^{-\tau_*}$ for large S , the distribution of durations T , which is predicted to scale as $T^{-\alpha_*}$, and the average avalanche size conditioned on the duration, which is predicted to scale as $T^{1/(\sigma_*\nu_*z_*)}$ [15]. These relations introduce the new critical exponents τ_* , α_* , and σ_* , in addition to the exponents $z_* = 2$, $\beta_{\text{AS}} = d/4$, and ν_* . These critical exponents are not independent, and

are related through the scaling relations [14]

$$\tau_* = 1 + \frac{\beta_{\text{AS}}}{(d + z_*)\nu_* - \beta_{\text{AS}}}, \quad (56)$$

$$\sigma_* = \frac{1}{(d + z_*)\nu_* - \beta_{\text{AS}}}, \quad (57)$$

$$\frac{\alpha_* - 1}{\tau_* - 1} = \frac{1}{\sigma_*\nu_*z_*}. \quad (58)$$

Given that ν_* appears to be predicted quite well by the ϵ -expansion for $2.78 \lesssim d \leq 4$, we obtain the estimates

$$\tau_* \approx \frac{3}{2} - \frac{5}{32}(4 - d) - \frac{1}{64}(4 - d)^2 + \dots \quad (59)$$

$$\sigma_* \approx \frac{1}{2} - \frac{1}{32}(4 - d) - \frac{3}{128}(4 - d)^2 + \dots \quad (60)$$

$$\alpha_* \approx 2 - \frac{3}{8}(4 - d) - \frac{1}{128}(4 - d)^2 + \dots \quad (61)$$

$$\frac{1}{\sigma_*\nu_*z_*} \approx 2 - \frac{4 - d}{8} + \frac{(4 - d)^2}{128} + \dots \quad (62)$$

In the range $2.78 \lesssim d \leq 4$ these estimates do not agree well with the experimental estimates obtained by [15]. A value of $d \approx 3.2 \sim 3.4$ yields predictions consistent with the ends of the ranges of the reported error bars ($\tau_* = 1.6 \pm 0.2$, $\alpha_* = 1.7 \pm 0.2$), but the estimate of $1/(\sigma_*\nu_*z_*) = 1.3 \pm 0.05$ is not consistent with any dimension in this range. This lack of consistency could be due to several factors, including the aforementioned fact that we expect randomness of synaptic connections to alter or obscure the critical exponents. Other important factors include the fact that actual slice networks are unlikely to have symmetric synaptic connections ($J_{ij} \neq J_{ji}$), which could give relevant perturbations to the fixed points, or the effective dimension could lie closer to $d = 2$, for which a different critical point is expected to control the universal properties of the absorbing state network.

In the spontaneous network at the spinodal critical point our perturbative expansion of the non-perturbative local potential $w_*(\tilde{z}, z)$ predicts

$$\beta_{\text{sp}} \simeq 1 - \frac{2}{9}(6 - d) - \frac{29}{649}(6 - d)^2 + \mathcal{O}((6 - d)^3).$$

For the Wilson-Fisher-like fixed point we find

$$\beta_{\text{WF}} \simeq \frac{1}{2} - \frac{1}{4}(4 - d) - \frac{1}{72}(4 - d)^2 + \mathcal{O}((4 - d)^3).$$

If we naively set $d = 3$ we obtain an estimate of 0.2361, which is close to the estimate of 0.2416 obtained by numerical solution of our $(2, \infty)$ truncation (Eqs. (53)-(54)). However, the series expansion differs from the ϵ -expansion obtained for the Wilson-Fisher fixed point by perturbative analysis of the ϕ^4 scalar field theory, $\beta_{\text{WF}} = 1/2 - (4 - d)/6 + \mathcal{O}((4 - d)^2)$. The current best estimate of β in the $d = 3$ Ising model is 0.325 [45].

This could be another sign that this fixed point is not really a Wilson-Fisher fixed point, along with the fact

that the dynamic exponent is fixed to $z_* = 2$ by our Ward-Takahashi identities. In the standard NPRG local potential approximation of the ϕ^4 theory or Ising model, which is equivalent to assuming $\varphi_{2s}(z) = 1$ here, the anomalous exponent $\delta\eta_*^X = \eta_*^X - (d+2)/4$ is zero and β has been estimated to be $0.32 \sim 0.325$ in $d = 3$ [29], close to the accepted value. A variation of the local potential approximation that incorporates a field renormalization (not applicable in the spiking model) yields an estimate of the anomalous exponent of $\delta\eta_*^X \approx 0.1$, larger than the generally accepted value of 0.036, giving a value of $\beta_{WF} = \nu_*(d-2+\delta\eta_*^X)/2 \approx 0.35$. Improvements on these estimates have required more sophisticated approximations, such as the derivative expansion [67, 70–72] or other hierarchy closing methods [24, 46, 73, 74]. It is possible that a generalization of the derivative expansion to the spiking network model would change the estimates of the critical exponents for the spiking network model, possibly bringing them into closer agreement with the estimates of the Wilson-Fisher fixed point, with the possible exception of the dynamical exponent z_* .

IV. DISCUSSION

In this work we have adapted the “non-perturbative renormalization group” (NPRG) formalism to apply to a spiking network model of neural activity, and used this formalism to study both universal and non-universal properties of the network statistics in both lattices and random networks. We have shown that this method

1. produces accurate quantitative predictions of the effective firing rate nonlinearity that describes the relationship between the mean firing rate of neurons and their mean membrane potentials, and the method works for different choices of the bare nonlinearity $\phi(V)$ and for different network architectures with symmetric connections, including excitatory lattices, excitatory graphs of random connections, and random networks with Gaussian synaptic connections (Figs. 3-6).
2. qualitatively captures non-universal behavior in the supercritical regime, which allows us to predict the properties of metastable states in excitatory networks and random Gaussian networks (Figs. 7-8).
3. predicts that the spiking network model supports two important non-equilibrium universality classes, a Directed-Percolation universality class in networks with an absorbing state and a spinodal fixed point like the Yang-Lee ϕ^3 theory universality class in spontaneous networks.
4. allows us to estimate non-mean-field values of critical exponents as a function of the effective network dimension d . Our method also predicts that the directed-percolation-like fixed point loses stability

to another fixed point around $d = 2.78$ (Figs. 9-10) although preliminary results suggest a more refined ansatz is required to identify spinodal fixed points below $d \simeq 5$ in spontaneous networks (Fig. 12).

5. identify a \mathbb{Z}_2 -symmetric fixed point similar to the well-known Wilson-Fisher fixed point, though this is unstable toward the spinodal fixed point (Fig. 11).

The non-universal predictions agree well with simulations, demonstrating the success of the extension to network models. We focused on calculating the effective nonlinearity $\Phi_1(y)$ using a hierarchy-closing scheme. In the sub-critical regime we are able to close the hierarchy at fourth order, while in the super-critical regime we could only calculate solutions at first order due to the non-analytic behavior that emerges. For similar reasons of numerically instability, we studied the non-universal nonlinearities only in the context of spontaneous networks, not the absorbing state networks that we consider in addition to spontaneous networks when investigating universal quantities. The numerical solution of the flow equations appears unreliable in the region where the bare nonlinearity vanishes, possibly due to the systematic issues observed in the spontaneous case in which the predicted nonlinearity underestimates the simulation data.

Our analysis of universal features makes several qualitative predictions regarding universality classes that spiking neural networks could be part of, though quantitative predictions of critical exponents require further refinement of the method and handling of the randomness of synaptic connections, to be discussed below. To arrive at our results we used a combination of a perturbative ϵ -expansion and non-perturbative truncations. Both yield roughly consistent results for dimensions not far from the upper critical dimensions, but may be unreliable too far from d_c because the local potential approximation neglects the frequency and λ dependence of the renormalized terms. Both sub-approaches have pros and cons: the perturbative expansion (which we stress follows already from a non-perturbative starting point, and hence is not fully perturbative) applies directly to the full dimensionless flow equation for $w_*(\tilde{z}, z)$, and so is “exact” within the local potential approximation. However, it is in principle limited to small $\epsilon = d_c - d$, where d_c is the upper critical dimension of the fixed point. The higher order non-perturbative truncations on the other hand necessarily omit information about hiring order couplings—which is the standard practical procedure in most RG schemes—but it is easier to estimate the critical exponent ν_* , and it reveals additional structure that the ϵ -expansion may not be able to detect. For example, in the absorbing-state network our truncation approach suggests the emergence of a new critical point at $d \simeq 2.78$, which is far enough below the upper critical dimension of 4 that an ϵ -expansion may not be able to detect it.

There are several other aspects of our results and their implications for neuroscience research that warrant

detailed discussion, including remaining mysteries surrounding the anomalous dimensions (IV A), limitations of the spiking model we use here and the local potential approximation (IV B), the role of disorder in the synaptic weight matrix J_{ij} (IV C), and potential implications for the critical brain hypothesis (IV D), to be discussed in turn below.

A. Anomalous dimensions

In the standard NPRG approach to other models in statistical physics on lattices or continuous media, anomalous exponents— $\delta\eta_s^X$ in this work—are best characterized by a proper treatment of the long-time, small momentum behavior of the model, which is not captured by the local potential approximation. Improved quantitative estimates can often be obtained by including field renormalization factors in the ansatz for the average effective action, dubbed the LPA' approximation. In the spontaneous network model our non-trivial choices of the running scale \tilde{X}_Λ are effectively like including a field renormalization of the noise, though is perhaps more like the redundant parameter in directed percolation field theories [56], as our Ward-Takahashi identities do not allow for direct field renormalization factors.

In order to improve on the predictions of the LPA' approach, previous NPRG work has implemented the “derivative expansion”, which amounts to expanding renormalized parameters as functions of the momentum and temporal frequency. In the spiking network model such an extension might involve expanding the function $U_\Lambda(\tilde{x}, y)$ in powers of the frequency ω and synaptic weight matrix eigenvalues λ . The derivative expansion has yielded very accurate estimates of critical exponents in the $O(N)$ model universality classes [71], though the technical implementation has been found to be sensitive to the smoothness of the regulator [67, 70]. Our eigenvalue regulator (19) is equivalent to the ultra-sharp regulator that has been used in previous NPRG approaches, which is known to cause issues for the derivative expansion.

An alternate approach to obtaining improved estimates of the anomalous exponents is a type of hierarchy closure scheme for vertex functions (derivatives of Γ), not related to our hierarchy Eqs. (25)-(27), called the Blaizot-Méndez Galain-Wschebor (BMW) approximation [75]. [24] introduce a variation of this approximation technique for a firing rate model. This could potentially be an approach that works even with our ultra-sharp regulator.

While the beyond-LPA methods discussed above may improve our estimates of the critical exponents, they are unlikely to resolve one of the peculiarities of our analysis, the trivial value of the dynamic exponent $z_* = 2$. Our Ward-Takahashi identities appear to restrict the dynamic exponent $z_* = 2$ in any dimension at any fixed point of this model. At most critical points that have been stud-

ied, like the directed percolation fixed point families or the dynamic Ising model families, the value of z_* deviates from 2. This poses a mystery, as the critical points we have identified for this model appear to be closely related to the directed percolation universality class in absorbing state networks and the Ising model family (with or without broken \mathbb{Z}_2 symmetry) in spontaneous networks, but the fact that $z_* = 2$ would suggest these fixed points belong to distinct universality classes.

There is some precedent for this situation: there are non-equilibrium extensions of the Ising model that have the same static critical exponents of the equilibrium Ising universality class, but different dynamic critical exponents. The most well-known examples are the so-called “Model A” and “Model B” formulations [76–78], in which the conservation of the order parameter in the latter formulation leads to a super-diffusive spread of fluctuations compared to the former, and hence the dynamic exponents differ. Model A has been studied using the NPRG in [30], which serves to highlight an important difference between Model A and the spiking network model studied here. In particular, in Model A the microscopic action admits a type of time-reversal symmetry, underlying a fluctuation-dissipation relationship, that is not present in the spiking network model. This symmetry imposes a relationship between the running scale of time and the running scale of the additive Gaussian noise in Model A. This correspondence turns out to decouple the flow of the dynamic exponent z_* from the flow of the local potential and the anomalous exponent η in Model A. In contrast, the spiking network model does not possess this time-reversal symmetry, and there is no relationship between the running time scale $\delta\Lambda^{z_*/2}$ and the running noise scale $\tilde{X}_\Lambda = \delta\Lambda^{\eta_s^X}$, so the static critical exponents are not protected from the influence of the running noise scale. This said, there are models in which $z_* = 2$ despite other critical exponents taking on non-mean-field values, such as the pure annihilation fixed point we briefly discussed [32] in Sec. III B.

Our best conjecture for the curious case of a trivial dynamical exponent is that it is due to the linear dynamics of the membrane potential in Eq. (1), which was an important element of the derivation of one of our Ward-Takahashi identities. We suspect that including additional nonlinearities in the membrane dynamics—which would couple $V_i(t)$ nonlinearly to its response field $\tilde{V}_i(t)$ and not just the spike response field $\tilde{n}_i(t)$ in the action (5)—would give rise to non-trivial values of z_* . We discuss this possible mechanism in more detail in the next section.

B. Limitations of the spiking model and the local potential approximation

The spiking network we have focused on here is a prototypical model in neuroscience and captures many of the essential features of spiking network activity. However,

there are possible changes to the model that could alter the critical properties we estimate in this work. The main features we discuss here are the form of the dynamics of the membrane potentials and spike train generation, as well as the properties of the synaptic connections.

As noted in the previous section, the dynamic response of the membrane potentials to spike input is linear in Eq. (1). Although spike generation depends nonlinearly on the membrane potential through the conditional Poisson process, Eq. (2), the linearity of the membrane potential dynamics allows us to solve for $V_i(t)$ entirely in terms of the spike trains $\dot{n}_i(t)$. It is this feature that allows us to derive one of the Ward-Takahashi identities that restricts the form of the average effective action $\Gamma[\tilde{\psi}, \psi, \tilde{\nu}, \nu]$. If the membrane potential dynamics were nonlinear, for example,

$$\tau \frac{dV_i(t)}{dt} = -\frac{V_i(t) - \mathcal{E}_i}{\tau} - aV_i(t)^2 + \sum_{j=1}^N J_{ij} \dot{n}_j(t),$$

then the solution for $V_i(t)$ will depend nonlinearly on the spike trains, which precludes the derivation of one of the Ward-Takahashi identity that relied on integrating out the membrane potential fields. The other Ward-Takahashi identity, which involved integrating out the spiking fields, remains. The consequence is that we can only restrict the form of the average effective action to

$$\Gamma[\chi] = \tilde{\nu} \cdot \nu - \tilde{\psi} \cdot J \cdot \nu + \Upsilon[\tilde{\psi}, \psi, \tilde{\nu}].$$

i.e., the renormalized terms would be functionals of three fields, instead of just $\tilde{\nu}$ and ψ . In this situation, the fact that the average effective action has the same structure as the bare action, plus all terms allowed by symmetry, becomes crucial, and the standard course of action is to make an ansatz that to lowest order Γ has the same form as the bare action but with renormalized coefficients, e.g.,

$$\begin{aligned} \Gamma_\Lambda[\chi] = \int \sum_i \left\{ \tilde{\psi}_i(t) \left[\tau_\Lambda \dot{\psi}_i(t) + \psi_i(t) - \mathcal{E}_i + a_\Lambda \psi_i(t)^2 \right. \right. \\ \left. \left. - \sum_j J_{ij}(t-t') \nu_j(t') \right] \right. \\ \left. + \tilde{\nu}_i(t) \nu_i(t) - U_\Lambda(\tilde{\nu}_i(t), \psi_i(t)) \right\}, \end{aligned}$$

where τ_Λ and a_Λ flow in addition to $U_\Lambda(\tilde{x}, y)$. Because these parameters flow they can contribute to the anomalous exponents in a way that was absent in the model with purely linear membrane potential dynamics. In particular, if $\tau_\Lambda \sim \delta\Lambda^{-\delta z_*/2}$ as $\delta\Lambda \rightarrow 0$, then the dynamic exponent would become $z_* = 2 + \delta z_*$; i.e., the dynamic exponent may no longer take on the trivial value $z_* = 2$. (See Appendix H).

Another important type of membrane nonlinearity is a multiplicative coupling between the membrane po-

tential and the spike train. In this stochastic spiking model a coupling of the form $\tilde{V}_i(t) \dot{n}_i(t) (V_i(t) - \mathcal{E}_{\text{reset}})$ has been used to implement a hard reset of the membrane potential to $\mathcal{E}_{\text{reset}}$ after a neuron spikes [26], as opposed to the soft resets implemented through negative diagonal terms $J_{ii} < 0$. Similarly, the synaptic currents that neurons inject into their targets depends on the membrane potential of the target, known as conductance-based coupling [79], which would replace the synaptic current injection $\tilde{V}_i(t) J_{ij} \dot{n}_j(t)$ in Eq. (1) with $-\tilde{V}_i(t) (V_i(t) - \mathcal{E}_{\text{syn}}) \sum_j G_{ij} \dot{n}_j(t)$, for some synaptic reversal potential \mathcal{E}_{syn} and conductances G_{ij} . Many types of behavior observed in conductance-based models can be reproduced with current based models, so this type of interaction could be irrelevant in the RG sense, at least near some critical points, but checking this could be challenging. These types of interactions would require a modified approach using the NRG method presented here, as they not only introduce a direct coupling between the spike train fields $\dot{n}_i(t)$ and the membrane potentials $V_i(t)$ in the model, but in the conductance-based model the synaptic interactions are no longer bilinear, and cannot be used to regulate the flow of models from the mean-field theory to the true model. A separate regulator would have to be introduced, perhaps more in the style of standard NRG work that achieves mean-field theory as a starting point by introducing a large “mass” term to freeze out stochastic fluctuations. We discuss a possible form of such a regulator in Appendix D 2.

Finally, a notable simplification of the analysis presented here is the restriction to symmetric synaptic connections $J_{ij} = J_{ji}$. While in principle our method will work for asymmetric matrices, the assumption of symmetry allows a dramatic simplification of the general flow equation for the local potential $U_\Lambda(\tilde{x}, y)$ (Eq. (17)), after which the $N \rightarrow \infty$ limit could be taken. While symmetric connections have been very useful in developing foundational theories in neuroscience, such as associative memory models like the Hopfield network [80], real neural circuits do not have perfectly symmetric connections. Connections are often highly reciprocally connected [81], and hence symmetric weights may be a reasonable approximation for some circuits; however, the behavior of firing rate networks is known to change qualitatively as the correlations between J_{ij} and J_{ji} vary from 1 to 0. For example, firing rate networks with perfectly symmetric connections exhibit spin-glass behavior with many metastable states [54], while non-symmetric connections display a transition to chaotic behavior [11]. In-between new phases controlled by marginally stable stables have even been shown to emerge [82]. We therefore expect correlations of reciprocal connections to be a relevant parameter in the RG flow of the spiking network model.

Allowing for asymmetric connections would also allow exploration of networks with multiple cell types, the classic case in neuroscience being populations of separate excitatory and inhibitory neurons (“E-I networks”), whose synapses are constrained to be positive or negative, re-

spectively. On one hand, we might expect these different populations to have different firing rate nonlinearities, owing to their different properties, which would not be captured by the current formalism. On the other hand, if one were to only measure a subset of neurons from a network and fit a generalized linear model—the name for the spiking network used in this work when fit to data—the inferred synaptic interactions would not naturally respect this dichotomy of cell types [42]. In this sense our random network model might still capture some aspects of E-I networks, though it may miss some collective pattern forming behavior driven by having separate populations of different cell types [9].

C. Impact of disorder on critical properties

Much of the renormalization group analysis presented was not affected by whether neurons were connected in a structured arrangement like a lattice or in a random network. Our calculation of the effective nonlinearity $\Phi_1(y)$ was insensitive to the origin of the eigenvalue density. Similarly, we find that the critical fixed points of the dimensionless flow equations only depend on the effective dimension d of the network, defined by the scaling of the eigenvalue distribution near the maximum bulk eigenvalue, $\rho_\lambda(\lambda) \sim |\Lambda_{\max} - \lambda|^{d/2-1}$. Consequently, at the level of the local potential approximation we make in this work, lattices of spatial dimension d and random networks of effective dimension d share the same critical points, and would appear to belong to the same universality class.

However, this conclusion is likely too naive. For one, extensions of the NRG beyond the local potential approximation (e.g., by generalizing the derivative expansion or implementing a BMW-esque closure scheme) may not have the convenient property that the eigenmodes of the weight distribution fall out of the flow equations, and hence could shape the critical properties of the network. This could even happen at the level of the LPA in asymmetric networks.

Second, we have already shown that the macroscopic dimensionful behavior of the system does depend on details of the synaptic weights J_{ij} . For instance, excitatory networks show two extremal metastable states (Fig. 7), while random networks with excitatory and inhibitory connections exhibit spin-glass behavior (Fig. 8). Moreover, simulations of absorbing state networks comprising excitatory neurons on lattices yield predictions of the critical exponents consistent with our estimates (Fig. 14), whereas simulations of absorbing state networks with Gaussian synaptic weights are not as easily verified.

It is well known that “disorder”, such as a random distribution of synaptic connections, can alter the critical properties of a continuous phase transition [51]. In equilibrium the Harris criterion predicts that when the correlation length exponent $\nu_* < 2/d$, then disorder is a relevant perturbation to a critical point. Similar cri-

teria also appear to hold in non-equilibrium absorbing state transitions [69]. If we assume this criterion holds for the spiking network model, then for the absorbing state $\nu_* - 2/d < 0$ for the estimates shown in Fig. 9, and we expect disorder to be relevant. In the spontaneous network model it is not clear if a Harris-like criterion applies to the spinodal point, which is associated with a first order transition.

One way to investigate how disorder impacts the behavior of the network would be to perform a dynamic mean-field calculation similar to the one we performed in Sec. II D to predict the behavior of random networks in the supercritical phase. At a critical point the analysis may be more difficult, as the self-consistent calculation would necessarily involve expectations over the non-analytic power law terms expected to be present in the critical nonlinearities (Eq. (55)). A possible means of investigating the impact of disorder on critical points in the dimensionless RG flow is by means of a replica calculation, similar to what has been done for the random-field $O(N)$ model in equilibrium [35, 83–85]. This would require a modification of the way we regulate the family of models in this work, in addition to the additional complications involved with performing the NRG analysis for replicated systems.

As a last note on the topic of disorder in the spiking network model, in our analysis of random networks with Gaussian synaptic connections in Sec. II D we tuned the rest potentials of each neuron to $\mathcal{E}_i = -\sum_j J_{ij} \Phi'_1(0)$ in order to tune the network to the critical point $\langle V_i(t) \rangle = 0$ for every neuron. In a real brain this seems like an extremely fine-tuned condition that may not be realistic. While possible that homeostatic mechanisms could tune a collective of neurons’ different rest potentials to different levels, a more natural model would be to assume a constant value of \mathcal{E} across all neurons of the same cell type, or even a random distribution but one uncorrelated with the synaptic weights J_{ij} . In this case the network would not be tuned to the critical point, and the spread of neural activity would appear like the simulations shown in Fig. 3, for which $\mathcal{E}_i = 0$ for all neurons. As a result, only a small fraction of the population would be close to $\langle V_i(t) \rangle = 0$, and it is not clear whether critical behavior would be visible. Potentially, such a scenario could give rise to “Griffiths phase”-like effects, in which rare regions of the network are close to criticality [86, 87]. In the standard Griffiths effect, these rare regions tend to be spatially localized, though signatures of the effect have been reported in random network models [88].

Understanding the impact of disorder on critical properties of spiking networks, and the influence on the sub- or super-critical collective behavior, while important, is non-trivial, and we leave investigations of these matters as avenues for future work.

D. Implications for the critical brain hypothesis

The possibility of criticality in neural tissue has been a subject of investigation for some time now. Much of the focus has centered on neural avalanches [13–15, 17], which display power law scaling in the distributions of quantities like avalanche size, duration, and even scaling forms of avalanche shapes [15]. Other lines of inquiry have looked for general signatures of criticality in, e.g., the retina [89]. These experimental analyses have spawned a variety of theoretical models to explain power law observations in neural data, including analyses that claim that many signatures of criticality may appear in non-critical models [19, 20], or could be due to the effects of subsampling [21, 22].

To date, most experimental analyses of criticality have looked for power law scaling, with a smaller subset attempting to perform Widom-style data collapses, a stronger signature of criticality [15]. Theoretically, most work has either focused on simulating network models that can produce power-law scaling in neural activity statistics, performed mean-field analyses to identify phases [90], or reinterpreted known models in statistical physics whose phase transition properties are well-studied [14]. The first and second cases typically do not directly invoke the renormalization group, and in the latter case the renormalization group may have been used to analyze models in their original context, but the reinterpretation in neuroscience must often be taken as a coarse-grained model of neural activity, rather than spiking activity.

Only recently have renormalization group methods been applied to models interpreted in the context of neuroscience [40]. [39] used ideas of renormalization-style coarse-graining as a data analysis tool, while [41] applied perturbative RG to the Wilson-Cowan neural field model, a model of coarse-grained neural activity, and found that in $d = 2$ the model had peculiar scaling behavior similar to the BTK transition in $d = 2$ $O(2)$ model. There has been some work applying the non-perturbative renormalization group in a neuroscience context, notably [24] introduces a BMW-like scheme for calculating correlation functions in firing rate models, and [91] explores possible equivalences between the NPRG and the information bottleneck neck in information theory, used in neural sensory coding work. To the author’s knowledge, our work is the first to apply renormalization group methods to spiking network models, both to calculate non-universal quantities like the firing rate nonlinearity, and to investigate critical points in the renormalization group flow.

Our results demonstrate that a spiking network model commonly used in neuroscience does possess non-trivial critical points in its renormalization group flow, and moreover that these critical points are accessed by tuning the gain of the neurons $\phi'(0)$ or the strength of the synaptic connections Λ_{\max} —in contrast to the possibility that such critical points may not be accessible and mean-field theory describes transitions in neural activity,

or more exotic possibilities like non-universal scaling. In networks with absorbing states our analysis predicts a regular continuous phase transition between an inactive state and an active state, which could be the universality class of avalanche dynamics observed *in vitro*, where the spontaneous activity of neurons is very low. In spontaneously active networks, however, which might be a better model for *in vivo* activity, our analysis predicts that the fixed point corresponds to a discontinuous transition associated with a spinodal point, owing to the fact that the dimensionless couplings are complex-valued. Despite the fact that this fixed point corresponds to a first order transition, it still boasts universal scaling. The spontaneous network critical point is very reminiscent of the Yang-Lee ϕ^3 theory, which is essentially the universality class of the Ising model in an external field. Thus, our results establish a firm renormalization-group-based foundation for the possibility that real networks could potentially be tuned to such critical points, but the full picture of the nature of these transitions may be much more complicated than the relatively simple second order transitions commonly associated with universality.

This said, it is important to distinguish between the possibility that neural circuit dynamics posses bona fide critical points separating different regimes of emergent collective activity from some of the stronger variations of the critical brain hypothesis, which posit that the brain’s homeostatic mechanisms actively maintain neural activity near a critical point. The results presented here say nothing about whether the brain tends to maintain itself near critical points. The most-studied mechanism by which the brain might tune itself to a critical point is through synaptic plasticity, a process through which the activity of the network alters the synaptic connections J_{ij} . The model presented here assumes fixed J_{ij} , but in principle one could add such dynamics to J_{ij} and study how this changes the renormalization group flow. This scenario is conceptually similar to direction percolation with a conserved quantity (DP-C) discussed earlier in this report, in which giving dynamics to a previously conserved quantity changes the critical exponents [61].

V. FUTURE DIRECTIONS

We have shown that we can extend the methods of the non-perturbative renormalization group (NPRG) to apply to an action for which the free theory is a Poisson, rather than Gaussian, process. Moreover, the dynamics may take place on either networks or lattices. While the context of our investigation is the collective activity of neural populations, but the underlying model, the non-linear Hawkes process, has been used in applications in other fields including epidemiology, ecology, and earth science [92–96].

The spiking network model presented here contains many simplifications that do not reflect the physiology of real neural circuitry, such as a single cell type neu-

rons with both excitatory and inhibitory connections and perfectly symmetric connections. However, the relative simplicity of the spiking model used in this work is what allowed it to become an important foundational model for extending the non-perturbative renormalization group to spiking neural networks. The linear membrane potential dynamics will remain valuable as a testing ground for further developments, in parallel with extensions that incorporate additional features like membrane nonlinearities.

In our discussion we have outlined many possible avenues for future extensions of the model and methods, including going beyond the local potential approximation, adding nonlinearities to the membrane potential dynamics, investigating how randomness in synaptic connections might alter critical properties, and investigating other network structures—in particular asymmetric networks and networks with multiple cell types.

Other avenues that can be investigated with the current model include studying the effects of fluctuations on dynamic phenomena, such as spinodal decomposition. Our finding that the spontaneous networks are controlled by a spinodal fixed point motivated investigating how a sudden quench—a change of the bare gain $\phi'(0)$ —could lead to phase separation, as shown in Fig. 1. A mean-field analysis of the dynamics would predict that one phase of the network typically takes over rather quickly, while simulations show that the stochastic fluctuations give rise to more complex spatiotemporal dynamics. Our method provides a means of taking the stochastic fluctuations into account in both the sub- and super-critical phases. Moreover, because our method is not restricted to lattices, we can probe deeper into the impact that other network structures have; a particular case of interest will be navigable-small world graphs, which interpolate from the lattice dynamics shown in Fig. 1A to the random network dynamics shown in Fig. 1B. By adapting the non-perturbative renormalization group to spiking networks, we have opened new doors to elucidating such phenomena.

The author thanks National Institute of Mental Health and National Institute for Neurological Disorders and Stroke grant UF-1NS115779-01 and Stony Brook University for financial support for this work, and Ari Pakman for feedback on an early version of this manuscript.

Appendix A: Path integral representation of the stochastic neural activity model

In the stochastic model of neural activity we consider in this work we have a network of N neurons connected synapses. Each neuron has a time-dependent membrane potential $V_i(t)$ and spike train history denoted by $\dot{n}_i(t)$. The dynamics of each neuron's membrane potential are given, in general, by the differential equation

$$\tau \frac{dV_i(t)}{dt} = E_i(t) + f(V_i(t)) + \sum_{j=1}^N \int_{-\infty}^{\infty} dt' K_{ij}(t-t') \dot{n}_j(t'), \quad (\text{A1})$$

where τ is a membrane time constant, $\mathcal{E}_i(t)$ is an external drive, $f(V_i(t))$ is a membrane nonlinearity, and $K_{ij}(t-t')$ is the time-dependent response of neuron i 's membrane potential at time t due to a spike from neuron j at time t' . If neuron j does not make a connection to neuron i , then $K_{ij}(t-t') = 0$ for all $t-t'$. In general K_{ij} need not be symmetric, though in this work we will limit our scope to symmetric networks.

The probability that neuron i fires $\dot{n}_i(t)dt$ spikes within an interval dt is given by

$$\text{Prob}(\text{spike} \in [t, t+dt]) = \phi_i(V_i(t)) dt, \quad (\text{A2})$$

where $\phi_i(V_i(t))$ is the neuron's firing rate nonlinearity. We assume that, given the value of the neuron's membrane potential at time t , the spiking activity is Poisson (or, equivalently for infinitesimal dt , Bernoulli):

$$\text{Prob}(\dot{n}_i(t)|V_i(t)) = \frac{(\phi_i(V_i(t))dt)^{\dot{n}_i(t)dt}}{(\dot{n}_i(t)dt)!} e^{-\phi_i(V_i(t))dt}.$$

Note that all neurons are conditionally independent once their membrane potential at the current time t is specified.

For general membrane nonlinearity $f(V)$ The dynamics of Eqs. (A1)-(A2) can be converted into a path integral formalism by modifying the Martin-Siggia-Rose-Janssen-De Dominicis (MSRJD) approach to converting stochastic differential equations into path integrals to take account of the fact that the “noise” $\dot{n}_i(t)$ is Poisson rather than Gaussian. Here we give a heuristic derivation of the procedure in continuous time; this procedure for generating the path integral should be understood as the formal continuous limit of the well-defined discrete-time formulation of the model. The derivation proceeds as

$$\begin{aligned} 1 &= \int \mathcal{D}[V, \dot{n}] \prod_{i,t} \delta \left(\frac{dV_i(t)}{dt} - \frac{E_i(t) + f(V_i(t)) + \sum_{j=1}^N \int_{-\infty}^{\infty} dt' K_{ij}(t-t') \dot{n}_j(t')}{\tau} \right) \frac{(\phi_i(V_i(t))dt)^{\dot{n}_i(t)dt}}{(\dot{n}_i(t)dt)!} e^{-\phi_i(V_i(t))dt} \\ &= \int \mathcal{D}[\tilde{V}, V, \tilde{n}, \dot{n}] e^{-\sum_i \int_{-\infty}^{\infty} dt \tilde{V}_i(t) \left[\frac{dV_i(t)}{dt} - \frac{E_i(t) + f(V_i(t)) + \sum_{j=1}^N \int_{-\infty}^{\infty} dt' K_{ij}(t-t') \dot{n}_j(t')}{\tau} \right] - \tilde{n}_i(t) \dot{n}_i(t) + (e^{\tilde{n}_i(t)} - 1) \phi_i(V_i(t))} \end{aligned}$$

where we used the Fourier representations of the Dirac delta function and the Poisson distribution, which introduces the auxiliary membrane potential field \tilde{V} and the auxiliary spike field \tilde{n} . This is the form of the path integral for general membrane nonlinearity $f(V)$; however, in this work we set the membrane potential nonlinearity $f(V_i(t)) = -V_i(t)$, such that we can formally solve for the membrane potential:

$$V_i(t) = \mathcal{E}_i(t) + \sum_{j=1}^N \int_{-\infty}^{\infty} dt' J_{ij}(t-t') \dot{n}_j(t'),$$

where $\mathcal{E}_i(t) = \int_{-\infty}^t dt'' \tau^{-1} e^{-(t-t'')/\tau} E_i(t'')$ and $J_{ij}(t-t') = \int_{-\infty}^t dt'' \tau^{-1} e^{-(t-t'')/\tau} K_{ij}(t''-t')$. We may thus instead directly enforce the solution,

$$\begin{aligned} 1 &= \int \mathcal{D}[V, \dot{n}] \prod_{i,t} \delta \left(V_i(t) = \mathcal{E}_i(t) + \sum_{j=1}^N \int_{-\infty}^{\infty} dt' J_{ij}(t-t') \dot{n}_j(t') \right) \frac{(\phi_i(V_i(t))dt)^{\dot{n}_i(t)dt}}{(\dot{n}_i(t)dt)!} e^{-\phi_i(V_i(t))dt} \\ &= \int \mathcal{D}[\tilde{V}, V, \tilde{n}, \dot{n}] e^{-\sum_i \int_{-\infty}^{\infty} dt \tilde{V}_i(t) [V_i(t) - \mathcal{E}_i(t) - \sum_{j=1}^N \int_{-\infty}^{\infty} dt' J_{ij}(t-t') \dot{n}_j(t')] - \tilde{n}_i(t) \dot{n}_i(t) + (e^{\tilde{n}_i(t)} - 1) \phi_i(V_i(t))}, \\ &\equiv \int \mathcal{D}[\tilde{V}, V, \tilde{n}, \dot{n}] e^{-S[\tilde{V}, V, \tilde{n}, \dot{n}]}, \end{aligned}$$

giving the action we work with in the main text:

$$S[\tilde{V}, V, \tilde{n}, \dot{n}] = \sum_{i=1}^N \int_{-\infty}^{\infty} dt \left\{ \tilde{V}_i(t) \left[V_i(t) - \mathcal{E}_i(t) - \sum_{j=1}^N \int_{-\infty}^{\infty} dt' J_{ij}(t-t') \dot{n}_j(t') \right] + \tilde{n}_i(t) \dot{n}_i(t) - \left(e^{\tilde{n}_i(t)} - 1 \right) \phi(V_i(t)) \right\}. \quad (\text{A3})$$

We may now introduce source terms to define the moment-generating functional (MGF) $\mathcal{Z}[\mathcal{A}]$,

$$\mathcal{Z}[\mathcal{A}] = \int \mathcal{D}[\tilde{V}, V, \tilde{n}, \dot{n}] e^{-S[\tilde{V}, V, \tilde{n}, \dot{n}] + \sum_i \int_{-\infty}^{\infty} dt \{ \tilde{V}_i(t) h_i(t) + V_i(t) \tilde{h}_i(t) + \tilde{n}_i(t) j_i(t) + \dot{n}_i(t) \tilde{j}_i(t) \}}, \quad (\text{A4})$$

where the source terms are $\mathcal{A} \equiv \{h, \tilde{h}, j, \tilde{j}\}$. Taking derivatives of this functional with respect to $\tilde{h}_i(t)$ or $\tilde{j}_i(t)$ and setting the sources to 0 will formally yield the statistical moments of the fields. Taking mixtures of derivatives with respect to $\tilde{h}_i(t)$ or $\tilde{j}_i(t)$ as well as the sources $h_i(t)$ or $j_i(t)$ will yield response functions. That is, all information about the statistics and responses of the network dynamics are contained in the MGF.

The MGF is related to two other important statistical functionals, the “cumulant generating functional” (CGF) $W[\mathcal{A}]$ and the “average effective action” (AEA) $\Gamma[\chi]$. The CGF is simply defined by the logarithm of the MGF,

$$W[\mathcal{A}] = \ln \mathcal{Z}[\mathcal{A}]. \quad (\text{A5})$$

The AEA is then defined as the Legendre transform of the CGF,

$$\Gamma[\chi] = -W[\mathcal{A}] + \mathcal{A} \cdot \chi; \quad (\text{A6})$$

where we introduce the fields $\chi \equiv \{\tilde{\psi}, \psi, \tilde{\nu}, \nu\}$ conjugate to the source fields $\mathcal{A} = \{y, \tilde{y}, j, \tilde{j}\}$. The notation $\mathcal{A} \cdot \chi$ is a shorthand for

$$\sum_i \int dt \left\{ h_i(t) \tilde{\psi}_i(t) + \tilde{h}_i(t) \psi_i(t) + j_i(t) \tilde{\nu}_i(t) + \tilde{j}_i(t) \nu_i(t) \right\},$$

and the fields are defined in terms of derivatives of W or Γ by

$$\tilde{\psi}_i(t) = \frac{\delta W[\mathcal{A}]}{\delta h_i(t)}, \quad \psi_i(t) = \frac{\delta W[\mathcal{A}]}{\delta \tilde{h}_i(t)}, \quad \tilde{\nu}_i(t) = \frac{\delta W[\mathcal{A}]}{\delta j_i(t)}, \quad \nu_i(t) = \frac{\delta W[\mathcal{A}]}{\delta \tilde{j}_i(t)}$$

and

$$h_i(t) = \frac{\delta \Gamma[\chi]}{\delta \tilde{\psi}_i(t)}, \quad \tilde{h}_i(t) = \frac{\delta \Gamma[\chi]}{\delta \psi_i(t)}, \quad j_i(t) = \frac{\delta \Gamma[\chi]}{\delta \tilde{\nu}_i(t)}, \quad \tilde{j}_i(t) = \frac{\delta \Gamma[\chi]}{\delta \nu_i(t)}.$$

All three functionals \mathcal{Z} , W , and Γ contain the full statistical and response information about the dynamics of the network, but have different advantages and disadvantages when performing calculations. The key advantage of the AEA Γ that is the focus of the non-perturbative renormalization group method exploits is that it shares the symmetries and constraints of the bare action S (Eq. (5)), whereas \mathcal{Z} and W tend to be more complicated objects.

Before we move on, a remark is in order regarding the values of the fields and sources. In principle, the auxiliary fields \tilde{V} and \tilde{n} are imaginary quantities, such that the integrals over these fields at each time point and for each neuron run from $-i\infty$ to $+i\infty$. The fields V and \dot{n} are real quantities. However, while we require \tilde{V} and \tilde{n} to be imaginary in order for the integrals to converge in general, the action $S[\tilde{V}, V, \tilde{n}, \dot{n}]$ may be trivially analytically continued to real values of \tilde{V} and \tilde{n} , as the dependence on these fields is already analytic.

In calculating the MGF $\mathcal{Z}[\mathcal{A}]$, the source fields h and j (conjugate to \tilde{V} and \tilde{n}) are real, with the restriction $j_i(t) \geq 0$, while the fields \tilde{h} and \tilde{j} (conjugate to V and \dot{n}) may be taken to be complex in general, subject to possible restrictions on the range of the real part. In the absence of coupling there are no such restrictions. We therefore take all source fields $\mathcal{A} = \{h, \tilde{h}, j, \tilde{j}\}$ to be real in computing the AEA $\Gamma[\chi]$, such that the fields $\chi = \{\tilde{\psi}, \psi, \tilde{\nu}, \nu\}$ may all be taken to be real. As with \tilde{V} in the bare action S , $\tilde{\psi}$ may be trivially analytically continued to the complex plane (as we will show that the dependence of $\Gamma[\chi]$ on $\tilde{\psi}$ is the same as the action S ’s dependence on \tilde{V}), and we will similarly assume that $\tilde{\nu}$ may be analytically continued to complex values, though this assumption will have to be justified after-the-fact. The reason for considering the values of these fields is that we will ultimately need to numerically evaluate a set of equations involving the fields $\tilde{\nu}$ and ψ ; having the freedom to choose $\tilde{\nu}$ to be real will aid in our numerical evaluations.

Appendix B: Derivation of the Wetterich flow equation for the spiking network model

The key idea behind the non-perturbative renormalization group (NPRG) approach is to introduce a family of models, here parametrized by a single parameter $\kappa \in [0, 1]$, that interpolates from a solvable theory to the true theory that incorporates all stochastic fluctuations. In the main text we parameterize the family of models by Λ , taken to be the threshold of the eigenvalues we are integrating over to generate the family of models. In this appendix we will take the threshold to be a function of the arbitrary parameter κ ; parametrizing the models by Λ is a matter of a simple change of variables.

The NPRG method creates this family of models in practice by deriving a differential equation for a functional Γ_κ , corresponding to the (modified) average effective action for this family of models. This differential equation is known as the Wetterich equation [47], which we derive for our model in this section.

The NPRG approach introduces a regulator into the action of the model, chosen to obey the symmetries of the model and such that at the initial value $\kappa = 0$ the functional Γ_0 coincides with the bare action of the theory—i.e., the “solvable” theory corresponds to the mean field theory of the model. The standard NPRG approach uses a bilinear regulator that introduces a mass-like term in the action, such that as $\kappa \rightarrow 0$ the mass grows so large that fluctuations are effectively frozen out, yielding the desired mean field theory. However, the standard proof of this effect for non-equilibrium path integral theories relies on the action being derived from a stochastic Langevin equation or the Doi-Peliti formalism applied to stochastic master equations [30]. Our action is not of these forms, and so the standard proof does not apply. Moreover, with four fields to deal with rather than two, it is not obvious which pairs of fields such a bilinear regulator ought to couple.

We therefore need to modify the NPRG approach to apply to the neural spiking model. Our adaptation is based on the observation that the moment-generating functional $\mathcal{Z}[\mathcal{A}]$ can be written in terms of an exponential derivative operator acting on the free theory $\mathcal{Z}_{\text{free}}[\mathcal{A}]$ which is not Gaussian but *Poisson*:

$$\begin{aligned} \mathcal{Z}[\mathcal{A}] &= \int \mathcal{D}[\tilde{V}, V, \tilde{n}, \dot{n}] e^{-S_{\text{free}}[\tilde{V}, V, \tilde{n}, \dot{n}] + \sum_{ij} \int dt dt' \tilde{V}_i(t) J_{\kappa;ij}(t-t') \dot{n}_j(t')} + \sum_i \int_{-\infty}^{\infty} dt \{ \tilde{V}_i(t) h_i(t) + V_i(t) \tilde{h}_i(t) + \tilde{n}_i(t) j_i(t) + \dot{n}_i(t) \tilde{j}_i(t) \} \\ &= e^{\sum_{ij} \int dt dt' \frac{\delta}{\delta h_i(t)} J_{\kappa;ij}(t-t') \frac{\delta}{\delta \tilde{j}_j(t')}} \int \mathcal{D}[\tilde{V}, V, \tilde{n}, \dot{n}] e^{-S_{\text{free}}[\tilde{V}, V, \tilde{n}, \dot{n}] + \sum_i \int_{-\infty}^{\infty} dt \{ \tilde{V}_i(t) h_i(t) + V_i(t) \tilde{h}_i(t) + \tilde{n}_i(t) j_i(t) + \dot{n}_i(t) \tilde{j}_i(t) \}} \\ &= e^{\sum_{ij} \int dt dt' \frac{\delta}{\delta h_i(t)} J_{\kappa;ij}(t-t') \frac{\delta}{\delta \tilde{j}_j(t')}} [\mathcal{Z}_{\text{free}}[\mathcal{A}]], \end{aligned}$$

where

$$S_{\text{free}} = \sum_{i=1}^N \int_{-\infty}^{\infty} dt \left\{ \tilde{V}_i(t) [V_i(t) - \mathcal{E}_i(t)] + \tilde{n}_i(t) \dot{n}_i(t) - \left(e^{\tilde{n}_i(t)} - 1 \right) \phi(V_i(t)) \right\} \quad (\text{B1})$$

is the “free” action corresponding to a non-homogeneous Poisson process with corresponding free moment-generating-functional $\mathcal{Z}_{\text{free}}[\mathcal{A}]$ which can be solved for exactly:

$$\mathcal{Z}_{\text{free}}[\mathcal{A}] = \exp \left(\sum_i \int_{-\infty}^{\infty} dt \left\{ \tilde{h}_i(t) [h_i(t) + \mathcal{E}_i(t)] + \tilde{j}_i(t) j_i(t) + (e^{\tilde{j}_i(t)} - 1) \phi(\mathcal{E}_i(t) + h_i(t)) \right\} \right), \quad (\text{B2})$$

The relationship between the true MGF $\mathcal{Z}[\mathcal{A}]$ and the free MGF $\mathcal{Z}_{\text{free}}[\mathcal{A}]$ motivates us to define our family of models by replacing the synaptic coupling $J_{ij}(t-t')$ by a regulated coupling $J_{\kappa;ij}(t-t')$ parametrized by κ such that $J_{\kappa=0;ij}(t-t') = 0$ and $J_{\kappa=1;ij}(t-t') = J_{ij}(t-t')$. The family of regulated MGFs is then given by

$$\mathcal{Z}_\kappa[\mathcal{A}] = \exp \left(\sum_{ij} \int dt dt' \frac{\delta}{\delta h_i(t)} J_{ij;\kappa}(t-t') \frac{\delta}{\delta \tilde{j}_j(t')} \right) \mathcal{Z}_{\text{free}}[\mathcal{A}] \quad (\text{B3})$$

This exponential operator cannot be evaluated analytically. Instead, the next step is to differentiate this expression with respect to κ , yielding the identity

$$\partial_\kappa \mathcal{Z}_\kappa[\mathcal{A}] = \sum_{ij} \int dt dt' \frac{\delta}{\delta h_i(t)} J_{ij;\kappa}(t-t') \frac{\delta}{\delta \tilde{j}_j(t')} \mathcal{Z}_\kappa[\mathcal{A}], \quad (\text{B4})$$

which can be taken to be a flow equation for $\mathcal{Z}_\kappa[\mathcal{A}]$ with initial condition $\mathcal{Z}_{\kappa=0}[\mathcal{A}] = \mathcal{Z}_{\text{free}}[\mathcal{A}]$. Although this flow

equation is linear, it is not as amenable to approximation as the flow equation for $\Gamma_\kappa[\chi]$ that we seek to derive. Defining the flowing CGF $W_\kappa[\mathcal{A}] = \ln \mathcal{Z}_\kappa[\mathcal{A}]$ yields a flow equation for $W_\kappa[\mathcal{A}]$,

$$\partial_\kappa W_\kappa[\mathcal{A}] = \sum_{ij} \int dt dt' \left\{ \partial_\kappa J_{\kappa;ij}(t-t') \frac{\delta^2 W_\kappa[\mathcal{A}]}{\delta h_i(t) \delta \tilde{j}_j(t')} + \frac{\delta W_\kappa[\mathcal{A}]}{\delta h_i(t)} \partial_\kappa J_{\kappa;ij}(t-t') \frac{\delta W_\kappa[\mathcal{A}]}{\delta \tilde{j}_j(t')} \right\} \quad (\text{B5})$$

with initial condition $W_{\kappa=0}[\mathcal{A}] = W_{\text{free}}[\mathcal{A}]$.

We now define the flowing average effective action $\Gamma_\kappa[\chi]$ by the *modified* Legendre transform

$$\Gamma_\kappa[\chi] + W_\kappa[\mathcal{A}] = \mathcal{A} \cdot \chi - \frac{1}{2} \chi \cdot \mathbf{R}_\kappa \cdot \chi, \quad (\text{B6})$$

where $\mathbf{R}_\kappa(t, t')$ is a $4N \times 4N$ (4 fields by N neurons) regulator related to $J_{\kappa;ij}(t-t')$. We require that this regulator vanishes as $\kappa \rightarrow 1$ in order to restore the proper definition of the Legendre transform, such that $\Gamma_{\kappa=1}[\chi] = \Gamma[\chi]$, the true AEA. We will determine the form of \mathbf{R}_κ momentarily. First, because we are working with a modified Legendre transform we must also suitably modify the definitions of the fields χ and \mathcal{A} . We take $\chi = \frac{\partial W_\kappa}{\partial \mathcal{A}}$ as in the true Legendre transform (with χ and \mathcal{A} corresponding to conjugate pairs of fields evaluated at the same neuron index and time), and must therefore require $\mathcal{A} = \frac{\delta \Gamma_\kappa}{\delta \chi} + \mathbf{R}_\kappa \cdot \chi$.

To obtain $\partial_\kappa \Gamma_\kappa[\chi]$, we differentiate Eq. (B6), accounting for the fact that the $\partial_\kappa W_\kappa$ derivative is taken holding the \mathcal{A} fields fixed, while we want to differentiate $\Gamma_\kappa[\chi]$ holding the fields χ fixed:

$$\partial_\kappa \Gamma_\kappa[\chi] \Big|_\chi = (\partial_\kappa \mathcal{A}) \cdot \chi - \partial_\kappa W_\kappa[\mathcal{A}] \Big|_\chi - \frac{1}{2} \chi \cdot \partial_\kappa \mathbf{R}_\kappa \cdot \chi.$$

The derivative $\partial_\kappa W_\kappa[\mathcal{A}] \Big|_\chi$ is related to $\partial_\kappa W_\kappa[\mathcal{A}] \Big|_\mathcal{A}$ by

$$\partial_\kappa W_\kappa[\mathcal{A}] \Big|_\chi = \partial_\kappa W_\kappa[\mathcal{A}] \Big|_\mathcal{A} + (\partial_\kappa \mathcal{A}) \cdot \chi.$$

We see that the $(\partial_\kappa \mathcal{A}) \cdot \chi$ terms cancel, giving

$$\partial_\kappa \Gamma_\kappa[\chi] \Big|_\chi = -\partial_\kappa W_\kappa[\mathcal{A}] \Big|_\mathcal{A} - \frac{1}{2} \chi \cdot \partial_\kappa \mathbf{R}_\kappa \cdot \chi,$$

where in the end we will express all \mathcal{A} dependence in terms of χ . Plugging in the flow equation for $\partial_\kappa W_\kappa$ gives

$$\partial_\kappa \Gamma_\kappa[\chi] \Big|_\chi = - \sum_{ij} \int dt dt' \left\{ \partial_\kappa J_{\kappa;ij}(t-t') \frac{\delta^2 W_\kappa[\mathcal{A}]}{\delta h_i(t) \delta \tilde{j}_j(t')} + \frac{\delta W_\kappa[\mathcal{A}]}{\delta h_i(t)} \partial_\kappa J_{\kappa;ij}(t-t') \frac{\delta W_\kappa[\mathcal{A}]}{\delta \tilde{j}_j(t')} \right\} - \frac{1}{2} \chi \cdot \partial_\kappa \mathbf{R}_\kappa \cdot \chi.$$

We identify $\frac{\delta W_\kappa[\mathcal{A}]}{\delta h_i(t)} = \tilde{\psi}_i(t)$ and $\frac{\delta W_\kappa[\mathcal{A}]}{\delta \tilde{j}_j(t')} = \nu_j(t')$, and realize that this term can be canceled if we choose $-\frac{1}{2} \chi \cdot \partial_\kappa \mathbf{R}_\kappa \cdot \chi = \tilde{\psi} \cdot \partial_\kappa \mathbf{J}_\kappa \cdot \nu$. (The factor of 1/2 comes from the implicit sum over the 4 field indices, which gives $\frac{1}{2} \chi \cdot \partial_\kappa \mathbf{R}_\kappa \cdot \chi = \frac{1}{2} \tilde{\psi} \cdot \partial_\kappa \mathbf{R}_\kappa \nu + \frac{1}{2} \nu \cdot \partial_\kappa \mathbf{R}_\kappa \cdot \tilde{\psi}$). If we write \mathbf{R}_κ as $\mathbf{R}_\kappa(t, t')$, a set 4×4 matrices of $N \times N$ blocks evaluated at times t and t' , it then has the form

$$\partial_\kappa \mathbf{R}_\kappa(t, t') = - \begin{bmatrix} \mathbf{0}_{N \times N} & \mathbf{0}_{N \times N} & \mathbf{0}_{N \times N} & \partial_\kappa \mathbf{J}_\kappa(t-t') \\ \mathbf{0}_{N \times N} & \mathbf{0}_{N \times N} & \mathbf{0}_{N \times N} & \mathbf{0}_{N \times N} \\ \mathbf{0}_{N \times N} & \mathbf{0}_{N \times N} & \mathbf{0}_{N \times N} & \mathbf{0}_{N \times N} \\ \partial_\kappa \mathbf{J}_\kappa^T(t-t') & \mathbf{0}_{N \times N} & \mathbf{0}_{N \times N} & \mathbf{0}_{N \times N} \end{bmatrix},$$

where the ordering of the χ indices from left to right and top to bottom is $\tilde{\psi}, \psi, \tilde{\nu}, \nu$. In order to ensure that $\mathbf{R}_{\kappa=1}(t-t') = \mathbf{0}_{4N \times 4N}$, we require

$$\mathbf{R}_\kappa(t-t) = \begin{bmatrix} \mathbf{0}_{N \times N} & \mathbf{0}_{N \times N} & \mathbf{0}_{N \times N} & \mathbf{J}(t-t') - \mathbf{J}_\kappa(t-t') \\ \mathbf{0}_{N \times N} & \mathbf{0}_{N \times N} & \mathbf{0}_{N \times N} & \mathbf{0}_{N \times N} \\ \mathbf{0}_{N \times N} & \mathbf{0}_{N \times N} & \mathbf{0}_{N \times N} & \mathbf{0}_{N \times N} \\ \mathbf{J}^T(t-t) - \mathbf{J}_\kappa^T(t-t) & \mathbf{0}_{N \times N} & \mathbf{0}_{N \times N} & \mathbf{0}_{N \times N} \end{bmatrix}, \quad (\text{B7})$$

With this, we have

$$\partial_\kappa \Gamma_\kappa[\chi] = - \sum_{ij} \int dt dt' \partial_\kappa J_{\kappa;ij}(t-t') \frac{\delta^2 W_\kappa[\mathcal{A}]}{\delta h_i(t) \delta \tilde{j}_j(t')},$$

leaving only the task of expressing second-order derivatives of $W_\kappa[\mathcal{A}]$ in terms of derivatives of $\Gamma_\kappa[\chi]$. To do so, we begin with the definition of the χ fields as derivatives of $W_\kappa[\mathcal{A}]$. Indexing the fields \mathcal{A} and χ by Greek indices $\alpha \in \{1, 2, 3, 4\}$, corresponding to the orderings of $\mathcal{A} = \{h, \tilde{h}, j, \tilde{j}\}$ and $\chi = \{\tilde{\psi}, \psi, \tilde{\nu}, \nu\}$ (i.e., $\mathcal{A}_1 = h$, $\chi_1 = \tilde{\psi}$, etc.), we have

$$\begin{aligned} \chi_\alpha &= \frac{\partial W_\kappa[\mathcal{A}]}{\partial \mathcal{A}_\alpha} \\ \Rightarrow \frac{\partial \chi_\alpha}{\partial \chi_\beta} &= \frac{\partial}{\partial \chi_\beta} \frac{\partial W_\kappa[\mathcal{A}]}{\partial \mathcal{A}_\alpha} \\ \Rightarrow \delta_{\alpha\beta} &= \sum_\gamma \frac{\partial \mathcal{A}_\gamma}{\partial \chi_\beta} \frac{\partial^2 W_\kappa[\mathcal{A}]}{\partial \mathcal{A}_\gamma \partial \mathcal{A}_\alpha}. \end{aligned}$$

Recall that the definition of the modified Legendre transform defining $\Gamma_\kappa[\chi]$ requires that $\mathcal{A} = \frac{\partial \Gamma_\kappa}{\partial \chi} + \mathbf{R}_\kappa \cdot \chi$. Differentiating this with respect to χ and inserting the result into the above equation yields

$$\delta_{\alpha\beta} = \sum_\gamma \left[\frac{\partial^2 \Gamma_\kappa[\chi]}{\partial \chi_\gamma \partial \chi_\beta} + (R_\kappa)_{\gamma\beta} \right] \frac{\delta^2 W_\kappa[\mathcal{A}]}{\delta \mathcal{A}_\gamma \delta \mathcal{A}_\alpha}.$$

If we rewrite this in terms of $4N \times 4N$ block matrices at times t and t' , this equation takes the form

$$\mathbb{I}_{4N \times 4N} \delta(t-t') = \int dt'' \left[\mathbf{\Gamma}_\kappa^{(2)}(t, t'') + \mathbf{R}_\kappa(t, t'') \right] \mathcal{G}_\kappa(t'', t'), \quad (\text{B8})$$

where we have defined the (field-dependent) ‘‘propagator’’ $\mathcal{G}_\kappa(t, t')$ as the $4N \times 4N$ block matrix of second order partial derivatives of $W_\kappa[\mathcal{A}]$ expressed in terms of the fields χ , i.e., with components $\mathcal{G}_{\kappa;ij}^{\gamma,\alpha}(t'', t') \equiv \frac{\delta^2 W_\kappa[\mathcal{A}]}{\delta \mathcal{A}_{\gamma,i}(t'') \delta \mathcal{A}_{\alpha,j}(t')}$. We also define

$$\mathbf{\Gamma}_\kappa^{(2)}(t, t') = \begin{bmatrix} \mathbf{0}_{N \times N} & \mathbb{I}_{N \times N} \delta(t-t') & \mathbf{0}_{N \times N} & -\mathbf{J}(t-t') \\ \mathbb{I}_{N \times N} \delta(t'-t) & \partial_{\psi\psi} \Upsilon_\kappa(t, t') & \partial_{\psi\tilde{\nu}} \Upsilon_\kappa(t, t') & \mathbf{0}_{N \times N} \\ \mathbf{0}_{N \times N} & \partial_{\tilde{\nu}\psi} \Upsilon_\kappa(t', t) & \partial_{\tilde{\nu}\tilde{\nu}} \Upsilon_\kappa(t', t) & \mathbb{I}_{N \times N} \delta(t-t') \\ -\mathbf{J}^T(t'-t) & \mathbf{0}_{N \times N} & \mathbb{I}_{N \times N} \delta(t'-t) & \mathbf{0}_{N \times N} \end{bmatrix}, \quad (\text{B9})$$

from which we have

$$\mathbf{\Gamma}_\kappa^{(2)}(t, t') + \mathbf{R}_\kappa(t, t') = \begin{bmatrix} \mathbf{0}_{N \times N} & \mathbb{I}_{N \times N} \delta(t-t') & \mathbf{0}_{N \times N} & -\mathbf{J}_\kappa(t-t') \\ \mathbb{I}_{N \times N} \delta(t'-t) & \partial_{\psi\psi} \Upsilon_\kappa(t, t') & \partial_{\psi\tilde{\nu}} \Upsilon_\kappa(t, t') & \mathbf{0}_{N \times N} \\ \mathbf{0}_{N \times N} & \partial_{\tilde{\nu}\psi} \Upsilon_\kappa(t', t) & \partial_{\tilde{\nu}\tilde{\nu}} \Upsilon_\kappa(t', t) & \mathbb{I}_{N \times N} \delta(t-t') \\ -\mathbf{J}_\kappa^T(t'-t) & \mathbf{0}_{N \times N} & \mathbb{I}_{N \times N} \delta(t'-t) & \mathbf{0}_{N \times N} \end{bmatrix}, \quad (\text{B10})$$

with $(\partial_{\psi\tilde{\nu}} \Upsilon_\kappa(t, t'))_{ij} = \frac{\delta^2 \Upsilon_\kappa[\tilde{\nu}, \psi]}{\delta \psi_i(t) \delta \tilde{\nu}_j(t')}$ and $(\partial_{\tilde{\nu}\psi} \Upsilon_\kappa(t', t))_{ji} = \frac{\delta^2 \Upsilon_\kappa[\tilde{\nu}, \psi]}{\delta \tilde{\nu}_i(t) \delta \psi_j(t')}$ is its transpose; similarly for $\partial_{\psi\psi} \Upsilon_\kappa(t, t')$ and $\partial_{\tilde{\nu}\tilde{\nu}} \Upsilon_\kappa(t, t')$. Formally inverting Eq. (B8) yields the representation

$$\mathcal{G}_\kappa(t, t') = \left[\mathbf{\Gamma}_\kappa^{(2)} + \mathbf{R}_\kappa \right]^{-1}(t, t').$$

In principle, we only need the component of \mathcal{G}_κ that corresponds to $\delta^2 W_\kappa / \delta h \delta \tilde{j}$, but these components can be picked out by $\partial_\kappa \mathbf{R}_\kappa$, and it will be convenient to write the flow equation as a trace over both neural indices ij and field indices $\alpha\beta$, corresponding to the four χ fields. We thus need to arrange things so that all of the ‘‘outer’’ indices

are the same, as in $(A_{ij}(t', t))_{\alpha\beta}(B_{ji}(t, t'))_{\beta\alpha}$. Identifying $\mathcal{G}_{\kappa;ij}^{\tilde{\psi},\nu}(t, t') = \frac{\partial^2 W_\kappa[\mathcal{A}]}{\partial h_i(t) \partial \tilde{j}_j(t')}$, we have

$$\begin{aligned}
\partial_\kappa \Gamma_\kappa[\chi] &= - \sum_{ij} \int dt dt' \partial_\kappa J_{\kappa;ij}(t - t') \frac{\delta^2 W_\kappa[\mathcal{A}]}{\delta h_i(t) \delta \tilde{j}_j(t')} \\
&= - \sum_{ij} \int dt dt' \partial_\kappa J_{\kappa;ij}(t - t') (\mathcal{G}_{\kappa;ij}(t, t'))_{\tilde{\psi}\nu} \\
&= - \sum_{ij} \int dt dt' \partial_\kappa (J_{\kappa;ji}^T(t - t')) (\mathcal{G}_{\kappa;ij}(t, t'))_{\tilde{\psi}\nu} \text{ (write as transpose of } J \text{ to swap neuron indices } i \text{ and } j) \\
&= + \sum_{ij} \int dt dt' \partial_\kappa (R_{\kappa;ji}(t', t))_{\nu\tilde{\psi}} (\mathcal{G}_{\kappa;ij}(t, t'))_{\tilde{\psi}\nu} \text{ (using the definition of } \partial_\kappa \mathbf{R}_\kappa(t, t') \text{ above; note order of time indices)} \\
&= + \sum_{ij\alpha\beta} \int dt dt' \partial_\kappa (R_{\kappa;ji}(t', t))_{\beta\alpha} (\mathcal{G}_{\kappa;ij}(t, t'))_{\alpha\beta} \text{ (using the fact that } R_{\alpha\beta} = 0 \text{ for any other components)} \\
&= \frac{1}{2} \sum_{ij\alpha\beta} \int dt dt' (\partial_\kappa (R_{\kappa;ji}(t', t))_{\beta\alpha} (\mathcal{G}_{\kappa;ij}(t, t'))_{\alpha\beta} + \partial_\kappa (R_{\kappa;ji}(t', t))_{\beta\alpha} (\mathcal{G}_{\kappa;ij}(t, t'))_{\alpha\beta}) \text{ (trivial duplication)} \\
&= \frac{1}{2} \sum_{ij\alpha\beta} (\partial_\kappa (R_{\kappa;ji}(t', t))_{\beta\alpha} (\mathcal{G}_{\kappa;ij}(t, t'))_{\alpha\beta} + \partial_\kappa (R_{\kappa;ij}(t, t'))_{\alpha\beta} (\mathcal{G}_{\kappa;ji}(t', t))_{\beta\alpha}) \\
&\quad \text{(relabelled all pairs of dummy indices in second term)}
\end{aligned}$$

Finally, we can recognize the expression as a trace over both the field indices α and β and the neuron indices i and j (as well as the time indices, but we will keep those explicit for a moment). We can thus write this expression as a trace over the $4N \times 4N$ block-matrix $\partial_\kappa \mathbf{R}_\kappa(t', t)$ and $\mathcal{G}_\kappa(t, t')$, giving

$$\partial_\kappa \Gamma_\kappa[\chi] = \frac{1}{2} \int dt dt' \text{tr} \left[\partial_\kappa \mathbf{R}_\kappa(t', t) \mathcal{G}_\kappa(t, t') \right], \quad (\text{B11})$$

where we the sums over neural indices ij and field indices $\alpha\beta$ are part of the matrix trace tr . We can include the time integrals in a “super-trace” Tr and write the flow equation in the form

$$\partial_\kappa \Gamma_\kappa[\chi] = \frac{1}{2} \text{Tr} \left[\partial_\kappa \mathbf{R}_\kappa \cdot \left[\mathbf{\Gamma}_\kappa^{(2)} + \mathbf{R}_\kappa \right]^{-1} \right] \quad (\text{B12})$$

This is formally the same as the Wetterich flow equation obtained in other NPRG work. This is why it was crucial to introduce the membrane potential fields as separate variables rather than integrating them out: it rendered the interaction term bilinear, allowing us to use it as the evolution operator.

The initial condition for the flow equation is given by

$$\begin{aligned}
\Gamma_{\kappa=0}[\chi] &= -W_{\kappa=0}[\mathcal{A}] + \mathcal{A} \cdot \chi - \frac{1}{2} \chi \cdot \mathbf{R}_{\kappa=0} \cdot \chi \\
&= \sum_i \int_{-\infty}^{\infty} dt \left\{ \tilde{\psi}_i(t) \left[\psi_i(t) - \mathcal{E}_i(t) - \sum_{j=1}^N \int_{-\infty}^{\infty} dt' J_{ij}(t - t') \nu_j(t') \right] + \tilde{\nu}_i(t) \nu_i(t) - \left(e^{\tilde{\nu}_i(t)} - 1 \right) \phi(\psi_i(t)) \right\}.
\end{aligned}$$

Note that the initial condition is *not* the AEA for the free theory, but is instead equal to the bare action evaluated at the fields χ . The average effective action being equal to the bare action corresponds to mean field theory. Thus, although the flow equations for $\mathcal{Z}_\kappa[\mathcal{A}]$ and $W_\kappa[\mathcal{A}]$ flow from the free theory for independent neurons towards the true theory, due to the modified Legendre transform the flow equation for $\Gamma_\kappa[\chi]$ interpolates from mean field theory to the true theory.

It is worth stressing that the flow equation Eq. (B12) is formally exact. It is much too difficult to solve, but forms the basis for tractable approximations. One of the most common approximations involves making an *ansatz* for the form of $\Gamma_\kappa[\chi]$. The success of this approach requires picking a suitable ansatz; to assist in restricting the form of $\Gamma_\kappa[\chi]$ we derive two Ward-Takahashi identities, below.

Appendix C: Derivation of the Ward-Takahashi identities

Two Ward-Takahashi identities can be derived for this model, allowing us to restrict the form of $\Gamma[\chi]$ and simplify the renormalization group flow. To do so, we derive two additional representations of $\mathcal{Z}[\mathcal{A}]$ by integrating out either the membrane potential fields $\{\tilde{V}, V\}$ or the spike fields $\{\tilde{n}, \dot{n}\}$. Integrating out the membrane potential fields yields

$$\mathcal{Z}[\mathcal{A}] = e^{\sum_i \int dt \tilde{h}_i(t)(h_i(t) + \mathcal{E}_i(t))} \int \mathcal{D}[\tilde{n}, \dot{n}] e^{-S_{\text{spike}}[\tilde{n}, \dot{n}; h] + \sum_i \int dt \{j_i(t)\tilde{n}_i(t) + (\tilde{j}_i(t) + \sum_j \int dt' \tilde{h}_j(t') J_{ji}(t' - t))\dot{n}_i(t)\}}, \quad (\text{C1})$$

where

$$S_{\text{spike}}[\tilde{n}, \dot{n}; h] = \sum_i \int dt \left[\tilde{n}_i(t)\dot{n}_i(t) - \left(e^{\tilde{n}_i(t)} - 1 \right) \phi \left(\sum_j \int dt' J_{ij}(t - t') \dot{n}_j(t') + \mathcal{E}_i(t) + h_i(t) \right) \right]$$

is the effective spike-only action with the source field $h_i(t)$ contributing to the input. For $h_i(t) = 0$ this is the action derived in [23]. Differentiating Eq. (C1) with respect to $\tilde{h}_i(t)$ gives

$$\frac{\delta \mathcal{Z}[\mathcal{A}]}{\delta \tilde{h}_i(t)} = (h_i(t) + \mathcal{E}_i(t))\mathcal{Z}[\mathcal{A}] + \sum_j \int dt' J_{ij}(t - t') \frac{\delta \mathcal{Z}[\mathcal{A}]}{\delta \tilde{j}_j(t')}$$

Inserting $Z[\mathcal{A}] = \exp(W[\mathcal{A}])$ yields an identity for the CGF,

$$\frac{\delta W[\mathcal{A}]}{\delta \tilde{h}_i(t)} = h_i(t) + \mathcal{E}_i(t) + \sum_j \int dt' J_{ij}(t - t') \frac{\delta W[\mathcal{A}]}{\delta \tilde{j}_j(t')}. \quad (\text{C2})$$

(The factor $\exp(W)$ cancels out after applying the derivatives). Recognizing $\psi_i(t) = \frac{\delta W[\mathcal{A}]}{\delta h_i(t)}$, $\nu_j(t') = \frac{\delta W[\mathcal{A}]}{\delta \tilde{j}_j(t')}$, and $h_i(t) = \frac{\delta \Gamma[\chi]}{\delta \tilde{\psi}_i(t)}$, we can re-write this identity as

$$\psi_i(t) = \frac{\delta \Gamma[\chi]}{\delta \tilde{\psi}_i(t)} + \mathcal{E}_i(t) + \sum_j \int dt' J_{ij}(t - t') \nu_j(t').$$

Integrating with respect to $\tilde{\psi}_i(t)$ gives

$$\Gamma[\chi] = \sum_i \int_{-\infty}^{\infty} dt \tilde{\psi}_i(t) \left(\psi_i(t) - \mathcal{E}_i(t) - \sum_j J_{ij}(t - t') \nu_j(t') \right) + \text{terms independent of } \tilde{\psi}.$$

To derive the second Ward-Takahashi identity, we integrate out the spike fields $\{\tilde{n}, \dot{n}\}$ to obtain the representation

$$\mathcal{Z}[\mathcal{A}] = e^{\sum_i \int dt j_i(t)\tilde{j}_i(t)} \int \mathcal{D}[\tilde{V}, V] e^{-S_{\text{volt}}[\tilde{V}, V; \tilde{j}, h] + \sum_i \int dt \{\tilde{V}_i(t)[h_i(t) + \mathcal{E}_i(t) + \sum_j \int dt' J_{ij}(t - t') j_j(t')] + \tilde{h}_i(t)V_i(t)\}}, \quad (\text{C3})$$

where the action for the membrane potentials is

$$S_{\text{volt}}[\tilde{V}, V; \tilde{j}, h] = \sum_i \int dt \left\{ \tilde{V}_i(t)V_i(t) - \phi(V_i(t)) \left(e^{\tilde{j}_i(t) + \sum_j \int dt' \tilde{V}_j(t') J_{ji}(t' - t)} - 1 \right) \right\}.$$

Differentiating Eq. (C3) with respect to $j_i(t)$ yields the identity

$$\frac{\delta \mathcal{Z}[\mathcal{A}]}{\delta j_i(t)} = \tilde{j}_i(t)\mathcal{Z}[\mathcal{A}] + \sum_j \int dt' \frac{\delta \mathcal{Z}[\mathcal{A}]}{\delta h_j(t')} J_{ji}(t' - t).$$

Inserting $\mathcal{Z}[\mathcal{A}] = \exp(W[\mathcal{A}])$ yields another identity for the CGF,

$$\frac{\delta W[\mathcal{A}]}{\delta j_i(t)} = \tilde{j}_i(t) + \sum_j \int dt' \frac{\delta W[\mathcal{A}]}{\delta h_j(t')} J_{ji}(t' - t). \quad (\text{C4})$$

Using $\tilde{\nu}_i(t) = \frac{\delta W}{\delta j_i(t)}$, $\tilde{\psi}_i(t) = \frac{\delta W}{\delta h_i(t)}$, and $\tilde{j}_i(t) = \frac{\delta \Gamma}{\delta \nu_i(t)}$ we can turn this into an identity for the effective action,

$$\tilde{\nu}_i(t) = \frac{\delta \Gamma}{\delta \nu_i(t)} + \sum_j \int dt' \tilde{\psi}_j(t') J_{ji}(t - t').$$

Integrating with respect to the fields ν gives

$$\Gamma[\chi] = \sum_i \int_{-\infty}^{\infty} dt \left\{ \tilde{\nu}_i(t) \nu_i(t) - \tilde{\psi}_i(t) \sum_j \int_{-\infty}^{\infty} dt' J_{ij}(t - t') \nu_j(t') \right\} + \text{terms independent of } \nu.$$

Putting our two identities together yields the general form of the average effective action quoted in the main text,

$$\Gamma[\tilde{\psi}, \psi, \tilde{\nu}, \nu] = \sum_i \int_{-\infty}^{\infty} dt \left\{ \tilde{\psi}_i(t) \left(\psi_i(t) - \mathcal{E}_i(t) - \sum_j J_{ij}(t - t') \nu_j(t') \right) + \tilde{\nu}_i(t) \nu_i(t) \right\} + \Upsilon[\tilde{\nu}, \psi], \quad (\text{C5})$$

where $\Upsilon[\tilde{\nu}, \psi]$ is an unknown functional of the fields $\tilde{\nu}$ and ψ only. Comparing to the bare action in Eq. (5) this result demonstrates that only the term $\sum_i \int dt (e^{\tilde{\nu}_i(t)} - 1) \phi(V_i(t))$ is renormalized by the stochastic fluctuations of the model. Thus, the most general form of the ansatz for our flow equation is

$$\Gamma_{\kappa}[\chi] = \sum_i \int_{-\infty}^{\infty} dt \left\{ \tilde{\psi}_i(t) \left(\psi_i(t) - \mathcal{E}_i(t) - \sum_j J_{ij}(t - t') \nu_j(t') \right) + \tilde{\nu}_i(t) \nu_i(t) \right\} + \Upsilon_{\kappa}[\tilde{\nu}, \psi]. \quad (\text{C6})$$

We therefore need only compute the renormalization group flow of the unknown functional $\Upsilon_{\kappa}[\tilde{\nu}, \psi]$.

In principle, we could try to restrict the form of $\Upsilon[\tilde{\nu}, \psi]$ further by differentiating $\mathcal{Z}[\mathcal{A}]$ with respect to the remaining source fields $h_i(t)$ and $\tilde{j}_i(t)$. The first of these choices turns out to correspond to an encoding of a shift symmetry of the membrane potential, reflecting the fact that only membrane potential differences are physically meaningful, while the second does not yield a tractable expression that can be turned into another identity. Let us show this briefly.

For the first case, as we have claimed that it will encode a shift symmetry, it is useful to make explicit an offset in the nonlinearity, setting $\phi(V) \rightarrow \phi(V - V_0)$, for a constant V_0 , and also making this explicit in $\Upsilon[\tilde{\nu}, \psi - V_0]$. Then, we may proceed by differentiating Eq. (C1) with respect to $h_i(t)$ to obtain

$$\frac{\delta \mathcal{Z}[\mathcal{A}]}{\delta h_i(t)} = \int \mathcal{D}[\tilde{n}, \dot{n}] \left\{ \tilde{h}_i(t) + \phi' \left(\mathcal{E}_i + \sum_j \int dt' J_{ij}(t - t') \dot{n}_j(t') + h_i(t) - V_0 \right) \right\} e^{-S_{\text{spike}}[\tilde{n}, \dot{n}; h] + \tilde{n} \cdot j + \dot{n} \cdot \tilde{j}}$$

We can eliminate the nonlinear term by summing over i and integrating over time,

$$\begin{aligned} & \sum_i \int dt \frac{\delta \mathcal{Z}[\mathcal{A}]}{\delta h_i(t)} \\ &= \int \mathcal{D}[\tilde{n}, \dot{n}] \left\{ \sum_i \int dt \tilde{h}_i(t) + \sum_i \int dt \phi' \left(\mathcal{E}_i + \sum_j \int dt' J_{ij}(t - t') \dot{n}_j(t') + h_i(t) - V_0 \right) \right\} e^{-S_{\text{spike}}[\tilde{n}, \dot{n}; h] + \tilde{n} \cdot j + \dot{n} \cdot \tilde{j}} \\ &= \int \mathcal{D}[\tilde{n}, \dot{n}] \left\{ \sum_i \int dt \tilde{h}_i(t) - \frac{\partial}{\partial V_0} \right\} e^{-S_{\text{spike}}[\tilde{n}, \dot{n}; h] + \tilde{n} \cdot j + \dot{n} \cdot \tilde{j}} \\ &= \left\{ \sum_i \int dt \tilde{h}_i(t) - \frac{\partial}{\partial V_0} \right\} \mathcal{Z}[\mathcal{A}] \end{aligned}$$

Plugging in $\mathcal{Z}[\mathcal{A}] = \exp(\mathcal{W}[\mathcal{A}])$ yields

$$\begin{aligned} \sum_i \int dt \frac{\delta \mathcal{W}[\mathcal{A}]}{\delta h_i(t)} &= \int \mathcal{D}[\tilde{n}, \dot{n}] \left\{ \sum_i \int dt \tilde{h}_i(t) - \frac{\partial}{\partial V_0} \right\} e^{-S_{\text{spike}}[\tilde{n}, \dot{n}; h] + \tilde{n} \cdot j + \dot{n} \cdot \tilde{j}} \\ &= \sum_i \int dt \tilde{h}_i(t) - \frac{\partial \mathcal{W}[\mathcal{A}]}{\partial V_0} \\ \Rightarrow \sum_i \int dt \tilde{\psi}_i(t) &= \left\{ \sum_i \int dt \frac{\delta \Gamma[\chi]}{\delta \psi_i(t)} + \frac{\partial \Gamma[\chi]}{\partial V_0} \right\} \end{aligned}$$

where we used the fact that $\frac{\partial \mathcal{W}[\mathcal{A}]}{\partial V_0} \Big|_{\mathcal{A}} = -\frac{\partial \Gamma[\chi]}{\partial V_0} \Big|_{\chi}$ (which holds for any parameter, not just V_0). Plugging in our general form of $\Gamma[\chi] = \tilde{\psi} \cdot (\psi - \mathcal{E} - J \cdot \nu) + \tilde{\nu} \cdot \nu + \Upsilon[\tilde{\nu}, \psi - V_0]$ yields the identity

$$\sum_i \int dt \frac{\delta \Upsilon[\tilde{\nu}, \psi - V_0]}{\delta \psi_i(t)} = -\frac{\partial \Upsilon[\tilde{\nu}, \psi - V_0]}{\partial V_0}$$

However, this identity trivially follows from the chain rule:

$$\begin{aligned} \frac{\partial \Upsilon[\tilde{\nu}, \psi - V_0]}{\partial V_0} &= \sum_i \int dt \frac{\delta \Upsilon[\tilde{\nu}, \psi - V_0]}{\delta (\psi_i(t) - V_0)} \frac{\partial (\psi_i(t) - V_0)}{\partial V_0} \\ &= -\sum_i \int dt \frac{\delta \Upsilon[\tilde{\nu}, \psi - V_0]}{\delta \psi_i(t)} \end{aligned}$$

Therefore, by explicitly including the shift V_0 in $\Upsilon[\tilde{\nu}, \psi - V_0]$ we have already accounted for this identity, and no further constraints on Υ are obtained. We note that this identify reflects the fact that only differences in membrane potentials are meaningful, which can be encoded as a symmetry $V_i(t) \rightarrow V_i(t) + \theta$, $\mathcal{E}_i \rightarrow \mathcal{E}_i + \theta$, and $V_0 \rightarrow V_0 + \theta$, for any constant θ . We are therefore free to make the choice $V_0 = 0$, as in the main text.

The last straightforward identity we could try to derive by differentiating with respect to the last remaining source field, $\tilde{j}_i(t)$, turns out to not be tractable. Differentiating Eq. (C3) with respect to $\tilde{j}_i(t)$,

$$\frac{\delta \mathcal{Z}[\mathcal{A}]}{\delta \tilde{j}_i(t)} = \int \mathcal{D}[\tilde{V}, V] \left\{ j_i(t) + \phi(V_i(t)) e^{\tilde{j}_i(t) + \sum_j \int dt' \tilde{V}_j(t') J_{j,i}(t' - t)} \right\} e^{-S_{\text{volt}}[\tilde{V}, V; j] + \tilde{V} \cdot h + V \cdot \tilde{h}}$$

Unfortunately, it does not appear that this can be reduced to an identity by summing over i and t and differentiating with respect to some parameter. For example, the nonlinear term can be partly simplified by setting $\phi(V) \rightarrow \beta \phi(V)$, making explicit a firing rate amplitude β , but at best this could be reduced to

$$\sum_i \int dt \frac{\delta \mathcal{Z}[\mathcal{A}]}{\delta \tilde{j}_i(t)} = \int \mathcal{D}[\tilde{V}, V] \left\{ j_i(t) + \beta \frac{\partial}{\partial \beta} + \beta \phi(V_i(t)) \right\} e^{-S_{\text{volt}}[\tilde{V}, V; j] + \tilde{V} \cdot h + V \cdot \tilde{h}},$$

which does not yield a tractable form of an identity that could further restrict $\Upsilon[\tilde{\nu}, \psi]$. Therefore, the most general form of the average effective action we have derived is

$$\Gamma[\tilde{\psi}, \psi, \tilde{\nu}, \nu] = \sum_i \int dt \left\{ \tilde{\psi}_i(t) \left[\psi_i(t) - \mathcal{E}_i(t) - \sum_j \int dt' J_{i,j}(t - t') \nu_j(t') \right] + \tilde{\nu}_i(t) \nu_i(t) \right\} + \Upsilon[\tilde{\nu}, \psi - V_0],$$

and we set $V_0 = 0$ as our reference point for the potential. Our ansatz for the renormalization group flow is implemented by allowing $\Upsilon_{\Lambda}[\tilde{\nu}, \psi]$ to run with the renormalization scale Λ .

Before we turn to our approximation scheme for Υ_{Λ} , a couple of remarks are in order. First, we note that the identities obtained here could be derived more succinctly by perturbing the fields $\tilde{V}_i(t) \rightarrow \tilde{V}_i(t) + \epsilon_i(t)$, $\dot{n}_i(t) \rightarrow \dot{n}_i(t) + \epsilon_i(t)$, and $V_i(t) \rightarrow V_i(t) + \epsilon$ for some infinitesimals $\epsilon_i(t)$ and ϵ , which is the standard approach [36]. However, this shift method does not work for the spike fields in the underlying discrete time theory, in which $\dot{n}_i(t)$ is the limit of $\Delta n_{it}/\Delta t$, where Δt is the time bin size and Δn_{it} is a non-negative integer corresponding to the number of spikes fired by neuron i in time bin t . As such, Δn_{it} could only be shifted by an integer quantity, which would change the range

of summation in the discrete-time formulation, rendering it unclear that shifting the fields produces a valid identity. The derivation of the Ward-Takahashi identities by differentiating the moment generating functional, however, carries through the same way in the discrete-time formulation, providing a solid foundation for the Ward-Takahashi identities.

The second important remark is that these Ward-Takahashi identities will not hold if the dynamics of the membrane potential are nonlinear; i.e., if $f(V)$ in Eq. (A1) is not linear in $V_i(t)$. Such a nonlinearity would introduce higher-order derivatives of $W[\mathcal{A}]$ that spoil the conversion to identities for $\Gamma[\chi]$. This would not prevent application of the NPRG method, but it means that more terms in the bare action are no longer protected from renormalization, and one's ansatz for $\Gamma_\kappa[\chi]$ may need to allow for additional mixing of the four fields. This would allow for additional contributions to anomalous dimensions.

Appendix D: Local potential approximation and derivation of the flow equation

To proceed with the NPRG method we must make some approximation to reduce the Wetterich equation to something that is tractable to solve. To this end, we follow the spirit of early NPRG approaches by making a “local potential approximation,” which amounts to assuming that the unknown functional $\Upsilon_\kappa[\tilde{\nu}, \psi]$ depends only on $\tilde{\nu}_i(t)$ and $\psi_i(t)$ at a single neural index i and time t :

$$\Upsilon_\kappa^{\text{LPA}}[\tilde{\nu}, \psi] = - \sum_{i=1}^N \int_{-\infty}^{\infty} dt U_\kappa(\tilde{\nu}_i(t), \psi_i(t)), \quad (\text{D1})$$

which defines the effective potential $U_\kappa(\tilde{\nu}_i(t), \psi_i(t))$, which has initial condition

$$U_{\kappa=0}(\tilde{\nu}_i(t), \psi_i(t)) = (e^{\tilde{\nu}_i(t)} - 1) \phi(\psi_i(t)).$$

Note that, as in the bare action, interactions between neurons result entirely from the synaptic coupling term $\tilde{\psi} \cdot J \cdot \nu$ in $\Gamma[\chi]$.

As the neurons are statistically homogeneous with the same bare rate nonlinearity $\phi(y)$, we similarly assume the local potential is the same for all neurons. We can isolate it by evaluating $\Upsilon_\kappa^{\text{LPA}}[\tilde{\nu}, \psi]$ at homogeneous fields $\tilde{\nu}_i(t) = \tilde{x}$ and $\psi_i(t) = y$:

$$-\Upsilon_\kappa[\tilde{\nu}, \psi] = NTU_\kappa(\tilde{x}, y)\Delta t.$$

The prefactors are N , the number of neurons, and T , the formally infinite duration of the spike train, i.e., $T = \int_{-\infty}^{\infty} dt 1$. These factors will ultimately cancel out in our reduced flow equation for $U_\kappa(\tilde{x}, y)$.

Inserting the local potential approximation into the Wetterich flow equation (Eq. (B12)) and setting $\tilde{\nu}_i(t) = \tilde{x}$ and $\psi_i(t) = y$ yields

$$-NT\partial_\kappa U_\kappa(\tilde{x}, y) = \frac{1}{2}\text{Tr} \left[\partial_\kappa \mathbf{R}_\kappa \cdot \mathcal{G}_\kappa \Big|_{\tilde{\nu}=\tilde{x}, \psi=y} \right].$$

We need to evaluate \mathcal{G}_κ at the homogeneous fields, using the fact that \mathcal{G}_κ is defined as the inverse of $\mathbf{\Gamma}_\kappa^{(2)} + \mathbf{R}_\kappa$.

Evaluated at homogeneous fields,

$$\mathbf{\Gamma}_\kappa^{(2)}(t, t') = \begin{bmatrix} \mathbf{0}_{N \times N} & \mathbb{I}_{N \times N} \delta(t - t') & \mathbf{0}_{N \times N} & -\mathbf{J}(t - t') \\ \mathbb{I}_{N \times N} \delta(t' - t) & -U_\kappa^{(0,2)}(\tilde{x}, y) \delta(t - t') & -U_\kappa^{(1,1)}(\tilde{x}, y) \delta(t - t') & \mathbf{0}_{N \times N} \\ \mathbf{0}_{N \times N} & -U_\kappa^{(1,1)}(\tilde{x}, y) \delta(t' - t) & -U_\kappa^{(2,0)}(\tilde{x}, y) \delta(t - t') & \mathbb{I}_{N \times N} \delta(t - t') \\ -\mathbf{J}^T(t' - t) & \mathbf{0}_{N \times N} & \mathbb{I}_{N \times N} \delta(t - t') & \mathbf{0}_{N \times N} \end{bmatrix}$$

where $U_\kappa^{(a,b)}(\tilde{x}, y) = \partial_{\tilde{x}}^a \partial_y^b U_\kappa(\tilde{x}, y)$ for brevity. Adding in our $\mathbf{R}_\kappa(t, t')$ we have

$$\mathbf{\Gamma}_\kappa^{(2)}(t, t') + \mathbf{R}_\kappa(t, t') = \begin{bmatrix} \mathbf{0}_{N \times N} & \mathbb{I}_{N \times N} \delta(t - t') & \mathbf{0}_{N \times N} & -\mathbf{J}_\kappa(t - t') \\ \mathbb{I}_{N \times N} \delta(t' - t) & -U_\kappa^{(0,2)}(\tilde{x}, y) \delta(t - t') & -U_\kappa^{(1,1)}(\tilde{x}, y) \delta(t - t') & \mathbf{0}_{N \times N} \\ \mathbf{0}_{N \times N} & -U_\kappa^{(1,1)}(\tilde{x}, y) \delta(t' - t) & -U_\kappa^{(2,0)}(\tilde{x}, y) \delta(t - t') & \mathbb{I}_{N \times N} \delta(t - t') \\ -\mathbf{J}_\kappa^T(t' - t) & \mathbf{0}_{N \times N} & \mathbb{I}_{N \times N} \delta(t - t') & \mathbf{0}_{N \times N} \end{bmatrix}.$$

It is not easy to find the inverse of this function in this form, as we must take the inverse over both matrix components and time. To this end, we now make use of the fact that, having evaluated $\tilde{\nu}_i(t)$ and $\psi_i(t)$ at time-independent homogeneous values \tilde{x} and y , our model is time-translation invariant; i.e., all remaining time-dependent functions only depend on the difference in times $t - t'$. We can then express these functions in frequency space, in which they will become diagonal in frequency, and the equation defining the propagator will reduce to a relatively simple matrix inversion.

Let

$$\mathcal{G}_\kappa(t - t') = \int_{-\infty}^{\infty} \frac{d\omega}{2\pi} e^{-i\omega(t-t')} \mathcal{G}_\kappa(\omega)$$

and

$$\mathbf{R}_\kappa(t - t') = \int_{-\infty}^{\infty} \frac{d\omega}{2\pi} e^{-i\omega(t-t')} \mathbf{R}_\kappa(\omega).$$

Inserting these into the flow equation gives

$$\begin{aligned} & \int_{-\infty}^{\infty} dt dt' \partial_\kappa \mathbf{R}_\kappa(t' - t) \mathcal{G}_\kappa(t - t') \\ &= \int_{-\infty}^{\infty} dt dt' \int_{-\infty}^{\infty} \frac{d\omega_1 d\omega_2}{(2\pi)^2} \partial_\kappa \mathbf{R}_\kappa(\omega_1) \mathcal{G}_\kappa(\omega_2) e^{-i\omega_1(t'-t) - i\omega_2(t-t')} \\ &= \int_{-\infty}^{\infty} \frac{d\omega_1 d\omega_2}{(2\pi)^2} \partial_\kappa \mathbf{R}_\kappa(\omega_1) \mathcal{G}_\kappa(\omega_2) \int_{-\infty}^{\infty} dt e^{-it(\omega_2 - \omega_1)} \int_{-\infty}^{\infty} dt' e^{-it'(\omega_1 - \omega_2)} \\ &= \int_{-\infty}^{\infty} \frac{d\omega_1 d\omega_2}{(2\pi)^2} \partial_\kappa \mathbf{R}_\kappa(\omega_1) \mathcal{G}_\kappa(\omega_2) \int_{-\infty}^{\infty} dt e^{-it(\omega_2 - \omega_1)} 2\pi \delta(\omega_1 - \omega_2) \\ &= \int_{-\infty}^{\infty} \frac{d\omega}{2\pi} \partial_\kappa \mathbf{R}_\kappa(\omega) \mathcal{G}_\kappa(\omega) \int_{-\infty}^{\infty} dt e^{-it \times 0}; \end{aligned}$$

where the delta functions imposed $\omega \equiv \omega_1 = \omega_2$, and we identify $\int_{-\infty}^{\infty} dt e^{-it \times 0} = T$, the formally infinite length of our spike train. This cancels with the factor of T in $-NT \partial_\kappa U_\kappa(\tilde{x}, y)$ on the left hand side of the flow equation, and hence write the flow equation for $U_\kappa(\tilde{x}, y)$ thus far as

$$\partial_\kappa U_\kappa(\tilde{x}, y) = -\frac{1}{2N} \int_{-\infty}^{\infty} \frac{d\omega}{2\pi} \text{tr} \left[\partial_\kappa \mathbf{R}_\kappa(\omega) \mathcal{G}_\kappa(\omega) \Big|_{\tilde{\nu}=\tilde{x}, \psi=y} \right]$$

where the lowercase tr trace is over matrix indices only (i.e., the neural indices). Now what remains is to determine $\mathcal{G}_\kappa(\omega) \Big|_{\tilde{\nu}=\tilde{x}, \psi=y}$. We can express Eq. (B8) in Fourier space as

$$\mathbb{I}_{4N \times 4N} = \left[\mathbf{\Gamma}_\kappa^{(2)}(\omega) + \mathbf{R}_\kappa(\omega) \right] \mathcal{G}_\kappa(\omega),$$

where in Fourier space

$$\mathbf{\Gamma}_\kappa^{(2)}(\omega) + \mathbf{R}_\kappa(\omega) = \begin{bmatrix} \mathbf{0}_{N \times N} & \mathbb{I}_{N \times N} & \mathbf{0}_{N \times N} & -\mathbf{J}_\kappa(\omega) \\ \mathbb{I}_{N \times N} & -U_\kappa^{(0,2)}(\tilde{x}, y) \mathbb{I}_{N \times N} & -U_\kappa^{(1,1)}(\tilde{x}, y) \mathbb{I}_{N \times N} & \mathbf{0}_{N \times N} \\ \mathbf{0}_{N \times N} & -U_\kappa^{(1,1)}(\tilde{x}, y) \mathbb{I}_{N \times N} & -U_\kappa^{(2,0)}(\tilde{x}, y) \mathbb{I}_{N \times N} & \mathbb{I}_{N \times N} \\ -\mathbf{J}_\kappa^T(-\omega) & \mathbf{0}_{N \times N} & \mathbb{I}_{N \times N} & \mathbf{0}_{N \times N} \end{bmatrix}.$$

Inverting this matrix will yield $\mathcal{G}_\kappa(\omega)$. Although the matrix is $4N \times 4N$, it is possible to invert it due to its simple structure. We are interested in synaptic interactions of the form $\mathbf{J}_\kappa(\omega) = \mathbf{J}_\kappa g(\omega)$, equivalent to $\mathbf{J}_\kappa(t - t') = \mathbf{J}_\kappa g(t - t')$ in the time domain. Here, \mathbf{J}_κ (with time or frequency arguments) is an $N \times N$ time-independent synaptic weight matrix and $g(\omega)$ is the Fourier transform of the temporal waveform $g(t - t')$. At this point we make the assumption that the weight matrix is symmetric and diagonalizable, such that $\mathbf{J}_\kappa = \mathbf{P} \mathbf{D}_\kappa \mathbf{P}^{-1}$, where \mathbf{P} is a matrix comprised of the eigenvectors of the true weight matrix \mathbf{J} , such that $\mathbf{P}^{-1} = \mathbf{P}^T$, and \mathbf{D}_κ is a diagonal matrix of the regulated eigenvalues of \mathbf{J}_κ , which we label λ_κ . We do not regulate the projection matrix \mathbf{P} . The assumption of symmetric

connections allows us to diagonalize $\mathbf{\Gamma}_\kappa^{(2)}(\omega) + \mathbf{R}_\kappa(\omega)$ by

$$\begin{aligned} & \mathbf{\Gamma}_\kappa^{(2)}(\omega) + \mathbf{R}_\kappa(\omega) \\ &= \begin{bmatrix} \mathbf{P} & \mathbf{0} & \mathbf{0} & \mathbf{0} \\ \mathbf{0} & \mathbf{P} & \mathbf{0} & \mathbf{0} \\ \mathbf{0} & \mathbf{0} & \mathbf{P} & \mathbf{0} \\ \mathbf{0} & \mathbf{0} & \mathbf{0} & \mathbf{P} \end{bmatrix} \begin{bmatrix} \mathbf{0} & \mathbb{I} & \mathbf{0} & -\mathbf{D}_\kappa g(\omega) \\ \mathbb{I} & -U_\kappa^{(0,2)}(\tilde{x}, y)\mathbb{I} & -U_\kappa^{(1,1)}(\tilde{x}, y)\mathbb{I} & \mathbf{0} \\ \mathbf{0} & -U_\kappa^{(1,1)}(\tilde{x}, y)\mathbb{I} & -U_\kappa^{(2,0)}(\tilde{x}, y)\mathbb{I} & \mathbb{I} \\ -\mathbf{D}_\kappa g(-\omega) & \mathbf{0} & \mathbb{I} & \mathbf{0} \end{bmatrix} \begin{bmatrix} \mathbf{P}^{-1} & \mathbf{0} & \mathbf{0} & \mathbf{0} \\ \mathbf{0} & \mathbf{P}^{-1} & \mathbf{0} & \mathbf{0} \\ \mathbf{0} & \mathbf{0} & \mathbf{P}^{-1} & \mathbf{0} \\ \mathbf{0} & \mathbf{0} & \mathbf{0} & \mathbf{P}^{-1} \end{bmatrix}. \end{aligned}$$

We have dropped the $N \times N$ subscript on the matrices $\mathbf{0}_{N \times N}$ and $\mathbb{I}_{N \times N}$ to save space. The matrix $\mathcal{G}_\kappa(\omega)$ may therefore be written as

$$\mathcal{G}_\kappa(\omega) = \begin{bmatrix} \mathbf{P} & \mathbf{0} & \mathbf{0} & \mathbf{0} \\ \mathbf{0} & \mathbf{P} & \mathbf{0} & \mathbf{0} \\ \mathbf{0} & \mathbf{0} & \mathbf{P} & \mathbf{0} \\ \mathbf{0} & \mathbf{0} & \mathbf{0} & \mathbf{P} \end{bmatrix} \begin{bmatrix} \mathbf{0} & \mathbb{I} & \mathbf{0} & -\mathbf{D}_\kappa g(\omega) \\ \mathbb{I} & -U_\kappa^{(0,2)}(\tilde{x}, y)\mathbb{I} & -U_\kappa^{(1,1)}(\tilde{x}, y)\mathbb{I} & \mathbf{0} \\ \mathbf{0} & -U_\kappa^{(1,1)}(\tilde{x}, y)\mathbb{I} & -U_\kappa^{(2,0)}(\tilde{x}, y)\mathbb{I} & \mathbb{I} \\ -\mathbf{D}_\kappa g(-\omega) & \mathbf{0} & \mathbb{I} & \mathbf{0} \end{bmatrix}^{-1} \begin{bmatrix} \mathbf{P}^{-1} & \mathbf{0} & \mathbf{0} & \mathbf{0} \\ \mathbf{0} & \mathbf{P}^{-1} & \mathbf{0} & \mathbf{0} \\ \mathbf{0} & \mathbf{0} & \mathbf{P}^{-1} & \mathbf{0} \\ \mathbf{0} & \mathbf{0} & \mathbf{0} & \mathbf{P}^{-1} \end{bmatrix}.$$

We still have a $4N \times 4N$ matrix to invert; we will address this momentarily. First, we plug this expression in our flow equation, along with the diagonalized matrix $\partial_\kappa \mathbf{R}_\kappa(\omega)$:

$$\partial_\kappa \mathbf{R}_\kappa(\omega) = \begin{bmatrix} \mathbf{P} & \mathbf{0} & \mathbf{0} & \mathbf{0} \\ \mathbf{0} & \mathbf{P} & \mathbf{0} & \mathbf{0} \\ \mathbf{0} & \mathbf{0} & \mathbf{P} & \mathbf{0} \\ \mathbf{0} & \mathbf{0} & \mathbf{0} & \mathbf{P} \end{bmatrix} \begin{bmatrix} \mathbf{0} & \mathbb{I} & \mathbf{0} & -\partial_\kappa \mathbf{D}_\kappa g(\omega) \\ \mathbb{I} & \mathbf{0} & \mathbf{0} & \mathbf{0} \\ \mathbf{0} & \mathbf{0} & \mathbb{I} & \mathbf{0} \\ -\partial_\kappa \mathbf{D}_\kappa g(-\omega) & \mathbf{0} & \mathbb{I} & \mathbf{0} \end{bmatrix} \begin{bmatrix} \mathbf{P}^{-1} & \mathbf{0} & \mathbf{0} & \mathbf{0} \\ \mathbf{0} & \mathbf{P}^{-1} & \mathbf{0} & \mathbf{0} \\ \mathbf{0} & \mathbf{0} & \mathbf{P}^{-1} & \mathbf{0} \\ \mathbf{0} & \mathbf{0} & \mathbf{0} & \mathbf{P}^{-1} \end{bmatrix}.$$

The inner projection matrices will cancel, and then we may use the cyclic property of the trace to simplify the flow equation to

$$\begin{aligned} & \partial_\kappa U_\kappa(\tilde{x}, y) \\ &= -\frac{1}{2N} \int_{-\infty}^{\infty} \frac{d\omega}{2\pi} \text{tr} \left(\begin{bmatrix} \mathbf{0} & \mathbb{I} & \mathbf{0} & -\partial_\kappa \mathbf{D}_\kappa g(\omega) \\ \mathbb{I} & \mathbf{0} & \mathbf{0} & \mathbf{0} \\ \mathbf{0} & \mathbf{0} & \mathbb{I} & \mathbf{0} \\ -\partial_\kappa \mathbf{D}_\kappa g(-\omega) & \mathbf{0} & \mathbb{I} & \mathbf{0} \end{bmatrix} \begin{bmatrix} \mathbf{0} & \mathbb{I} & \mathbf{0} & -\mathbf{D}_\kappa g(\omega) \\ \mathbb{I} & -U_\kappa^{(0,2)}(\tilde{x}, y)\mathbb{I} & -U_\kappa^{(1,1)}(\tilde{x}, y)\mathbb{I} & \mathbf{0} \\ \mathbf{0} & -U_\kappa^{(1,1)}(\tilde{x}, y)\mathbb{I} & -U_\kappa^{(2,0)}(\tilde{x}, y)\mathbb{I} & \mathbb{I} \\ -\mathbf{D}_\kappa g(-\omega) & \mathbf{0} & \mathbb{I} & \mathbf{0} \end{bmatrix}^{-1} \right) \end{aligned}$$

We now need to perform the $4N \times 4N$ matrix inverse. The key is to note that we can rearrange the matrices from their current configurations—a 4×4 block matrix of $N \times N$ blocks—into an $N \times N$ block matrix of 4×4 blocks. In this configuration the diagonalized $\mathcal{G}_\kappa(\omega)$ is block-diagonal, and hence the inverse is simply a block-diagonal matrix of the inverse of the 4×4 matrices. Each 4×4 block to be inverted is of the form

$$\begin{bmatrix} 0 & 1 & 0 & -\lambda_\kappa g(\omega) \\ 1 & -U_\kappa^{(0,2)}(\tilde{x}, y) & -U_\kappa^{(1,1)}(\tilde{x}, y) & 0 \\ 0 & -U_\kappa^{(1,1)}(\tilde{x}, y) & -U_\kappa^{(2,0)}(\tilde{x}, y) & 1 \\ -\lambda_\kappa g(-\omega) & 0 & 1 & 0 \end{bmatrix}.$$

This matrix can be inverted exactly. The result is somewhat lengthy, so we omit it here. The result, after evaluating the matrix multiplication and taking the trace over neural and field indices, is

$$\partial_\kappa U_\kappa(\tilde{x}, y) = \frac{1}{N} \sum_{\lambda} \int_{-\infty}^{\infty} \frac{d\omega}{2\pi} \left[\frac{\partial_\kappa \lambda_\kappa g(-\omega) \left[U_\kappa^{(1,1)}(\tilde{x}, y) - \lambda_\kappa g(\omega) \left(U_\kappa^{(1,1)}(\tilde{x}, y)^2 - U_\kappa^{(2,0)}(\tilde{x}, y)U_\kappa^{(0,2)}(\tilde{x}, y) \right) \right]}{1 - (\lambda_\kappa g(\omega) + \lambda_\kappa g(-\omega)) U_\kappa^{(1,1)}(\tilde{x}, y) + \lambda_\kappa^2 |g(\omega)|^2 \left(U_\kappa^{(1,1)}(\tilde{x}, y) - U_\kappa^{(0,2)}(\tilde{x}, y)U_\kappa^{(2,0)}(\tilde{x}, y) \right)} \right], \quad (\text{D2})$$

where we sum over the N eigenvalue λ , which enter through the regulated eigenvalues $\lambda_\kappa = \lambda_\kappa(\lambda)$. Finally, we take the $N \rightarrow \infty$ limit, in which the sum over the eigenvalues becomes an average over the eigenvalue density $\rho_\lambda(\lambda)$, which

we assume to be independent of N ,

$$\begin{aligned} & \partial_\kappa U_\kappa(\tilde{x}, y) \\ &= \int d\lambda \rho_\lambda(\lambda) \int_{-\infty}^{\infty} \frac{d\omega}{2\pi} \left[\frac{\partial_\kappa \lambda_\kappa g(-\omega) \left[U_\kappa^{(1,1)}(\tilde{x}, y) - \lambda_\kappa g(\omega) \left(U_\kappa^{(1,1)}(\tilde{x}, y)^2 - U_\kappa^{(2,0)}(\tilde{x}, y)U_\kappa^{(0,2)}(\tilde{x}, y) \right) \right]}{1 - (\lambda_\kappa g(\omega) + \lambda_\kappa g(-\omega)) U_\kappa^{(1,1)}(\tilde{x}, y) + \lambda_\kappa^2 |g(\omega)|^2 \left(U_\kappa^{(1,1)}(\tilde{x}, y)^2 - U_\kappa^{(0,2)}(\tilde{x}, y)U_\kappa^{(2,0)}(\tilde{x}, y) \right)} \right], \end{aligned} \quad (\text{D3})$$

with initial condition $U_{\kappa=0}(\tilde{x}, y) = (e^{\tilde{x}} - 1)\phi(y)$. We note that this integral retains the 1-loop structure of the Wetterich equation, such that we may write it in the form

$$\begin{aligned} \partial_\kappa U_\kappa(\tilde{x}, y) &= -\frac{1}{4} \int d\lambda \rho_\lambda(\lambda) \int_{-\infty}^{\infty} \frac{d\omega}{2\pi} \\ &\quad \times \partial_\kappa \lambda_\kappa \frac{\partial}{\partial \lambda_\kappa} \ln \left[1 - 2\lambda_\kappa \text{Re}[g(\omega)] U_\kappa^{(1,1)}(\tilde{x}, y) + \lambda_\kappa^2 |g(\omega)|^2 \left(U_\kappa^{(1,1)}(\tilde{x}, y)^2 - U_\kappa^{(0,2)}(\tilde{x}, y)U_\kappa^{(2,0)}(\tilde{x}, y) \right) \right]. \end{aligned} \quad (\text{D4})$$

To obtain Eq. (D3) after evaluating the derivative, split the $\text{Re}[g(\omega)]$ term in the numerator into two terms and change variables to $\omega \rightarrow -\omega$ in one of the terms.

For completeness, we record here the general result for any $\mathbf{J}_\kappa(\omega)$, obtained by inverting $\mathbf{\Gamma}_\kappa^{(2)}(\omega) + \mathbf{R}_\kappa(\omega)$ by block-matrix inversion. The calculation is somewhat tedious, so we give only the final result:

$$\begin{aligned} \partial_\Lambda U_\Lambda(\tilde{x}, y) &= \frac{1}{2} \int_{-\infty}^{\infty} \frac{d\omega}{2\pi} \text{tr} \left[\partial_\Lambda \mathbf{J}_\Lambda(\omega) \left[U_\Lambda^{(1,1)}(\tilde{x}, y) \mathbb{I}_{N \times N} - \left(U_\Lambda^{(1,1)}(\tilde{x}, y)^2 - U_\Lambda^{(2,0)}(\tilde{x}, y)U_\Lambda^{(0,2)}(\tilde{x}, y) \right) \mathbf{J}_\Lambda^T(-\omega) \right] \mathbf{\Xi}_\Lambda(\omega) \right. \\ &\quad \left. + \partial_\Lambda \mathbf{J}_\Lambda^T(-\omega) \mathbf{\Xi}_\Lambda(\omega) \left[U_\Lambda^{(1,1)}(\tilde{x}, y) \mathbb{I}_{N \times N} - \left(U_\Lambda^{(1,1)}(\tilde{x}, y)^2 - U_\Lambda^{(2,0)}(\tilde{x}, y)U_\Lambda^{(0,2)}(\tilde{x}, y) \right) \mathbf{J}_\Lambda(\omega) \right] \right]. \end{aligned}$$

where the trace tr is over neural indices and

$$\mathbf{\Xi}_\Lambda(\omega) = \left[\mathbb{I}_{N \times N} - U_\Lambda^{(1,1)}(\tilde{x}, y) (\mathbf{J}_\Lambda(\omega) + \mathbf{J}_\Lambda^T(-\omega)) + \left(U_\Lambda^{(1,1)}(\tilde{x}, y)^2 - U_\Lambda^{(2,0)}(\tilde{x}, y)U_\Lambda^{(0,2)}(\tilde{x}, y) \right) \mathbf{J}_\Lambda(\omega) \mathbf{J}_\Lambda^T(-\omega) \right]^{-1}.$$

This form would be useful for networks with asymmetric connections $\mathbf{J} \neq \mathbf{J}^T$, or networks for which $\mathbf{J}(\omega)$ is not separable (e.g., $\mathbf{J}(\omega) = \sum_\ell \mathbf{J}^{(\ell)} g_\ell(\omega)$ for synaptic matrices $\mathbf{J}^{(\ell)}$ that are not diagonalizable in the same basis) or for which $\mathbf{J}(\omega)$ is not diagonalizable, such as purely feedforward networks with repeated entrees along the diagonal (which would be the case for cell types with homogeneous self-connections, though we could allow a random distribution of self-connections, for which the probability of any two neurons having exactly the same self-connections vanishes, though for a finite realization the network might be poorly-conditioned).

1. Evaluation of the frequency integral for exponential synaptic filters

For the case of an exponential synaptic filter $g(t - t') = \tau^{-1} e^{-(t-t')/\tau} \Theta(t - t')$, which gives $g(\omega) = 1/(1 - i\omega\tau)$, we can exactly evaluate the frequency integral in Eq. (D3) using the residue theorem. However, there is a subtlety that we must account for that arises from the continuous time limit that we have taken in this presentation. As is the case in other applications of the NPRG method to non-equilibrium problems [30], to obtain the correct result we must introduce a small delay τ_d , such that $g(\omega) = e^{i\omega\tau_d}/(1 - i\omega\tau)$. It appears to be sufficient to add the $\exp(i\omega\tau_d)$ factor only in $\partial_\kappa \mathbf{R}_\kappa$, which enters as a multiplicative factor to the entire integrand. After including this factor, we multiply numerator and denominator by the appropriate factors of $1 \pm i\omega\tau$, and after some rearrangement of terms we arrive at the integral

$$\int_{-\infty}^{\infty} \frac{d\omega}{2\pi} \frac{e^{-i\omega\tau_d}}{\tau^2} \frac{(1 - i\omega\tau)U_\kappa^{(1,1)} - \lambda_\kappa \left((U_\kappa^{(1,1)})^2 - U_\kappa^{(0,2)}U_\kappa^{(2,0)} \right)}{(\omega - \omega_+)(\omega - \omega_-)},$$

where

$$\omega_{\pm} = \pm i \frac{\sqrt{(1 - \lambda_{\kappa} U_{\kappa}^{(1,1)}(0, y))^2 - \lambda_{\kappa}^2 U_{\kappa}^{(0,2)}(0, y) U_{\kappa}^{(2,0)}(0, y)}}{\tau}.$$

In order to evaluate the integral, we need to know where these poles lie in the complex ω plane. There are two factors that determine where the poles are: whether the eigenvalues λ and their regulated counterparts λ_{κ} are real or complex, and the (unknown) values of $U_{\kappa}(\tilde{x}, y)$ and its derivatives. With regard to the eigenvalues, in this work we have chosen to focus on the case of symmetric synaptic weight matrices \mathcal{J} , such that all of its eigenvalues λ (and λ_{κ}) are purely real. The eigenvalues of asymmetric matrices are complex and may have complicated distributions, making it difficult to determine where the poles are. We leave the case of asymmetric synaptic weight matrices for future work.

With regard to the values of $U_{\kappa}(\tilde{x}, y)$, we need to make some assumptions about the nature of the solutions. As discussed earlier, we may choose \tilde{x} to be real or imaginary; for the sake of both numerical stability and determining the location of the poles it is most convenient to take \tilde{x} to be real. Then, we need only determine the sign of the radicand, $(1 - \lambda_{\kappa} U_{\kappa}^{(1,1)}(\tilde{x}, y))^2 - \lambda_{\kappa}^2 U_{\kappa}^{(0,2)}(\tilde{x}, y) U_{\kappa}^{(2,0)}(\tilde{x}, y)$. The poles are imaginary when this is positive and real when this is negative.

In general, we expect the radicand to remain positive and the roots to be imaginary, at least for values of \tilde{x} close to zero, our primary regime of interest, as the firing rates and correlation functions are related to derivatives of $U_{\kappa=1}(\tilde{x}, y)$ with respect to \tilde{x} evaluated at $\tilde{x} = 0$. We expect this to be the case because we require $U_{\kappa}(0, y) = 0$ for all y and κ (we will prove this holds after performing the frequency integrals). Accordingly, $U_{\kappa}^{(0,2)}(0, y) = 0$ as well and when \tilde{x} is small the leading order term of the radicand will be $(1 - \lambda_{\kappa} U_{\kappa}^{(1,1)}(0, y))^2$, which is positive. In practice, assuming the radicand is non-negative in a range of \tilde{x} around 0 holds reasonably well, but numerical errors when the radicand is small occasionally lead to violations of this assumption, introducing imaginary terms to the solution. These imaginary terms are typically small except near the boundaries of the solution, where interpolation starts to break down. To prevent this numerical instability it is useful to evaluate the integral for both real and imaginary poles.

When the poles are imaginary the integral can be evaluated by straightforward application of the residue theorem. The factor of $e^{-i\omega\tau_d}$ indicates that the contour must be closed in the lower-half ω plane and hence only ω_- contributes to the residue. As such, in order for ω to run from $-\infty$ to ∞ the contour must be closed travelling clockwise, meaning the residue acquires an overall minus sign when employing the residue theorem. When the poles are real the integral becomes ambiguous as both poles lie along the $\omega \in (-\infty, \infty)$ contour, and it is therefore not obvious which of the poles, if either, should be taken to contribute to the residue. A careful analysis in discrete time shows that if we allow the real roots to be complex (e.g., by giving the radicand an infinitesimal imaginary component), then ω_+ lies entirely outside the contour and does not contribute to the integral, while ω_- lies inside the contour and does contribute, and therefore the integral evaluates to zero when $(1 - \lambda_{\kappa} U_{\kappa}^{(1,1)}(\tilde{x}, y))^2 - \lambda_{\kappa}^2 U_{\kappa}^{(0,2)}(\tilde{x}, y) U_{\kappa}^{(2,0)}(\tilde{x}, y) < 0$. Putting this all together we may evaluate the integral for both cases and then set $\tau_d \rightarrow 0$, yielding

$$\partial_{\kappa} U_{\kappa}(\tilde{x}, y) = -\frac{1}{2\tau} \int d\lambda \rho_{\lambda}(\lambda) \partial_{\kappa} \lambda_{\kappa} \left\{ U_{\kappa}^{(1,1)}(\tilde{x}, y) - \frac{(1 - \lambda_{\kappa} U_{\kappa}^{(1,1)}(\tilde{x}, y)) U_{\kappa}^{(1,1)}(\tilde{x}, y) + \lambda_{\kappa} U_{\kappa}^{(0,2)}(\tilde{x}, y) U_{\kappa}^{(2,0)}(\tilde{x}, y)}{\sqrt{(1 - \lambda_{\kappa} U_{\kappa}^{(1,1)}(\tilde{x}, y))^2 - \lambda_{\kappa}^2 U_{\kappa}^{(0,2)}(\tilde{x}, y) U_{\kappa}^{(2,0)}(\tilde{x}, y)}} \right\} \times \Theta \left((1 - \lambda_{\kappa} U_{\kappa}^{(1,1)}(\tilde{x}, y))^2 - \lambda_{\kappa}^2 U_{\kappa}^{(0,2)}(\tilde{x}, y) U_{\kappa}^{(2,0)}(\tilde{x}, y) \right) \quad (\text{D5})$$

The Heaviside Theta factor enforces the condition that $(1 - \lambda_{\kappa} U_{\kappa}^{(1,1)}(\tilde{x}, y))^2 - \lambda_{\kappa}^2 U_{\kappa}^{(0,2)}(\tilde{x}, y) U_{\kappa}^{(2,0)}(\tilde{x}, y) \geq 0$. We will omit the Heaviside factor in analytic calculations as we generally expect this condition to be satisfied, a conjecture supported after-the-fact by the success of our results. Omitting the Heaviside factor, this equation retains the “one-loop structure,” allowing us to write it in the form given in the main text:

$$\partial_{\kappa} U_{\kappa}(\tilde{x}, y) = -\frac{1}{2\tau} \int d\lambda \rho_{\lambda}(\lambda) \partial_{\kappa} \lambda_{\kappa} \frac{\partial}{\partial \lambda_{\kappa}} \left\{ \lambda_{\kappa} U_{\kappa}^{(1,1)}(\tilde{x}, y) + \sqrt{(1 - \lambda_{\kappa} U_{\kappa}^{(1,1)}(\tilde{x}, y))^2 - \lambda_{\kappa}^2 U_{\kappa}^{(0,2)}(\tilde{x}, y) U_{\kappa}^{(2,0)}(\tilde{x}, y)} \right\}. \quad (\text{D6})$$

This form is useful for easily proving that in the subcritical regime $U_{\kappa}(0, y) = 0$ for any point along the flow, given that it holds at the initial condition $\kappa = 0$. Plugging this assumption into the flow equation causes the term $U_{\kappa}^{(0,2)}(0, y) U_{\kappa}^{(2,0)}(0, y) = 0$, and then assuming (or requiring) that $\sqrt{(1 - \lambda_{\kappa} U_{\kappa}^{(1,1)}(0, y))^2} = 1 - \lambda_{\kappa} U_{\kappa}^{(1,1)}(0, y)$ results

in $\frac{\partial}{\partial \lambda_\kappa} \{1\}$, which vanishes, giving $\partial_\kappa U_\kappa(0, y) = 0$. The assumption that $\sqrt{(1 - \lambda_\kappa U_\kappa^{(1,1)}(0, y))^2} = 1 - \lambda_\kappa U_\kappa^{(1,1)}(0, y)$ means $1 - \lambda_\kappa U_\kappa^{(1,1)}(0, y) > 0$, or $1 > \lambda_\kappa \Phi_{1,\kappa}(y)$, where $\Phi_{1,\kappa}(y) = U_\kappa^{(1,1)}(0, y)$ is the $m = 1$ effective nonlinearity (written as a function of κ instead Λ). This condition must hold for all λ_κ and y , so it means that $1 - \Lambda_{\max} \Phi_{1,\kappa=1}(y) > 0$ only when the maximum gain of the nonlinearity at any input y cannot exceed the maximum eigenvalue Λ_{\max} when $\Lambda_{\max} > 0$. As we argue in the main text, we expect that this condition is not violated, at least for the classes of bounded nonlinearities investigated in this work, because the solution develops non-analytic regions such that $1 \geq \lambda_\kappa \Phi_{1,\kappa}(y)$ for all κ and y .

2. Regulating the eigenvalue integral

In this work we regulate the eigenvalues of the synaptic weight matrix J_{ij} , leaving the eigenvectors as is. The regulator must satisfy certain properties. In particular, by the end of the NRG flow the effects of the regulator must be removed, such that $\Gamma_{\kappa=1}[\chi]$ is the true AEA of the theory (or would be, if we could solve the flow equations exactly). In principle, the choice of regulator does not matter as long as it does not break any symmetries of the model. However, in practice artifacts of the choice of regulator can enter through the approximations performed as part of the NRG calculations [48, 68, 97, 98]. In better-studied models like the Ising family of models, many different regulators have been tested and even optimized; in this first work applying the NRG method to spiking we will only investigate one regulator, but we briefly discuss some possible other options in this section.

a. Sharp regulator

The primary regulator we employ in this work is the sharp regulator

$$\lambda_\kappa = \lambda \Theta(\Lambda_\kappa - \lambda).$$

This regulator sets all eigenvalues less than a threshold $\Lambda_\kappa \in [\Lambda_{\min}, \Lambda_{\max}]$ to 0, such that at $\kappa = 0$ the synaptic weights are $J_{ij;\kappa=0} = 0$ and the network is completely coupled in both neurons and time, allowing for the exact evaluation of the moment generating functional of the model. (The possibility of instead setting all of the eigenvalues to a constant is discussed in the ‘‘Mean-field regulator’’ section). As $\kappa \rightarrow 1$ all of the eigenvalues take on their true values and $J_{ij;\kappa=1} = J_{ij}$.

This sharp regulator must be interpreted as the limit of a smooth regulator,

$$\lambda_\kappa = \lim_{\epsilon \rightarrow 0} \lambda f\left(\frac{\Lambda_\kappa - \lambda}{\epsilon}\right),$$

where $f(y)$ is a sigmoidal function that tends to 0 as $y \rightarrow -\infty$ and 1 as $y \rightarrow +\infty$. This interpretation is necessary to properly evaluate the eigenvalue integrals in the flow equation, similar to the introduction of the family of smooth regulators in [50]. This regulator is convenient for analytically simplifying the flow equation, though it has some undesirable features. In particular, this regulator discontinuously sets all eigenvalues greater than Λ_κ to 0. In general, many eigenvalues will be negative, and the flow begins by discontinuously turning on the largest magnitude negative eigenvalues. The overall magnitude of the weights $J_{ij;\kappa}$ will remain small due to the fact that most eigenvalues are still 0, but given that sharp momentum cutoffs have caused problems in lattice systems and continuous media, we might worry that such a sharp cutoff will cause some artifacts in the flow equations. Despite this worry, this regulator appears to be an effective choice that yields reasonably good numerical results, though future studies will need to investigate the possibility that it introduces artifacts in the dimensionless RG flow. We therefore focus on this regulator in the present work.

b. Mean-field regulator

Another style of regulator we might wish to employ is the Litim-Dupuis-Machado (LDM) regulator introduced for lattice models in [29] and studied in detail for the Ising model in [48, 68]. This regulator appears superficially similar to our sharp regulator, the key difference between that whereas our sharp regulator initially sets all eigenvalues to 0 the LDM regulator would initially set all of the eigenvalues to the same constant, the initial value of the threshold

Λ_0 . That is,

$$\lambda_\kappa = \begin{cases} \Lambda_\kappa, & \lambda > \Lambda_\kappa \\ \lambda, & \lambda < \Lambda_\kappa \end{cases},$$

with $\Lambda_0 \leq \Lambda_\kappa \leq \Lambda_{\max}$. Similarly to the bilateral regulator, these eigenvalues change continuously as the threshold is adjusted.

The key difference between the LDM regulator and the previous two regulators is that although the initial condition of the flow will yield a population of *independent* neurons—as all of the eigenvalues of J_{ij} will be equal and hence $J_{ij} = \Lambda_0 \delta_{ij}$ —it will *not* decouple each neuron’s spiking activity from its past history. As a result, we cannot analytically evaluate the initial condition $\Gamma_{\kappa=0}$, which would require that we solve for the single-neuron CGF, an intractable problem even numerically.

Other work has gotten around this issue by the equivalent of taking the limit $\Lambda_0 \rightarrow -\infty$. For many models of interest this limit forces $\Gamma_{\kappa=0}[\tilde{\psi}, \psi, \tilde{\nu}, \nu]$ to be equal to the bare action $S[\tilde{\psi}, \psi, \tilde{\nu}, \nu]$ (up to an infinite constant), i.e., the mean-field theory. However, the proof that $\Gamma_{\kappa=0}$ tends to the mean-field theory fails for this model: the fact that only the \tilde{V} and \tilde{n} fields are coupled means they will tend to $\tilde{\psi}$ and ν as $\Lambda_0 \rightarrow -\infty$, but the fields V and \tilde{n} are not forced to ψ and $\tilde{\nu}$ and must still be integrated out, which remains an intractable calculation. One way around this could be to introduce an additional regulator that couples V and \tilde{n} and vanishes by the end of the flow. For example, a possible regulator could be a coupling $R_{ij;\kappa}^{\psi\tilde{\nu}}(t, t') = \delta_{ij} \delta(t - t') \left(1 - \frac{\Lambda_\kappa}{\Lambda_{\max}}\right)$. Because this coupling only exists in the regulator, it does not affect the derivation of the Ward-Takahashi identities for $\Gamma[\chi]$, and only introduces new terms into the flow equation through $\partial_\kappa \mathbf{R}_\kappa$ and $[\mathbf{\Gamma}_\kappa^{(2)} + \mathbf{R}_\kappa]^{-1}$. With such a regulator the proof that $\Gamma_{\kappa=0}[\tilde{\psi}, \psi, \tilde{\nu}, \nu] = S[\tilde{\psi}, \psi, \tilde{\nu}, \nu]$ will succeed, at the cost of complicating the flow equations.

We can easily derive the flow equation for this dual-regulator model from our previous results by noting that adding a term proportional to $V \cdot \tilde{n}$ to $\mathbf{\Gamma}_\kappa^{(2)} + \mathbf{R}_\kappa$ will shift $\lambda_\kappa(\lambda) U_\kappa^{(1,1)}(\tilde{x}, y) \rightarrow -\mu_\kappa(\lambda) + \lambda_\kappa(\lambda) U_\kappa^{(1,1)}(\tilde{x}, y)$, where $\mu_\kappa(\lambda)$ is the $V \cdot \tilde{n}$ regulator $R_\kappa^{\psi\tilde{\nu}}$ in λ -space. Then, from the one-loop property of the Wetterich flow equation, we must have

$$\partial_\kappa U_\kappa(\tilde{x}, y) = -\frac{1}{2\tau} \int d\lambda \rho_\lambda(\lambda) \tilde{\partial}_\kappa \left\{ -\mu_\kappa(\lambda) + \lambda_\kappa(\lambda) U_\kappa^{(1,1)}(\tilde{x}, y) + \sqrt{\left(1 + \mu_\kappa(\lambda) - \lambda_\kappa(\lambda) U_\kappa^{(1,1)}(\tilde{x}, y)\right)^2 - \lambda_\kappa(\lambda)^2 U_\kappa^{(0,2)}(\tilde{x}, y) U_\kappa^{(2,0)}(\tilde{x}, y)} \right\}, \quad (\text{D7})$$

where $\tilde{\partial}_\kappa$ acts only on $\mu_\kappa(\lambda)$ and $\lambda_\kappa(\lambda)$, not U_κ .

We could now pick a specific form of the regulator $\mu_\kappa(\lambda)$. A simple choice would be the regulator mentioned above, which would give rise to $\mu_\kappa(\lambda) = 1 - \Lambda_\kappa/\Lambda_{\max}$ for all λ . This regulator is inconvenient analytically, as it would not allow for the λ integral to be performed in closed form.

A different choice that simplifies the λ integrals could be

$$\mu_\kappa(\lambda) = \begin{cases} \Lambda_\kappa/\Lambda_{\max}, & \lambda > \Lambda_\kappa \\ 0, & \lambda < \Lambda_\kappa \end{cases}.$$

Because $\partial_\kappa \mu_\kappa = 0$ for $\lambda < \Lambda_\kappa$, the integral will vanish on this interval, whereas it will be non-zero for $\lambda > \Lambda_\kappa$. Because $\lambda_\kappa(\lambda) = \Lambda_\kappa$ on the non-zero interval, the λ integral reduces to the prefactor $\int_{\Lambda_\kappa}^{\Lambda_{\max}} d\lambda \rho_\lambda(\lambda)$. However, we note that this regulator is discontinuous in λ , similar to our sharp regulator, except for the fact that $\partial_\kappa \mu_\kappa \neq 0$ for $\lambda > \Lambda_\kappa$. This appears sufficient to avoid using the limit of smooth regulators to define the integral, though it is not clear if the discontinuity is of any concern.

c. Proportional regulators

Another type of regulator we could consider would scale the eigenvalues down from their true values:

$$\lambda_\kappa = \kappa^n \lambda$$

for some constant n and $\kappa \in [0, 1]$ as usual. A possible use of this choice is to perform a comparison of results obtained using different values of n , to evaluate the sensitivity of the flow to the choice of regulator, at least within this class.

This regulator, however, has some downsides. For one, the λ integral generally cannot be done analytically, making numerical evaluation of the flow equations more difficult than it already is in cases in which the integrals can be evaluated. The other potential downside is that it is not clear if the critical properties of the model can be studied with such a regulator, as all eigenvalues contribute to the flow simultaneously.

3. Evaluation of the eigenvalue integral for a sharp regulator

We may evaluate this flow equation for particular eigenvalue statistics, choices of the initial nonlinearity $\Phi_0(y) = \phi(y)$, and regulators λ_κ . As we focus on the case of bounded eigenvalue distributions with a minimum eigenvalue Λ_{\min} and maximum eigenvalue Λ_{\max} , the most convenient regulator is a sharp cutoff for which

$$\lambda_\kappa(\lambda) = \lambda \Theta(\Lambda_\kappa - \lambda), \quad (\text{D8})$$

where we define the threshold $\Lambda_\kappa = (\Lambda_{\max} - \Lambda_{\min})\kappa + \Lambda_{\min}$ such that $\Lambda_0 = \Lambda_{\min}$ and $\Lambda_1 = \Lambda_{\max}$. This regulator sets all eigenvalues greater than Λ_κ to be zero; therefore, at $\kappa = 0$ the synaptic interactions vanish and $\Gamma_{\kappa=0}$ is given by mean field theory, as required by our construction. As Λ_κ is raised, eigenvalues are set to their true values and contribute to the flow of the model.

Using the regulator (D8) to evaluate the λ integral in the flow equation requires some care; in particular, one has to properly define integrals of the form $\int dy \delta(x - y) \mathcal{F}(\Theta(x - y))$. We thus interpret Eq. (D8) as the limit of a smooth regulator,

$$\lambda_\kappa(\lambda; \epsilon) = \lambda f\left(\frac{\Lambda_\kappa - \lambda}{\epsilon}\right), \quad (\text{D9})$$

where $f(y)$ is a sigmoidal function that is 0 as $y \rightarrow -\infty$ and 1 as $y \rightarrow +\infty$. In the limit $\epsilon \rightarrow 0$ this tends to the step function. We can now formally evaluate the integral in our flow equation, using $\partial_\kappa \lambda_\kappa = \lambda f'((\Lambda_\kappa - \lambda)/\epsilon) \partial_\kappa \Lambda_\kappa / \epsilon$.

$$\begin{aligned} & \int_{\Lambda_{\min}}^{\Lambda_{\max}} d\lambda \rho_\lambda(\lambda) \partial_\kappa \lambda_\kappa \left\{ U_\kappa^{(1,1)}(\tilde{x}, y) - \frac{\left(1 - \lambda_\kappa U_\kappa^{(1,1)}(\tilde{x}, y)\right) U_\kappa^{(1,1)}(\tilde{x}, y) + \lambda_\kappa U_\kappa^{(0,2)}(\tilde{x}, y) U_\kappa^{(2,0)}(\tilde{x}, y)}{\sqrt{\left(1 - \lambda_\kappa U_\kappa^{(1,1)}(\tilde{x}, y)\right)^2 - \lambda_\kappa^2 U_\kappa^{(0,2)}(\tilde{x}, y) U_\kappa^{(2,0)}(\tilde{x}, y)}} \right\} \\ &= \int_{\Lambda_{\min}}^{\Lambda_{\max}} d\lambda \rho_\lambda(\lambda) \lambda f'\left(\frac{\Lambda_\kappa - \lambda}{\epsilon}\right) \frac{\partial_\kappa \Lambda_\kappa}{\epsilon} \\ & \quad \times \left\{ U_\kappa^{(1,1)}(\tilde{x}, y) - \frac{\left(1 - \lambda f\left(\frac{\Lambda_\kappa - \lambda}{\epsilon}\right) U_\kappa^{(1,1)}(\tilde{x}, y)\right) U_\kappa^{(1,1)}(\tilde{x}, y) + \lambda f\left(\frac{\Lambda_\kappa - \lambda}{\epsilon}\right) U_\kappa^{(0,2)}(\tilde{x}, y) U_\kappa^{(2,0)}(\tilde{x}, y)}{\sqrt{\left(1 - \lambda f\left(\frac{\Lambda_\kappa - \lambda}{\epsilon}\right) U_\kappa^{(1,1)}(\tilde{x}, y)\right)^2 - \left(\lambda f\left(\frac{\Lambda_\kappa - \lambda}{\epsilon}\right)\right)^2 U_\kappa^{(0,2)}(\tilde{x}, y) U_\kappa^{(2,0)}(\tilde{x}, y)}} \right\} \end{aligned}$$

Now, make the change of variables $y = (\Lambda_\kappa - \lambda)/\epsilon$, with $\lambda = \Lambda_\kappa - \epsilon y$ and $d\lambda = -\epsilon dy$:

$$\begin{aligned} & \int_{(\Lambda_\kappa - \Lambda_{\max})/\epsilon}^{(\Lambda_\kappa - \Lambda_{\min})/\epsilon} dy \rho_\lambda(\Lambda_\kappa - \epsilon y) (\Lambda_\kappa - \epsilon y) f'(y) \partial_\kappa \Lambda_\kappa \\ & \quad \times \left\{ U_\kappa^{(1,1)}(\tilde{x}, y) - \frac{\left(1 - (\Lambda_\kappa - \epsilon y) f(y) U_\kappa^{(1,1)}(\tilde{x}, y)\right) U_\kappa^{(1,1)}(\tilde{x}, y) + (\Lambda_\kappa - \epsilon y) f(y) U_\kappa^{(0,2)}(\tilde{x}, y) U_\kappa^{(2,0)}(\tilde{x}, y)}{\sqrt{\left(1 - (\Lambda_\kappa - \epsilon y) f(y) U_\kappa^{(1,1)}(\tilde{x}, y)\right)^2 - ((\Lambda_\kappa - \epsilon y) f(y))^2 U_\kappa^{(0,2)}(\tilde{x}, y) U_\kappa^{(2,0)}(\tilde{x}, y)}} \right\} \end{aligned}$$

Now, we take the $\epsilon \rightarrow 0$ limit. Inside the integral we may essentially just set $\epsilon = 0$. The integration bounds require some care, as they tend to different limits depending on the value of Λ_κ . The integration bounds diverge in opposite directions for $\Lambda_{\min} < \Lambda_\kappa < \Lambda_{\max}$. If $\Lambda_\kappa < \Lambda_{\min} < \Lambda_{\max}$ then both bounds diverge to $-\infty$ and the integral is 0. Similarly, if $\Lambda_{\min} < \Lambda_{\max} < \Lambda_\kappa$ then both bounds diverge to $+\infty$ and the integral is again 0. The last case is when Λ_κ is at one of the bounds, in which case one of the limits is 0. However, we need not worry about these two points. If we formally integrate $\partial_\kappa U_\kappa$ over κ , then the points at which $\Lambda_\kappa = \Lambda_{\max}$ or Λ_{\min} are just two points in the integral

over κ , which can be removed without changing the value of the integral. Therefore, as $\epsilon \rightarrow 0$ our integral becomes

$$\begin{aligned}
& \lim_{\epsilon \rightarrow 0} \int_{(\Lambda_\kappa - \Lambda_{\max})/\epsilon}^{(\Lambda_\kappa - \Lambda_{\min})/\epsilon} dy \rho_\lambda(\Lambda_\kappa - \epsilon y)(\Lambda_\kappa - \epsilon y)f'(y) \partial_\kappa \Lambda_\kappa \\
& \times \left\{ U_\kappa^{(1,1)}(\tilde{x}, y) - \frac{\left(1 - (\Lambda_\kappa - \epsilon y)f(y)U_\kappa^{(1,1)}(\tilde{x}, y)\right)U_\kappa^{(1,1)}(\tilde{x}, y) + (\Lambda_\kappa - \epsilon y)f(y)U_\kappa^{(0,2)}(\tilde{x}, y)U_\kappa^{(2,0)}(\tilde{x}, y)}{\sqrt{\left(1 - (\Lambda_\kappa - \epsilon y)f(y)U_\kappa^{(1,1)}(\tilde{x}, y)\right)^2 - ((\Lambda_\kappa - \epsilon y)f(y))^2 U_\kappa^{(0,2)}(\tilde{x}, y)U_\kappa^{(2,0)}(\tilde{x}, y)}} \right\} \\
& \rightarrow \rho_\lambda(\Lambda_\kappa) \partial_\kappa \Lambda_\kappa \Lambda_\kappa \int_{-\infty}^{+\infty} dy f'(y) \\
& \times \left\{ U_\kappa^{(1,1)}(\tilde{x}, y) - \frac{\left(1 - \Lambda_\kappa f(y)U_\kappa^{(1,1)}(\tilde{x}, y)\right)U_\kappa^{(1,1)}(\tilde{x}, y) + \Lambda_\kappa f(y)U_\kappa^{(0,2)}(\tilde{x}, y)U_\kappa^{(2,0)}(\tilde{x}, y)}{\sqrt{\left(1 - \Lambda_\kappa f(y)U_\kappa^{(1,1)}(\tilde{x}, y)\right)^2 - (\Lambda_\kappa f(y))^2 U_\kappa^{(0,2)}(\tilde{x}, y)U_\kappa^{(2,0)}(\tilde{x}, y)}} \right\} \\
& = \rho_\lambda(\Lambda_\kappa) \partial_\kappa \Lambda_\kappa \Lambda_\kappa \int_0^1 df \\
& \times \left\{ U_\kappa^{(1,1)}(\tilde{x}, y) - \frac{\left(1 - \Lambda_\kappa f U_\kappa^{(1,1)}(\tilde{x}, y)\right)U_\kappa^{(1,1)}(\tilde{x}, y) + \Lambda_\kappa f U_\kappa^{(0,2)}(\tilde{x}, y)U_\kappa^{(2,0)}(\tilde{x}, y)}{\sqrt{\left(1 - \Lambda_\kappa f U_\kappa^{(1,1)}(\tilde{x}, y)\right)^2 - (\Lambda_\kappa f)^2 U_\kappa^{(0,2)}(\tilde{x}, y)U_\kappa^{(2,0)}(\tilde{x}, y)}} \right\}.
\end{aligned}$$

In going to the last line we used the fact that $dy f'(y) = df$. This final integral can be evaluated exactly due to the “1-loop” property of the flow equation mentioned earlier. The result is

$$\partial_\kappa U_\kappa(\tilde{x}, y) = \frac{1}{2\tau} \rho_\lambda(\Lambda_\kappa) \partial_\kappa \Lambda_\kappa \left\{ 1 - \Lambda_\kappa U_\kappa^{(1,1)}(\tilde{x}, y) - \sqrt{\left(1 - \Lambda_\kappa U_\kappa^{(1,1)}(\tilde{x}, y)\right)^2 - \Lambda_\kappa^2 U_\kappa^{(0,2)}(\tilde{x}, y)U_\kappa^{(2,0)}(\tilde{x}, y)} \right\}. \quad (\text{D10})$$

We may reparameterize the model in favor of Λ over κ by a change of variables, which eliminates the factor of $\partial_\kappa \Lambda_\kappa$ on the right-hand-side of the equation.

We can solve this equation numerically for specific choices of $\rho_\lambda(\lambda)$, corresponding to eigenvalue density of different (symmetric) synaptic weight matrices, and “bare” nonlinearities $\phi(y)$, which enters through the initial condition $U_0(\tilde{x}, y) = (e^{\tilde{x}} - 1) \phi(y)$. The formalism holds for any type of network which gives continuous and bounded eigenvalue distributions, including both lattices and random matrices. In this study we have focused on the particular cases of lattices, random regular graphs, and Gaussian random matrices.

a. Lattices

On lattices, the eigenvalue density of the synaptic weight matrix can be computed semi-analytically using the method of [53], which we use in our numerical calculations in this work. For networks with uniform excitatory strength J and self-coupling of equal magnitude, $J_{\text{self}} = -J$, the maximum eigenvalue is $\Lambda_{\max} = (2d - 1)J$ and the minimum eigenvalue is $\Lambda_{\min} = -(2d + 1)J$. In standard NRG work the flow is typically regulated in terms of momentum instead of the eigenvalues, which are related to energy, but this procedure does not generalize easily to non-translation invariant systems.

While the exact form of the eigenvalue distribution is not tractable, for any spatial dimension d one can show that the density scales as

$$\rho_\lambda(\lambda) \sim |\Lambda_{\max} - \lambda|^{d/2-1}$$

for λ near the maximum eigenvalue density Λ_{\max} . We use this scaling to define the effective dimension d for random networks.

b. Random regular graphs

The adjacency matrix of a finite random regular graph of degree k (the number of connections each neuron makes) has bulk eigenvalue spectrum

$$\rho_\lambda(\lambda) = \frac{k}{2\pi} \frac{\sqrt{4(k-1) - \lambda^2}}{k^2 - \lambda^2},$$

where $|\lambda| \leq 2\sqrt{k-1}$, and is 0 outside of this interval [99]. The adjacency matrix also has a single isolated eigenvalue at $\lambda = k$. This eigenvalue is greater than the maximum eigenvalue of the bulk spectrum.

In order to scale the adjacency matrix of the random regular graph to a synaptic weight matrix J_{ij} , we divide the adjacency matrix by $\sqrt{k-1}$ and multiply by the uniform excitatory strength J , such that the maximum eigenvalue of the bulk spectrum is $\Lambda_{\max} = 2J$. If we add a negative self-coupling J_{self} to implement a soft refractory period, the eigenvalues are all shifted by this amount.

The fact that the random regular graph has a single isolated eigenvalue greater than the bulk distribution's Λ_{\max} could potentially be an issue for the dynamics of the network. In the infinite network limit this eigenvalue is a negligible part of the eigenvalue density. We therefore neglect it in our calculations of the effective nonlinearities, and it does not appear to cause any discrepancies, though this may not be the case in finite networks, particularly small networks.

Lastly, we note that for any degree k the eigenvalue distribution scales as $\sqrt{\Lambda_{\max} - \lambda}$ near the maximum bulk eigenvalue, meaning that random regular graphs of any degree $k > 2$ have effective dimension $d = 3$.

c. Random networks

For networks with random distributions of both synaptic connections and the weights of the connections, we start with a fully connected graph with Gaussian distributed weights: $J_{ij} \sim \mathcal{N}(0, J_0^2/N)$, with $J_{ij} = J_{ji}$ and $J_{ii} = J_{\text{self}}$, where $J_{\text{self}} < 0$ is the inhibitory self-coupling that implements a soft-refractory period. In the large network limit this yield the well-known semi-circle law

$$\rho_\lambda(\lambda) = \frac{\sqrt{(\Lambda_{\max} - \lambda)(\lambda - \Lambda_{\min})}}{\frac{\pi}{2} \left(\frac{\Lambda_{\max} - \Lambda_{\min}}{2} \right)^2}, \quad (\text{D11})$$

where $\Lambda_{\min} = -2J_0 + J_{\text{self}}$ and $\Lambda_{\max} = 2J_0 + J_{\text{self}}$. For simplicity in this work we set $J_{\text{self}} = 0$. We note that Erdos-Reyni graphs with connection probability p , drawn independently for each connection, share this same eigenvalue distribution. As a result, fully connected networks and sparse networks will have the same effective nonlinearities.

Like the random regular graph, the Gaussian random network has effective dimension $d = 3$. To explore the impact of the “effective dimension” d , we create “beta networks,” constructed by generating a symmetric Gaussian random network, diagonalizing it, and replacing the eigenvalues with ordered eigenvalues drawn from a beta distribution,

$$\rho_\lambda(\lambda) = \frac{\Gamma\left(\frac{d_+ + d_-}{2}\right)}{\Gamma\left(\frac{d_+}{2}\right)\Gamma\left(\frac{d_-}{2}\right)} \frac{|\Lambda_{\max} - \lambda|^{d_+/2-1} |\lambda - \Lambda_{\min}|^{d_-/2-1}}{(\Lambda_{\max} - \Lambda_{\min})^{d_+/2 + d_-/2 - 1}}, \quad (\text{D12})$$

where the parameters d_+ and d_- define the effective dimensions and $\Gamma(\cdot)$ is the Gamma function. In this work we focus on the symmetric case $d_+ = d_- = d$, though even in the asymmetric case $d_- \neq d_+$ we expect only d_+ to control the critical behavior of the network. This distribution reduces to the semi-circle law when $d = 3$.

Appendix E: Numerical solutions of the flow equation

Although we drastically simplified the Wetterich equation down to a partial differential equation for $U_\kappa(\tilde{x}, y)$, Eq. (20) is still difficult to solve, even numerically. Straightforward explicit finite-difference schemes, as have been used in other NPRG works to numerically solve flow equations [38], are very sensitive to the discretization step sizes in κ , \tilde{x} , and y . We had some success solving the flow equation using Mathematica's `NDSolve` function with the `PDEDiscritization` method, using the options `MethodOfLines` and `SpatialDiscritization` with options

`TensorProductGrid` and sufficiently many points in each \tilde{x} and y dimension. The results were sensitive to various factors, particularly the range of \tilde{x} and y used.

Due to the fact that $\tilde{x} \in \mathbb{R}_+$ and $y \in \mathbb{R}$ or \mathbb{R}_+ it is difficult to properly supply boundary conditions for this problem. We expect that as $\tilde{x} \rightarrow -\infty$ the solution will decay to 0, while it diverges as $\tilde{x} \rightarrow +\infty$; accordingly, we cut off \tilde{x} just above 0. The behavior in y depends on the choice of bare nonlinearity. For the choices considered in this work, we expect that $\lim_{|y| \rightarrow \infty} U^{(0,1)}(\tilde{x}, y) \rightarrow 0$; however, some choices of nonlinearity, such as $\phi(y) = \exp(y)$, could diverge in this limit; we have not explored these cases. Because these boundary conditions occur at ∞ , it is non-trivial to implement them. One option is to simply omit the boundary conditions, which will prompt warnings from Mathematica. The other option is to assume that for large $|y|$ that the boundary conditions asymptotically match the bare rate function $U_0(\tilde{x}, y) = (e^{\tilde{x}} - 1)\phi(y)$. This yielded results that were mostly consistent with the solutions obtained by omitting the boundary conditions, but still suffered numerical instability as we approach the supercritical regime. The main issue is the square root: even though we expect that $(1 - \lambda_\kappa U_\kappa^{(1,1)}(\tilde{x}, y))^2 - \lambda_\kappa^2 U_\kappa^{(2,0)}(\tilde{x}, y)U_\kappa^{(0,2)}(\tilde{x}, y) \geq 0$, this may become negative due to numerical inaccuracy, introducing imaginary components into the numerical solution. Trying to enforce this condition with piecewise conditions, like the Heaviside factor, or replacing the radicand with 0 if it went negative, only traded one source of numerical instability for another.

In order to improve numerical instability and explore the supercritical regime, we developed the approach of deriving a hierarchy of flow equations for the effective nonlinearities $\Phi_{m,\kappa}(y) \equiv U_\kappa^{(m,0)}(0, y)$, eliminating the difficulties with the variable \tilde{x} . As explained in the main text, this hierarchy is infinite, so to solve the equations we must make some approximation to close the hierarchy of equations. We opted to close the equations at order m by approximating $\Phi_{m,\kappa}(y) = \phi(y)$, allowing us to solve the equations. In practice, we solved the equations numerically in Mathematica using the `PDEDiscritization` method with the `MethodOfLines` option and the `SpatialDiscritization` option with setting `TensorProductGrid` and `MinPoints` of 400. We use the bare nonlinearity $\phi(y)$ as the boundary conditions at large y . We closed the approximation at order $m = 4$ for subcritical values of Λ_{\max} , and at order $m = 1$ for the supercritical cases, for which Mathematica's `NDSolve` is unable to integrate through the development of the non-analyticity.

To compare the non-perturbative method to perturbative results, shown in Fig. 3, we used the Python code provided by Ref. [23], modified for our particular choices of the bare nonlinearity $\phi(y)$, synaptic filters $g(t - t')$, and Gaussian random networks, to calculate the 1-loop predictions of the firing rates. We note that although our method works better than the perturbative results near and above the critical regime, the perturbative methods of Refs. [23, 25] apply to any network architecture, and are not limited to the symmetric networks we have focused on.

Exact result for the 1-loop approximation on random networks

In our hierarchy of nonlinearities the 1-loop approximation amounts to approximating the nonlinearities on the right-hand-sides of the equations by their bare, Λ -independent values. In this case the effective nonlinearities within this approximation can be obtained by integrating with respect to Λ . The 1-loop approximation for the first nonlinearity, $\Phi_1(y)$, is given by

$$\Phi_1(y) = \phi(y) + \frac{\phi(y)\phi''(y)}{2\tau} \left\langle \frac{\lambda^2}{1 - \lambda\phi'(y)} \right\rangle,$$

where the angled brackets denote an expectation over the eigenvalues of the weight matrix J_{ij} . We present the result for $J_{ij} \sim \mathcal{N}(0, J_0^2/N)$, yielding a Wigner semi-circle distribution of eigenvalues, $\rho_\lambda(\lambda) = \frac{2}{\pi\Lambda_{\max}^2} \sqrt{\Lambda_{\max}^2 - \lambda^2}$, with $\Lambda_{\max} = 2J_0$, for which the even moments are $\langle \lambda^{2\ell} \rangle = J_0^{2\ell} C_\ell$, where $C_\ell = \frac{(2\ell)!}{(\ell!)^2(\ell+1)}$ are Catalan numbers. The odd moments are 0 by symmetry.

Because we require $\lambda\phi'(y) < 1$, we can expand the result in a geometric series and use the result for the moments

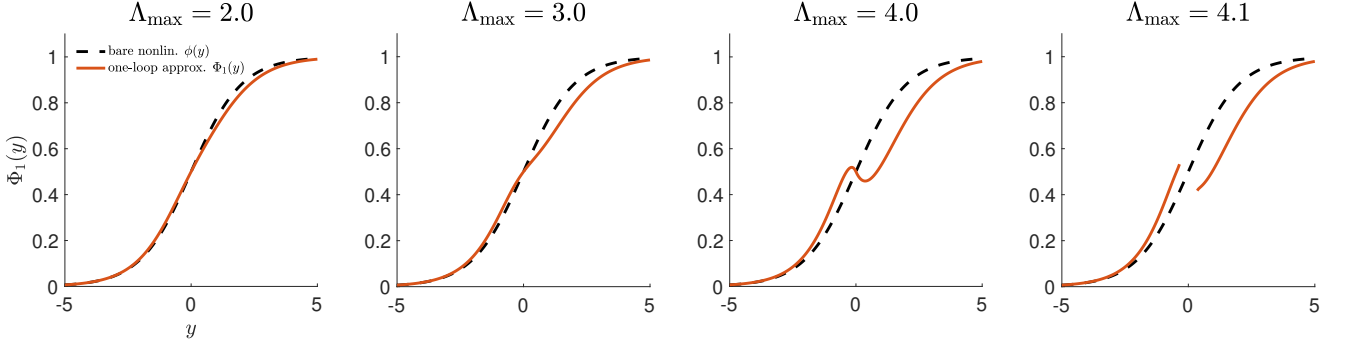


FIG. 15. **One-loop approximation of the effective nonlinearity.** As the maximum eigenvalue of the synaptic weight varies the slope of the effective nonlinearity (solid red) decreases compared to the bare nonlinearity (black dashed). As the mean-field critical value $\Lambda_{\max} = 1/\phi'(0) = 4$ is approached the effective nonlinearity becomes non-monotonic, and breaks down in the supercritical regime.

of the distribution:

$$\begin{aligned}
\Phi_1(y) &= \phi(y) + \frac{\phi(y)\phi''(y)}{2\tau} \left\langle \frac{\lambda^2}{1 - \lambda\phi'(y)} \right\rangle \\
&= \phi(y) + \frac{\phi(y)\phi''(y)}{2\tau} \sum_{\ell=0}^{\infty} \langle \lambda^{2+\ell} \rangle \phi'(y)^\ell \\
&= \phi(y) + \frac{\phi(y)\phi''(y)}{2\tau} \sum_{m=0}^{\infty} \langle \lambda^{2+2m} \rangle \phi'(y)^{2m} \\
&= \phi(y) + \frac{\phi(y)\phi''(y)}{2\tau} \sum_{m=0}^{\infty} (J_0)^{2+2m} \frac{(2+2m)!}{((1+m)!)^2 (2+m)} \phi'(y)^{2m} \\
&= \phi(y) + \frac{J_0^2 \phi(y)\phi''(y)}{2\tau} \frac{1 - 2(J_0\phi'(y))^2 - \sqrt{1 - 4(J_0\phi'(y))^2}}{2(J_0\phi'(y))^4} \\
&= \phi(y) + \frac{\Lambda_{\max}^2 \phi(y)\phi''(y)}{\tau} \frac{1 - \frac{1}{2}(\Lambda_{\max}\phi'(y))^2 - \sqrt{1 - (\Lambda_{\max}\phi'(y))^2}}{(\Lambda_{\max}\phi'(y))^4}
\end{aligned}$$

Although $\phi'(y)$ appears in the denominator here, the limit as $\phi'(y) \rightarrow 0$ is well-defined. As expected, this solution is only valid for $\Lambda_{\max}\phi'(y) < 1$, above which it develops erroneously complex values due to the square root. However, even in the approach to this breakdown, we see the failure of the loop approximation, as the effective nonlinearity becomes non-monotonic near $y = 0$. The 1-loop approximation for $\Phi_1(y)$ also no longer obeys the property $\phi(-y) = 1 - \phi(y)$ exhibited by the bare nonlinearity.

Appendix F: Dynamic mean-field theory treatment of the mean membrane potential dynamics

In order to characterize the dynamics and statistics of the network model when the synaptic connections are Gaussian random variables $J_{ij} \sim \mathcal{N}(0, J_0^2/N)$, $J_{ij} = J_{ji}$ (with $J_{ii} = 0$ for simplicity), we turn to dynamic mean-field theory, which has previously been used to study spin-glasses and the emergence of chaos in rate-based network models [24, 54, 55].

The dynamics of the mean-membrane potential $\psi_i(t)$ follows

$$\tau\psi_i(t) = -\psi_i(t) + \sum_{j=1}^N J_{ij} (\Phi_1(\psi_j(t)) - \Phi_1(0)),$$

where we have inserted $\mathcal{E}_1 = -\sum_{j=1}^N J_{ij} \Phi_1(0)$; i.e., we have tuned the rest potentials so that individual neurons

experience no bias away from $\psi_i = 0$. For convenience, we will write

$$\delta\Phi_1(\psi) = \Phi_1(\psi) - \Phi_1(0)$$

for the calculations in this section. Note that $\delta\Phi_1(0) = 0$ and is negative for $\psi < 0$ and positive for $\psi > 0$.

In the large N limit, at least away from the critical point at $1 = \Lambda_{\max}\Phi'_1(0)$, we expect the sum of inputs to each neuron to act like a Gaussian input noise due to the randomness of J_{ij} . This motivates us to write the mean dynamics as a path integral and then take the expectation over the synaptic weights.

The deterministic equation of the means can be written as a path integral

$$P[\psi|J] = \int \mathcal{D}\tilde{\psi} e^{-S_{\text{mean}}[\tilde{\psi}, \psi]},$$

with action

$$S_{\text{mean}}[\tilde{\psi}, \psi] = \int dt \sum_i \tilde{\psi}_i(t) \left[\dot{\psi}_i(t) + \frac{\psi_i(t)}{\tau} - \frac{1}{\tau} \sum_j J_{ij} \delta\Phi_1(\psi_j(t)) \right].$$

Now, we average the probability $P[\psi|J]$ over J_{ij} , taking account of the fact that $J_{ij} = J_{ji}$. This requires us to write

$$\begin{aligned} \sum_{ij} \tilde{\psi}_i(t) J_{ij} \delta\Phi_1(\psi_j(t)) &= \sum_{i,j < i} \tilde{\psi}_i(t) J_{ij} \delta\Phi_1(\psi_j(t)) + \sum_{i,j > i} \tilde{\psi}_i(t) J_{ij} \delta\Phi_1(\psi_j(t)) \\ &= \sum_{i,j < i} \tilde{\psi}_i(t) J_{ij} \delta\Phi_1(\psi_j(t)) + \sum_{i,j < i} \tilde{\psi}_j(t) J_{ji} \delta\Phi_1(\psi_i(t)) \\ &= \sum_{i,j < i} J_{ij} \left[\tilde{\psi}_i(t) \delta\Phi_1(\psi_j(t)) + \tilde{\psi}_j(t) \delta\Phi_1(\psi_i(t)) \right]. \end{aligned}$$

These terms are integrated over time. We can now perform the average, giving an averaged action of

$$S_{\text{eff}}[\tilde{\psi}, \psi] = \int dt \sum_i \tilde{\psi}_i(t) \left[\dot{\psi}_i(t) + \frac{\psi_i(t)}{\tau} \right] - \frac{J_0^2}{2N\tau^2} \sum_{i,j < i} \left(\int dt \left\{ \tilde{\psi}_i(t) \delta\Phi_1(\psi_j(t)) + \tilde{\psi}_j(t) \delta\Phi_1(\psi_i(t)) \right\} \right)^2.$$

Expanding the square, we may write the non-local part of the action as

$$\begin{aligned} &\sum_{i,j < i} \left(\int dt \left\{ \tilde{\psi}_i(t) \delta\Phi_1(\psi_j(t)) + \tilde{\psi}_j(t) \delta\Phi_1(\psi_i(t)) \right\} \right)^2 \\ &= \sum_{i,j < i} \int dt_1 dt_2 \left\{ \tilde{\psi}_i(t_1) \delta\Phi_1(\psi_j(t_1)) + \tilde{\psi}_j(t_1) \delta\Phi_1(\psi_i(t_1)) \right\} \left\{ \tilde{\psi}_i(t_2) \delta\Phi_1(\psi_j(t_2)) + \tilde{\psi}_j(t_2) \delta\Phi_1(\psi_i(t_2)) \right\} \\ &= \sum_{i,j < i} \int dt_1 dt_2 \left\{ \tilde{\psi}_i(t_1) \delta\Phi_1(\psi_j(t_1)) \tilde{\psi}_i(t_2) \delta\Phi_1(\psi_j(t_2)) + \tilde{\psi}_i(t_1) \delta\Phi_1(\psi_j(t_1)) \tilde{\psi}_j(t_2) \delta\Phi_1(\psi_i(t_2)) \right. \\ &\quad \left. + \tilde{\psi}_j(t_1) \delta\Phi_1(\psi_i(t_1)) \tilde{\psi}_i(t_2) \delta\Phi_1(\psi_j(t_2)) + \tilde{\psi}_j(t_1) \delta\Phi_1(\psi_i(t_1)) \tilde{\psi}_j(t_2) \delta\Phi_1(\psi_i(t_2)) \right\} \\ &= \sum_{i \neq j} \int dt_1 dt_2 \left\{ \tilde{\psi}_i(t_1) \tilde{\psi}_i(t_2) \delta\Phi_1(\psi_j(t_1)) \delta\Phi_1(\psi_j(t_2)) + \tilde{\psi}_i(t_1) \delta\Phi_1(\psi_i(t_2)) \tilde{\psi}_j(t_2) \delta\Phi_1(\psi_j(t_1)) \right\} \\ &\approx \sum_{i,j} \int dt_1 dt_2 \left\{ \tilde{\psi}_i(t_1) \tilde{\psi}_i(t_2) \delta\Phi_1(\psi_j(t_1)) \delta\Phi_1(\psi_j(t_2)) + \tilde{\psi}_i(t_1) \delta\Phi_1(\psi_i(t_2)) \tilde{\psi}_j(t_2) \delta\Phi_1(\psi_j(t_1)) \right\}, \end{aligned}$$

where we added back in the $i = j$ term, which we expect to be $\mathcal{O}(N)$ and negligible compared to the $\mathcal{O}(N^2)$ amount of $i \neq j$ terms.

The next step is to render the action local in neuron indices, though not time, by introducing a pair of fields,

$$NQ_1(t_1, t_2) = \sum_{i=1}^N \delta\Phi_1(\psi_i(t_1))\delta\Phi_1(\psi_i(t_2)), \quad (\text{F1})$$

$$N\tilde{Q}_2(t_1, t_2) = \sum_{i=1}^N \tilde{\psi}_i(t_1)\delta\Phi_1(\psi_i(t_2)), \quad (\text{F2})$$

enforcing this change of variables by functional delta functions, represented in Fourier space and thereby introducing two additional fields $\tilde{Q}_1(t_1, t_2)$ and $Q_2(t_1, t_2)$. The effective action will become

$$S_{\text{eff}}[\tilde{\psi}, \psi | Q_1, \tilde{Q}_2] = \int dt \sum_i \tilde{\psi}_i(t) \left[\dot{\psi}_i(t) + \frac{\psi_i(t)}{\tau} \right] - \frac{J_0^2}{2N\tau^2} \int dt_1 dt_2 \left\{ \sum_i \tilde{\psi}_i(t_1) \tilde{\psi}_i(t_2) NQ_1(t_1, t_2) + N^2 \tilde{Q}_2(t_1, t_2) \tilde{Q}_2(t_2, t_1) \right\}. \quad (\text{F3})$$

The probability distribution for the fields Q_1 and \tilde{Q}_2 will be

$$P[Q_1, \tilde{Q}_2] \equiv \int \mathcal{D}[\tilde{Q}_1, Q_2, \tilde{\psi}, \psi] e^{-\tilde{Q}_1 \cdot (NQ_1 - \sum_i \delta\Phi_1(\psi_i(t_1))\delta\Phi_1(\psi_i(t_2))) - Q_2 \cdot (N\tilde{Q}_2 - \sum_i \tilde{\psi}_i(t_1)\delta\Phi_1(\psi_i(t_2)))} \times e^{-S_{\text{eff}}[\tilde{\psi}, \psi | Q_1, \tilde{Q}_2]} \quad (\text{F4})$$

$$= \int \mathcal{D}[\tilde{Q}_1, Q_2] e^{-N \left\{ \tilde{Q}_1 \cdot Q_1 - Q_2 \cdot \tilde{Q}_2 - \frac{J_0^2}{2\tau^2} \int dt_1 dt_2 \tilde{Q}_2(t_1, t_2) \tilde{Q}_2(t_2, t_1) \right\} + \sum_i W_{\text{local}}^{(i)}[Q_1, \tilde{Q}_1, Q_2]}, \quad (\text{F5})$$

where

$$e^{W_{\text{local}}^{(i)}[Q_1, \tilde{Q}_1, Q_2]} \equiv \int \mathcal{D}[\tilde{\psi}, \psi] e^{-\int dt \tilde{\psi}_i(t) [\dot{\psi}_i(t) + \psi_i(t)/\tau - \int dt_2 Q_2(t, t_2) \delta\Phi_1(\psi_i(t_2))]} \times e^{\int dt_1 dt_2 \{ \tilde{\psi}_i(t_1) Q_1(t_1, t_2) \tilde{\psi}_i(t_2) + \delta\Phi_1(\psi_i(t_1)) \tilde{Q}_1(t_1, t_2) \delta\Phi_1(\psi_i(t_2)) \}}. \quad (\text{F6})$$

We notice that W_{local} decouples over each of the neurons, and may in fact be written as N copies of the same action, $\sum_i W_{\text{local}} = NW_{\text{local}}$. We can then take the $N \rightarrow \infty$ limit of our action and evaluate it by the method of steepest descents. We define

$$S_Q[Q_1, \tilde{Q}_1, Q_2, \tilde{Q}_2] = \int dt_1 dt_2 \left\{ \tilde{Q}_1(t_1, t_2) Q_1(t_1, t_2) + \tilde{Q}_2(t_1, t_2) Q_2(t_1, t_2) - \frac{J_0^2}{2\tau^2} \tilde{Q}_2(t_1, t_2) \tilde{Q}_2(t_2, t_1) \right\} - W_{\text{local}}[Q_1, \tilde{Q}_1, Q_2].$$

We have four saddle-point equations to solve for:

$$\begin{aligned} \frac{\delta S_Q[Q_1, \tilde{Q}_1, Q_2, \tilde{Q}_2]}{\delta \tilde{Q}_1(t, t')} &= Q_1(t, t') - \frac{\delta W_{\text{local}}}{\delta \tilde{Q}_1(t, t')} \\ \frac{\delta S_Q[Q_1, \tilde{Q}_1, Q_2, \tilde{Q}_2]}{\delta Q_1(t, t')} &= \tilde{Q}_1(t, t') - \frac{\delta W_{\text{local}}}{\delta Q_1(t, t')} \\ \frac{\delta S_Q[Q_1, \tilde{Q}_1, Q_2, \tilde{Q}_2]}{\delta \tilde{Q}_2(t, t')} &= Q_2(t, t') - \frac{J_0^2}{\tau^2} \tilde{Q}_2(t', t) \\ \frac{\delta S_Q[Q_1, \tilde{Q}_1, Q_2, \tilde{Q}_2]}{\delta Q_2(t, t')} &= \tilde{Q}_2(t, t') - \frac{\delta W_{\text{local}}}{\delta Q_2(t, t')} \end{aligned}$$

The derivatives over the local action yield

$$\begin{aligned}
\frac{\delta W_{\text{local}}}{\delta \tilde{Q}_1(t, t')} &= e^{-W_{\text{local}}} \int \mathcal{D}[\tilde{\psi}, \psi] \delta\Phi_1(\psi(t)) \delta\Phi_1(\psi(t')) e^{-\int dt \tilde{\psi}(t) [\dot{\psi}(t) + \psi(t)/\tau - \int dt_2 Q_2(t, t_2) \delta\Phi_1(\psi(t_2))]} \\
&\quad \times e^{\int dt_1 dt_2 \{ \tilde{\psi}(t_1) Q_1(t_1, t_2) \tilde{\psi}(t_2) + \delta\Phi_1(\psi(t_1)) \tilde{Q}_1(t_1, t_2) \delta\Phi_1(\psi(t_2)) \}} \\
&= \langle \delta\Phi_1(\psi(t)) \delta\Phi_1(\psi(t')) \rangle_Q \\
\frac{\delta W_{\text{local}}}{\delta Q_1(t, t')} &= e^{-W_{\text{local}}} \int \mathcal{D}[\tilde{\psi}, \psi] \tilde{\psi}(t) \tilde{\psi}(t') e^{-\int dt \tilde{\psi}(t) [\dot{\psi}(t) + \psi(t)/\tau - \int dt_2 Q_2(t, t_2) \delta\Phi_1(\psi(t_2))]} \\
&\quad \times e^{\int dt_1 dt_2 \{ \tilde{\psi}(t_1) Q_1(t_1, t_2) \tilde{\psi}(t_2) + \delta\Phi_1(\psi(t_1)) \tilde{Q}_1(t_1, t_2) \delta\Phi_1(\psi(t_2)) \}} \\
&= \langle \tilde{\psi}(t) \tilde{\psi}(t') \rangle_Q \\
\frac{\delta W_{\text{local}}}{\delta Q_2(t, t')} &= e^{-W_{\text{local}}} \int \mathcal{D}[\tilde{\psi}, \psi] \tilde{\psi}(t) \delta\Phi_1(\psi(t')) e^{-\int dt \tilde{\psi}(t) [\dot{\psi}(t) + \psi(t)/\tau - \int dt_2 Q_2(t, t_2) \delta\Phi_1(\psi(t_2))]} \\
&\quad \times e^{\int dt_1 dt_2 \{ \tilde{\psi}(t_1) Q_1(t_1, t_2) \tilde{\psi}(t_2) + \delta\Phi_1(\psi(t_1)) \tilde{Q}_1(t_1, t_2) \delta\Phi_1(\psi(t_2)) \}} \\
&= \langle \tilde{\psi}(t) \delta\Phi_1(\psi(t')) \rangle_Q,
\end{aligned}$$

where all of these averages, denoted with the subscript Q , are over the stochastic process $\psi(t)$ with response field $\tilde{\psi}(t)$ that obeys the Langevin equation

$$\dot{\psi}(t) = -\psi(t)/\tau + \int dt' Q_2(t, t') \delta\Phi_1(\psi(t')) + \eta(t),$$

where $\eta(t)$ is a Gaussian noise with mean zero and covariance $Q_1(t, t')$. These averages must be computed self-consistently in order to solve for the Q 's, as our saddle-point equations reduce to

$$\begin{aligned}
Q_1(t, t') &= \langle \delta\Phi_1(\psi(t)) \delta\Phi_1(\psi(t')) \rangle_Q \\
\tilde{Q}_1(t, t') &= \langle \tilde{\psi}(t) \tilde{\psi}(t') \rangle_Q \\
Q_2(t, t') &= \frac{J_0^2}{\tau^2} \tilde{Q}_2(t', t), \\
\tilde{Q}_2(t, t') &= \langle \tilde{\psi}(t) \delta\Phi_1(\psi(t')) \rangle_Q.
\end{aligned}$$

Some comments on these equations are in order. The first question dictates that the noise covariance of the effective noisy process of the mean dynamics is equal to the covariance of the nonlinearities over the stochastic mean process. The second equation is the covariance of the response fields, but in the steady-state, which we focus on in this work, this expectation must be zero, or it would violate causality [24, 54]. The last two fields end up being proportional but with opposite time-arguments, resulting in $Q_2(t, t')$ being proportional to the linear response of the nonlinearity to changes in the membrane potential.

Solving the self-consistent equations is difficult due to the nonlinearity, which is not even analytic in the supercritical regime. However, in the supercritical regime there is an extended linear region of the nonlinearity, which we might hope will enable an approximate solution.

In order to evaluate the expectations involving the nonlinearities, $\langle \tilde{\psi}(t) \delta\Phi_1(\psi(t')) \rangle_Q$ and $\langle \delta\Phi_1(\psi(t)) \delta\Phi_1(\psi(t')) \rangle_Q$, we will introduce a fictitious spiking process, and then evaluate the response and correlation functions using a mean-field approximation. We do not necessarily expect this approximation to be quantitatively accurate, but hope it will produce qualitatively reasonable results. The extended action including the spiking process becomes

$$S_1[\tilde{\psi}, \psi, \tilde{r}, r] = \int dt \left\{ \tilde{\psi}(t) \left[\dot{\psi}(t) + \psi(t)/\tau + q_2 r_0 - \int dt' Q_2(t - t') r(t') \right] - \frac{1}{2} \int dt' \tilde{\psi}(t) Q_1(t - t') \tilde{\psi}(t') \right\} \quad (\text{F7})$$

$$+ \tilde{r}(t) r(t) - \left(e^{\tilde{r}(t)} - 1 \right) \Phi_1(\psi(t)) \right\}, \quad (\text{F8})$$

where $q_2 = \int dt' Q_2(t - t')$ and $r_0 = \Phi_1(0)$. The steady-state mean-field equations give $\tilde{\psi} = \tilde{r} = 0$ and

$$\begin{aligned}\psi &= q_2\tau(r - r_0) \\ r &= \Phi_1(\psi).\end{aligned}$$

We require the mean membrane potential to be zero, which in turn implies $r = r_0$. We expand the action around these mean-field values, $r(t) = r_0 + \delta r$, $\psi = \delta\psi$, and similarly for the response fields. We also use the fact that the nonlinearity is approximately linear in the supercritical regime to write $\Phi_1(\psi) \approx r_0 + g\delta\psi$ in the action, where we set $g = \Phi'_1(0)$ for brevity in the following calculations (not to be confused with the dimensionless couplings g_{mn} in the non-dimensionalized flow equations). Keeping only quadratic terms yields

$$\begin{aligned}S_1[\tilde{\psi}, \delta\psi, \tilde{r}, \delta r] &\approx \int dt \left\{ \tilde{\psi}(t) \left[\dot{\psi}(t) + \psi(t)/\tau - \int dt' Q_2(t - t')\delta r(t') \right] - \frac{1}{2} \int dt' \tilde{\psi}(t)Q_1(t - t')\tilde{\psi}(t') \right. \\ &\quad \left. + \tilde{r}(t)(r_0 + \delta r(t)) - \left(\tilde{r}(t) + \frac{1}{2}\tilde{r}(t)^2 \right) \{r_0 + g\delta\psi(t)\} \right\} \\ &= \int dt \left\{ \tilde{\psi}(t) \left[\dot{\psi}(t) + \psi(t)/\tau - \int dt' Q_2(t - t')\delta r(t') \right] - \frac{1}{2} \int dt' \tilde{\psi}(t)Q_1(t - t')\tilde{\psi}(t') \right. \\ &\quad \left. + \tilde{r}(t)\delta r(t) - g\tilde{r}(t)\delta\psi(t) - \frac{1}{2}\tilde{r}(t)^2 r_0 \right\} \\ &= \int dt dt' \left\{ \tilde{\psi}(t) \left[\left(\frac{d}{dt} + \frac{1}{\tau} \right) \delta(t - t') \right] \psi(t') - \tilde{\psi}(t)Q_2(t - t')\delta r(t') - \frac{1}{2}\tilde{\psi}(t)Q_1(t - t')\tilde{\psi}(t') \right. \\ &\quad \left. + \tilde{r}(t)\delta(t - t')\delta r(t) - \tilde{r}(t)g\delta(t - t')\delta\psi(t) - \frac{1}{2}\tilde{r}(t)r_0\delta(t - t')\tilde{r}(t') \right\}.\end{aligned}$$

The action is entirely of convolutional form, which motivates transforming into frequency space. In frequency space the action becomes (using the Fourier convention $f(t) = (2\pi)^{-1} \int_{-\infty}^{\infty} d\omega e^{i\omega t} f(\omega)$, which differs from our convention in Appendix G)

$$\begin{aligned}S_1[\tilde{\psi}, \delta\psi, \tilde{r}, \delta r] &= \int d\omega \left\{ \tilde{\psi}(-\omega) (i\omega + \tau^{-1}) \psi(\omega) - \tilde{\psi}(-\omega)Q_2(\omega)\delta r(\omega) - \frac{1}{2}\tilde{\psi}(-\omega)Q_1(\omega)\tilde{\psi}(\omega) \right. \\ &\quad \left. + \tilde{r}(-\omega)\delta r(\omega) - \tilde{r}(-\omega)g\delta\psi(\omega) - \frac{1}{2}\tilde{r}(-\omega)r_0\tilde{r}(\omega) \right\}.\end{aligned}$$

We may write this as

$$\begin{aligned}S_1[\tilde{\psi}, \delta\psi, \tilde{r}, \delta r] &= \frac{1}{2} \int d\omega \left\{ \tilde{\psi}(-\omega) (i\omega + \tau^{-1}) \psi(\omega) - \tilde{\psi}(-\omega)Q_2(\omega)\delta r(\omega) - \tilde{\psi}(-\omega)Q_1(\omega)\tilde{\psi}(\omega) \right. \\ &\quad \left. + \tilde{r}(-\omega)\delta r(\omega) - \tilde{r}(-\omega)g\delta\psi(\omega) - \tilde{r}(-\omega)r_0\tilde{r}(\omega) + \{\omega \leftrightarrow -\omega\} \right\},\end{aligned}$$

which allows us to write the action in matrix form

$$S_1[\tilde{\psi}, \delta\psi, \tilde{r}, \delta r] = -\frac{1}{2} \int d\omega \begin{bmatrix} \tilde{\psi}(-\omega) \\ \psi(-\omega) \\ \tilde{r}(-\omega) \\ r(-\omega) \end{bmatrix}^T \begin{bmatrix} Q_1(\omega) & -(i\omega + \tau^{-1}) & 0 & Q_2(\omega) \\ -(-i\omega + \tau^{-1}) & 0 & g & 0 \\ 0 & g & r_0 & -1 \\ Q_2(-\omega) & 0 & -1 & 0 \end{bmatrix} \begin{bmatrix} \tilde{\psi}(\omega) \\ \psi(\omega) \\ \tilde{r}(\omega) \\ r(\omega) \end{bmatrix}.$$

The matrix in this form is the inverse-covariance/response matrix in frequency space. Performing the matrix inversion will yield the (Gaussian approximation to the) covariance and response functions.

We get

$$\langle \tilde{\psi} \delta r \rangle_Q(\omega) = \frac{g}{-i\omega + \tau^{-1} - gQ_2(-\omega)}, \quad (\text{F9})$$

$$\langle \delta r \delta r \rangle_Q(\omega) = \frac{r_0(\omega^2 + \tau^{-2}) + g^2 Q_1(\omega)}{|i\omega + \tau^{-1} - gQ_2(\omega)|^2}, \quad (\text{F10})$$

$$\langle \psi \psi \rangle_Q(\omega) = \frac{Q_1(\omega) + r_0|Q_2(\omega)|^2}{|i\omega + \tau^{-1} - gQ_2(\omega)|^2}. \quad (\text{F11})$$

Our self-consistent equations impose

$$Q_2(\omega) = \frac{J_0^2}{\tau^2} \frac{g}{-i\omega + \tau^{-1} - gQ_2(-\omega)}.$$

We can solve this as a system of equations for $z_1 = Q_2(\omega)$ and $z_2 = Q_2(-\omega)$. We find multiple solutions, but the correct solution that numerically integrates to a legitimate response function is

$$Q_2(\omega) = \frac{i\omega\tau + 1 - \sqrt{(i\omega\tau + 1)^2 - 4J_0^2g^2}}{2g\tau}. \quad (\text{F12})$$

Note that for the supercritical nonlinearity we have $4g^2J_0^2 = 1$.

Next, we solve for $Q_1(\omega)$,

$$Q_1(\omega) = \frac{r_0(\omega^2 + \tau^{-2}) + g^2 Q_1(\omega)}{|i\omega + \tau^{-1} - gQ_2(\omega)|^2}.$$

We use the fact that we may write

$$|Q_2(\omega)|^2 = \left(\frac{J_0^2 g}{\tau^2} \right)^2 \frac{1}{|i\omega + \tau^{-1} - gQ_2(\omega)|^2}$$

to simplify the right-hand-side, and solve for $Q_1(\omega)$ in terms of $Q_2(\omega)$:

$$Q_1(\omega) = r_0 \left(\frac{\tau^2}{J_0^2 g} \right)^2 |Q_2(\omega)|^2 \frac{\omega^2 + \tau^{-2}}{1 - g^2 \left(\frac{\tau^2}{J_0^2 g} \right)^2 |Q_2(\omega)|^2}. \quad (\text{F13})$$

We will not simplify this expression further. We plug it into the expression for the membrane-potential covariance, Eq. (F11). By integrating the result over frequency we can obtain an estimate of the membrane potential variance across the population. The numerical solution breaks down if $g = \Lambda_{\max}^{-1}$ is too large, as is expected because we anticipate our calculation is only valid well into the supercritical regime.

A final note on this dynamic mean-field calculation: in applying this method we assumed we could use the effective nonlinearity $\Phi_1(\psi)$, which has already been calculated using the $N \rightarrow \infty$ limit. We then take a subsequent $N \rightarrow \infty$ for the mean dynamics. In principle, these limits should be taken simultaneously, and we are assuming that taking the limits separately will yield the same result as taking a single simultaneous limit. The reason for this subtlety is that for finite N the effective nonlinearity is a random quantity depending on the specific realization of J_{ij} , and would therefore couple to J_{ij} in the dynamic mean-field calculation. Our calculation assumes such a coupling will be negligible in the $N \rightarrow \infty$ limit.

Appendix G: Derivation of the dimensionless flow equation

We derive the dimensionless flow equation for the effective potential $W_\Lambda(\tilde{x}, y)$, defined by $U_\Lambda(\tilde{x}, y) = \Lambda_{\max}^{-1} \tilde{x}y + W_\Lambda(\tilde{x}, y)$. We remove the factor of Λ_{\max}^{-1} because we anticipate that at a critical point we must have $U_{\Lambda=\Lambda_{\max}}^{(1,1)}(0, 0) = \Lambda_{\max}^{-1}$, and removing this term will allow us to isolate the singular contributions to the scaling that arise from $\delta\Lambda = \Lambda_{\max} - \Lambda$, the generalization of the running momentum k^2 to non-lattice models. We define the dimensionless potential

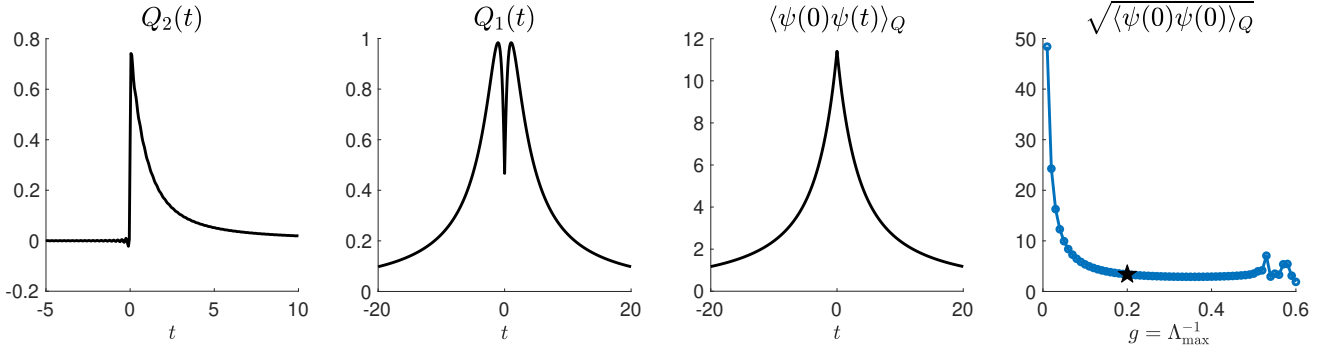


FIG. 16. **Numerical estimates of the self-consistent population statistics in supercritical regime.** Computed numerically in Mathematica by evaluating Eqs. (F9)-(F11) using Eqs. (F12) and (F13) and numerically integrating against $\exp(i\omega t)$. The estimates break down for large $g = \Lambda_{\max}^{-1}$, for which the network is no longer in the supercritical regime and our approximations may not be expected to work well. The plot of $\sqrt{\langle\psi(0)\psi(0)\rangle_Q}$ shows a wider range of g values compared to Fig. 8 in the main text.

$w_s(\tilde{z}, z)$ by

$$W_\Lambda(\tilde{x}, y) = \Omega_\Lambda w_s(\tilde{z}, z), \quad \tilde{z} = \tilde{x}/X_\Lambda, \quad z = y/Y_\Lambda,$$

where Ω_Λ is a running amplitude, X_Λ is a running spike response scale, and Y_Λ is a running membrane potential scale. We have also denoted $w_s(\tilde{z}, z)$ to depend on the “RG-time” $s = -\ln\left(\frac{\Lambda_{\max}-\Lambda}{\Lambda_{\max}-\Lambda_{\min}}\right)$ rather than Λ ; our definition of the RG-time runs from 0 to $+\infty$, in contrast to the convention in some NRG studies that define s to be negative. The running scales Ω_Λ and Y_Λ will be chosen in such a way to render the flow equation asymptotically autonomous as $s \rightarrow \infty$, which will determine how they scale with $\delta\Lambda$. The running scale X_Λ will be chosen to help isolate fixed point solution expected for some different universality classes.

We begin by considering the right-hand-side of the flow equation,

$$\begin{aligned} & \frac{\rho_\lambda(\Lambda)}{2\tau} \left(1 - \Lambda U_\Lambda^{(1,1)}(\tilde{x}, y) - \sqrt{(1 - \Lambda U_\Lambda^{(1,1)}(\tilde{x}, y))^2 - \Lambda^2 U_\Lambda^{(0,2)}(\tilde{x}, y) U_\Lambda^{(2,0)}(\tilde{x}, y)} \right) \\ &= \frac{\rho_\lambda(\Lambda)}{2\tau} \left(1 - \frac{\Lambda}{\Lambda_{\max}} - \Lambda W_\Lambda^{(1,1)}(\tilde{x}, y) - \sqrt{\left(1 - \frac{\Lambda}{\Lambda_{\max}} - \Lambda W_\Lambda^{(1,1)}(\tilde{x}, y)\right)^2 - \Lambda^2 W_\Lambda^{(0,2)}(\tilde{x}, y) W_\Lambda^{(2,0)}(\tilde{x}, y)} \right) \\ &= \frac{\rho_\lambda(\Lambda)}{2\tau} \left(\frac{\delta\Lambda}{\Lambda_{\max}} - \Lambda W_\Lambda^{(1,1)}(\tilde{x}, y) - \sqrt{\left(\frac{\delta\Lambda}{\Lambda_{\max}} - \Lambda W_\Lambda^{(1,1)}(\tilde{x}, y)\right)^2 - \Lambda^2 W_\Lambda^{(0,2)}(\tilde{x}, y) W_\Lambda^{(2,0)}(\tilde{x}, y)} \right). \end{aligned}$$

Next, we insert our definition $W_\Lambda(\tilde{x}, y) = \Omega_\Lambda w_s(\tilde{z}, z)$, using $W_\Lambda^{(m,n)}(\tilde{x}, y) = \Omega_\Lambda X_\Lambda^{-m} Y_\Lambda^{-n} w_s^{(m,n)}(\tilde{z}, z)$:

$$\frac{\rho_\lambda(\Lambda)}{2\tau} \left(\frac{\delta\Lambda}{\Lambda_{\max}} - \frac{\Lambda \Omega_\Lambda}{X_\Lambda Y_\Lambda} w_s^{(1,1)}(\tilde{z}, z) - \sqrt{\left(\frac{\delta\Lambda}{\Lambda_{\max}} - \frac{\Lambda \Omega_\Lambda}{Y_\Lambda} w_s^{(1,1)}(\tilde{z}, z)\right)^2 - \left(\frac{\Lambda \Omega_\Lambda}{X_\Lambda Y_\Lambda}\right)^2 w_s^{(0,2)}(\tilde{z}, z) w_s^{(2,0)}(\tilde{z}, z)} \right)$$

The first step to render this “asymptotically autonomous” is to impose

$$\frac{\Omega_\Lambda}{X_\Lambda Y_\Lambda} \equiv \frac{\delta\Lambda}{\Lambda_{\max}^2}, \quad (G1)$$

giving an RHS of

$$\frac{\rho_\lambda(\Lambda)\delta\Lambda}{2\Lambda_{\max}\tau} \left(1 - \frac{\Lambda}{\Lambda_{\max}} w_s^{(1,1)}(\tilde{z}, z) - \sqrt{\left(1 - \frac{\Lambda}{\Lambda_{\max}} w_s^{(1,1)}(\tilde{z}, z)\right)^2 - \left(\frac{\Lambda}{\Lambda_{\max}}\right)^2 w_s^{(0,2)}(\tilde{z}, z) w_s^{(2,0)}(\tilde{z}, z)} \right),$$

having factored out $\delta\Lambda/\Lambda_{\max}$ from the square root. The RHS side has an explicit dependence on Λ/Λ_{\max} , but this tends to 1 asymptotically as the end of the RG flow is approached.

We now turn to the left-hand-side (LHS) of the flow equation:

$$\begin{aligned}\partial_\Lambda U_\Lambda(\tilde{x}, y) &= \partial_\Lambda W_\Lambda(\tilde{x}, y) \\ &= \partial_\Lambda [\Omega_\Lambda w_s(\tilde{x}/X_\Lambda, y/Y_\Lambda)] \Big|_{\tilde{x}, y}\end{aligned}$$

To simplify the LHS we need to account for the fact that the derivative ∂_Λ is taken holding \tilde{x} and y fixed (denoted explicitly by $\Big|_{\tilde{x}, y}$), and must be converted to a derivative holding \tilde{z} and z fixed. This gives rise to the “dimensional flow” terms (as called in other NPRG works) that permit the existence of fixed points. We may expand $\partial_\Lambda [\Omega_\Lambda w_s(\tilde{x}/X_\Lambda, y/Y_\Lambda)]$ as follows:

$$\partial_\Lambda [\Omega_\Lambda w_s(\tilde{x}/X_\Lambda, y/Y_\Lambda)] \Big|_{\tilde{x}, y} = \Omega_\Lambda \partial_\Lambda w_s(\tilde{z}, z) \Big|_{\tilde{z}, z} + \frac{\partial_\Lambda \Omega_\Lambda}{\Omega_\Lambda} \Omega_\Lambda w_s(\tilde{z}, z) - \Omega_\Lambda \frac{\partial_\Lambda X_\Lambda}{X_\Lambda} \tilde{z} w_s^{(1,0)}(\tilde{z}, z) - \Omega_\Lambda \frac{\partial_\Lambda Y_\Lambda}{Y_\Lambda} z w_s^{(0,1)}(\tilde{z}, z),$$

which follows from an application of the chain rule to each Λ -dependent term and inserting $\tilde{z} = \tilde{x}/X_\Lambda$ and $z = y/Y_\Lambda$. As we have converted everything to \tilde{z} and z now we will again drop the explicit notation denoting which variables are held constant during partial differentiation.

At this point, let us put everything from the LHS and RHS together, dividing the factor of Ω_Λ on the LHS over to the RHS:

$$\begin{aligned}\partial_\Lambda w_s(\tilde{z}, z) + \frac{\partial_\Lambda \Omega_\Lambda}{\Omega_\Lambda} w_s(\tilde{z}, z) - \frac{\partial_\Lambda X_\Lambda}{X_\Lambda} \tilde{z} w_s^{(1,0)}(\tilde{z}, z) - \frac{\partial_\Lambda Y_\Lambda}{Y_\Lambda} z w_s^{(0,1)}(\tilde{z}, z) \\ = \frac{\rho_\lambda(\Lambda) \delta\Lambda}{2\Lambda_{\max} \Omega_\Lambda \tau} \left[1 - \frac{\Lambda}{\Lambda_{\max}} w_s^{(1,1)}(\tilde{z}, z) - \sqrt{\left(1 - \frac{\Lambda}{\Lambda_{\max}} w_s^{(1,1)}(\tilde{z}, z)\right)^2 - \left(\frac{\Lambda}{\Lambda_{\max}}\right)^2 w_s^{(0,2)}(\tilde{z}, z) w_s^{(2,0)}(\tilde{z}, z)} \right]\end{aligned}$$

To get the LHS into the desired form for identifying fixed points, we want to convert this fully to a function of the RG-time s . We may do so by noting that $\partial_\Lambda = -\partial_{\delta\Lambda}$ and multiplying both sides by $\delta\Lambda$. We may then write $-\delta\Lambda \partial_{\delta\Lambda} = \partial_s$. Thus,

$$\begin{aligned}\partial_s w_s(\tilde{z}, z) + (\partial_s \ln \Omega_\Lambda) w_s(\tilde{z}, z) - (\partial_s \ln X_\Lambda) \tilde{z} w_s^{(1,0)}(\tilde{z}, z) - (\partial_s \ln Y_\Lambda) z w_s^{(0,1)}(\tilde{z}, z) \\ = \frac{\rho_\lambda(\Lambda) \delta\Lambda^2}{2\Lambda_{\max} \Omega_\Lambda \tau} \left[1 - \frac{\Lambda}{\Lambda_{\max}} w_s^{(1,1)}(\tilde{z}, z) - \sqrt{\left(1 - \frac{\Lambda}{\Lambda_{\max}} w_s^{(1,1)}(\tilde{z}, z)\right)^2 - \left(\frac{\Lambda}{\Lambda_{\max}}\right)^2 w_s^{(0,2)}(\tilde{z}, z) w_s^{(2,0)}(\tilde{z}, z)} \right]\end{aligned}$$

Now, we can make a choice of Ω_Λ that renders our flow equation fully asymptotically autonomous. Noting that $\rho_\lambda(\Lambda) \rightarrow c\delta\Lambda^{d_+/2-1}$ as $\delta\Lambda \rightarrow 0$, for some dimensionful constant c that depends on the exact eigenvalue distribution, we choose to define Ω_Λ as

$$\Omega_\Lambda \equiv \frac{c \delta\Lambda^{d_+/2+1}}{2\Lambda_{\max} \tau}. \quad (\text{G2})$$

For this choice the prefactor on the RHS of the low equation tends to 1 as $s \rightarrow \infty$. Note that in principle we could have chosen to impose $\Omega_\Lambda = \rho_\lambda(\Lambda) \delta\Lambda^2 / (2\Lambda_{\max} \tau)$ so that this prefactor is 1 exactly, but because $\rho_\lambda(\Lambda)$ scales as $|\Lambda - \Lambda_{\min}|^{d_-/2-1}$ as $\Lambda \rightarrow \Lambda_{\min}$ ($s \rightarrow 0$) for some dimension d_- , this would result in $\Omega_\Lambda \rightarrow 0$, resulting in divergences in the flow equation and the initial conditions of $w_s(\tilde{z}, z)$ that ultimately balance out but would make analytical and numerical analyses difficult. It is simpler to define Ω_Λ as above, as it remains finite as $s \rightarrow 0$.

Now that we have defined Ω_Λ , we may evaluate the logarithmic derivatives appearing on the LHS of the flow equation. Using $\delta\Lambda = (\Lambda_{\max} - \Lambda_{\min})e^{-s}$, we have

$$\begin{aligned}\partial_s \ln \Omega_\Lambda &= \partial_s \ln \left(\frac{c (\Lambda_{\max} - \Lambda_{\min})^{d_+/2+1} e^{-s(d_+/2-1)}}{2\Lambda_{\max} \tau} \right) \\ &= -\left(\frac{d_+}{2} + 1\right),\end{aligned}$$

and

$$\begin{aligned}\partial_s \ln Y_\Lambda &= \partial_s \ln \left(\frac{\Lambda_{\max} \Lambda_{\max} \Omega_\Lambda}{\delta \Lambda} \right) \\ &= \partial_s \ln \left(\text{const.} \times \frac{\delta \Lambda^{d_+/2}}{X_\Lambda} \right) \\ &= - \left(\frac{d_+}{2} - \eta_s^X \right),\end{aligned}$$

where we used the definition $\eta_s^X \equiv -\partial_s \ln X_\Lambda$.

Our flow equation, with explicit non-autonomous terms, simplifies to

$$\begin{aligned}\partial_s w_s(\tilde{z}, z) - \left(\frac{d_+}{2} + 1 \right) w_s(\tilde{z}, z) + \eta_s^X \tilde{z} w_s^{(1,0)}(\tilde{z}, z) + \left(\frac{d_+}{2} - \eta_s^X \right) z w_s^{(0,1)}(\tilde{z}, z) \\ = \frac{\rho_\lambda(\Lambda)}{c \delta \Lambda^{d_+/2-1}} \left[1 - \frac{\Lambda}{\Lambda_{\max}} w_s^{(1,1)}(\tilde{z}, z) - \sqrt{\left(1 - \frac{\Lambda}{\Lambda_{\max}} w_s^{(1,1)}(\tilde{z}, z) \right)^2 - \left(\frac{\Lambda}{\Lambda_{\max}} \right)^2 w_s^{(0,2)}(\tilde{z}, z) w_s^{(2,0)}(\tilde{z}, z)} \right].\end{aligned}$$

We may finally take the asymptotic limit $\delta \Lambda \rightarrow 0$ ($s \rightarrow \infty$) to obtain the flow equation given in the main text:

$$\begin{aligned}\partial_s w_s(\tilde{z}, z) - \left(\frac{d_+}{2} + 1 \right) w_s(\tilde{z}, z) + \eta_s^X \tilde{z} w_s^{(1,0)}(\tilde{z}, z) + \left(\frac{d_+}{2} - \eta_s^X \right) z w_s^{(0,1)}(\tilde{z}, z) \\ = 1 - w_s^{(1,1)}(\tilde{z}, z) - \sqrt{\left(1 - w_s^{(1,1)}(\tilde{z}, z) \right)^2 - w_s^{(0,2)}(\tilde{z}, z) w_s^{(2,0)}(\tilde{z}, z)}.\end{aligned}$$

Again, we retain the derivative $\partial_s w_s$ to help with determining linear stability of fixed point solutions.

Lastly, we give the initial conditions for $w_0(\tilde{z}, z)$, given our macroscopic initial condition $U_{\Lambda_{\min}}(\tilde{x}, y) = (e^{\tilde{x}} - 1) \phi(y)$. Using our definition $W_\Lambda(\tilde{x}, y) = \Omega_\Lambda w_s(\tilde{z}, z) = U_\Lambda(\tilde{x}, y) - \Lambda_{\max}^{-1} \tilde{x} y$ and our choice of the running scales, we have

$$\begin{aligned}w_0(\tilde{z}, z) &= \Omega_{\Lambda_{\min}}^{-1} \left[U_{\Lambda_{\min}}(\tilde{z} X_{\Lambda_{\min}}, z Y_{\Lambda_{\min}}) - \frac{X_{\Lambda_{\min}} Y_{\Lambda_{\min}}}{\Lambda_{\max}} \tilde{z} z \right] \\ &= \Omega_{\Lambda_{\min}}^{-1} U_{\Lambda_{\min}}(\tilde{z} X_{\Lambda_{\min}}, z Y_{\Lambda_{\min}}) - \frac{\Lambda_{\max}}{\Lambda_{\max} - \Lambda_{\min}} \tilde{z} z.\end{aligned}$$

By construction, the initial condition for $w_0(\tilde{z}, z)$ is simply a scaled and finite version of $W_{\Lambda_{\min}}(\tilde{x}, y)$. For concreteness, we evaluate the scale factors for the shifted Beta eigenvalue distribution,

$$\rho_\lambda(\lambda) = \frac{\Gamma(\frac{d_++d_-}{2})}{\Gamma(d_+/2)\Gamma(d_-/2)} \frac{|\Lambda_{\max} - \lambda|^{d_+/2-1} |\Lambda_{\min} - \lambda|^{d_-/2-1}}{|\Lambda_{\max} - \Lambda_{\min}|^{(d_++d_-)/2-1}}. \quad (\text{G3})$$

and the choices of X_Λ we focus on in this work. For this eigenvalue distribution the constant

$$c = \frac{\Gamma(\frac{d_++d_-}{2})}{\Gamma(d_+/2)\Gamma(d_-/2)} |\Lambda_{\max} - \Lambda_{\min}|^{-d_+/2}.$$

For the pure annihilation fixed point case $X_\Lambda = 1$, we then have

$$w_0(\tilde{z}, z) = \left(\frac{\Gamma(\frac{d_++d_-}{2})}{\Gamma(d_+/2)\Gamma(d_-/2)} \frac{|\Lambda_{\max} - \Lambda_{\min}|}{2\Lambda_{\max}\tau} \right)^{-1} U_{\Lambda_{\min}} \left(\tilde{z}, z \frac{\Gamma(\frac{d_++d_-}{2})}{\Gamma(d_+/2)\Gamma(d_-/2)} \frac{\Lambda_{\max}}{2\tau} \right) - \frac{\Lambda_{\max}}{\Lambda_{\max} - \Lambda_{\min}} \tilde{z} z$$

with anomalous exponent $\eta_s^X = 0$ for all s .

Next, for the spontaneous network with $X_\Lambda = \sqrt{\Omega_\Lambda/G_{20,\Lambda}}$, the initial value is $X_{\Lambda_{\min}} = \sqrt{\Omega_{\Lambda_{\min}}/\phi(0)}$, and so

$$w_0(\tilde{z}, z) = \left(\frac{\Gamma(\frac{d_++d_-}{2})}{\Gamma(d_+/2)\Gamma(d_-/2)} \frac{|\Lambda_{\max} - \Lambda_{\min}|}{2\Lambda_{\max}\tau} \right)^{-1} \times \\ U_{\Lambda_{\min}} \left(\tilde{z} \sqrt{\frac{\Gamma(\frac{d_++d_-}{2})}{\Gamma(d_+/2)\Gamma(d_-/2)} \frac{|\Lambda_{\max} - \Lambda_{\min}|}{2\Lambda_{\max}\tau\phi(0)}}, z \sqrt{\frac{\Gamma(\frac{d_++d_-}{2})}{\Gamma(d_+/2)\Gamma(d_-/2)} \frac{2\Lambda_{\max}\tau\phi(0)}{|\Lambda_{\max} - \Lambda_{\min}|} \frac{\Lambda_{\max}}{2\tau}} \right) \\ - \frac{\Lambda_{\max}}{\Lambda_{\max} - \Lambda_{\min}} \tilde{z}z.$$

The anomalous exponent simplifies to $\eta_s^X = -\frac{1}{2}\partial_s \ln(\Omega_\Lambda/G_{20,\Lambda})$, which gives $\eta_0^X = \frac{1}{2} \left(\frac{d_+}{2} + 1 \right)$ (assuming $G_{20,\Lambda}$ does not scale as some power of e^{-s} as $s \rightarrow 0$).

Finally, for the absorbing state network with $X_\Lambda = \sqrt{\frac{\Lambda_{\max}^2}{\delta\Lambda} \Omega_\Lambda \left(-\frac{G_{21,\Lambda}}{G_{12,\Lambda}} \right)}$, the initial scale is $X_{\Lambda_{\min}} = \sqrt{\frac{\Lambda_{\max}^2}{\Lambda_{\max} - \Lambda_{\min}} \Omega_{\Lambda_{\min}} \left(-\frac{\phi'(0)}{\phi''(0)} \right)}$ and we have

$$w_0(\tilde{z}, z) = \left(\frac{\Gamma(\frac{d_++d_-}{2})}{\Gamma(d_+/2)\Gamma(d_-/2)} \frac{|\Lambda_{\max} - \Lambda_{\min}|}{2\Lambda_{\max}\tau} \right)^{-1} \times \\ U_{\Lambda_{\min}} \left(\tilde{z} \sqrt{\frac{\Gamma(\frac{d_++d_-}{2})}{\Gamma(d_+/2)\Gamma(d_-/2)} \frac{\Lambda_{\max}}{2\tau} \left(-\frac{\phi'(0)}{\phi''(0)} \right)}, z \sqrt{\frac{\Gamma(\frac{d_++d_-}{2})}{\Gamma(d_+/2)\Gamma(d_-/2)} \frac{\Lambda_{\max}}{2\tau} \left(-\frac{\phi''(0)}{\phi'(0)} \right)} \right) \\ - \frac{\Lambda_{\max}}{\Lambda_{\max} - \Lambda_{\min}} \tilde{z}z.$$

The anomalous exponent is $\eta_0^X = \frac{d_+}{4}$ (assuming $-G_{21,\Lambda}/G_{12,\Lambda}$ does not scale as a power of e^{-s} in this limit).

In all cases, if we expand U to extract the bilinear $\tilde{z}z$ term, we find it is equal to

$$-\frac{\Lambda_{\max}}{\Lambda_{\max} - \Lambda_{\min}} (1 - \Lambda_{\max}\phi'(0)) \tilde{z}z.$$

We note that this vanishes if we choose $\phi'(0) = \Lambda_{\max}^{-1}$, the mean field prediction for the critical point. In simulations and numerical solutions of $U_{\Lambda_{\max}}$ from the macroscopic flow equation we find that the critical point occurs for $\Lambda_{\max}\phi'(0) > 1$, such that $g_{11,0}$ is positive.

Appendix H: Non-dimensionalization of the full average effective action

Our derivation of the dimensionless potential does not address how to non-dimensionalize the full average effective action. We show this here, as the derivation requires a careful consideration of the $N \rightarrow \infty$ limit, and involves the eigenmodes of the synaptic connectivity matrix J_{ij} , which did not contribute to our flow equation. Importantly, this derivation reveals that time should scale as $\delta\Lambda^{-1}$, giving the usual dynamic critical exponent $z = 2$ (at the level of the LPA approximation), despite the fact that the potential W_Λ , which has units of time $^{-1}$, scales as $\delta\Lambda^{d/2+1}$.

To facilitate this calculation, we will first manipulate the AEA to put the membrane potential dynamics in differential form. We do so explicitly for pulse coupled networks. In this case, the membrane potential terms read

$$\sum_i \int dt \tilde{\psi}_i(t) \left[\psi_i(t) - \mathcal{E}_i - \sum_j \int dt' J_{ij} g(t-t') \nu_j(t') \right],$$

where $g(t-t') = \exp(-(t-t')/\tau)\Theta(t-t')/\tau$ is an exponential filter. This filter is the Green's function of the linear differential operator $\hat{\mathcal{L}} = \tau\partial_t + 1$, such that $\hat{\mathcal{L}}g(t-t') = \delta(t-t')$. We may redefine the field $\tilde{\psi}_i(t) \rightarrow \hat{\mathcal{L}}^\dagger \tilde{\psi}_i(t)$, where $\hat{\mathcal{L}}^\dagger = -\tau\partial_t + 1$ is the adjoint operator of $\hat{\mathcal{L}}$ (assuming vanishing boundary conditions), and we are abusing notation by using the same symbol $\tilde{\psi}_i(t)$. By integrating by parts we move the differential operator off the new $\tilde{\psi}_i(t)$ and onto

the membrane potential dynamics and synaptic input, giving the differential form

$$\Gamma_\Lambda[\tilde{\psi}, \psi, \tilde{\nu}, \nu] = \sum_i \int dt \left\{ \tilde{\psi}_i(t) \left[\tau \partial_t \psi_i(t) + \psi_i(t) - \mathcal{E}_i - \sum_j J_{ij} \nu_j(t) \right] + \tilde{\nu}_i(t) \nu_i(t) - U_\Lambda(\tilde{\nu}_i(t), \psi_i(t)) \right\}.$$

We have performed this operation so that we obtain a more convenient form of the action that results from our next step: extremizing over the spike fields ν and $\tilde{\nu}$ to obtain an AEA purely in terms of the membrane response fields ψ and $\tilde{\psi}$, which we will then be able to non-dimensionalize. Extremizing Γ_Λ with respect to $\tilde{\nu}$ and ν gives the equations of state

$$\begin{aligned} \frac{\delta \Gamma_\Lambda}{\delta \tilde{\nu}_i(t)} &= \nu_i(t) - U_\Lambda(\tilde{\nu}_i(t), \psi_i(t)) = 0 \\ \frac{\delta \Gamma_\Lambda}{\delta \nu_i(t)} &= \tilde{\nu}_i(t) - \sum_j \tilde{\psi}_j(t) J_{ji} = 0. \end{aligned}$$

We can straightforwardly solve these for $\tilde{\nu}_i(t)$ and $\nu_i(t)$ and plug the result into the AEA. The $\sum_{ij} \tilde{\psi}_i(t) J_{ij} \nu_j(t)$ and $\sum_i \tilde{\nu}_i(t) \nu_i(t)$ cancel out, leaving the reduced AEA

$$\Gamma_\Lambda[\tilde{\psi}, \psi] = \sum_i \int dt \left\{ \tilde{\psi}_i(t) \left[\tau \partial_t \psi_i(t) + \psi_i(t) - \mathcal{E}_i \right] - U_\Lambda \left(\sum_j \tilde{\psi}_j(t) J_{ji}, \psi_i(t) \right) \right\}.$$

Now, we insert $U_\Lambda(\tilde{x}, y) = \Phi_\Lambda(0)\tilde{x} + \Lambda_{\max}^{-1}\tilde{x}y + W_\Lambda(\tilde{x}, y)$, which gives

$$\Gamma_\Lambda[\tilde{\psi}, \psi] = \sum_i \int dt \left\{ \tilde{\psi}_i(t) \left[\tau \partial_t \psi_i(t) + \sum_j \left[\delta_{ij} - \frac{J_{ij}}{\Lambda_{\max}} \right] \psi_j(t) - \left(\mathcal{E}_i + \sum_j J_{ij} \Phi_\Lambda(0) \right) \right] - W_\Lambda \left(\sum_j \tilde{\psi}_j(t) J_{ji}, \psi_i(t) \right) \right\}.$$

As discussed in the main text, to be at a critical point we require $\mathcal{E}_i + \sum_j J_{ij} \Phi_\Lambda(0) = 0$ as $\Lambda \rightarrow \Lambda_{\max}$, and we will drop this term from the action in this limit.

The next step is to pass from the neural index representation to the synaptic eigenmode basis, diagonalizing the membrane potential dynamics. We will also do this for the local potential W_Λ , but it is cumbersome, so we will consider it separately. Defining $J_{ij} = \sum_{\alpha\beta} P_{i\alpha} \lambda_\alpha \delta_{\alpha\beta} (P^T)_{\beta j}$, $N^{-1} \tilde{\psi}_\alpha(t) = \sum_i (P^T)_{\alpha i} \tilde{\psi}_i(t)$, and $N^{-1} \psi_\alpha(t) = \sum_i (P^T)_{\alpha i} \psi_i(t)$, the linear part of the action becomes

$$\frac{1}{N} \sum_\alpha \int dt \tilde{\psi}_\alpha \left[\tau \partial_t \psi_\alpha + \frac{\Lambda_{\max} - \lambda_\alpha}{\Lambda_{\max}} \psi_\alpha \right].$$

Now, we may take the limit $N \rightarrow \infty$, assuming the spectrum λ_α becomes continuous with density $\rho_\lambda(\lambda)$ and modes $P_{i\alpha} \rightarrow P_i(\lambda)$, and replacing $\tilde{\psi}_\alpha(t) \rightarrow \tilde{\psi}(\lambda, t)$ and $\psi_\alpha(t) \rightarrow \psi(\lambda, t)$. In this way we may write

$$\psi_i(t) = \int d\lambda \rho_\lambda(\lambda) P_i(\lambda) \psi(\lambda, t) \tag{H1}$$

$$\tilde{\psi}_i(t) = \int d\lambda \rho_\lambda(\lambda) P_i(\lambda) \tilde{\psi}(\lambda, t), \tag{H2}$$

and the AEA's linear term becomes

$$\begin{aligned} & \int_{\Lambda_{\min}}^{\Lambda_{\max}} d\lambda \rho_\lambda(\lambda) \int dt \tilde{\psi}(\lambda, t) \left[\tau \partial_t \psi(\lambda, t) + \frac{\Lambda_{\max} - \lambda}{\Lambda_{\max}} \psi(\lambda, t) \right] \\ &= \int_0^{\Lambda_{\max} - \Lambda_{\min}} d\delta\lambda \rho_\lambda(\Lambda_{\max} - \delta\lambda) \int dt \tilde{\psi}(\lambda, t) \left[\tau \partial_t \psi(\delta\lambda, t) + \frac{\delta\lambda}{\Lambda_{\max}} \psi(\delta\lambda, t) \right], \end{aligned}$$

where in going to the second line we defined $\delta\lambda = \Lambda_{\max} - \lambda$. We are now ready to introduce running scales and non-dimensionalize this term. Let $\delta\lambda \rightarrow \delta\hat{\lambda}\delta\Lambda$, $t \rightarrow \hat{t}\delta\Lambda^{[t]}$, $\tilde{\psi}(\delta\lambda, t) \rightarrow \hat{\tilde{\psi}}(\delta\hat{\lambda}, \hat{t})\delta\Lambda^{[\tilde{\psi}(\delta\lambda, t)]}$, and $\psi(\delta\lambda, t) \rightarrow \hat{\psi}(\delta\hat{\lambda}, \hat{t})\delta\Lambda^{[\psi(\delta\lambda, t)]}$, where $[\dots]$ is the scaling exponents for the associated quantity. Our goal will be to choose these scaling exponents so

that the AEA is asymptotically finite as $\delta\Lambda \rightarrow 0$. Inserting these scalings, and using the fact that $\rho_\lambda(\lambda) \sim \delta\lambda^{d/2-1}$ for small $\delta\lambda$, we have

$$\int_0^{(\Lambda_{\max} - \Lambda_{\min})/\delta\Lambda} d\delta\hat{\lambda} (\delta\hat{\lambda})^{d/2-1} \int dt \hat{\tilde{\psi}}(\delta\Lambda)^{d/2+[t]+[\tilde{\psi}(\delta\lambda, t)]} \left[(\delta\Lambda)^{-[t]+[\psi(\delta\lambda, t)]} \tau \partial_t \hat{\psi} + (\delta\Lambda)^{1+[\psi(\delta\lambda, t)]} \frac{\delta\hat{\lambda}}{\Lambda_{\max}} \hat{\psi} \right].$$

We have dropped the arguments on the fields for brevity, except in the $[\dots]$, as we will later use the arguments to distinguish the scaling exponents of the fields $\tilde{\psi}$ and ψ in the different bases. Inspection of the above results shows that in order to have the time derivative scale like $\delta\lambda$ (the equivalent of time scaling like the diffusion operator in a lattice or continuum model), we must have $[t] = -1$. It then follows that

$$\frac{d}{2} + [\tilde{\psi}(\delta\lambda, t)] + [\psi(\delta\lambda, t)] = 0.$$

From Eqs. (H1) and (H2) we can also determine the scaling exponents of the membrane fields in the neuron index basis. We assume that $P_i(\lambda)$ is dimensionless and does not scale with $\delta\Lambda$; this is the direct analog of the basis $e^{i\mathbf{q}\cdot\mathbf{x}}$ not scaling with the running momentum in a lattice model. Then, with $d\lambda \rho_\lambda(\lambda) \sim \delta\Lambda^{d/2}$, it follows that

$$\begin{aligned} [\psi_i(t)] &= \frac{d}{2} + [\psi(\delta\lambda, t)] \\ [\tilde{\psi}_i(t)] &= \frac{d}{2} + [\tilde{\psi}(\delta\lambda, t)], \end{aligned}$$

and hence

$$-\frac{d}{2} + [\tilde{\psi}_i(t)] + [\psi_i(t)] = 0.$$

This renders the linear part of the AEA scale invariant as $\delta\Lambda \rightarrow 0$. (The upper limit on the $\delta\hat{\lambda}$ integral becomes infinite in this limit, and the contributions from this region are suppressed by $\rho_\lambda(\lambda)$ near Λ_{\min}). We next need to show that the potential term is invariant with these choices of scaling. Doing so requires a careful treatment of the $N \rightarrow \infty$ limit, which is easiest to perform in the λ basis.

We first consider the argument $\sum_j \tilde{\psi}_j(t) J_{ji}$. We may write this in the discrete λ_α basis as $N^{-1} \sum_\alpha \tilde{\psi}_\alpha \lambda_\alpha (P^T)_{\alpha i} = N^{-1} \sum_\alpha \tilde{\psi}_\alpha \lambda_\alpha P_{i,\alpha}$. Taking the infinite limit, this becomes $\int d\lambda \rho_\lambda(\lambda) \lambda P_i(\lambda) \tilde{\psi}(\lambda, t)$. Changing variables to $\delta\lambda$ gives

$$\sum_j \tilde{\psi}_j(t) J_{ji} \sim \int d\delta\lambda (\delta\lambda)^{d/2-1} (\Lambda_{\max} - \delta\lambda) P_i(\lambda) \tilde{\psi}(\lambda, t).$$

Scaling the fields with $\delta\Lambda \rightarrow 0$, we have $\Lambda_{\max} - \delta\hat{\lambda}\delta\Lambda \sim \Lambda_{\max}$ and

$$\sum_j \tilde{\psi}_j(t) J_{ji} \sim (\delta\Lambda)^{d/2+[\tilde{\psi}(\delta\lambda, t)]} \int d\delta\hat{\lambda} (\delta\hat{\lambda})^{d/2-1} \Lambda_{\max} P_i(\delta\hat{\lambda}) \hat{\tilde{\psi}}(\delta\hat{\lambda}, t),$$

where we assume that $P_i(\lambda) = P_i(\delta\hat{\lambda})$ does not scale with $\delta\Lambda$. We may identify this overall scaling exponent as being equal to $[\tilde{\psi}_i(t)]$ from our earlier argument. Because this term was equal to $\tilde{\nu}_i(t)$, this shows that $[\tilde{\nu}_i(t)] = [\tilde{\psi}_i(t)]$, so long as $\Lambda_{\max} \neq 0$. We will use this result shortly.

Finally, we show that the scaling of the potential W_Λ derived by demanding the dimensionless flow equation be asymptotically autonomous will yield a fixed point in the full AEA (i.e., it will not diverge or scale to zero). We

expand the potential in a power series (which we may do since it is analytic for $\Lambda < \Lambda_{\max}$),

$$\begin{aligned} & \sum_i \int dt W_\Lambda \left(\sum_j \tilde{\psi}_j(t) J_{ji}, \psi_i(t) \right) \\ &= \sum_i \int dt \sum_{mn} \frac{G_{mn,\Lambda}}{m!n!} \left(\int d\lambda \rho_\lambda(\lambda) P_i(\lambda) \tilde{\psi}(\lambda, t) \right)^m \left(\int d\lambda \rho_\lambda(\lambda) P_i(\lambda) \psi(\lambda, t) \right)^n \\ &= \sum_{mn} \frac{G_{mn,\Lambda}}{m!n!} \int dt d\lambda_1 \dots d\lambda_{m+n} \rho_\lambda(\lambda_1) \dots \rho_\lambda(\lambda_{m+n}) \left[\sum_i P_i(\lambda_1) \dots P_i(\lambda_{m+n}) \right] \tilde{\psi}(\lambda_1, t) \dots \tilde{\psi}(\lambda_m, t) \psi(\lambda_{m+1}, t) \dots \psi(\lambda_{m+n}, t). \end{aligned}$$

We now change variables to $\delta\lambda \rightarrow \delta\hat{\lambda}\delta\Lambda$ and $t = \hat{t}\delta\Lambda^{-1}$ and use the scalings $\tilde{\psi}(\lambda, t) = (\delta\Lambda)^{[\tilde{\psi}(\lambda, t)]} \hat{\tilde{\psi}}(\delta\hat{\lambda}, \hat{t})$, $\psi(\lambda, t) = (\delta\Lambda)^{[\psi(\lambda, t)]} \hat{\psi}(\delta\hat{\lambda}, \hat{t})$, and $G_{mn,\Lambda} = (\delta\Lambda)^{d/2+1-m} [\tilde{\psi}_i(t)] - n [\psi_i(t)] g_{mn,s}$, where we used $\Omega_\Lambda \sim \delta\Lambda^{d/2+1}$ and $[\tilde{\nu}_i(t)] = [\tilde{\psi}_i(t)]$. Omitting the integrals and factors of $\rho_\lambda(\lambda) \sim (\delta\hat{\lambda})^{d/2-1}$ for brevity, the potential scales as

$$\begin{aligned} & \sum_i \int dt W_\Lambda \left(\sum_j \tilde{\psi}_j(t) J_{ji}, \psi_i(t) \right) \\ & \sim g_{mn,s} (\delta\Lambda)^{d/2+(m+n)(d/2)-m[\tilde{\psi}_i(t)]-n[\psi_i(t)]+m[\tilde{\psi}(\lambda, t)]+n[\psi(\lambda, t)]} \left[\sum_i P_i(\lambda_1) \dots P_i(\lambda_{m+n}) \right] \hat{\tilde{\psi}}(\delta\hat{\lambda}_1, t) \dots \hat{\psi}(\delta\hat{\lambda}_{m+n}, t). \end{aligned}$$

Using the relationship between $[\psi_i(t)]$ and $[\psi(\lambda, t)]$, etc., the overall scaling reduces to

$$\sum_i \int dt W_\Lambda \left(\sum_j \tilde{\psi}_j(t) J_{ji}, \psi_i(t) \right) \sim (\delta\Lambda)^{d/2} \left[\sum_i P_i(\lambda_1) \dots P_i(\lambda_{m+n}) \right].$$

In order for this to achieve a scale invariant value in the AEA, we thus need $\sum_i P_i(\lambda_1) \dots P_i(\lambda_{m+n})$ to scale like $\delta\Lambda^{-d/2}$. We argue that this will indeed be the case. In a continuum limit of a lattice model, $P_j(\lambda(\mathbf{q})) \sim e^{i\mathbf{q} \cdot \mathbf{x}_j}$, and $\sum_i P_i(\lambda_1) \dots P_i(\lambda_{m+n})$ becomes $\delta(\mathbf{q}_1 + \dots + \mathbf{q}_{m+n})$. In the NPRG approach to such a model, one would scale the momentum by a running scale k , such that

$$\begin{aligned} \delta(\mathbf{q}_1 + \dots + \mathbf{q}_{m+n}) & \rightarrow \delta(k\hat{\mathbf{q}}_1 + \dots + k\hat{\mathbf{q}}_{m+n}) \\ & = k^{-d} \delta(\hat{\mathbf{q}}_1 + \dots + \hat{\mathbf{q}}_{m+n}) \end{aligned}$$

using the scaling property of the Dirac delta function. Since $k \sim \delta\Lambda^{1/2}$, we argue that $\sum_i P_i(\lambda_1) \dots P_i(\lambda_{m+n}) \sim \delta\Lambda^{-d/2}$, and so $\sum_i \int dt W_\Lambda \left(\sum_j \tilde{\psi}_j(t) J_{ji}, \psi_i(t) \right)$ will indeed scale overall as $\delta\Lambda^0$, giving a finite contribution to the rescaled AEA.

Another way to argue this last scaling is to consider a continuum limit in the neural index i as $N \rightarrow \infty$:

$$\sum_{i=1}^N \sim \int_0^N di.$$

As we integrate out modes in the eigenvalue basis, the number of remaining modes left over is $N' = N \int_\Lambda^{\Lambda_{\max}} d\lambda \rho_\lambda(\lambda) \sim N \delta\Lambda^{d/2}$. Writing the index integral in terms of the new N' gives

$$\begin{aligned} \int_0^N di &= \int_0^{N' \delta\Lambda^{-d/2}} di \\ &= \delta\Lambda^{-d/2} \int_0^{N'} di', \end{aligned}$$

where we changed variables to $\hat{i} = \delta\Lambda^{-d/2}i$. Using this argument, we again find

$$\begin{aligned} \sum_i P_i(\lambda_1) \dots P_i(\lambda_{m+n}) &\rightarrow \int_0^N di P_i(\lambda_1) \dots P_i(\lambda_{m+n}) \\ &= \delta\Lambda^{-d/2} \int_0^{N'} d\hat{i} P_{\hat{i}}(\delta\hat{\lambda}_1) \dots P_{\hat{i}}(\delta\hat{\lambda}_{m+n}), \end{aligned}$$

where we again assume $P_i(\lambda) = P_{\hat{i}}(\delta\hat{\lambda})$ does not scale with $\delta\Lambda$.

This completes our demonstration that the scalings used in the flow equation lead to a fixed point average effective action, at least at the level of the local potential approximation.

Appendix I: Linear stability of trivial critical points and upper critical dimensions

In this section we analyze the linear stability of the trivial critical points for the pure annihilation fixed point, absorbing state networks, and spontaneous networks. We use the asymptotic form of the flow equation,

$$\partial_s w_s - \left(\frac{d}{2} + 1\right) w_s + \eta_s^X \tilde{z} w_s^{(1,0)} + \left(\frac{d}{2} - \eta_s^X\right) z w_s^{(0,1)} = 1 - w_s^{(1,1)} - \sqrt{\left(1 - w_s^{(1,1)}\right)^2 - w_s^{(0,2)} w_s^{(2,0)}},$$

to perform our analysis.

1. Pure annihilation fixed point

For the pure annihilation fixed point the trivial solution is $w_*(\tilde{z}, z) = 0$ and $\eta_s^X = 0$ for all s . Linearizing the flow equation for $w_s(\tilde{z}, z) = \sum_{mn} \delta g_{mn}(s) \tilde{z}^m z^n / (m!n!)$ yields a system of equations for the perturbations of the couplings,

$$\partial_s \delta g_{mn}(s) = \left(1 + \frac{d}{2}(1-n)\right) g_{mn}(s),$$

which has solution

$$\delta g_{mn}(s) = \delta g_{mn}(0) \exp\left(s \left[1 + \frac{d}{2}(1-n)\right]\right).$$

The coupling is relevant when its eigenvalue $\mu_{m,n} = 1 + (1-n)d/2$ is positive. We see that this is always the case for $n = 0, 1$, meaning the couplings $g_{m0}(s)$ and $g_{m1}(s)$ are both relevant in any dimension. The remaining couplings have upper critical dimensions

$$d_{mn} = \frac{2}{n-1}.$$

We see that these critical dimensions are independent of m , and all irrelevant above $d > 2$, progressively becoming relevant below this dimension.

2. Absorbing state networks

For the absorbing state network the trivial solution is $w_*(\tilde{z}, z) = 0$ and $\eta_*^X = d/4$. The flowing equation for η_s^X is

$$\eta_*^X = \frac{d}{4} + \frac{1}{2} \frac{g_{13}^* - g_{31}^*}{1 - g_{11}^*}.$$

We perturb $w_s(\tilde{z}, z) = \delta w_s(\tilde{z}, z)$ and $\eta_s^X = d/4 + \delta\eta_s^X$ and expand to linear order. It turns out the running anomalous exponent does not couple to $\delta w_s(\tilde{z}, z)$. We expand $\delta w_s(\tilde{z}, z) = \sum_{mn} \frac{\delta g_{mn}(s)}{m!n!} \tilde{z}^m z^n$, giving a flow equation

$$\partial_s \delta g_{mn}(s) = \left(1 + \frac{2-m-n}{4}\right) \delta g_{mn}(s) \quad (\text{I1})$$

which has solution

$$\delta g_{mn}(s) = \delta g_{mn}(0) \exp\left(s \left[1 + \frac{2-m-n}{4}\right]\right).$$

Relevant perturbations will grow with RG time s , while irrelevant perturbations will decay. We thus see that $\delta g_{11}(s)$ is always a relevant perturbation, hence why it must be tuned to make the network critical. The remaining couplings become relevant for effective dimensions less than the critical dimensions

$$d_{mn}^{\text{AS}} = \frac{4}{m+n-2}. \quad (\text{I2})$$

Notably, for $m = 1$, the first coupling to become unstable is the z^2 coupling in $d = 4$, which occurs simultaneously with the $(m, n) = (2, 1)$ coupling, as must be the case because we scaled the model so that $g_{12} = -g_{21}$ for all RG times s . The next couplings $(m, n) = (1, 3)$ or $(3, 1)$ and $(2, 2)$ become relevant in $d < 2$.

For completeness, the perturbed equation for $\delta\eta_s^X$ is

$$\delta\eta_s^X = \frac{1}{2} (\delta g_{13}(s) - \delta g_{31}(s)),$$

which will decay to 0 in $d > 2$.

3. Spontaneous networks

For the spontaneous network the trivial solution is $w_*(\tilde{z}, z) = \tilde{z}^2/2$ and $\eta_*^X = (d+2)/4$, where

$$\begin{aligned} \eta_s^X &= \frac{d+2}{4} + \frac{1}{4} \frac{g_{22,s} + 2g_{12,s}g_{30,s}}{1 - g_{11,s}} \\ &\quad + \frac{1}{2} \frac{g_{12,s}g_{21,s}}{(1 - g_{11,s})^2} + \frac{1}{8} \frac{g_{12,s}^2}{(1 - g_{11,s})^3}. \end{aligned}$$

Expanding $w_s(\tilde{z}, z) = \tilde{z}^2/2 + \sum_m e^{\mu_m s} \delta\varphi_m(z)$ and $\eta_s^X = (d+2)/4 + \delta\eta_s^X$ yields the linearized system of equations

$$\begin{aligned} \delta\eta_s^X &= \frac{1}{4} e^{\mu_m s} \delta\varphi_2''(0), \\ \delta\varphi_m''(z) &= \frac{d-2}{2} z \delta\varphi_m(z) + [-(d+2) + 2\mu_m] \delta\varphi_m(z) + \delta_{m,2} \delta\varphi_2''(0), \end{aligned}$$

where the value of $\delta\varphi_2''(0)$ will need to be determined self-consistently. Demanding that the solutions are polynomially bounded restricts the allowed values of μ_m to a countably infinite set for each m .

For $m = 1$ we have

$$\delta\varphi_1^{(n)}(z) = H_n \left(\frac{\sqrt{d-2}}{2} z \right),$$

where $H_n(\cdot)$ Hermite Polynomials of integer order n , which must be equal to

$$n = \frac{2+d-(d-2)\mu_{1,n}}{4}.$$

This constraint fixes the eigenvalues $\mu_{1,n}$. When the exponent $\mu_{1,n}$ is positive the eigenmode is relevant. For $n = 1$ the exponent is $\mu_{1,1} = 1$, and the mode $\delta\varphi_1^{(1)}(z) = \sqrt{d-2}z$ is always relevant. The critical dimensions of the remaining

$m = 1$ modes are given by

$$d_{1,n} = 2 \frac{n+1}{n-1},$$

from which we verify that the first coupling to become relevant is g_{12} in $d = 6$, and then next is g_{13} in $d = 4$.

The $m = 2$ term is slightly trickier to solve because it involves the contribution from $\delta\eta_s^X = e^{\mu_2 s} \delta\varphi_2''(0)$. This ultimately only adds a constant factor of $\delta\varphi_2''(0)/\mu_2$ to the homogeneous solution, from which it follows that $\delta\varphi_2''(0) = H_n''(0)$. The overall solution for the $m = 2$ mode can be written

$$\delta\varphi_2^{(n)}(z) = -\frac{(n-1)2^{n-2}}{\Gamma(\frac{3-n}{2})} + H_n\left(\frac{\sqrt{d-2}}{2}z\right),$$

with

$$n = -\frac{4\mu_{2,n}}{d-2}.$$

We see that the $m = 2$ modes are irrelevant for any $d > 2$, and marginal in $d = 2$. While it appears that these modes are relevant in $d < 2$, note that the factors of $\sqrt{d-2}$ will become imaginary. While our spinodal fixed point is complex-valued, it is known that in the Ising universality class the lower critical dimension is 2, below which the system does not order, and this result may be a reflection of that fact.

The case $m > 2$ yields the general solution

$$\delta\varphi_m^{(n)}(z) = H_n\left(\frac{\sqrt{d-2}}{2}z\right),$$

with

$$n = \frac{4 + 2d - 2m - md - 4\mu_{m,n}}{d-2},$$

or

$$\mu_{m,n} = \frac{(2+d)(2-m) + (2-d)n}{4}.$$

Solving for the critical dimension we obtain

$$d_{mn} = -2 \frac{m-2-n}{m-2+n};$$

we see that the critical dimension is less than 2 for any choice of $(m > 2, n)$, and so these modes are always irrelevant for any $d > 2$.

Finally, we note that in both the absorbing state and spontaneous network's trivial fixed points the $(m, n) = (1, 1)$ mode had an eigenvalue of $\mu_{1,1} = 1$. The correlation length exponent is related to this eigenvalue by $\nu_* = 1/(2\mu_{1,1}) = 1/2$ at the trivial fixed points, as expected. In the spontaneously network the $(m, n) = (1, 0)$ mode is also relevant in any dimension, with eigenvalue $\mu_{1,0} = (d+2)/(d-2)$. However, this mode only contributes to the renormalized value of $\Phi_1(0)$, and does not drive the flow of any other coupling, so we do not expect it to determine the correlation length exponent of the spontaneous networks.

Appendix J: Approximate fixed point solutions of the flow equation

Finding non-trivial fixed points of the flow equation analytically is generally quite difficult. In this work have used two methods: non-perturbative solutions obtained by truncating $w_s(\tilde{z}, z) = \sum_{mn} g_{mn}^* \tilde{z}^m z^n / (m! n!)$ at a finite order in \tilde{z} and z . For both absorbing state networks and spontaneous networks we first truncated at a low order (just a few couplings g_{mn}^*) in order to obtain an analytic solution. This solution reveals how the couplings scale with the distance from the upper critical dimension of the model.

This motivated a perturbative ϵ -expansion that is not restricted to a finite number of couplings, but only valid near

the upper critical dimensions. The perturbative solution proceeds by expanding around the trivial solution,

$$w_*(\tilde{z}, z) = \epsilon^{1/2} w_1(\tilde{z}, z) + \epsilon w_2(\tilde{z}, z) + \epsilon^{3/2} w_3(\tilde{z}, z) + \epsilon^2 w_4(\tilde{z}, z) + \dots$$

$$\eta_*^X = 1 + \epsilon^{1/2} \delta\eta_1 + \epsilon \delta\eta_2 + \epsilon^{3/2} \delta\eta_3 + \epsilon^2 \delta\eta_4 + \dots$$

for the absorbing state network model ($\epsilon = 4 - d$) and

$$w_*(\tilde{z}, z) = \tilde{z}^2/2 + \epsilon^{1/2} w_1(\tilde{z}, z) + \epsilon w_2(\tilde{z}, z) + \epsilon^{3/2} w_3(\tilde{z}, z) + \epsilon^2 w_4(\tilde{z}, z) + \dots$$

$$\eta_*^X = 2 + \epsilon^{1/2} \delta\eta_1 + \epsilon \delta\eta_2 + \epsilon^{3/2} \delta\eta_3 + \epsilon^2 \delta\eta_4 + \dots$$

near the spinodal fixed point ($\epsilon = 6 - d$) and

$$w_*(\tilde{z}, z) = \tilde{z}^2/2 + \epsilon w_1(\tilde{z}, z) + \epsilon^2 w_2(\tilde{z}, z) + \dots$$

$$\eta_*^X = 3/2 + \epsilon \delta\eta_1 + \epsilon^2 \delta\eta_2 + \dots$$

near the Wilson-Fisher-like fixed point ($\epsilon = 4 - d$).

Expanding the flow equation (32) in a series around $\epsilon = 0$ and collecting terms of equal powers yields a system of linear equations to solve, where each order is coupled to the previous order. As mentioned in the main text, we determine integration constants at each order by demanding that the solution is polynomially bounded in z .

The ϵ -expansion solutions are in principle exact (within the local potential approximation) close to the upper critical dimension of the fixed point. This allows us to use these results as initial guesses in a root-finding algorithm for the non-perturbative truncation approach at high orders.

Appendix K: Numerical solution of the Wilson-Fisher fixed point in spontaneous networks

Solving the dimensionless flow equations for $w_s(\tilde{z}, z)$ is extremely difficult, due to the fact that the solution diverges unless tuned to a critical manifold. Solving the flow equations for the effective nonlinearities $\varphi_{1,s}(z)$ and $\varphi_{2,s}(z)$ (Eqs. (53)-(54)) is also challenging, but feasible, at least for identifying the \mathbb{Z}_2 -symmetric fixed; we have not succeeded in numerically solving for the spinodal fixed point due to the complex-valued nature of the solution.

Our solution of the Wilson-Fisher-like $\mathbb{Z} - 2$ fixed point was aided by previous work solving the flow equations for the Ising model [48, 68]. In the Ising case the flow equations are derived for the anti-derivative of our $\varphi_{1,s}(z)$, fixing $\varphi_{2,s}(z) = 1$ for all z , when translated to our notation. We could therefore leverage the asymptotic solutions predicted for the Ising case to help identify the numerical solution by a dichotomy method tuning the initial value of the coupling $g_{11,0}$.

We solve the flow equations (53)-(54) numerically using a semi-implicit Euler scheme, in which the nonlinear terms are treated explicitly, while the linear terms are treated implicitly, in order to improve the stability of the numerical solution, which is otherwise quite delicate. We solve the flow equations using the initial conditions $\varphi_{1,0}(z) = g_{11,0}z - 2g_{11,0}(1 - g_{11,0})\frac{z^3}{3!} - \mathcal{A}_d \text{sgn}(z)|z|^{\frac{d+2}{d-2}}$, where the last term is the expected asymptotic behavior of $\varphi_{1*}(z)$ at the Wilson-Fisher critical point for the truncation $\varphi_{2s}(z) = 1$. This term is included purely as a regularizer, as without the asymptotic term the numerical solution is not as stable. The numerical value of \mathcal{A}_d is therefore not quantitatively important, and we use the $d = 3$ value $\mathcal{A}_3 = 0.0182058164$ obtained by [48] for all dimensions. For $\varphi_{2s}(z)$ we use the initial condition $\varphi_{2,0}(z) = 1$. For each initial condition $g_{11,0} > 0$ we vary the value until the numerical solution diverges within an RG-time of $s_{\max} = 30$, with $z \in [-20, 20]$ and $dz = 0.1$, $ds = 0.001$. The critical values g_{11}^c reported in Table I are those values for which increasing the value further results in a divergent numerical solution. Because these are non-universal values, and we start this flow in the asymptotic regime where memory of our actual initial condition for $w_s(\tilde{z}, z)$ is lost, these values cannot be used to predict the critical value of $\Lambda_{\max}\phi'(0)$, unlike in our solution of the flow equation for the macroscopic potential $U_{\Lambda}(\tilde{x}, y)$.

The discretized semi-implicit equations we use are

$$\left\{ \mathbb{I} + \Delta s \left[-\left(\frac{d+2}{4} \right) \mathbb{I} + \left(\frac{d-2}{4} \right) z \frac{\partial}{\partial z} \right] \right\} \varphi_{1,s+\Delta s} = \varphi_{1,s} + \Delta s \left[-\delta\eta_s \varphi_{1,s} + \delta\eta_s z \varphi'_{1,s} + F_{1,s} \right]$$

$$\left\{ \mathbb{I} + \Delta s \left[\left(\frac{d-2}{4} \right) z \frac{\partial}{\partial z} \right] \right\} \varphi_{2,s+\Delta s} = \varphi_{2,s} + \Delta s \left[-2\delta\eta_s \varphi_{2,s} + \delta\eta_s z \varphi'_{2,s} + F_{2,s} \right],$$

where $F_{1,s}$ and $F_{2,s}$ are the right-hand-sides of Eqs. (53)-(54) and $\delta\eta_s^X$ is the deviation from the mean-field value $(d+2)/4$, computed using Eq. (39). We solve the equations numerically in Matlab, using a 5-point stencil to compute

d	$g_{11,0}^c$	g_{11}^*	$\eta_*^X - \frac{d+2}{4}$
4.0	0.16922141	-0.0005	$\mathcal{O}(10^{-13})$
3.5	0.3109490006	0.00059	$\mathcal{O}(10^{-7})$
3.2	0.461971091	0.0754	0.00055
3.0	0.659959128	0.3178	0.08

TABLE I. Critical value of the bare coupling $g_{11,s=0}$, the fixed point value g_{11}^* , and anomalous exponent $\eta_*^X - \frac{d+2}{4}$ for the spontaneous network model for a few choices of the effective dimension d . Values of $g_{11,0}^c$ are determined by dichotomy, attempting to achieve convergence by an RG time of $s = 30$. The procedure becomes extremely sensitive below $d = 3$, possibly due to the emergence of multiple critical points. These values are determined for $g_{21,s=0} = 0$ and an initial condition $\varphi_{1,0}(z) = g_{11,0}z - 2g_{11,0}(1 - g_{11,0})\frac{z^3}{3!} - \mathcal{A}_3 \text{sgn}(z)|z|^{\frac{d+2}{d-2}}$, with \mathcal{A}_3 a constant.

the derivatives.

In principle, the equation updating $\delta\eta_s^X$ should impose that $\varphi_{2,s}(0) = 1$ for all s , but due to numerical error this quickly deviates from 1. We therefore normalize $\varphi_{2,s}(z)$ by dividing by the actual numerical value of $\varphi_{2,s}(0)$ at the end of each time step to ensure this holds exactly. This results in a much more numerically stable solution. We also remove the value of $\varphi_{1,s}(0)$ from $\varphi_{1,s}(z)$ at the end of each time step. This value does not contribute to the flow of any other components of the solution, but does increase numerically, and removing it improves numerical stability and prevents possible overflow errors.

Appendix L: Flow equation of continuum scalar field theories with ultra-sharp regulators

In this section we show that the standard NPRG method applied to continuum limit field theories with an ultra-sharp regulator yields flow equations very similar to the flow equation for $W_\Lambda(\tilde{x}, y)$ and $w_s(\tilde{z}, z)$, with the equations for the asymptotic fixed point equation for $w_*(\tilde{z}, z)$ being exactly the same. This demonstrates that the different models can achieve, in principle, the same critical points. Which critical points are accessible in practice depends on the initial condition of the flow.

We consider a field theory for the fields $\phi(\mathbf{x}, t)$ and $\tilde{\phi}(\mathbf{x}, t)$, which may be derived from either a Langevin equation in the MSRJD formalism or from master equation models using the Doi-Peliti method for reaction-diffusion models [30]. In many cases of interest, the ansatz employed for the average effective action takes the form

$$\Gamma_k[\tilde{\phi}, \phi] = \int d\mathbf{x} dt \left\{ \tilde{\phi}(\mathbf{x}, t) [Z_k \partial_t - D_k \nabla^2] \phi(\mathbf{x}, t) + W_k(\tilde{\phi}, \phi) \right\},$$

chosen to be a function of the running momentum scale k . Z_k and D_k are field renormalization factors, which are taken to be constants independent of k in the local potential approximation. For some models, these factors can be shown to be unrenormalized when fluctuations are accounted for (e.g., the pure annihilation or coagulation models [32]), similar to the spiking network model. We will choose units in which $Z_k = D_k = 1$. In Langevin models driven by additive noise, one often makes a stronger ansatz, assuming $W_k(\tilde{\phi}, \phi)$ may be truncated at quadratic order in $\tilde{\phi}$ and that only the ϕ -dependent coefficient of $\tilde{\phi}$ flows, but we will work with the full local potential here.

Within the local potential approximation, the Wetterich equation for this ansatz gives (after integrating over time or frequency):

$$\partial_k W_k(\tilde{x}, y) = \frac{1}{2} \int \frac{d\mathbf{q}}{(2\pi)^d} \partial_k R_k(\mathbf{q}) \frac{q^2 + R_k(\mathbf{q}) + W_k^{(1,1)}}{\sqrt{\left(q^2 + R_k(\mathbf{q}) + W_k^{(1,1)}\right)^2 - W_k^{(2,0)} W_k^{(0,2)}}},$$

where \mathbf{q} is the d -dimensional momentum, $q^2 = |\mathbf{q}|^2$, assumed to have a maximum value $q = \Lambda$, and $R_k(\mathbf{q})$ is the regulator that diverges as $q \rightarrow \Lambda$ and vanishes as $q \rightarrow 0$.

In most recent NPRG work, the regulator $R_k(\mathbf{q})$ is chosen to be a smooth regulator, which is not analytically tractable, or the so-called Litim-Machado-Dupuis (LMD) regulator, $R_k(\mathbf{q}) = (k^2 - q^2)\Theta(k^2 - q^2)$, for which the momentum integrals can be evaluated and the flow equations studied in more detail. Earlier NPRG work on equilibrium models also used the “ultra-sharp” regulator $R_k(\mathbf{q}) = \beta k^2 \Theta(k^2 - q^2)$, with the limit $\beta \rightarrow 0$. This ultra-sharp regulator was found to have some undesirable features, notably it introduced artifacts when attempting to go beyond the LPA using the derivative expansion [67, 70], and in the Ising model predicted some incorrect features of the magnetization

[48], but otherwise gave a qualitatively accurate picture of the RG fixed point structure. The author is not aware of any publications that have written out the flow equation for the effective potential of non-equilibrium systems with the ultra-sharp regulator, so we derive it here to demonstrate the similarity to the flow equation for the spiking network model.

To evaluate the \mathbf{q} integral, we need to regularize the Heaviside step function, which we take to be the limit of a smooth sigmoidal function $f(\frac{k^2-q^2}{\epsilon})$ as $\epsilon \rightarrow 0$. Then, we may write the derivative as

$$\partial_k R_k(\mathbf{q}) = 2\beta k f\left(\frac{k^2-q^2}{\epsilon}\right) + \beta k^2 f'\left(\frac{k^2-q^2}{\epsilon}\right) \frac{2k}{\epsilon}.$$

Because the ultra-sharp regulator only depends on the magnitude of the momentum, we may write $\int d\mathbf{q} = C_d \int dq q^{d-1}$, where C_d is a d -dependent constant. Then,

$$\partial_k W_k = \frac{C_d}{2} \int_0^\Lambda dq q^{d-1} \left[2\beta k f\left(\frac{k^2-q^2}{\epsilon}\right) + \beta k^2 f'\left(\frac{k^2-q^2}{\epsilon}\right) \frac{2k}{\epsilon} \right] \frac{q^2 + \beta k^2 f\left(\frac{k^2-q^2}{\epsilon}\right) + W_k^{(1,1)}}{\sqrt{\left(q^2 + \beta k^2 f\left(\frac{k^2-q^2}{\epsilon}\right) + W_k^{(1,1)}\right)^2 - W_k^{(2,0)} W_k^{(0,2)}}}.$$

Next, we set $y = (k^2 - q^2)/\epsilon$:

$$\partial_k W_k = \frac{C_d}{2} \int_{(k^2-\Lambda^2)/\epsilon}^{k^2/\epsilon} dy (k^2 - \epsilon y)^{(d-2)/2} \frac{\epsilon}{2} \left[2\beta k f(y) + \beta k^2 f'(y) \frac{2k}{\epsilon} \right] \frac{k^2 - \epsilon y + \beta k^2 f(y) + W_k^{(1,1)}}{\sqrt{\left(k^2 - \epsilon y + \beta k^2 f(y) + W_k^{(1,1)}\right)^2 - W_k^{(2,0)} W_k^{(0,2)}}}.$$

We now take $\epsilon \rightarrow 0$ (for fixed k^2 , such that $k^2/\epsilon \rightarrow +\infty$ and $(k^2 - \Lambda^2)/\epsilon \rightarrow -\infty$), giving

$$\partial_k W_k = \frac{C_d}{2} \int_{-\infty}^{\infty} dy k^{d+1} \beta f'(y) \frac{k^2 + \beta k^2 f(y) + W_k^{(1,1)}}{\sqrt{\left(k^2 + \beta k^2 f(y) + W_k^{(1,1)}\right)^2 - W_k^{(2,0)} W_k^{(0,2)}}}.$$

Now we may make a change of variables $dy f'(y) = df$, with $f \in [0, 1]$. The resulting integral can be exactly evaluated due to the one-loop structure of the flow equation, similar to our evaluation of the spiking network model:

$$\begin{aligned} \partial_k W_k &= \frac{C_d k^{d+1} \beta}{2} \int_0^1 df \frac{k^2 + \beta k^2 f + W_k^{(1,1)}}{\sqrt{\left(k^2 + \beta k^2 f + W_k^{(1,1)}\right)^2 - W_k^{(2,0)} W_k^{(0,2)}}} \\ &= \frac{C_d k^{d+1} \beta}{2} \frac{1}{\beta k^2} \sqrt{\left(k^2 + \beta k^2 f + W_k^{(1,1)}\right)^2 - W_k^{(2,0)} W_k^{(0,2)}} \Big|_0^1 \\ &= \frac{C_d k^{d-1}}{2} \left[\sqrt{\left(k^2 + \beta k^2 + W_k^{(1,1)}\right)^2 - W_k^{(2,0)} W_k^{(0,2)}} - \sqrt{\left(k^2 + W_k^{(1,1)}\right)^2 - W_k^{(2,0)} W_k^{(0,2)}} \right]. \end{aligned}$$

At this point we make a minor modification to the flow equation to remove an infinite flowing constant that most NPRG papers ignore. We set $W_k(\tilde{x}, y) \rightarrow W_k(\tilde{x}, y) + K_k$. We expect that $W_k(0, 0) = 0$, so plugging this change into the flow equation and setting $\tilde{x} = y = 0$ yields $\partial_k K_k = \frac{C_d k^{d+1}}{2} \beta k^2$. We may thus write

$$\partial_k W_k = \frac{C_d k^{d-1}}{2} \left[\sqrt{\left(k^2 + \beta k^2 + W_k^{(1,1)}\right)^2 - W_k^{(2,0)} W_k^{(0,2)}} - \beta k^2 - \sqrt{\left(k^2 + W_k^{(1,1)}\right)^2 - W_k^{(2,0)} W_k^{(0,2)}} \right].$$

Finally, we will take the $\beta \rightarrow \infty$ limit:

$$\begin{aligned} \sqrt{\left(k^2 + \beta k^2 + W_k^{(1,1)}\right)^2 - W_k^{(2,0)} W_k^{(0,2)}} - \beta k^2 &= \beta k^2 \sqrt{\left(1 + \frac{k^2 + W_k^{(1,1)}}{\beta k^2}\right)^2 - \frac{W_k^{(2,0)} W_k^{(0,2)}}{(\beta k^2)^2} - \beta k^2} \\ &\approx \beta k^2 \left(1 + \frac{1}{2} \frac{2(k^2 + W_k^{(1,1)})}{\beta k^2}\right) - \beta k^2 \\ &= k^2 + W_k^{(1,1)}. \end{aligned}$$

Putting everything together, the flow equation becomes

$$\partial_k W_k = \frac{C_d k^{d-1}}{2} \left[k^2 + W_k^{(1,1)} - \sqrt{\left(k^2 + W_k^{(1,1)}\right)^2 - W_k^{(2,0)} W_k^{(0,2)}} \right].$$

Identifying $k^2 \sim \delta\Lambda$, $C_d k^{d-2} \sim \rho_\lambda(\Lambda)$ (the extra k^{-1} comes from changing variables $\partial_k W_k = 2k \partial_{k^2} W_k$), and $W_k \sim -W_\Lambda$, we see that this flow equation very nearly has the same form as the flow equation we derived for the spiking network model. The main difference is a missing factor of the analog of Λ multiplying W_k on the right-hand side. It is worth noting that in the derivation of the flow equation for the spiking network model there was no need to invoke a secondary limit $\beta \rightarrow \infty$ after regularizing the Θ function, so the correspondence of the two derivations is not trivial.

While the macroscopic flow equations are not perfectly identical between the standard scalar field theory and spiking network models, the asymptotic fixed point flow equations do match. To see this, we define the dimensionless potential by $W_k(\tilde{x}, y) = k^{d+2} w_s(\tilde{x}, yk^{-d})$, with $\tilde{x} = \tilde{x}$ and $z = y/k^d$. The left hand side becomes $\partial_k W_k = (d+2)k^{d+1} w_s + k^{d+2} \partial_k w_s - k^{d+1} z w_s^{(0,1)}$. Dividing through by k^{d+1} and defining the RG time by $k \partial_k = -\partial_s$ yields

$$\partial_s w_s - (d+2)w_s + dz w_s^{(0,1)} = -\frac{C_d}{2} \left[1 + w_s^{(1,1)} - \sqrt{(1 + w_s^{(1,1)})^2 - w_s^{(2,0)} w_s^{(0,2)}} \right].$$

Rescaling $w_s(\tilde{z}, z) \rightarrow -\frac{C_d}{2} w_s(\tilde{z}, 2z/C_d)$ will eliminate the constant C_d and send $d+2 \rightarrow d/2+1$ and $d \rightarrow d/2$, $w_s \rightarrow -w_s$, and the resulting flow equation will identically match the asymptotic flow equation for our spiking model. Thus, the possible fixed point solutions of the spiking network model and usual scalar field theories are identical. The primary differences reside in the initial conditions, with the symmetries of the initial conditions constraining which critical points the model may flow by. However, it is also worth noting that in many scalar field theories there is no protection against field renormalization. Including a field renormalization in the ansatz for the average effective action Γ is one method for going beyond the local potential approximation in scalar field theories to derive non-trivial (i.e., non-mean-field) estimates of the critical exponents. The spiking network model is protected from such field renormalizations by our Ward identities, although the scaling of the spike response fields $\tilde{\nu}_i(t)$ perhaps plays a similar role. In any case, beyond the local potential approximation the correspondence between scalar field theories driven by Gaussian noise and the spiking network model may differ.

[1] R. E. Kass, S.-I. Amari, K. Arai, E. N. Brown, C. O. Diekman, M. Diesmann, B. Doiron, U. T. Eden, A. L. Fairhall, G. M. Fiddymont, T. Fukai, So. Grün, M. T. Harrison, M. Helias, H. Nakahara, J.-N. Teramae, P. J. Thomas, M. Reimers, J. Rodu, H. G. Rotstein, E. Shea-Brown, H. Shimazaki, S. Shinomoto, B. M. Yu, and M. A. Kramer. Computational neuroscience: Mathematical and statistical perspectives. *Annual Review of Statistics and Its Application*, 5(1):183–214, 2018.

[2] A. A. Faisal, L.P. J. Selen, and D. M. Wolpert. Noise in the nervous system. *Nat. Rev. Neurosci.*, 9(4):292–303, 2008.

[3] Mikhail I Rabinovich, Pablo Varona, Allen I Selverston, and Henry DI Abarbanel. Dynamical principles in neuroscience. *Reviews of modern physics*, 78(4):1213, 2006.

[4] Kechen Zhang. Representation of spatial orientation by the intrinsic dynamics of the head-direction cell ensemble: a theory. *Journal of Neuroscience*, 16(6):2112–2126, 1996.

[5] Carlo R Laing and Carson C Chow. Stationary bumps in networks of spiking neurons. *Neural computation*, 13(7):1473–1494, 2001.

[6] Klaus Wimmer, Duane Q Nykamp, Christos Constantinidis, and Albert Compte. Bump attractor dynamics in prefrontal cortex explains behavioral precision in spatial working memory. *Nature neuroscience*, 17(3):431–439, 2014.

[7] Sung Soo Kim, Hervé Rouault, Shaul Druckmann, and Vivek Jayaraman. Ring attractor dynamics in the drosophila central brain. *Science*, 356(6340):849–853, 2017.

- [8] G Bard Ermentrout and Jack D Cowan. A mathematical theory of visual hallucination patterns. *Biological cybernetics*, 34(3):137–150, 1979.
- [9] Paul C Bressloff. Metastable states and quasicycles in a stochastic wilson-cowan model of neuronal population dynamics. *Physical Review E*, 82(5):051903, 2010.
- [10] Thomas Charles Butler, Marc Benayoun, Edward Wallace, Wim van Drongelen, Nigel Goldenfeld, and Jack Cowan. Evolutionary constraints on visual cortex architecture from the dynamics of hallucinations. *Proceedings of the National Academy of Sciences*, 109(2):606–609, 2012.
- [11] H. Sompolinsky, A. Crisanti, and H. J. Sommers. Chaos in random neural networks. *Phys. Rev. Lett.*, 61:259–262, Jul 1988.
- [12] David Dahmen, Sonja Grün, Markus Diesmann, and Moritz Helias. Second type of criticality in the brain uncovers rich multiple-neuron dynamics. *Proceedings of the National Academy of Sciences*, 116(26):13051–13060, 2019.
- [13] John M Beggs and Dietmar Plenz. Neuronal avalanches in neocortical circuits. *Journal of neuroscience*, 23(35):11167–11177, 2003.
- [14] Michael A Buice and Jack D Cowan. Field-theoretic approach to fluctuation effects in neural networks. *Physical Review E*, 75(5):051919, 2007.
- [15] N. Friedman, S. Ito, B. A. W. Brinkman, M. Shimono, R. E. L. DeVille, K. A. Dahmen, J. M. Beggs, and T. C. Butler. Universal critical dynamics in high resolution neuronal avalanche data. *Phys. Rev. Lett.*, 108:208102, May 2012.
- [16] Woodrow L Shew, Hongdian Yang, Shan Yu, Rajarshi Roy, and Dietmar Plenz. Information capacity and transmission are maximized in balanced cortical networks with neuronal avalanches. *Journal of neuroscience*, 31(1):55–63, 2011.
- [17] J. Beggs and N. Timme. Being critical of criticality in the brain. *Frontiers in Physiology*, 3:163, 2012.
- [18] W. L. Shew and D. Plenz. The functional benefits of criticality in the cortex. *The Neuroscientist*, 19(1):88–100, 2013. PMID: 22627091.
- [19] Jonathan Touboul and Alain Destexhe. Can power-law scaling and neuronal avalanches arise from stochastic dynamics? *PloS one*, 5(2):e8982, 2010.
- [20] Jonathan Touboul and Alain Destexhe. Power-law statistics and universal scaling in the absence of criticality. *Physical Review E*, 95(1):012413, 2017.
- [21] Marcel Nonnenmacher, Christian Behrens, Philipp Berens, Matthias Bethge, and Jakob H Macke. Signatures of criticality arise from random subsampling in simple population models. *PLoS computational biology*, 13(10):e1005718, 2017.
- [22] Anna Levina and Viola Priesemann. Subsampling scaling. *Nature communications*, 8(1):1–9, 2017.
- [23] G. K. Ocker, K. Josić, E. Shea-Brown, and M. A. Buice. Linking structure and activity in nonlinear spiking networks. *PLOS Computational Biology*, 13(6):1–47, 06 2017.
- [24] Jonas Stapmanns, Tobias Kühn, David Dahmen, Thomas Luu, Carsten Honerkamp, and Moritz Helias. Self-consistent formulations for stochastic nonlinear neuronal dynamics. *Physical Review E*, 101(4):042124, 2020.
- [25] M. Kordovan and S. Rotter. Spike train cumulants for linear-nonlinear poisson cascade models, 2020.
- [26] Gabriel Koch Ocker. Dynamics of stochastic integrate-and-fire networks. *Phys. Rev. X*, 12:041007, Oct 2022.
- [27] L. Canet, B. Delamotte, O. Deloubrière, and N. Wschebor. Nonperturbative renormalization-group study of reaction-diffusion processes. *Phys. Rev. Lett.*, 92:195703, May 2004.
- [28] Léonie Canet, Hugues Chaté, Bertrand Delamotte, Ivan Dornic, and Miguel A Munoz. Nonperturbative fixed point in a nonequilibrium phase transition. *Physical review letters*, 95(10):100601, 2005.
- [29] T. Machado and N. Dupuis. From local to critical fluctuations in lattice models: A nonperturbative renormalization-group approach. *Phys. Rev. E*, 82:041128, Oct 2010.
- [30] L. Canet, H. Chaté, and B. Delamotte. General framework of the non-perturbative renormalization group for non-equilibrium steady states. *Journal of Physics A: Mathematical and Theoretical*, 44(49):495001, Nov 2011.
- [31] A. Rançon and N. Dupuis. Nonperturbative renormalization group approach to strongly correlated lattice bosons. *Phys. Rev. B*, 84:174513, Nov 2011.
- [32] A. A. Winkler and E. Frey. Long-range and many-body effects in coagulation processes. *Phys. Rev. E*, 87:022136, Feb 2013.
- [33] Ingo Homrighausen, Anton A. Winkler, and Erwin Frey. Fluctuation effects in the pair-annihilation process with lévy dynamics. *Phys. Rev. E*, 88:012111, Jul 2013.
- [34] T. Kloss, L. Canet, B. Delamotte, and N. Wschebor. Kardar-parisi-zhang equation with spatially correlated noise: A unified picture from nonperturbative renormalization group. *Phys. Rev. E*, 89:022108, Feb 2014.
- [35] Ivan Balog and Gilles Tarjus. Activated dynamic scaling in the random-field ising model: A nonperturbative functional renormalization group approach. *Physical Review B*, 91(21):214201, 2015.
- [36] Léonie Canet, Bertrand Delamotte, and Nicolás Wschebor. Fully developed isotropic turbulence: Symmetries and exact identities. *Physical Review E*, 91(5):053004, 2015.
- [37] P. Jakubczyk and A. Eberlein. Thermodynamics of the two-dimensional XY model from functional renormalization. *Phys. Rev. E*, 93:062145, Jun 2016.
- [38] C. Duclut and B. Delamotte. Nonuniversality in the erosion of tilted landscapes. *Phys. Rev. E*, 96:012149, Jul 2017.
- [39] Leenoy Meshulam, Jeffrey L Gauthier, Carlos D Brody, David W Tank, and William Bialek. Coarse graining, fixed points, and scaling in a large population of neurons. *Physical review letters*, 123(17):178103, 2019.
- [40] Serena Bradde and William Bialek. PCA meets RG. *Journal of statistical physics*, 167(3):462–475, 2017.
- [41] Lorenzo Tiberi, Jonas Stapmanns, Tobias Kühn, Thomas Luu, David Dahmen, and Moritz Helias. Gell-mann–low criticality in neural networks. *Physical Review Letters*, 128(16):168301, 2022.
- [42] Braden AW Brinkman, Fred Rieke, Eric Shea-Brown, and Michael A Buice. Predicting how and when hidden neurons

skew measured synaptic interactions. *PLoS computational biology*, 14(10):e1006490, 2018.

[43] Bertrand Delamotte. An introduction to the nonperturbative renormalization group. In *Renormalization group and effective field theory approaches to many-body systems*, pages 49–132. Springer, 2012.

[44] Léonie Canet. Reaction–diffusion processes and non-perturbative renormalization group. *Journal of Physics A: Mathematical and General*, 39(25):7901, 2006.

[45] L. Canet and H. Chaté. A non-perturbative approach to critical dynamics. *Journal of Physics A: Mathematical and Theoretical*, 40(9):1937–1949, feb 2007.

[46] Nicolas Dupuis, L Canet, Astrid Eichhorn, W Metzner, Jan M Pawłowski, M Tissier, and N Wschebor. The nonperturbative functional renormalization group and its applications. *Physics Reports*, 910:1–114, 2021.

[47] C. Wetterich. Exact evolution equation for the effective potential. *Physics Letters B*, 301(1):90 – 94, 1993.

[48] Jean-Michel Caillol. The non-perturbative renormalization group in the ordered phase. *Nuclear Physics B*, 855(3):854–884, 2012.

[49] James Cooper Robinson and C Pierre. Infinite-dimensional dynamical systems: An introduction to dissipative parabolic pdes and the theory of global attractors. cambridge texts in applied mathematics. *Appl. Mech. Rev.*, 56(4):B54–B55, 2003.

[50] Juergen Berges, Nikolaos Tetradis, and Christof Wetterich. Non-perturbative renormalization flow in quantum field theory and statistical physics. *Physics Reports*, 363(4–6):223–386, 2002.

[51] Nigel Goldenfeld. *Lectures on Phase Transitions and the Renormalization Group*. Westview Press, 1992.

[52] Solving Burger’s equation with NDSolve at large time. StackExchange; accessed January 18 2023.

[53] Yen Lee Loh. Accurate calculation of green functions on the d-dimensional hypercubic lattice. *Journal of Physics A: Mathematical and Theoretical*, 44(27):275201, 2011.

[54] Haim Sompolinsky and Annette Zippelius. Relaxational dynamics of the edwards-anderson model and the mean-field theory of spin-glasses. *Physical Review B*, 25(11):6860, 1982.

[55] Jannis Schuecker, Sven Goedeke, and Moritz Helias. Optimal sequence memory in driven random networks. *Physical Review X*, 8(4):041029, 2018.

[56] Hans-Karl Janssen, Frédéric van Wijland, Olivier Deloubrière, and Uwe C. Täuber. Pair contact process with diffusion: Failure of master equation field theory. *Phys. Rev. E*, 70:056114, Nov 2004.

[57] Michel Droz and László Sasvári. Renormalization-group approach to simple reaction-diffusion phenomena. *Physical Review E*, 48(4):R2343, 1993.

[58] John Cardy and Uwe C Täuber. Theory of branching and annihilating random walks. *Physical review letters*, 77(23):4780, 1996.

[59] Pierre-Antoine Rey and Michel Droz. A renormalization group study of a class of reaction-diffusion models, with particles input. *Journal of Physics A: Mathematical and General*, 30(4):1101, 1997.

[60] John L Cardy and Uwe C Täuber. Field theory of branching and annihilating random walks. *Journal of statistical physics*, 90(1):1–56, 1998.

[61] Hans-Karl Janssen and Uwe C Täuber. The field theory approach to percolation processes. *Annals of Physics*, 315(1):147–192, 2005.

[62] Malo Tarpin, Federico Benitez, Léonie Canet, and Nicolás Wschebor. Nonperturbative renormalization group for the diffusive epidemic process. *Physical Review E*, 96(2):022137, 2017.

[63] Malte Henkel, Haye Hinrichsen, and Sven Lübeck. Universality classes different from directed percolation. *Non-Equilibrium Phase Transitions: Volume I: Absorbing Phase Transitions*, pages 197–259, 2008.

[64] Fan Zhong. Imaginary fixed points can be physical. *Physical Review E*, 86(2):022104, 2012.

[65] Fan Zhong. Renormalization-group theory of first-order phase transition dynamics in field-driven scalar model. *Frontiers of Physics*, 12(5):1–31, 2017.

[66] Xin An, David Mesterházy, and Mikhail A Stephanov. Functional renormalization group approach to the yang-lee edge singularity. *Journal of High Energy Physics*, 2016(7):1–19, 2016.

[67] Tim R Morris. Properties of derivative expansion approximations to the renormalization group. *International Journal of Modern Physics B*, 12(12n13):1343–1354, 1998.

[68] Jean-Michel Caillol. Critical line of the $\phi 4$ theory on a simple cubic lattice in the local potential approximation. *Nuclear Physics B*, 865(2):291–307, 2012.

[69] Jef Hooyberghs, Ferenc Iglói, and Carlo Vanderzande. Absorbing state phase transitions with quenched disorder. *Physical Review E*, 69(6):066140, 2004.

[70] Tim R Morris. Derivative expansion of the exact renormalization group. *Physics Letters B*, 329(2-3):241–248, 1994.

[71] Léonie Canet, Bertrand Delamotte, Dominique Mouhanna, and Julien Vidal. Nonperturbative renormalization group approach to the ising model: a derivative expansion at order ∂^4 . *Physical Review B*, 68(6):064421, 2003.

[72] N Defenu and Alessandro Codello. Scaling solutions in the derivative expansion. *Physical Review D*, 98(1):016013, 2018.

[73] Federico Benitez, J-P Blaizot, Hugues Chaté, Bertrand Delamotte, R Méndez-Galain, and Nicolás Wschebor. Solutions of renormalization-group flow equations with full momentum dependence. *Physical Review E*, 80(3):030103, 2009.

[74] F Benitez, J-P Blaizot, H Chaté, B Delamotte, R Méndez-Galain, and N Wschebor. Nonperturbative renormalization group preserving full-momentum dependence: Implementation and quantitative evaluation. *Physical Review E*, 85(2):026707, 2012.

[75] J-P Blaizot, R Méndez Galain, and N Wschebor. Non-perturbative renormalization group calculation of the transition temperature of the weakly interacting bose gas. *EPL (Europhysics Letters)*, 72(5):705, 2005.

[76] Uwe C Täuber. Field-theory approaches to nonequilibrium dynamics. In *Ageing and the Glass Transition*, pages 295–348. Springer, 2007.

[77] Uwe C Täuber. Renormalization group: applications in statistical physics. *Nuclear Physics B-Proceedings Supplements*, 228:7–34, 2012.

[78] Uwe C Täuber. *Critical dynamics: a field theory approach to equilibrium and non-equilibrium scaling behavior*. Cambridge University Press, 2014.

[79] Wulfram Gerstner, Werner M Kistler, Richard Naud, and Liam Paninski. *Neuronal dynamics: From single neurons to networks and models of cognition*. Cambridge University Press, 2014.

[80] John J Hopfield. Neural networks and physical systems with emergent collective computational abilities. *Proceedings of the national academy of sciences*, 79(8):2554–2558, 1982.

[81] Sen Song, Per Jesper Sjöström, Markus Reigl, Sacha Nelson, and Dmitri B Chklovskii. Highly nonrandom features of synaptic connectivity in local cortical circuits. *PLoS biology*, 3(3):e68, 2005.

[82] Kevin Berlemont and Gianluigi Mongillo. Glassy phase in dynamically-balanced neural networks. *bioRxiv*, 2022.

[83] Gilles Tarjus and Matthieu Tissier. Nonperturbative functional renormalization group for random-field models: The way out of dimensional reduction. *Physical review letters*, 93(26):267008, 2004.

[84] Gilles Tarjus and Matthieu Tissier. Nonperturbative functional renormalization group for random field models and related disordered systems. i. effective average action formalism. *Physical Review B*, 78(2):024203, 2008.

[85] Matthieu Tissier and Gilles Tarjus. Nonperturbative functional renormalization group for random field models and related disordered systems. ii. results for the random field $\phi(n)$ model. *Physical Review B*, 78(2):024204, 2008.

[86] Mohit Randeria, James P Sethna, and Richard G Palmer. Low-frequency relaxation in ising spin-glasses. *Physical review letters*, 54(12):1321, 1985.

[87] AJ Bray. Nature of the griffiths phase. *Physical review letters*, 59(5):586, 1987.

[88] Miguel A Munoz, Róbert Juhász, Claudio Castellano, and Géza Ódor. Griffiths phases on complex networks. *Physical review letters*, 105(12):128701, 2010.

[89] Gašper Tkačik, Thierry Mora, Olivier Marre, Dario Amodei, Stephanie E Palmer, Michael J Berry, and William Bialek. Thermodynamics and signatures of criticality in a network of neurons. *Proceedings of the National Academy of Sciences*, 112(37):11508–11513, 2015.

[90] Rashid V Williams-García, Mark Moore, John M Beggs, and Gerardo Ortiz. Quasicritical brain dynamics on a nonequilibrium widom line. *Physical Review E*, 90(6):062714, 2014.

[91] Adam G Kline and Stephanie E Palmer. Gaussian information bottleneck and the non-perturbative renormalization group. *New Journal of Physics*, 24(3):033007, 2022.

[92] A. Skrondal and S. Rabe-Hesketh. Some applications of generalized linear latent and mixed models in epidemiology: Repeated measures, measurement error and multilevel modeling. *Norsk Epidemiologi*, 13(2), Oct. 2003.

[93] D. I. Warton and L. C. Shepherd. Poisson point process models solve the “pseudo-absence problem” for presence-only data in ecology. *Ann. Appl. Stat.*, 4(3):1383–1402, 09 2010.

[94] A. Bray and F. P. Schoenberg. Assessment of point process models for earthquake forecasting. *Statist. Sci.*, 28(4):510–520, 11 2013.

[95] Braden AW Brinkman, Michael LeBlanc, Yehuda Ben-Zion, Jonathan T Uhl, and Karin A Dahmen. Probing failure susceptibilities of earthquake faults using small-quake tidal correlations. *Nature communications*, 6(1):1–7, 2015.

[96] Braden AW Brinkman, Michael P LeBlanc, Jonathan T Uhl, Yehuda Ben-Zion, and Karin A Dahmen. Probabilistic model of waiting times between large failures in sheared media. *Physical Review E*, 93(1):013003, 2016.

[97] Léonie Canet, Bertrand Delamotte, Dominique Mouhanna, and Julien Vidal. Optimization of the derivative expansion in the nonperturbative renormalization group. *Physical Review D*, 67(6):065004, 2003.

[98] Charlie Duclut and Bertrand Delamotte. Frequency regulators for the nonperturbative renormalization group: A general study and the model a as a benchmark. *Physical Review E*, 95(1):012107, 2017.

[99] Brendan D McKay. The expected eigenvalue distribution of a large regular graph. *Linear Algebra and its Applications*, 40:203–216, 1981.